Mathematical Modelling of Aortic Dissection

by

Beibei Li

A thesis completed in the
School of Mathematics and Statistics,
submitted to the
College of Science and Engineering
at the University of Glasgow
for the degree of
Doctor of Philosophy

January - 2013

I would like to express my deep and sincere gratitude to my supervisors, Professor Nicholas Hill and Dr. Steven Roper. Their enthusiasm, inspiration, patience, and great efforts to explain things clearly and simply have been great value for me. They have been supportive and given big help since I started my PhD study. Their insightful discussions, suggestions and guidance help me get on the right track to my project. I am very grateful to their sound advice and lots of good ideas to guide me to cope with all the problems on my research. Throughout my PhD study and my thesis-writing period, they spend plenty of time to help me to solve problems and check my thesis. I also would like to thank Professor Xiaoyu Luo to her enthusiastic and valuable discussions and suggestions. Thanks to Lei Wang for his data on comparing our work with his numerical work.

I would like to thank my mum and my dad for their love and encouragement. Thanks to my friends, Yu Guan, Yue Han, Charis Kap, Di Xu, Nadia Murdoch, Rui Ji, Weiwei Chen, Nan Qi, for all the caring and happiness they provided. To my office mates, Ewan Morrisons, Fawad Hussain, Joseph Mullaney, Steve O'Hagan, Yujue Hao, thanks for the help during the four years.

Thanks for China Scholarship Council, who has funded my research during my studies. The financial support from School of Mathematics and Statistics of the University of Glasgow during my thesis writing up is acknowledged.

Abstract

An aortic dissection is a tear of the intima of the aortic wall that spreads into the media or between the media and adventitia. In addition to the original lumen for blood flow, the dissection creates a new flow channel, the 'false' lumen that may cause the artery to narrow or even close off entirely. Aortic dissection is a medical emergency and can quickly lead to death.

The mechanical property of the aorta has been described by the strain energy function given by Holzapfel et al. [2000]. The aorta is idealized as an elastic axisymmetric thick-walled tube with 3 layers. We focus on the dissection in media, which is considered as a composite reinforced by two families of fibres. We assume the dissection in the media is axisymmetric. The mathematical model for the dissection is presented. The 2D plane crack problem in linear elastic infinity plane and 2D strip, the axisymmetric crack problem in linear elastic compressible and incompressible tube, the axisymmetric crack problem in an incompressible axisymmetric aorta are applied to obtain solutions to three different problems. And the fluid flow inside the crack has been studied.

The 2D plane crack problem in linear elastic infinity plane has been solved analytically. The 2D plane crack problem in linear elastic compressible and incompressible strip is modelled respectively and solved numerically.

The models for axisymmetric crack problem in linear elastic compressible and incompressible tube are presented respectively. The numerical solutions for the crack problems are expressed, and the results are analyzed.

The mathematical model of the incompressible aorta axisymmetric dissection is given, and the solutions are found numerically. The results change along with the different parameters in the strain energy function, which are analyzed and compared.

The fluid flow inside the tear is assumed very thin which is expressed as the lubrication theory. We use the implicit method to model the Stokes equation numerically, and test the crack opening change along with time.

Contents

Chapter 1

Introduction

The aorta is the largest artery in the body, originating from the left ventricle of the heart and extending down to the abdomen, where it bifurcates into two smaller arteries. The aorta distributes oxygenated blood to all parts of the body through the systemic circulation. The aorta is usually divided into three segments: the ascending aorta, the arch of aorta and the descending aorta as shown in Fig 1.1. The descending aorta is composed of thoracic aorta, the half of the descending aorta above the diaphragm, and abdominal aorta, the half of the descending aorta below the diaphragm.

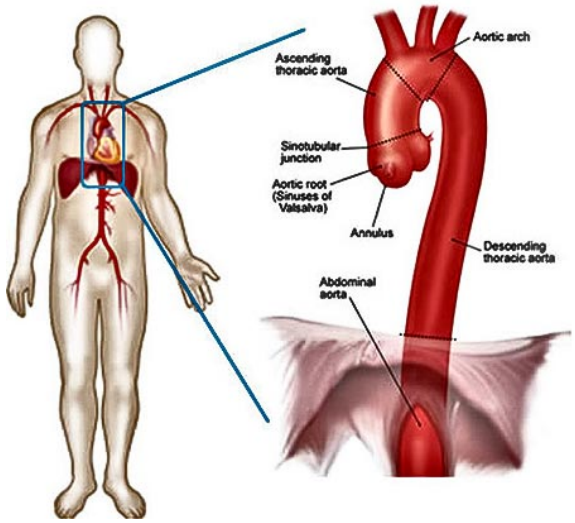

Figure 1.1: The aorta is divided into three segments: the ascending aorta, the arch of aorta and the descending aorta.

An aortic dissection (Holzapfel [2009]) is a tear of the delicate intima of the aortic wall that

spreads into the media or between the media and adventitia. In addition to the original lumen for blood flow, the dissection creates a new flow channel, the 'false' lumen that may cause the artery to narrow or even close off entirely. Simultaneously, the dissection may cause the formation of a thrombus from which fragments embolize. Aortic dissection is a medical emergency and can quickly lead to death, even with optimal treatment. If the dissection tears the aorta completely open (through all three layers), massive and rapid blood loss occurs. Aortic dissections resulting in rupture have an 80 % mortality rate, and 50 % of patients die before they even reach the hospital. Aortic dissection is divided into acute and chronic types (Khan and Nair [2002]), depending on the duration of symptoms. Acute aortic dissection is present when the diagnosis is made within 2 weeks after the initial onset of symptoms, and chronic aortic dissection is present when the initial symptoms are more than 2 weeks duration. About one third of patients with aortic dissection fall into the chronic category. The most common site of initiation of aortic dissection is the ascending aorta (50 % of the cases) followed by the aortic regions in the vicinity of the ligamentum arteriosum.

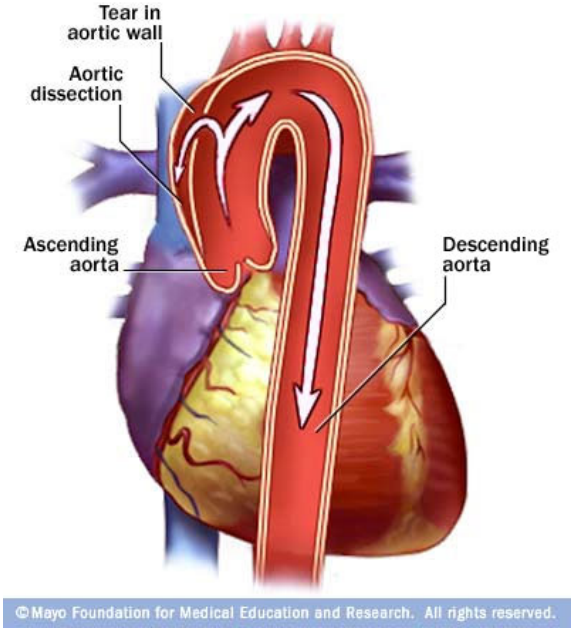

Figure 1.2: The sketch of an aorta and aortic dissection.

Several different classification systems have been used to describe aortic dissections. One is the DeBakey system (DeBakey et al. [1961]),which categorizes the dissection based on where the original intimal tear is located and the extent of the dissection: Type I orig-

inates in the ascending aorta, propagates at least to the aortic arch and often beyond it distally; Type II originates in and is confined to the ascending aorta; Type III originates in the descending aorta, rarely extends proximally but will extend distally. The Stanford classification consists of the following two types. Type A, which involves the ascending aorta and/or aortic arch, and possibly the descending aorta. The tear can originate in the ascending aorta, the aortic arch, or, more rarely, in the descending aorta. It includes DeBakey type I, II and retrograde type III (dissection originating in the descending aorta or aortic arch but extending into the ascending aorta). Type B, which involves the descending aorta or the arch (distal to right brachiocephalic artery origin), without involvement of the ascending aorta. It includes DeBakey type III without retrograde extension into the ascending aorta.

Aortic dissections are observed in clinical practice. Suzuki et al. [2003] have analyzed 384 patients with acute type B aortic dissection enrolled in the International Registry of Acute Aortic Dissection (IRAD). The effect of tear depth on the propagation of aortic dissections in isolated porcine thoracic aorta is observed by Tam et al. [1998], which determines the relationship between the depth of tear and propagation pressure of a bleb using an in vitro porcine model. Sixteen patients with descending thoracic aortic dissection, intimal disruption close to the subclavian artery, and extension of the dissection into the aortic arch or the ascending aorta are described in Segesser et al. [1994]. Parker et al. [1975] outlines the rationale for therapy and the current method of managing acute dissection. The pathophysiology, classification, clinical manifestations, early diagnosis, and management of acute aortic dissection is discussed by Kamalakannan et al. [2007]. Nineteen consecutive patients with aortic dissection underwent open surgery, which all received aortic reconstruction with vascular grafts, are studied by Wei et al. [2009].

The arterial histology has been studied by Holzapfel et al. [2000].

> A health elastic artery is composed of three layers: the intima, the media, the adventitia. The intima is the innermost layer consisting of a single layer endothelial cells that rests on a thin basal membrane and a subendothelial layer whose thickness varies with topography, age and disease. In healthy young individuals, the intima is very thin and makes an insignificant contribution to the solid mechanical properties of the arterial wall. However, it should be

noted that the intima thickens and stiffens with age (arteriosclerosis) so that the mechanical contribution may become significant.

The media is composed of smooth muscle cells, a network of elastic and collagen fibrils and elastic laminae which separate the media into a number of fibre-reinforced layers. The media is separated from the intima and adventitia by the so-called internal elastic lamina and external elastic lamina (absent in cerebral blood vessels), respectively. The orientation of and close interconnection between the elastic and collagen fibrils, elastic laminae, and smooth muscle cells together constitute a continuous fibrous helix. The helix has a small pitch so that the fibrils in the media are almost circumferentially oriented. This structured arrangement gives the media high strength, resilience and the ability to resist loads in both the longitudinal and circumferential directions. From the mechanical perspective, the media is the most significant layer in a healthy artery.

The adventitia is the outermost layer of the artery and consists mainly of fibroblasts and fibrocytes (cells that produce collagen and elastin), histological ground substance and thick bundles of collagen fibrils forming a fibrous tissue. The adventitia is surrounded continuously by loose connective tissue. The primary constituents of the adventitia are thick bundles of collagen fibrils arranged in helical structures. The wavy collagen fibrils are arranged in helical structures and serve to reinforce the wall. They contribute significantly to the stability and strength of the arterial wall. The adventitia is much less stiff in the load-free configuration and at low strains than the media. However, at higher strain the collagen fibres reach their straightened lengths and the adventitia changes to a stiff jacket-like tube which prevents the artery from overstretch and rupture.

The structure of the media give it high strength, resilience and the ability to resist loads in both the longitudinal and circumferential directions. From the mechanical perspective (Holzapfel et al. [2000]), the media is the most significant layer in a healthy artery. Dissections usually happen in media or between the media and adventitia. In this thesis we mainly focus on the dissection in media, the artery is considered as incompressible material since it does not change their volume within the physiological range of deformation.

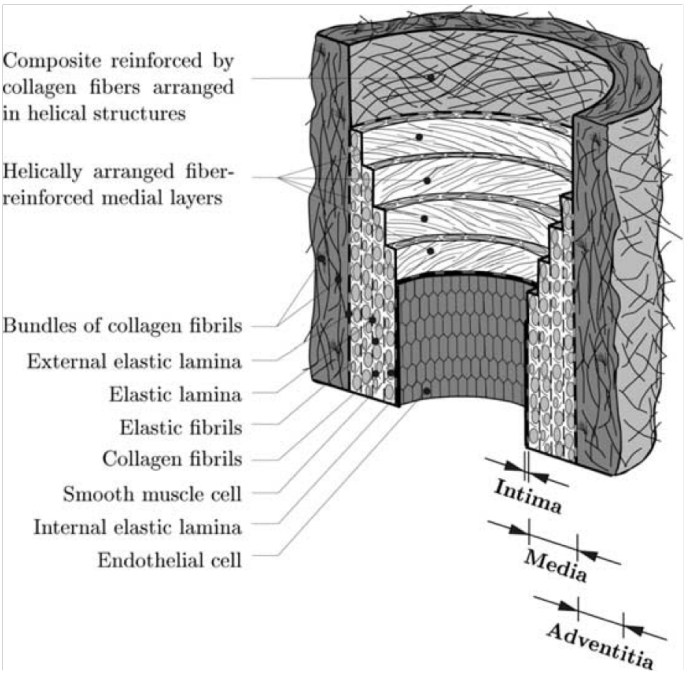

Figure 1.3: Diagrammatic model (Holzapfel et al. [2000]) of the major components of a healthy elastic artery composed of three layers.

A Continuum-mechanical framework is specified in Holzapfel et al. [2000]. They provide the general continuum description of the deformation and the hyperelastic stress response of the material. The artery is considered as a thick-walled circular cylindrical tube subjected to various loads. The strain measures to be used are specified and the equilibrium equations are discussed. Residual stress and pre-stretch play important roles in the artery. The active mechanical behaviour of arterial walls is governed mainly by the intrinsic properties of elastin and collagen fibres and by the degree of activation of smooth muscles. Some constitutive models for arterial walls are introduced by Holzapfel et al. [2000].

In addition, a new constitutive model for arterial walls is given by Holzapfel et al. [2000], They proposed strain energy functions that model each layer of the artery as a fibre-reinforced composite. A constitutive model which incorporates some histological information is formulated. The material parameters involved may be associated with the histological structure of arterial walls (i.e. fibre directions). Arteries are composed of (thick-walled) layers with a separate strain-energy function. From the engineering point

of view, each layer may be considered as a composite reinforced by two families of (collagen) fibres which are arranged in symmetrical spirals. Each layer responds with similar mechanical characteristics and therefore the same form of strain-energy function for each layer is used (but a different set of material parameters). In a healthy young arterial segment (with no pathological intimal changes), the innermost layer of the artery is not of solid mechanical interest, and they therefore focus attention on modelling the two remaining layers, i.e. the media and the adventitia. It is then appropriate to model the artery as a two-layer thick-walled tube (with residual strains) using the strain-energy functions in Holzapfel et al. [2000].

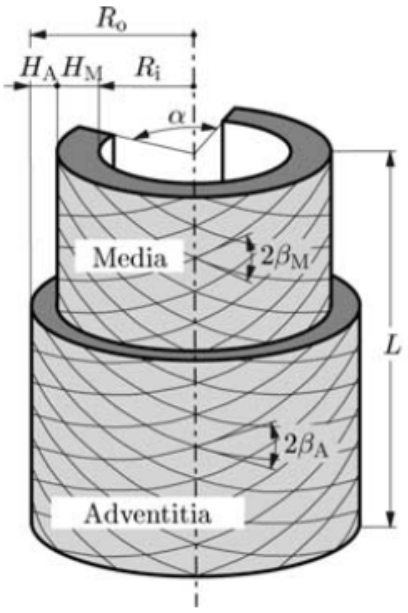

Figure 1.4: Diagrammatic model of media and adventitia as two-layer thick-walled tube.

Arterial dissection has been studied by Gasser and Holzapfel [2006], which focus on the solid mechanical and structure aspects and the geometry of the artery, and captures the displacement discontinuity during arterial dissection they employ the Heaviside function up to an enhanced displacement field. A single-field variational formulation leads to two variational statements, which, together with their consistent linearizations, form the basis for implementations in a finite element program. Geometrically non-linear and consistently linearized embedded strong discontinuity models for 3D problems with an application to the dissection analysis of soft biological tissues have been studied by Gasser and Holzapfel

[2003].

The blood inside the dissection is connecting with the blood in the aorta. Referring to Benson et al. [1957] if there is a tear in the overlying media and intima, a column of blood under aortic pressure may then enter the false lumen and cause a more rapid and complete dissection due to Bernoulli's law. This happens because the lateral pressure of the stagnant column of blood and clot within the dissection will exceed that in the swiftly flowing main column of blood. According to Benson et al. [1957] a second tear in the aortic wall may follow. If the second defect is through the adventitia, massive hemorrhage and death usually occur. If the second defect is through the internal layer, the lateral pressure in the false lumen will drop, again in accord with Bernoulli's law, and further dissection may occur. Therefore the tear propagation need to be considered. We won't be discussing these in this thesis, however it is an important direction.

In order to understand the tear of the elastic material we review several articles. The evaluation of stress intensity factors for plane cracks in residual stress fields by Wilks et al. [1993] gives the modelling of residual stress, and analyze the crack by using the dislocation density method. In Yang et al. [2001] a cohesive zone model for fatigue crack initiation and growth in quasibrittle materials is proposed. Leise et al. [2010] considers the problem of the dynamic, transient propagation of a semiinfinite, mode I crack in an infinite elastic body with a nonlinear, viscoelastic cohesive zone. And they presented a combined analytical/numerical solution method that involves reducing the problem to a Dirichlet-to-Neumann map along the crack face plane, resulting in a integro-differential equation relating the displacement and stress along the crack faces and within the cohesive zone. Ortiz and Pandolfi [1999] has developed a three-dimensional finite-deformation cohesive element and a class of irreversible cohesive laws which enable the accurate and efficient tracking of dynamically growing cracks. A method is outlined for the determination of cohesive zone properties in soft materials in Nilsson [2005]. The goal of the study was to extend earlier work assuming linear kinematics and linear elasticity to include non-linear kinematics and finite elasticity. Explicit results for cohesive traction determination are given and discussed.

The following papers indicate how to deal with the jump conditions of the crack face

for the axisymmetric crack problems. Axisymmetric crack problems has been solved as the singular stress-displacement field resulting from the introduction of a Somigliana ring dislocation in an isotropic linear elastic solid by Demir et al. [1992]. The Burgers vector of this dislocation has two components, one being normal to the plane of the circular ring dislocation (Vulterra type) and the other being in the radial direction of the ring dislocation everywhere (Somigliana type). The analytical solution, in terms of complete elliptic integrals of the first, second and third kinds, is obtained using the Love stress function and Fourier transform. In Korsunsky [1995] the fundamental eigenstrain solutions are derived for axisymmetric crack problems. The solutions are found in terms of Papkovich-Neuber potentials, which in turn are expressed using one function from the family of Lipschitz-Hankel integrals. In order to achieve the most concise form, two methods are used in the analysis: integration method for the axial opening eigenstrain ring and direct solution method for the radial opening eigenstrain ring and the ring of shear.

Above works on the axisymmetric tear focus on the linear elastic material, which can not be used for the aorta. Our model studies the aorta, whose material is non-linear and is described by the strain energy function Holzapfel et al. [2000]. The Cauchy stress, nominal stress, and incremental nominal stress for the tear problem are deduced from the strain energy function, and are used to establish the equilibrium equations with boundary conditions and jump conditions to model the axisymmetric aorta tear problem.

The aim of this thesis is to construct a mathematical model of aortic dissection. We consider the aorta an incompressible elastic cylindrical tube, the mechanics of which is described by the strain energy function given by Holzapfel et al. [2000] and the dissection is axisymmetric. Residual stress and axial stretch play important roles. Hence take the stress-free artery with an open angle as the reference configuration, and the closed artery with residual stress as the current configuration. The dissection of the artery is idealised as the incremental elastic deformation on the configuration with residual stress. The equilibrium equations, which are from Cauchy's law of motion, together with boundary conditions and jump conditions for the crack face are the mathematical description for the 3D crack problem. The methods to solve the problem and the results are included as well.

1.1 Structure

This thesis has solved the 2D plane crack problem in a linear elastic strip, the axisymmetric crack problem in a linear elastic cylindrical tube, and the axisymmetric crack problem in a non-linear elastic cylindrical aorta based on the strain energy function given by Holzapfel et al. [2000]. Each chapter will start with an introduction, following by a problem formulation, then the solutions and main results will be given. The fluid flow inside the tear is analyzed at last.

Chapter 2 introduces basic mathematical formula for idealized artery, then the elastic moduli and incremental moduli. Residual stress and axial stretch are pre-stretch for an unloaded artery. They need to be considered before we think over the tear. The concept of incremental moduli is presented, which will be used to describe the stresses and deformations of the tear. An example is given to explain these concepts. Last but not least, the crack discontinuity is modelled as jump condition, which is introduced by Demir et al. [1992] and Korsunsky [1995].

In Chapter 3 2D plane crack problem in an infinite plane and an elastic strip are presented. The general method to solve a crack problem is given. The traction and displacement components of the tear are written as the integral of Green's function weighted by the displacement of each point along the crack. These Green's functions will be obtained from the calculations of the equilibrium equations with the boundary conditions and jump conditions. So when the traction is given on the tear face, the displacement will be obtained. We use this approach to solve the 2D plane crack in compressible and incompressible elastic strip respectively.

Chapter 4 focuses on the axisymmetric crack problem. We use the similar method as Chapter 3 to solve the axisymmetric crack problem in a compressible and an incompressible linear elastic tube.

In Chapter 5 we model the axisymmetric crack in an elastic incompressible cylindrical thick-walled aorta, which is described as a composite reinforced by two families of collagen fibres which are arranged in symmetrical spirals by the strain energy function given by Holzapfel et al. [2000]. The equilibrium equations for Cauchy stress and incremental nom-

inal stress are given with the boundary conditions and jump conditions. The approach to model the tear is similar as Chapter 3. The results for different parameters are compared and explained.

Chapter 6 discusses the fluid flow inside the crack. Assuming the tear is very thin we use the lubrication theory to describe it, and we use implicit method to test how the opening will change along with time.

Chapter 2

Background material

2.1 Background material

In this section we introduce the concept of residual stress, which plays a very important role in the in-vivo artery. A load-free artery is not a stress-free artery, therefore before we consider any other stress acting on the artery we have to describe the residual stress and axial stretch first. In addition, the strain energy function used to describe the deformation of the artery in Chapter 5 is introduced here. Then an example to explain how to calculate the stress, in which the residual stress and axial stretch are involved, is presented.

2.1.1 Residual stress

We consider the artery as an incompressible thick-walled cylindrical tube subject to various loads referring to Holzapfel et al. [2000]. The load free artery, which is cut along the axial direction as the figure 2.1, is not stress-free artery and will open up with an angle α due to the residual stress. Thus, we take the stress-free opening artery as the reference (undeformed) configuration Ω_0, and the closed artery with residual stress and axial stretch as the current (deformed) configuration Ω.

Refering to Holzapfel et al. [2000], we use the cylindrical polar coordinates (R, Θ, Z) to describe the region Ω_0:

$$R_i \leqslant R \leqslant R_o, \;\; 0 \leqslant \Theta \leqslant (2\pi - \alpha), \;\; 0 \leqslant Z \leqslant L, \tag{2.1}$$

where R_i, R_o, α and L denote the inner and outer radii, the opening angle and length of the undeformed tube, respectively.

In terms of cylindrical polar coordinates (r, θ, z), the geometry of the deformed configura-

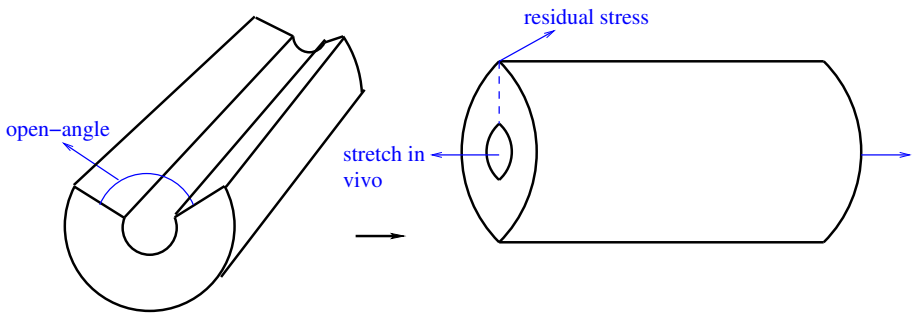

Figure 2.1: Arterial ring in the (stress-free) reference configuration Ω_0, and the (load-free) current configuration Ω.

tion Ω is given by

$$r_{in} \leqslant r \leqslant r_{out}, \quad 0 \leqslant z \leqslant l, \tag{2.2}$$

where r_{in}, r_{out} and l denote the inner and outer radii and the length of the deformed tube, respectively.

From Holzapfel et al. [2000] the deformation χ, which is taken to be isochoric, is written as

$$\chi = r\mathbf{e}_r + z\mathbf{e}_z \tag{2.3}$$

with reference to the basis vectors $\{\mathbf{e}_r, \mathbf{e}_\theta, \mathbf{e}_z\}$ associated with the cylindrical polar coordinates (r, θ, z), where

$$r = \sqrt{\frac{R^2 - R_i^2}{k\lambda} + r_{in}^2}, \quad z = \lambda, \quad k = \frac{2\pi}{2\pi - \alpha} \tag{2.4}$$

λ is the axial stretch, the parameter k is a convenient measure of the tube opening angle in the unstressed configuration.

The Cauchy stress tensor $\boldsymbol{\sigma}$ is decoupled into volumetric contribution $\boldsymbol{\sigma}_{vol}$ and isochoric contribution $\overline{\boldsymbol{\sigma}}$ as shown in Holzapfel et al. [2000]

$$\boldsymbol{\sigma} = \boldsymbol{\sigma}_{vol} + \overline{\boldsymbol{\sigma}} = -p\boldsymbol{I} + \overline{\boldsymbol{\sigma}}, \tag{2.5}$$

where p is the hydrostatic pressure. In the absence of body forces the equilibrium equations are

$$\operatorname{div} \boldsymbol{\sigma} = 0, \tag{2.6}$$

because of the geometrical and constitutive symmetry, the only non-trivial component of (2.6) is

$$\frac{d\sigma_{rr}}{dr} + \frac{\sigma_{rr} - \sigma_{\theta\theta}}{r} = 0. \tag{2.7}$$

From this equation (2.7) and the boundary condition $\sigma_{rr}|_{r=r_{out}} = 0$ on the outer surface of the tube, the radial Cauchy stress σ_{rr} may be calculated as

$$\sigma_{rr}(\xi) = \int_{\xi}^{r_{out}} \frac{(\sigma_{rr} - \sigma_{\theta\theta})}{r} dr, \quad r_{in} \leq \xi \leq r_{out} \tag{2.8}$$

The internal pressure is written as $p_{in} = -\sigma_{rr}|_{r=r_{in}} = \int_{r_{in}}^{r_{out}} \frac{(\sigma_{\theta\theta} - \sigma_{rr})}{r} dr$. Due to (2.5) the components of $\boldsymbol{\sigma}$ have the decompositions $\sigma_{\theta\theta} = -p + \overline{\sigma}_{\theta\theta}$ and $\sigma_{rr} = -p + \overline{\sigma}_{rr}$. Hence the internal pressure

$$\begin{aligned} p_{in} &= \int_{r_{in}}^{r_{out}} \frac{(\sigma_{\theta\theta} - \sigma_{rr})}{r} dr \\ &= \int_{r_{in}}^{r_{out}} \frac{(\overline{\sigma}_{\theta\theta} - \overline{\sigma}_{rr})}{r} dr. \end{aligned} \tag{2.9}$$

The axial force N can be calculated via the definitions

$$\begin{aligned} N &= 2\pi \int_{r_{in}}^{r_{out}} \sigma_{zz} r dr \\ &= 2\pi \int_{r_i}^{r_{out}} (-p + \overline{\sigma}_{zz})\, r dr \\ &= 2\pi \int_{r_{in}}^{r_{out}} (\sigma_{rr} - \overline{\sigma}_{rr} + \overline{\sigma}_{zz})\, r dr \\ &= 2\pi \int_{r_{in}}^{r_{out}} (\sigma_{rr}(\xi) - \overline{\sigma}_{rr} + \overline{\sigma}_{zz})\, \xi d\xi \\ &= 2\pi \int_{r_{in}}^{r_{out}} \left(\int_{\xi}^{r_{out}} \frac{(\sigma_{rr} - \sigma_{\theta\theta})}{r} dr - \overline{\sigma}_{rr} + \overline{\sigma}_{zz} \right) \xi d\xi \\ &= 2\pi \int_{r_{in}}^{r_{out}} \left(\int_{\xi}^{r_{out}} \frac{(\overline{\sigma}_{rr} - \overline{\sigma}_{\theta\theta})}{r} dr - \overline{\sigma}_{rr} + \overline{\sigma}_{zz} \right) \xi d\xi \end{aligned} \tag{2.10}$$

The reduced axial force can be expressed as

$$\begin{aligned} F &= N - {r_{in}}^2 \pi p_{in} \\ &= 2\pi \int_{r_{in}}^{r_{out}} \left(\int_{\xi}^{r_{out}} \frac{(\overline{\sigma}_{rr} - \overline{\sigma}_{\theta\theta})}{r} dr - \overline{\sigma}_{rr} + \overline{\sigma}_{zz} \right) \xi d\xi - {r_{in}}^2 \pi p_i \\ &= 2\pi \int_{r_{in}}^{r_{out}} \int_{\xi}^{r_{out}} \frac{(\overline{\sigma}_{rr} - \overline{\sigma}_{\theta\theta})}{r} dr \xi d\xi - 2\pi \int_{r_{in}}^{r_{out}} (\overline{\sigma}_{rr} - \overline{\sigma}_{zz})\, \xi d\xi - {r_{in}}^2 \pi p_i \\ &= 2\pi \int_{r_{in}}^{r_{out}} \int_{r_{in}}^{r} (\overline{\sigma}_{rr} - \overline{\sigma}_{\theta\theta}) \xi d\xi \frac{dr}{r} - 2\pi \int_{r_{in}}^{r_{out}} (\overline{\sigma}_{rr} - \overline{\sigma}_{zz})\, \xi d\xi - {r_{in}}^2 \pi p_i \\ &= 2\pi \int_{r_{in}}^{r_{out}} \frac{r^2 - {r_{in}}^2}{2} (\overline{\sigma}_{rr} - \overline{\sigma}_{\theta\theta}) \frac{dr}{r} - 2\pi \int_{r_{in}}^{r_{out}} (\overline{\sigma}_{rr} - \overline{\sigma}_{zz})\, \xi d\xi - {r_{in}}^2 \pi \int_{r_{in}}^{r_{out}} \frac{(\overline{\sigma}_{\theta\theta} - \overline{\sigma}_{rr})}{r} dr \\ &= \pi \int_{r_{in}}^{r_{out}} (2\overline{\sigma}_{zz} - \overline{\sigma}_{\theta\theta} - \overline{\sigma}_{rr}) r dr. \end{aligned} \tag{2.11}$$

The hydrostatic pressure p can be calculated from

$$\frac{dp}{dr} = \frac{d\overline{\sigma}_{rr}}{dr} + \frac{\overline{\sigma}_{rr} - \overline{\sigma}_{\theta\theta}}{r}. \tag{2.12}$$

We will use these results to calculate the internal pressure, the reduced axial force and the hydrostatic pressure in §2.1.3.

2.1.2 Strain energy function

The artery is composed of the intima, media, and adventitia. According to Holzapfel et al. [2000] the intima is not of mechanical interest, and therefore the artery is considered as a two-layer thick-walled tube with residual stress and pre-stretch in the longitudinal direction. The structures of the two layers are same, which have the strain energy function

$$\Psi = U(J) + \overline{\Psi} \tag{2.13}$$

where $U(J)$ is volumetric contribution and $\overline{\Psi}$ is given by Holzapfel et al. [2000]

$$\overline{\Psi} = \frac{1}{2}c\left(\overline{I}_1 - 3\right) + \frac{k_1}{2k_2}\left[\Psi_f\left(\overline{I}_4\right) + \Psi_f\left(\overline{I}_6\right)\right]. \tag{2.14}$$

In equation (2.13) and equation (2.14)

$$J = \det \mathbf{A}, \quad \overline{I}_1 = J^{-2/3}\mathrm{tr}\left(\mathbf{A}^T\mathbf{A}\right), \quad \overline{I}_4 = J^{-2/3}\mathrm{tr}\left(\mathbf{M}_+\mathbf{A}^T\mathbf{A}\right), \quad \overline{I}_6 = J^{-2/3}\mathrm{tr}\left(\mathbf{M}_-\mathbf{A}^T\mathbf{A}\right) \tag{2.15}$$

and

$$\Psi_f(x) = \exp\left[k_2\left(x-1\right)^2\right] - 1. \tag{2.16}$$

In a cylindrical polar coordinate system the tensor $\mathbf{A}$ is the deformation gradient, and the matrices $\mathbf{M}_\pm$ are given by

$$\mathbf{M}_\pm = \begin{bmatrix} 0 & 0 & 0 \\ 0 & \cos^2\beta & \pm\cos\beta\sin\beta \\ 0 & \pm\cos\beta\sin\beta & \sin^2\beta \end{bmatrix}, \tag{2.17}$$

and

$$\mathrm{Sym}\left(\mathbf{M}\right) = \frac{1}{2}\left(\mathbf{M} + \mathbf{M}^T\right), \tag{2.18}$$

where 2β is the angle between collagen fibers as shown in Figure 2.2. The media and adventitia have same strain-energy function (2.14). The differences for media and adventitia are the material parameters c, k_1, k_2. The parameter c is associated with the non-collagenous matrix of the material, and describes the isotropic part of the overall response of the tissue. The parameters k_1 and k_2 are associated with the anisotropic contribution of collagen to the overall response. The material parameters are constants and do not depend on the geometry, opening angle or fibre angle.

The strain energy function (2.13) will be used to construct the aortic dissection model in Chapter 5.

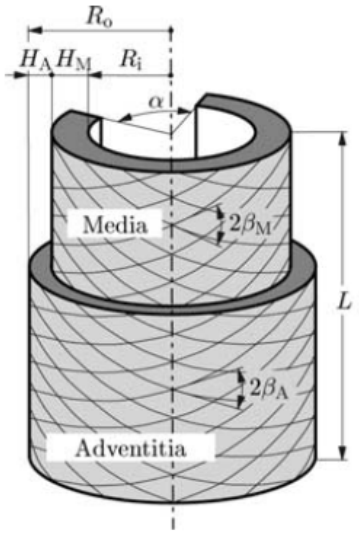

Figure 2.2: Sketch of the media and adventitia from Holzapfel et al. [2000].

2.1.3 Example for residual stress and axial stretch

Here is an example using above theory to calculate stress when residual stress and axial stretch are included. For a general incompressible hyperelastic material the deformation gradient due to residual stress and pre-stretch is

$$\mathbf{A} = \begin{bmatrix} \dfrac{\partial r}{\partial R} & 0 & 0 \\ 0 & k\dfrac{r}{R} & 0 \\ 0 & 0 & \dfrac{\partial z}{\partial Z} \end{bmatrix} \tag{2.19}$$

where $\frac{\partial z}{\partial Z} = \lambda$, $r = r(R)$ defined in (2.4). The incompressibility constraint $J = \det\mathbf{A} = 1$ leads to $\frac{\partial r}{\partial R} = \frac{R}{kr\lambda_z}$, and therefore

$$\mathbf{A} = \begin{bmatrix} \dfrac{R}{kr\lambda_z} & 0 & 0 \\ 0 & k\dfrac{r}{R} & 0 \\ 0 & 0 & \lambda \end{bmatrix}. \tag{2.20}$$

Refer to Holzapfel et al. [2000] the isochoric contribution in (2.5) is

$$\begin{aligned}\overline{\sigma} &= \mathrm{dev}(\overline{\mathbf{A}}\frac{\partial\overline{\Psi}}{\partial\overline{\mathbf{E}}}\overline{\mathbf{A}}^T) \\ &= \mathrm{dev}(\mathbf{A}\frac{\partial\overline{\Psi}}{\partial\mathbf{E}}\mathbf{A}^T) \\ &= \mathbf{A}\frac{\partial\overline{\Psi}}{\partial\mathbf{E}}\mathbf{A}^T - \frac{1}{3}[(\mathbf{A}\frac{\partial\overline{\Psi}}{\partial\mathbf{E}}\mathbf{A}^T) : \mathbf{I}]\mathbf{I}\end{aligned} \tag{2.21}$$

where $\overline{\mathbf{A}} = \left(J^{-\frac{1}{3}}\mathbf{I}\right)\mathbf{A} = \mathbf{A}$, $\mathrm{dev}(\cdot) = (\cdot) - (\frac{1}{3})\mathrm{tr}(\cdot)$ and $\overline{\mathbf{E}} = \mathbf{E}$ due to incompressibility, in which Green-Lagrange strain tensor $\mathbf{E} = \frac{1}{2}(\mathbf{C} - \mathbf{I})$ and right Cauchy-Green tensor $\mathbf{C} = \mathbf{A}^T\mathbf{A}$.

$$\frac{1}{2}\left(\overline{I}_1 - 3\right) = \frac{1}{2}\left(\mathrm{tr}\left(\overline{\mathbf{C}}\right) - 3\right) = \frac{1}{2}\mathrm{tr}(\mathbf{C} - \mathbf{I}) = \mathrm{tr}(\mathbf{E}), \tag{2.22}$$

$$\overline{I}_4 = \mathrm{tr}\left(\mathbf{M}_+\mathbf{A}^T\mathbf{A}\right) = \mathrm{tr}\left(\mathbf{M}_+\mathbf{A}^T\mathbf{A} - \mathbf{M}_+\right) + \mathrm{tr}\left(\mathbf{M}_+\right) = 2\mathrm{tr}\left(\mathbf{M}_+\mathbf{E}\right) + \mathrm{tr}\left(\mathbf{M}_+\right), \tag{2.23}$$

$$\overline{I}_6 = \mathrm{tr}\left(\mathbf{M}_-\mathbf{A}^T\mathbf{A}\right) = \mathrm{tr}\left(\mathbf{M}_-\mathbf{A}^T\mathbf{A} - \mathbf{M}_-\right) + \mathrm{tr}\left(\mathbf{M}_-\right) = 2\mathrm{tr}\left(\mathbf{M}_-\mathbf{E}\right) + \mathrm{tr}\left(\mathbf{M}_-\right), \tag{2.24}$$

$$\frac{\partial\overline{I}_4}{\partial\mathbf{E}} = 2\mathbf{M}_+, \quad \frac{\partial\overline{I}_6}{\partial\mathbf{E}} = 2\mathbf{M}_-, \tag{2.25}$$

Hence

$$\frac{\partial\overline{\Psi}}{\partial\mathbf{E}} = c\mathbf{I} + 2k_1\exp\left[k_2\left(\overline{I}_4 - 1\right)^2\right]\left(\overline{I}_4 - 1\right)\mathbf{M}_+ + 2k_1\exp\left[k_2\left(\overline{I}_6 - 1\right)^2\right]\left(\overline{I}_6 - 1\right)\mathbf{M}_-. \tag{2.26}$$

Then the components of $\overline{\boldsymbol{\sigma}}$ are

$$\begin{aligned}\overline{\sigma}_{rr} &= c\left(\frac{R}{kr\lambda}\right)^2 \\ &- \frac{1}{3}\left\{c\left[\left(\frac{R}{kr\lambda}\right)^2 + k^2\left(\frac{r}{R}\right)^2 + \lambda^2\right] + 4k_1Qe^{4k_2Q^2}\left[\cos^2\beta k^2\left(\frac{r}{R}\right)^2 + \sin^2\beta\lambda^2\right]\right\}\end{aligned}$$

$$\begin{aligned}\overline{\sigma}_{\theta\theta} &= ck^2\left(\frac{r}{R}\right)^2 + 4k_1Qe^{4k_2Q^2}k^2\left(\frac{r}{R}\right)^2 \\ &- \frac{1}{3}\left\{c\left[\left(\frac{R}{kr\lambda}\right)^2 + k^2\left(\frac{r}{R}\right)^2 + \lambda^2\right] + 4k_1Qe^{4k_2Q^2}\left[\cos^2\beta k^2\left(\frac{r}{R}\right)^2 + \sin^2\beta\lambda^2\right]\right\}\end{aligned}$$

$$\begin{aligned}\overline{\sigma}_{zz} &= c\lambda^2 + 4k_1Qe^{4k_2Q^2}\sin^2\beta\lambda^2 \\ &- \frac{1}{3}\left\{c\left[\left(\frac{R}{kr\lambda}\right)^2 + k^2\left(\frac{r}{R}\right)^2 + \lambda^2\right] + 4k_1Qe^{4k_2Q^2}\left[\cos^2\beta k^2\left(\frac{r}{R}\right)^2 + \sin^2\beta\lambda^2\right]\right\}\end{aligned}$$

where

$$Q = 2\mathrm{tr}\left(\mathbf{M}_+\mathbf{E}\right) = \left[\cos^2\beta\left(k\frac{r}{R}\right)^2 + \sin^2\beta\lambda^2 - 1\right].$$

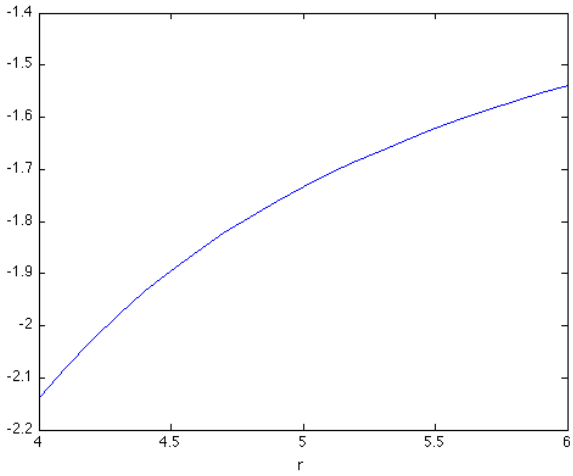

Figure 2.3: Plot of $\overline{\sigma}_{rr}$ when $r_{in} = 4$, $r_{out} = 6$, $\mu = 3$, $\lambda = 1.1$, $\beta = \frac{\pi}{3}$, $k_1 = 2.3632$, $k_2 = 0.8393$, $\alpha = \frac{\pi}{6}$.

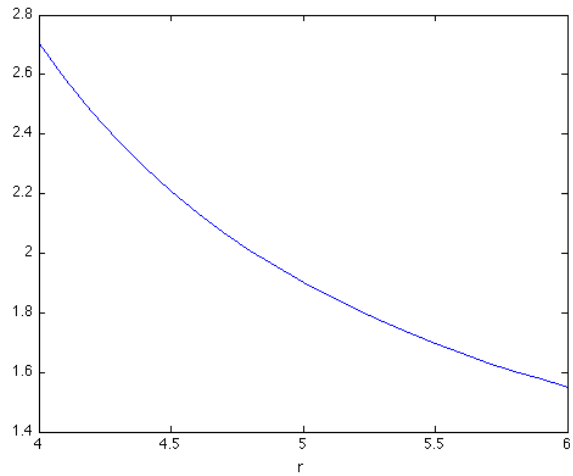

Figure 2.4: Plot of $\overline{\sigma}_{\theta\theta}$ when $r_{in} = 4$, $r_{out} = 6$, $\mu = 3$, $\lambda = 1.1$, $\beta = \frac{\pi}{3}$, $k_1 = 2.3632$, $k_2 = 0.8393$, $\alpha = \frac{\pi}{6}$.

In figures 2.3, 2.4, and 2.5 we plot $\overline{\sigma}_{rr}$, $\overline{\sigma}_{\theta\theta}$, $\overline{\sigma}_{zz}$. And the internal pressure p_{in}, the reduced axial force F and the hydrostatic pressure p can be calculated from equation (2.9), equation (2.11) and equation (2.12) respectively

$$p_{in} = \int_{r_{in}}^{r_{out}} (-\mu \frac{R^2}{k^2\lambda^2 r^3} + \mu k^2 \frac{r}{R^2} + 4k_1 Q e^{4k_2 Q^2} k^2 (\frac{r}{R})^2) dr,$$

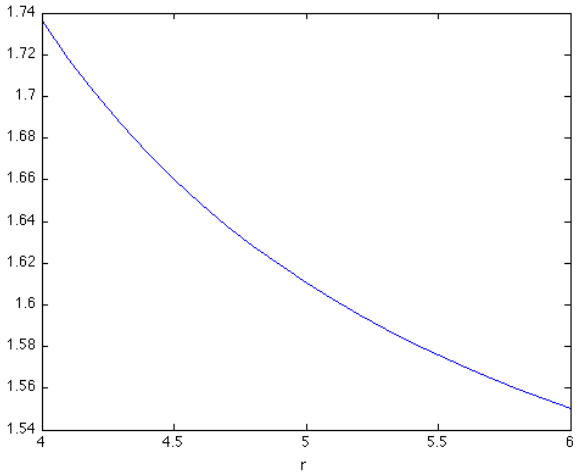

Figure 2.5: Plot of $\overline{\sigma}_{zz}$ when $r_{in} = 4$, $r_{out} = 6$, $\mu = 3$, $\lambda = 1.1$, $\beta = \frac{\pi}{3}$, $k_1 = 2.3632$, $k_2 = 0.8393$, $\alpha = \frac{\pi}{6}$.

$$\begin{aligned} F &= \int_{r_{in}}^{r_{out}} \pi \left(2\,\mu\lambda^2 + 8\,k_1 \sin^2(\beta)\lambda^2 Q e^{k_2 Q^2}\right) r \\ &- \pi \left(\frac{cR^2}{k^2\lambda^2 r^2} + \frac{ck^2 r^2}{R^2} + 4\,\frac{k_1 Q e^{k_2 Q^2}\cos^2(\beta)k^2 r^2}{R^2}\right) r dr, \end{aligned}$$

$$\begin{aligned} p &= \int_{r_{in}}^{r_{out}} 1/3\,\frac{\mu R^2}{k^2 r^3 \lambda^2} + 5/3\,\frac{ck^2 r}{R^2} \\ &+ 4\,\frac{k_1 e^{k_2 Q^2}\left(\cos(\beta)\right)^2 k^2 r\left(4/3\,k_2\left(Q^3 - Q^2\right) + 1/3\,Q - 2/3\right)}{R^2} dr. \end{aligned}$$

These integrals can be calculated numerically.

2.2 Incremental moduli and elastic moduli

The stress-free artery is taken as reference configuration, and the configuration with residual stress as current configuration. We consider the aortic dissection as an incremental deformation, whose definition is

> If the displacement $\delta\mathbf{x}$ is 'small' for each $\mathbf{X} \in \Omega_0$ so that terms of order $|\delta\mathbf{x}|^2$ are negligible in comparison with those of order $|\delta\mathbf{x}|$, then we refer to $\delta\chi$ as an incremental deformation from the configuration described by χ.

referring to R.W.Ogden [1997]. In the following sections (§2.2.1-§2.2.5) the explanation of elastic moduli, incremental elastic deformations, etc are from R.W.Ogden [1997]. In

addition, an example is given to explain how to use the incremental deformation in practice. In the end of this section, we introduce the aortic dissection as axisymmetric tear problem, and give the ideas about how to model the axisymmetric tear.

2.2.1 Elastic moduli

An elastic material, which has a strain-energy function, is called a hyperelastic material. The mechanical propertities of such a material are characterized by the strain-energy function W. The nominal stress, whose transpose is first Piola-Kirchhoff stress, can be written as

$$\mathbf{S} = \frac{\partial W}{\partial \mathbf{A}}. \tag{2.27}$$

The nominal stress has following relation with Cauchy stress,

$$\mathbf{S} = J\mathbf{B}^T\boldsymbol{\sigma} \tag{2.28}$$

where $\mathbf{B} = (\mathbf{A}^{-1})^T$. For a Green-elastic material subject to a single constraint $C(\mathbf{A}) = 0$, the nominal stress is given by

$$\mathbf{S} = \mathbf{H}(\mathbf{A}) + q\frac{\partial C(\mathbf{A})}{\partial \mathbf{A}}, \tag{2.29}$$

where q is an arbitrary scalar, which has the role of a Lagrange multiplier, and $\mathbf{H}$ is the material response function

$$\mathbf{H}(\mathbf{A}) = \frac{\partial W}{\partial \mathbf{A}}. \tag{2.30}$$

For the incompressible constraint we have $C(\mathbf{A}) = \det \mathbf{A} - \mathbf{I} = 0$ and $\frac{\partial C(\mathbf{A})}{\partial \mathbf{A}} = \mathbf{B}^T$. The nominal stress becomes

$$\mathbf{S} = \frac{\partial W}{\partial \mathbf{A}} - p\mathbf{B}^T. \tag{2.31}$$

where we have replaced q by $-p$, p being referred to as the arbitrary hydrostatic pressure.

2.2.2 Deformation increments

The deformation of a body in the current configuration can be written as

$$\mathbf{x} = \chi(\mathbf{X}) \tag{2.32}$$

where $\mathbf{X}$ is the position in the reference configuration Ω_0. Suppose that the deformation is changed to χ' and let

$$\mathbf{x}' = \chi'(\mathbf{X}) \quad \mathbf{X} \in \Omega_0. \tag{2.33}$$

The displacement of a material particle due to this change is

$$\mathbf{x}' - \mathbf{x} = \chi'(\mathbf{X}) - \chi(\mathbf{X}). \tag{2.34}$$

We write this as

$$\delta\mathbf{x} = \delta\chi(\mathbf{X}) \tag{2.35}$$

where the operator δ is defined by $\delta\chi = \chi' - \chi$.

2.2.3 Stress increments

The deformation gradient is $\mathbf{A}$, and the relative incremental deformation gradient is $\delta\mathbf{A}$. The nominal stress increment may be written

$$\delta\mathbf{S} = \mathcal{A}^1\delta\mathbf{A}, \tag{2.36}$$

where $\mathcal{A}^1$ is elastic moduli

$$\mathcal{A}^1 = \frac{\partial\mathbf{S}}{\partial\mathbf{A}}, \tag{2.37}$$

and in componenets

$$\mathcal{A}^1_{\alpha i\beta j} = \frac{\partial^2 W}{\partial A_{i\alpha}\partial A_{j\beta}}. \tag{2.38}$$

2.2.4 Instantaneous moduli

On page 333 of R.W.Ogden [1997], the definitions of *fixed-reference moduli* and *instantaneous moduli* are given

> Suppose we now consider a fixed reference configuration and let $\mathbf{A}$ be the deformation gradient which relates this to the current configuration. We then refer to the moduli as *fixed-reference moduli*.
>
> We take the reference configuration to coincide with the current configuration at any stage of the deformation. The resulting elastic moduli are called *instantaneous moduli*.

Now the current configuration is used as the reference configuration, and $\delta\mathbf{A}_0$ is the value of $\delta\mathbf{A}$ in this configuration, which leads to the relation

$$\delta\mathbf{A} = (\delta\mathbf{A}_0)\,\mathbf{A}. \tag{2.39}$$

In addition

$$\delta \mathbf{S}_0 = J^{-1}\mathbf{A}\delta\mathbf{S} \tag{2.40}$$

where $\delta\mathbf{S}$ is the incremental nominal stress for the fixed configuration, and $\delta\mathbf{S_0}$ is its value relative to the current configuration. The relation between the incremental deformation gradient and incremental nominal stress for the fixed configuration is

$$\delta\mathbf{S} = \mathcal{A}^1\delta\mathbf{A}, \tag{2.41}$$

and for the current configuration it is

$$\delta\mathbf{S}_0 = \mathcal{A}^1_0\delta\mathbf{A}_0, \tag{2.42}$$

where

$$\mathcal{A}^1_{0ijkl} = J^{-1}A_{i\alpha}A_{k\beta}\mathcal{A}^1_{\alpha j\beta l}. \tag{2.43}$$

Hence when the strain energy function W is given, the nominal stress $\mathbf{S}$ and incremental nominal stress $\delta\mathbf{S}_0$ for current configuration could be calculated as following

$$S_{aj} = \frac{\partial W}{\partial A_{j\alpha}}, \quad \mathcal{A}^1_{\alpha j\beta l} = \frac{\partial S_{\alpha j}}{\partial A_{l\beta}}, \quad \mathcal{A}^1_{0ijkl} = J^{-1}A_{i\alpha}A_{k\beta}\mathcal{A}^1_{\alpha j\beta l}, \quad \delta S_{0ij} = \mathcal{A}^1_{0ijkl}\delta A_{0lk}. \tag{2.44}$$

Constraint

For a material with a single constraint, the incremental nominal stress is

$$\delta\mathbf{S} = \mathcal{A}^1\delta\mathbf{A} + \delta q\frac{\partial C}{\partial \mathbf{A}} + q\left(\frac{\partial^2 C}{\partial \mathbf{A}^2}\right)\delta\mathbf{A}, \tag{2.45}$$

and for an incompressible material this becomes

$$\delta\mathbf{S} = \mathcal{A}^1\delta\mathbf{A} + \delta q\mathbf{B}^T - q\mathbf{B}^T\left(\delta\mathbf{A}\right)\mathbf{B}^T. \tag{2.46}$$

When the reference configuration is chosen to coincide with the current configuration, the equation becomes

$$\delta\mathbf{S}_0 = \mathcal{A}^1_0\delta\mathbf{A}_0 + \delta q\mathbf{I} - q\delta\mathbf{A}_0. \tag{2.47}$$

Similar to the unconstrained material, when the strain energy function W is given, the nominal stress $\mathbf{S}$ and incremental nominal stress $\delta\mathbf{S}_0$ could be calculated as following

$$S_{aj} = \frac{\partial W}{\partial A_{j\alpha}} - pB_{j\alpha}, \quad \mathcal{A}^1_{\alpha j\beta l} = \frac{\partial S_{\alpha j}}{\partial A_{l\beta}}, \quad \mathcal{A}^1_{0ijkl} = J^{-1}A_{i\alpha}A_{k\beta}\mathcal{A}^1_{\alpha j\beta l}, \quad \delta S_{0ij} = \mathcal{A}^1_{0ijkl}\delta A_{0lk}. \tag{2.48}$$

2.2.5 Structure and properties of the incremental equations

Refering to R.W.Ogden [1997] for a body whose reference configuration is Ω_0 we write the boundary conditions as

$$\boldsymbol{x} = \boldsymbol{\xi}(\mathbf{X}) \quad \text{on} \quad \partial\Omega_0^{\boldsymbol{x}}, \tag{2.49}$$

$$\mathbf{S}^T\mathbf{N} = \boldsymbol{t}(\mathbf{X}, \mathbf{x}, \mathbf{A}) \quad \text{on} \quad \partial\Omega_0^{\boldsymbol{t}}, \tag{2.50}$$

where $\boldsymbol{\xi}$ and $\boldsymbol{t}$ are prescribed functions of their arguments, $\mathbf{x} = \chi(\mathbf{X})$ for $\mathbf{X} \in \Omega_0$ defines the deformation, and $\mathbf{A} = \text{Grad}\chi(\mathbf{X})$. In R.W.Ogden [1997] the pressure P per unit current area is considered as the loading. The true traction is then given by

$$\boldsymbol{\sigma n} = -P\boldsymbol{n} \quad \text{on} \quad \partial\Omega. \tag{2.51}$$

The corresponding nominal traction has the form

$$\mathbf{S}^T\mathbf{N} = -JP\mathbf{BN} \quad \text{on} \quad \partial\Omega_0. \tag{2.52}$$

The nominal stress $\mathbf{S}$ is given by an appropriate form of elastic constitutive law. In particular,

$$\mathbf{S} = \frac{\partial W}{\partial \mathbf{A}} \tag{2.53}$$

for an unconstrained hyperelastic material, and this is modified to

$$\mathbf{S} = \frac{\partial W}{\partial \mathbf{A}} + q\mathbf{B}^T \tag{2.54}$$

for an incompressible material. The equilibrium equation is

$$\text{Div}\mathbf{S} + \rho_0\mathbf{b} = 0 \tag{2.55}$$

where $\boldsymbol{b}$ is the body force and ρ_0 is the mass density of the body in the configuration Ω_0 .

In R.W.Ogden [1997] the boundary conditions (2.49) is subjected to the increments

$$\delta\boldsymbol{x} = \delta\boldsymbol{\xi}(\mathbf{X}) \quad \text{on} \quad \partial\Omega_0^{\boldsymbol{x}}, \tag{2.56}$$

$$\delta\mathbf{S}^T\mathbf{N} = \delta\boldsymbol{t}(\mathbf{X}, \mathbf{x}, \mathbf{A}) \quad \text{on} \quad \partial\Omega_0^{\boldsymbol{t}}, \tag{2.57}$$

where $\delta\mathbf{S}$ is the increment in nominal stress. In the case of pressure loading (2.51) we have $\boldsymbol{t} = -JP\mathbf{BN}$ and

$$\delta\boldsymbol{t} = -\delta PJ\mathbf{BN} - JP\text{tr}\left(\mathbf{B}^T\delta\mathbf{A}\right)\mathbf{BN} + JP\mathbf{B}\delta\mathbf{A}^T\mathbf{BN} \tag{2.58}$$

where δP is the prescribed increment in P. The incremental counterpart of the equilibrium equation is

$$\mathrm{Div}\delta\mathbf{S} + \rho_0\delta\mathbf{b} = 0, \tag{2.59}$$

where we have

$$\delta\mathbf{S} = \mathcal{A}^1\delta\mathbf{A} \tag{2.60}$$

for an unconstrained material, and

$$\delta\mathbf{S} = \mathcal{A}^1\delta\mathbf{A} + \delta q\mathbf{B}^T - \delta q\mathbf{B}^T\delta\mathbf{A}\mathbf{B}^T \tag{2.61}$$

for an incompressible material. This is accompanied by the incompressibility constraint $\delta\left(\det\mathbf{A}\right) = 0$ which may be written

$$\mathrm{tr}\left(\mathbf{B}^T\delta\mathbf{A}\right) = 0. \tag{2.62}$$

When the reference configuration is chosen to coincide with the current configuration the equilibrium equation becomes

$$\mathrm{div}\delta\mathbf{S}_0 + \rho\delta\mathbf{b} = 0, \tag{2.63}$$

where

$$\delta\mathbf{S}_0 = \mathcal{A}_0^1\delta\mathbf{A}_0 \tag{2.64}$$

for an unconstraint material, and

$$\delta\mathbf{S}_0 = \mathcal{A}_0^1\delta\mathbf{A}_0 + \delta q\mathbf{I} - \delta q\delta\mathbf{A}_0 \tag{2.65}$$

for an incompressible material with

$$\mathrm{tr}\left(\delta\mathbf{A}_0\right) = 0. \tag{2.66}$$

The boundary condition becomes

$$\delta\mathbf{S}_0^T\mathbf{n} = \delta\boldsymbol{t_0} = -\delta P\mathbf{n} - P\mathrm{tr}\left(\delta\mathbf{A}_0\right)\mathbf{n} + P\delta\mathbf{A}_0^T\mathbf{n} \tag{2.67}$$

where $\mathbf{n}$ is the unit normal to the current boundary $\partial\Omega$ of the body, and the middle term on the right-hand side vanishing for an incompressible material.

2.2.6 An example

Here is an example to show how to use above theory to calculate incremental deformation. Consider a stress-free solid incompressible elastic cylinder as the reference configuration. Then the ends of the cylinder are stretched with the stretch ratio λ and take the deformed configuration as the current configuration. Then we press the cylinder along the circumferential direction in the middle of the axial directionwith pressure P which is axisymmetric in the incremental deformation. The coordinate system is (r, θ, z), and assume the radius of the cylinder in the current configuration is $r = a$.

Consider a Neo-Hookean like material with strain-energy density

$$W = \mu \left[\frac{1}{2} \left(\lambda_1^2 + \lambda_2^2 + \lambda_3^2 \right) - \log J \right] + \kappa g \left(J \right) \tag{2.68}$$

where $J = \det\mathbf{A}$ and let λ_i are the principal stretches of the deformation gradient $\mathbf{A}$. The function $g(J)$ satisfies $g(1) = g'(1) = 0$ and $g''(1) = 1$. The strain-energy function becomes

$$W = \mu \left[\frac{1}{2} \mathrm{tr} \left(\mathbf{A}^T \mathbf{A} - \mathbf{I} \right) - \log \left(\det \mathbf{A} \right) \right] + \kappa g \left(\det \mathbf{A} \right). \tag{2.69}$$

The first nominal stress is given by

$$\mathbf{S} = \frac{\partial W}{\partial \mathbf{A}}, \tag{2.70}$$

and write it in the form of strain tensor

$$S_{\alpha i} = \frac{\partial W}{\partial A_{i\alpha}}. \tag{2.71}$$

We use some standard results to generate the expression for $\mathbf{S}$. First

$$\frac{\partial}{\partial \mathbf{A}} \left[\mathrm{tr}\, \mathbf{A}^T \mathbf{A} \right] \tag{2.72}$$

the α-ith component of this tensor is

$$\frac{\partial}{\partial A_{i\alpha}} \left[A_{k\beta} A_{k\beta} \right] = 2 A_{k\beta} \delta_{ik} \delta_{\alpha\beta} = 2 A_{i\alpha} = 2 \left(\mathbf{A}^T \right)_{\alpha i}, \tag{2.73}$$

so that

$$\frac{\partial}{\partial \mathbf{A}} \left[\mathrm{tr}\, \mathbf{A}^T \mathbf{A} \right] = 2 \mathbf{A}^T. \tag{2.74}$$

Next we use the result

$$\frac{\partial}{\partial \mathbf{A}} \left[\det \mathbf{A} \right] = \left(\det \mathbf{A} \right) \mathbf{A}^{-1} \tag{2.75}$$

which in component form is

$$\frac{\partial}{\partial A_{i\alpha}} J = J \left(\mathbf{A}^{-1} \right)_{\alpha i}. \tag{2.76}$$

Any function of J can be differentiated easily

$$\frac{\partial}{\partial \mathbf{A}} F\left(\det \mathbf{A}\right) = \left(\det \mathbf{A}\right) F'\left(\det \mathbf{A}\right) \mathbf{A}^{-1}. \tag{2.77}$$

These results allow us to write that

$$\mathbf{S} = \mu \mathbf{A}^T + \left(\kappa J g'\left(J\right) - \mu\right) \mathbf{A}^{-1} \tag{2.78}$$

for the Neo-Hookean energy. The elastic moduli, based in incremental deformation on top of the finite deformation represented by $\mathbf{A}$ are

$$\mathcal{A}^1 = \frac{\partial \mathbf{S}}{\partial \mathbf{A}}. \tag{2.79}$$

In component form we have

$$\mathcal{A}^1_{\alpha i \beta j} = \frac{\partial S_{\alpha i}}{\partial A_{j\beta}}. \tag{2.80}$$

Before we begin the computation we perform a helpful calculation

$$\begin{aligned}
\frac{\partial}{\partial A_{j\beta}} \left[\left(A^{-1}\right)_{\alpha k} A_{k\gamma}\right] &= \frac{\partial}{\partial A_{j\beta}} \delta_{\alpha\gamma} = 0 \\
&= \frac{\partial}{\partial A_{j\beta}} \left[\left(A^{-1}\right)_{\alpha k}\right] A_{k\gamma} + \left(A^{-1}\right)_{\alpha k} \frac{\partial}{\partial A_{j\beta}} [A_{k\gamma}] \\
&= \frac{\partial}{\partial A_{j\beta}} \left[\left(A^{-1}\right)_{\alpha k}\right] A_{k\gamma} + \left(A^{-1}\right)_{\alpha k} \delta_{jk} \delta_{\beta\gamma} \\
\frac{\partial}{\partial A_{j\beta}} \left[\left(A^{-1}\right)_{\alpha k}\right] A_{k\gamma} \left(A^{-1}\right)_{\gamma i} &= -\left(A^{-1}\right)_{\alpha k} \delta_{jk} \delta_{\beta\gamma} \left(A^{-1}\right)_{\gamma i}
\end{aligned} \tag{2.81}$$

giving the final result that

$$\frac{\partial}{\partial A_{j\beta}} \left[\left(A^{-1}\right)_{\alpha i}\right] = -A^{-1}_{\alpha j} A^{-1}_{\beta i}. \tag{2.82}$$

Using this result we may write

$$\mathcal{A}^1_{\alpha i \beta j} = \mu \left[\delta_{ij}\delta_{\alpha\beta} + A^{-1}_{\alpha j} A^{-1}_{\beta i}\right] + \kappa J g'\left(J\right) \left[A^{-1}_{\alpha i} A^{-1}_{\beta j} - A^{-1}_{\alpha j} A^{-1}_{\beta i}\right] + \kappa J^2 g''\left(J\right) A^{-1}_{\alpha i} A^{-1}_{\beta j}. \tag{2.83}$$

For the moduli when the current configuration is the new reference configuration we have

$$\begin{aligned}
\mathcal{A}^1_{0ijkl} &= J^{-1} A_{i\alpha} A_{k\beta} \mathcal{A}^1_{\alpha j \beta l} \\
&= J^{-1} A_{i\alpha} A_{k\beta} \mu \left[\delta_{ij}\delta_{\alpha\beta} + A^{-1}_{\alpha l} A^{-1}_{\beta j}\right] \\
&+ J^{-1} A_{i\alpha} A_{k\beta} \mu \left(\kappa J g'\left(J\right) \left[A^{-1}_{\alpha j} A^{-1}_{\beta l} - A^{-1}_{\alpha l} A^{-1}_{\beta j}\right] + \kappa J^2 g'' J A^{-1}_{\alpha j} A^{-1}_{\beta l}\right) \\
&= \mu J^{-1} \left(\delta_{jl} A_{i\alpha} A_{k\alpha} + \delta_{il}\delta_{jk}\right) \\
&+ \kappa g'\left(J\right) \left(\delta_{ij}\delta_{kl} - \delta_{il}\delta jk\right) + \kappa J g''\left(J\right) \delta_{ij}\delta_{kl}.
\end{aligned} \tag{2.84}$$

If the deformation $\mathbf{A} = \mathbf{I}$, so that $J = 1$ and $A_{pq} = \delta_{pq}$ then

$$\mathcal{A}^1_{0ijkl} = \mu\left(\delta_{ik}\delta_{jl} + \delta_{il}\delta_{jk}\right) + \kappa\delta_{ij}\delta_{kl} \tag{2.85}$$

which is the isotropic 4th rank tensor for linear elasticity with Lamé moduli μ and κ.

Constraint—Incompressible

The stress-deformation relation for the nominal stress is

$$\mathbf{S} = \frac{\partial W}{\partial \mathbf{A}} + q\frac{\partial C(\mathbf{A})}{\partial \mathbf{A}} \tag{2.86}$$

with $J = 1$ and $\mathrm{tr}\left(\delta\mathbf{A}_0\right) = 0$, since the cylinder is incompressible. When we take the incremental configuration as same as the current configuration we have the incremental nominal stress as

$$\delta\mathbf{S}_0 = \mathcal{A}^1_0\delta\mathbf{A}_0 + \delta q\mathbf{I} - q\delta\mathbf{A}_0, \tag{2.87}$$

Use equation (2.84) we have

$$\begin{aligned}
\left(\delta S_0\right)_{ij} &= \mathcal{A}^1_{0ijkl}\left(\delta A_0\right)_{lk} + \delta q\delta_{ij} - q\left(\delta A_0\right)_{ij} \qquad (2.88)\\
&= \mu J^{-1}A_{i\alpha}A_{k\alpha}\delta_{ij}\left(\delta A_0\right)_{lk} + J^{-1}\mu\delta_{il}\delta_{kj}\left(\delta A_0\right)_{lk}\\
&+ \kappa g''\left(J\right)J\delta_{ji}\delta_{lk}\left(\delta A_0\right)_{lk} + \delta q\delta_{ij} - q\left(\delta A_0\right)_{ij} - q\left(\delta A_0\right)_{ij}\\
&= \mu J^{-1}A_{i\alpha}A^T_{\alpha k}\left(\delta A_0\right)_{kl}\delta^T_{lj} + J^{-1}\mu\delta_{il}\left(\delta A_0\right)_{lk}\delta_{kj} + \kappa g''\left(J\right)J\delta^T_{ij},
\end{aligned}$$

which leads to

$$\delta\mathbf{S}_0 = \mu J^{-1}\mathbf{A}\mathbf{A}^T\delta\mathbf{A}_0{}^T\mathbf{I}^T + J^{-1}\mu\mathbf{I}\delta\mathbf{A}_0\mathbf{I} + \kappa g''\left(J\right)J\mathbf{I}^T\mathrm{tr}\left(\delta\mathbf{A}_0\right) + \delta q\mathbf{I} - q\delta\mathbf{A}_0. \tag{2.89}$$

The deformation gradient is

$$\mathbf{A} = \begin{bmatrix} \frac{R}{r\lambda} & 0 & 0 \\ 0 & \frac{r}{R} & 0 \\ 0 & 0 & \lambda \end{bmatrix}, \tag{2.90}$$

and the solid cylinder is axisymmetric so the incremental deformation gradient is

$$\delta\mathbf{A}_0 = \begin{bmatrix} \frac{\partial\delta r}{\partial r} & 0 & \frac{\partial\delta r}{\partial z} \\ 0 & \frac{\delta r}{r} & 0 \\ \frac{\partial\delta z}{\partial r} & 0 & \frac{\partial\delta z}{\partial z} \end{bmatrix}. \tag{2.91}$$

In details the (2.89) is written as

$$\delta\mathbf{S}_0 = \begin{bmatrix} \mu\left(\frac{1}{\lambda}+1\right)\frac{\partial\delta r}{\partial r}+\delta q-q\frac{\partial\delta r}{\partial r} & 0 & \mu\left(\frac{1}{\lambda}\frac{\partial\delta z}{\partial r}+\frac{\partial\delta r}{\partial z}\right)-q\frac{\partial\delta r}{\partial z} \\ 0 & \mu\left(\frac{1}{\lambda}+1\right)\frac{\delta r}{r}+\delta q-q\frac{\delta r}{r} & 0 \\ \mu\left(\lambda^2\frac{\partial\delta r}{\partial z}+\frac{\partial\delta z}{\partial r}\right)-q\frac{\partial\delta z}{\partial r} & 0 & \mu\left(\lambda^2+1\right)\frac{\partial\delta z}{\partial z}+\delta q-q\frac{\partial\delta z}{\partial z} \end{bmatrix}. \tag{2.92}$$

In following parts we use u to replace δr, and w to replace δz .

Equilibrium equations and boundary conditions

Consider a stress-free solid incompressible elastic cylinder as the reference configuration. Then the ends of the cylinder are stretched with the stretch ratio λ and take the deformed configuration as the current configuration. The radius in the current configuration is $r = a$ The equilibrium equation and boundary condition for nominal stress are

$$\begin{aligned} \mathrm{div}\mathbf{S} &= 0 && (2.93)\\ \mathbf{S^T N} &= -PJ\mathbf{BN} \quad \text{on} \quad r=a. && (2.94) \end{aligned}$$

Then we press the cylinder along the circumferential direction in the middle of the axial direction with pressure P which is axisymmetric in the incremental deformation. The equilibrium equation and boundary condition for incremental nominal stress are

$$\begin{aligned} \mathrm{div}\,\delta\mathbf{S}_0 &= 0 && (2.95)\\ \delta\mathbf{S}_0^T\mathbf{n} &= -\delta P\mathbf{n}-P\mathrm{tr}\left(\delta\mathbf{A}_0\right)\mathbf{n}+P\delta\mathbf{A}_0^T\mathbf{n} \quad \text{on} \quad r=a. && (2.96) \end{aligned}$$

The equilibrium equations (2.95) are

$$\begin{aligned} \mu\frac{1}{\lambda}\left[\frac{\partial^2 u}{\partial r^2}+\frac{1}{r}\frac{\partial u}{\partial r}-\frac{u}{r^2}\right]+\mu\lambda^2\frac{\partial^2 u}{\partial z^2}+\frac{\partial\delta q}{\partial r} &= 0, && (2.97)\\ \mu\frac{1}{\lambda}\left(\frac{\partial^2 w}{\partial r^2}+\frac{1}{r}\frac{\partial w}{\partial r}\right)+\mu\lambda^2\frac{\partial^2 w}{\partial z^2}+\frac{\partial\delta q}{\partial z} &= 0, && (2.98)\\ \frac{1}{r}\frac{\partial}{\partial r}\left(ru\right)+\frac{\partial w}{\partial z} &= 0. && (2.99) \end{aligned}$$

The boundary conditions (2.96) on $r = a$ are

$$\begin{aligned} \frac{\mu}{\lambda}\frac{\partial u}{\partial r}+\left(\mu-P-q\right)\frac{\partial u}{\partial r}+\delta q+\delta P &= 0, && (2.100)\\ \frac{\mu}{\lambda}\frac{\partial w}{\partial r}+\left(\mu-P-q\right)\frac{\partial u}{\partial z} &= 0. && (2.101) \end{aligned}$$

Let $\delta q = -\mu Q$ and $\delta P = \mu \overline{P}$, so the equilibrium equations and boundary conditions become

$$\begin{aligned} \mu \frac{1}{\lambda}\left[\frac{\partial^2 u}{\partial r^2} + \frac{1}{r}\frac{\partial u}{\partial r} - \frac{u}{r^2}\right] + \mu\lambda^2 \frac{\partial^2 u}{\partial z^2} - \mu \frac{\partial Q}{\partial r} &= 0, \\ \mu \frac{1}{\lambda}\left(\frac{\partial^2 w}{\partial r^2} + \frac{1}{r}\frac{\partial w}{\partial r}\right) + \mu\lambda^2 \frac{\partial^2 w}{\partial z^2} - \mu \frac{\partial Q}{\partial z} &= 0, \\ \frac{1}{r}\frac{\partial}{\partial r}(ru) + \frac{\partial w}{\partial z} &= 0, \end{aligned} \tag{2.102}$$

and

$$\begin{aligned} \frac{\mu}{\lambda}\frac{\partial u}{\partial r} + (\mu - P - q)\frac{\partial u}{\partial r} - \mu Q + \mu \overline{P} &= 0, \\ \frac{\mu}{\lambda}\frac{\partial w}{\partial r} + (\mu - P - q)\frac{\partial u}{\partial z} &= 0 \quad \text{on} \quad r = a. \end{aligned} \tag{2.103}$$

Solutions

Let

$$\boldsymbol{u} = \nabla \wedge \psi \boldsymbol{e}_\theta \tag{2.104}$$

$$= \frac{1}{r}\frac{\partial (r\psi)}{\partial r}\boldsymbol{e}_z - \frac{\partial \psi}{\partial z}\boldsymbol{e}_r, \tag{2.105}$$

that means let $w = \dfrac{1}{r}\dfrac{\partial (r\psi)}{\partial r}$ and let $u = -\dfrac{\partial \psi}{\partial z}$. Put them into equations (2.102), and reduce them to

$$\begin{aligned} &\frac{1}{\lambda}\frac{\partial^4 \psi}{\partial r^4} + \lambda^2 \frac{\partial^4 \psi}{\partial z^4} + \left(\lambda^2 + \frac{1}{\lambda}\right)\frac{\partial^4 \psi}{\partial z^2 \partial r^2} + \frac{2}{\lambda r}\partial^3 \psi \partial r^3 + \left(\frac{\lambda^2}{r} + \frac{1}{\lambda r}\right) \\ &\frac{\partial^3 \psi}{\partial z^2 \partial r} - \left(\frac{\lambda^2}{r^2} + \frac{1}{\lambda r^2}\right)\frac{\partial^2 \psi}{\partial z^2} - \frac{3}{\lambda r^2}\frac{\partial^2 \psi}{\partial r^2} + \frac{3}{\lambda r^3}\frac{\partial \psi}{\partial r} - \frac{3}{\lambda r^4}\psi = 0. \end{aligned} \tag{2.106}$$

To factorize the equation into two parts

$$\left[\frac{1}{\lambda}\left(\frac{\partial^2}{\partial r^2} + \frac{1}{r}\frac{\partial}{\partial r} - \frac{1}{r^2}\right) + \lambda^2 \frac{\partial^2}{\partial z^2}\right]\left[\frac{\partial^2}{\partial r^2} + \frac{1}{r}\frac{\partial}{\partial r} - \frac{1}{r^2} + \frac{\partial^2}{\partial z^2}\right]\psi = 0, \tag{2.107}$$

so we change the 4th order equation into two 2nd order equations

$$\left[\frac{1}{\lambda}\left(\frac{\partial^2}{\partial r^2} + \frac{1}{r}\frac{\partial}{\partial r} - \frac{1}{r^2}\right) + \lambda^2 \frac{\partial^2}{\partial z^2}\right]\phi = 0, \tag{2.108}$$

$$\left[\frac{\partial^2}{\partial r^2} + \frac{1}{r}\frac{\partial}{\partial r} - \frac{1}{r^2} + \frac{\partial^2}{\partial z^2}\right]\psi = \phi. \tag{2.109}$$

Use Fourier transformation

$$\begin{aligned} \mathcal{F}[\phi] &= \int_{-\infty}^{+\infty} \phi(r,z)e^{-ikz}dz = \widehat{\phi}(r,k), \quad \phi(r,z) = \frac{1}{2\pi}\int_{-\infty}^{+\infty} \widehat{\phi}(r,k)e^{ikz}dk, \\ \mathcal{F}[\frac{d\phi}{dr}] &= \int_{-\infty}^{+\infty} \frac{d\phi}{dr}e^{-ikz}dz = \frac{d\widehat{\phi}(r,k)}{dr}, \quad \mathcal{F}[\frac{d^2\phi}{dr^2}] = \int_{-\infty}^{+\infty} \frac{d^2\phi}{dr^2}e^{-ikz}dz = \frac{d^2\widehat{\phi}(r,k)}{dr^2}, \\ \mathcal{F}[\frac{d\phi}{dz}] &= \int_{-\infty}^{+\infty} \frac{d\phi}{dz}e^{-ikz}dz = ik\widehat{\phi}, \quad \mathcal{F}[\frac{d^2\phi}{dz^2}] = -k^2\widehat{\phi}, \end{aligned}$$

so equation (2.108) changes to

$$\frac{\partial^2\widehat{\phi}}{\partial r^2}+\frac{1}{r}\frac{\partial\widehat{\phi}}{\partial r}-\frac{\widehat{\phi}}{r^2}-\lambda^3k^2\widehat{\phi}=0. \tag{2.110}$$

Let $t=\lambda^{3/2}kr$ and change it to Modified Bessel equation

$$\frac{\partial^2\widehat{\phi}}{\partial t^2}+\frac{1}{t}\frac{\partial\widehat{\phi}}{\partial t}-\frac{\widehat{\phi}}{t^2}-\widehat{\phi}=0. \tag{2.111}$$

The solution of this equation is $\widehat{\phi}=a(k)I_1(\lambda^{3/2}k,\,r)+b(k)K_1(\lambda^{3/2}k,\,r)$.
When $r\to 0$, $K_1\to\infty$, so $b=0$ and $\widehat{\phi}=a(k)I_1(\lambda^{3/2}k,\,r)$.

Now we want to solve the second equation (2.109). After Fourier transformation the general solution of the homogenous equation

$$\left[\frac{\partial^2}{\partial r^2}+\frac{1}{r}\frac{\partial}{\partial r}-\frac{1}{r^2}+\frac{\partial^2}{\partial z^2}\right]\psi=0 \tag{2.112}$$

is

$$\widehat{\psi}=C(k)I_1(k,\,r)+D(k)K_1(k,\,r). \tag{2.113}$$

When $r\to 0$, $K_1\to\infty$, so $D=0$ and $\widehat{\psi}=C(k)I_1(k,\,r)$.
We show that $\frac{\hat{\phi}}{k^2(\lambda^3-1)}$ is the particular solution for the nonhomogeneous equation after Fourier transformation, where $\widehat{\phi}=a(k)I_1(\lambda^{3/2}k,\,r)$.

Proof :

$$\begin{aligned}
LHS &= \frac{1}{k^2\left(\lambda^3-1\right)}\left[a(k)\lambda^3k^2I_1''(\lambda^{3/2}k,\,r)+\frac{1}{t}a(k)\lambda^3k^2I'(\lambda^{3/2}k,\,r)\right]\\
&- \frac{1}{k^2\left(\lambda^3-1\right)}\left[\frac{1}{t}^2\,a(k)\lambda^3k^2I(\lambda^{3/2}k,\,r)+a(k)k^2I(\lambda^{3/2}k,\,r)\right]\\
&= \frac{1}{k^2\left(\lambda^3-1\right)}\left[a(k)\lambda^3k^2I_1(\lambda^{3/2}k,\,r)-a(k)k^2I(\lambda^{3/2}k,\,r)\right]\\
&= a(k)I(\lambda^{3/2}k,\,r)\\
&= \hat{\phi}\\
&= RHS
\end{aligned}$$

So the particular solution of equation (2.109) after Fourier transform is

$$\frac{a(k)I_1(\lambda^{3/2}k,\,r)}{k^2\left(\lambda^3-1\right)}. \tag{2.114}$$

So the solution of equation (2.109) after Fourier transformation is

$$A(k)I_1(\lambda^{3/2}k,\,r)+C(k)I_1(k,\,r). \tag{2.115}$$

In boundary conditions (2.103) we define $\delta q = -\mu Q$, and $\delta P = \mu\overline{P}$.

And we have $P + q = \mu(1 - \frac{1}{\lambda})$. This is from the boundary condition (2.94), which is in components as

$$\mu\left(\frac{R}{r\lambda} - \frac{r}{R}\lambda\right) + q\frac{r}{R}\lambda \;=\; -P\lambda\frac{r}{R} \quad \text{on} \quad r = a,$$

where

$$r = \sqrt{\frac{R^2 - R_i^2}{\lambda} + r_i^2} \quad \text{for the solid cylinder we have} \quad R_i = 0 \quad \text{and} \quad r_i = 0.$$

So boundary conditions (2.103) become

$$\frac{2}{\lambda}\frac{\partial u}{\partial r} - Q + \overline{P} \;=\; 0, \tag{2.116}$$

$$\frac{\partial w}{\partial r} + \frac{\partial u}{\partial z} \;=\; 0 \quad \text{on} \quad r = a. \tag{2.117}$$

Put $w = \frac{1}{r}\frac{\partial(r\psi)}{\partial r}$ and $u = -\frac{\partial\psi}{\partial z}$ into these equations

$$-\frac{2}{\lambda}\frac{\partial^2\psi}{\partial r\partial z} - Q + \overline{P} \;=\; 0, \tag{2.118}$$

$$\frac{\partial^2\psi}{\partial r^2} + \frac{1}{r}\frac{\partial\psi}{\partial r} - \frac{\psi}{r^2} - \frac{\partial^2\psi}{\partial z^2} \;=\; 0 \quad \text{on} \quad r = a. \tag{2.119}$$

After Fourier transformation we put $\psi = A(k)I_1(\lambda^{3/2}k, r) + C(k)I_1(k, r)$ into boundary condition (2.119) we write $A(k)$ in the form of $C(k)$

$$A(k) = \frac{-C(k)I_1(k,a)(a^2 + k^2 - 1 + k^2a^2)}{I_1(k\lambda^{\frac{3}{2}}, a)(a^2 + k^2\lambda^3 - 1 + k^2a^2)}. \tag{2.120}$$

Now we use the boundary condition (2.118) and the equilibrium equation (6.28) to get the value of $A(k)$ and $C(k)$,

$$\mu\frac{1}{\lambda}\left(\frac{\partial^2 w}{\partial r^2} + \frac{1}{r}\frac{\partial w}{\partial r}\right) + \mu\lambda^2\frac{\partial^2 w}{\partial z^2} - \mu\frac{\partial Q}{\partial z} \;=\; 0, \tag{2.121}$$

$$-\frac{2}{\lambda}\frac{\partial^3\psi}{\partial r\partial z^2} - \frac{\partial Q}{\partial z} + \frac{\partial\overline{P}}{\partial z} \;=\; 0. \tag{2.122}$$

Eliminate $\frac{\partial Q}{\partial z}$ term from these equations, and use Fourier transformation to change the PDE to ODE. Let $\mathcal{F}[\overline{P}(z)] = \int_{-\infty}^{+\infty}\overline{P}(z)e^{-ikz}dz = \widehat{\overline{P}(k)}$. The values of $A(k)$ and $C(k)$ are known, which include $\widehat{\overline{P}(k)}$. Then $\psi(r,k) = A(k)I_1(\lambda^{3/2}k, r) + C(k)I_1(k, r)$ is known as well. Now we use numerical way to integral $\psi(r,z) = \frac{1}{2\pi}\int_{-\infty}^{+\infty}\psi(r,k)e^{ikz}dk$, $w = \frac{1}{r}\frac{\partial(r\psi)}{\partial r}$

and $u = -\frac{\partial \psi}{\partial z}$

$$
\begin{aligned}
\psi(r,z) &= \frac{1}{2\pi}\int_{-\infty}^{+\infty} \psi(r,k)e^{ikz}dk \qquad (2.123)\\
&= \frac{1}{2\pi}\int_{-\infty}^{+\infty} [\Re\psi(r,k) + i\Im\psi(r,k)]\,[\cos(kz) + i\sin(kz)]dk\\
&= -\frac{1}{2\pi}\int_{-\infty}^{+\infty} [\Im\psi(r,k)]\,[\sin(kz)]dk\\
u &= -\frac{\partial \psi}{\partial z}\\
&= -\frac{1}{2\pi}\int_{-\infty}^{+\infty} \psi(r,k)ike^{ikz}dk\\
&= -\frac{1}{2\pi}i\int_{-\infty}^{+\infty} k\,[\Re\psi(r,k) + i\Im\psi(r,k)]\,[\cos(kz) + i\sin(kz)]dk\\
&= \frac{1}{2\pi}\int_{-\infty}^{+\infty} k\,[\Im\psi(r,k)]\,[\cos(kz)]dk\\
w &= \frac{1}{r}\frac{\partial\,(r\psi)}{\partial r}\\
&= \frac{1}{2\pi}\int_{-\infty}^{+\infty} \left[\frac{\psi}{r}e^{ikz} + \frac{\partial\psi}{\partial r}e^{ikz}\right]dk\\
&= -\frac{1}{2r\pi}\int_{-\infty}^{+\infty} [\Im\psi(r,k)]\,[\sin(kz)]dk - \frac{1}{2\pi}\int_{-\infty}^{+\infty} \frac{\partial\Im\psi(r,k)}{\partial r}\sin(kz)dk
\end{aligned}
$$

where $\Re$ is the real part, and $\Im$ is the imaginary part.

In this case $\overline{P}(z) = \frac{1}{\epsilon}$, and $\widehat{\overline{P}(k)} = \int_{-\frac{\epsilon}{2}}^{+\frac{\epsilon}{2}} \frac{1}{\epsilon}e^{-ikz}dz = \frac{\sin(\frac{\epsilon k}{2})}{\frac{\epsilon k}{2}}$. Now we assume the outer radius $a = 1$, $\lambda = 1.1$, and $\epsilon = 0.1$, then we get the displacement as Figure 2.6

Conclusion

In this example we use the equilibrium equations of incremental nominal stress with pressure on boundary to describe the problem. And we use Fourier transform (F.T.) to change PDE to ODE, and solve the ODE analytically and invert it by inverse F.T. to obtain the final displacement. For solving the axisymmetric crack problem we will use the F.T. and incremental deformation. The main procedures are similar, but we consider the crack as jump conditions, which is introduced in next part. In additional the ODE is solved numerically.

2.2.7 Aortic dissection–Axisymmetric crack problem

We idealized the aorta as an axisymmetric thick-walled cylindrical tube with residual stress and pre-stretch in axial direction. We assume the crack is axisymmetric in the

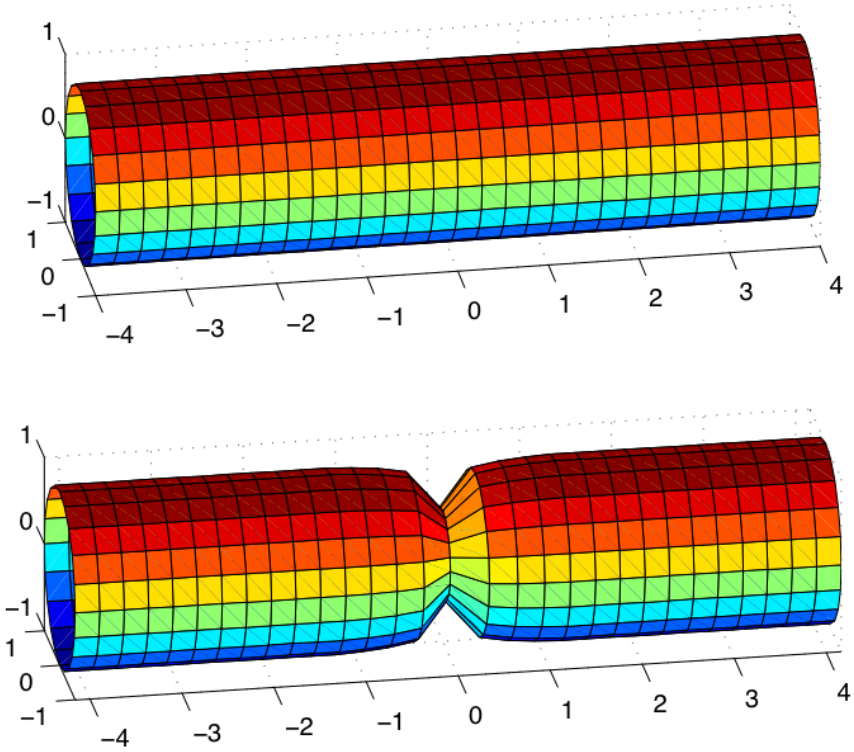

Figure 2.6: The cylinder before and after deformation.

wall as shown in Figure 2.7. We take the stress-free artery with an open angle as the

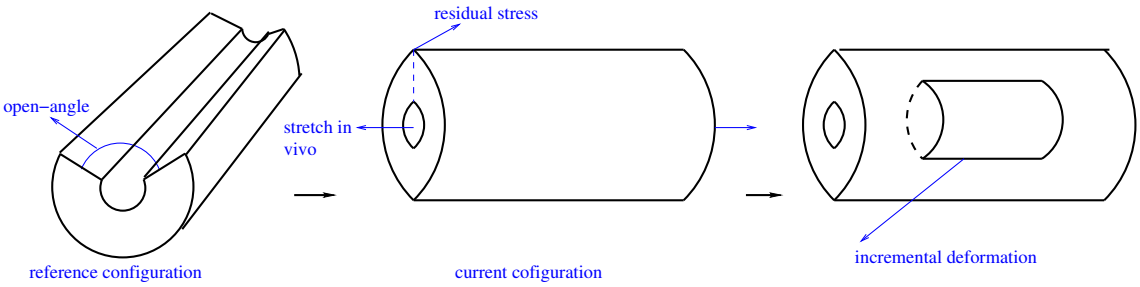

Figure 2.7: Axisymmetric aortic dissection on a thick-walled cylindrical tube with residual stress and pre-stretch.

reference configuration, and the closed artery with residual stress and axial stretch as the *current* configuration. The dissection of the artery is idealised as the *incremental* elastic deformation on the configuration with residual stress. In current configuration the equilibrium equation and boundary condition for Cauchy Stress are equations (5.1). Take

the configuration with residual stress in as the same configuration for the incremental deformation, and the equilibrium equation and boundary conditions for the incremental nominal stress are equations (5.2). For the crack problem we still need jump conditions, which will be discussed in §2.3.2 .

2.3 Axisymmetric crack problem

We assume that the aortic dissection is axisymmetric. The tear discontinuity is considered as the jump conditions which has been studied by Demir et al. [1992] and Korsunsky [1995]. We will use the similar jump conditions to solve the crack problem in Chapter 3—Chapter 5.

2.3.1 Axisymmetric crack

According to Demir et al. [1992] for an isotropic elastic material the axisymmetric crack problem is convenient to use the Love stress function ϕ which satisfies the equilibrium condition. The problem is reduced to solving for the Love stress function ϕ which must satisfy the biharmonic equation

$$\nabla^2\nabla^2\phi = 0, \tag{2.124}$$

for the axisymmetric case under consideration, the Laplacian ∇^2 is given by

$$\nabla^2 = \frac{\partial^2}{\partial r^2} + \frac{1}{r}\frac{\partial}{\partial r} + \frac{\partial^2}{\partial z^2}. \tag{2.125}$$

The stress and displacement components are given by

$$\sigma_{rr} = \frac{\partial}{\partial z}\left(\nu\nabla^2\phi - \frac{\partial^2\phi}{\partial r^2}\right), \tag{2.126}$$

$$\sigma_{\theta\theta} = \frac{\partial}{\partial z}\left(\nu\nabla^2\phi - \frac{1}{r}\frac{\partial\phi}{\partial r}\right), \tag{2.127}$$

$$\sigma_{zz} = \frac{\partial}{\partial z}\left[(2-\nu)\nabla^2\phi - \frac{\partial^2\phi}{\partial z^2}\right], \tag{2.128}$$

$$\sigma_{rz} = \frac{\partial}{\partial r}\left[(1-\nu)\nabla^2\phi - \frac{\partial^2\phi}{\partial z^2}\right], \tag{2.129}$$

$$2Gu = -\frac{\partial^2\phi}{\partial r\partial z}, \tag{2.130}$$

$$2Gw = 2(1-\nu)\nabla^2\phi - \frac{\partial^2\phi}{\partial z^2}, \tag{2.131}$$

where z is the axis of symmetry, r is the radial coordinate, σ_{rr}, $\sigma_{\theta\theta}$, σ_{zz}, σ_{rz} are the radial, transverse, axial and shear stress components respectively. u and w are the radial and

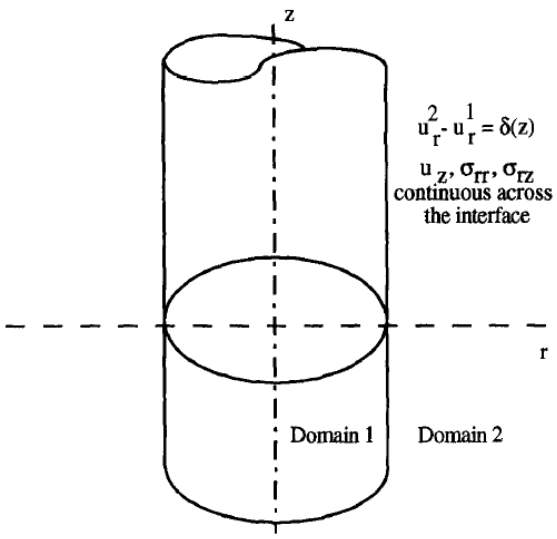

Figure 2.8: Korsunsky [1995]

axial displacements respectively, and G is the shear modulus of elasticity and ν is the Poisson's ratio. Equation 2.124 is solved by use of the Fourier transform pair

$$\phi = \frac{1}{\sqrt{2\pi}} \int_{-\infty}^{\infty} \hat{\phi}(r,\xi) e^{-i\xi z} d\xi, \quad \hat{\phi} = \frac{1}{\sqrt{2\pi}} \int_{-\infty}^{\infty} \phi(r,z) e^{i\xi z} dz, \tag{2.132}$$

where ξ is the Fourier transformation variable. Then upon applying the Fourier transform to equation 2.124 we obtain a Bessel differential equation for ϕ whose solution is given by

$$\xi^2 \phi\left(\hat{r},\xi\right) = iA\left(\xi\right) I_0\left(\xi r\right) + \xi r B\left(\xi\right) I_1\left(\xi r\right) + iC\left(\xi\right) K_0\left(\xi r\right) + \xi r D\left(\xi\right) K_1\left(\xi r\right) \tag{2.133}$$

where $I_{0,1}$ and $K_{0,1}$ are the modified Bessel functions of the first and second kinds respectively, and $A\left(\xi\right)$, $B\left(\xi\right)$, $C\left(\xi\right)$ and $D\left(\xi\right)$ are functions of the transform variable ξ and should be chosen in connection with the boundary conditions.
Results for stress and displacements can be found in The Somigliana ring dislocation by Demir et al. [1992].

2.3.2 Jump conditions

We consider the discontinuity of the crack face in the elastic cylinder as 'Jump condition'. Korsunsky [1995] used the following jump conditions to solve the axisymmetric crack

problem.

$$\left(u^2 - u^1\right) = \delta(z), \quad -\infty < z < \infty, \tag{2.134}$$

$$\left(w^2 - w^1\right) = 0, \quad -\infty < z < \infty, \tag{2.135}$$

$$\sigma_{rz}^2 - \sigma_{rz}^1 = 0, \quad -\infty < z < \infty, \tag{2.136}$$

$$\sigma_{rr}^2 - \sigma_{rr}^1 = 0, \quad |z| > 0, \tag{2.137}$$

where u is the displacement component in radial direction and w is the displacement component in axial direction, and the superscript '2' means domain 2 and the superscript '1' means domain 1. By using these conditions $A(\xi)$, $B(\xi)$, $C(\xi)$ and $D(\xi)$ in equation (2.133) can be solved.

Results are given by Demir et al. [1992] and Korsunsky [1995].

We got the idea form these jump conditions to use similar methods to cope with the crack discontinuity in the crack problem in Chapter 3—Chapter 5.

2.4 Conclusions

We have illustrated the ideas of residual stress, incremental moduli, elastic moduli, the strain energy function of an artery, axisymmetric crack problem and the jump conditions for the crack. In Chapter 5 we will use all of these to build a model of a tear in the aorta.

Chapter 3

Static tears in compressible and incompressible linear elastic 2D strips

3.1 Introduction

Our aim in this chapter is to introduce a method for the solution of 2D crack problems. We illustrate aspects of the method by considering a straight crack in an infinite domain and derive an integral equation relating crack opening to traction on the crack faces. We then consider a straight crack in an inifnite 2D strip, in which the crack is aligned with the strip direction. The approach leads us to consider a numerical scheme to solve for crack opening and displacements given the tractions on the crack faces. We discuss the important parts of this scheme as it will be used in Chapters 4 and 5 to solve axisymmetric crack problems in Chapter 4 and used to solve our idealised tear problem in the aortic media.

3.1.1 General crack problem in plane strain

We consider a cracked body in 2D occupying a domain D with boundary ∂D as shown in Figure 3.1. Let an arclength coordinate along L, and crack lies along L in D. The displacement discontinuity across the crack is $\boldsymbol{U}(s)$, where s is an arbitrary point on L. The displacement discontinuity $\boldsymbol{U}(s)$ is decomposed to give the normal jump $U(s)$ and the tangential jump $V(s)$. The outer normal to ∂D is $\mathbf{n}^b$. The boundary ∂D is traction free

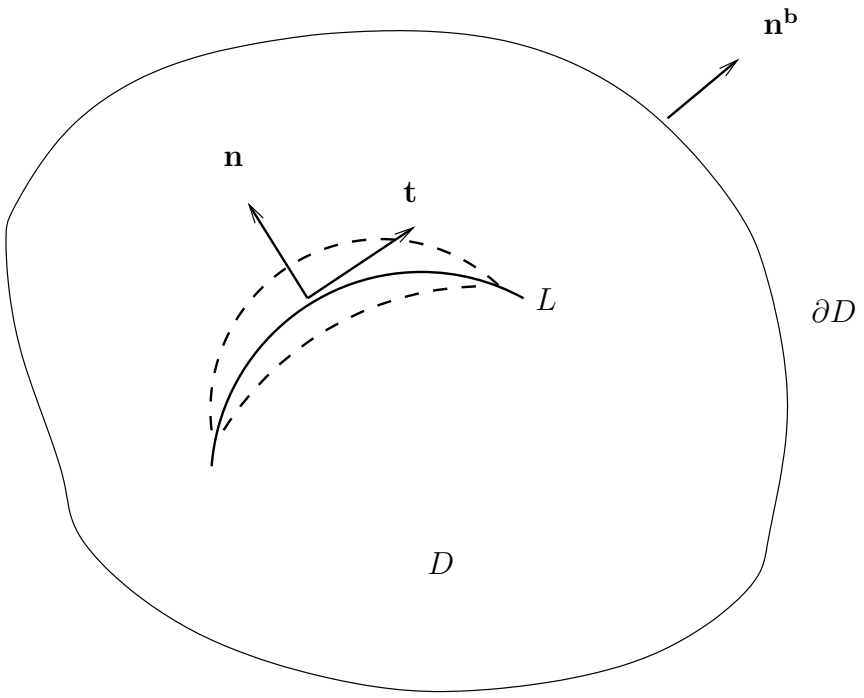

Figure 3.1: Crack on an arbitrary 2D body.

so

$$\boldsymbol{T} \cdot \mathbf{n}^b = 0 \quad \text{on} \quad \partial D$$

where $\boldsymbol{T}$ is the traction. The traction is decomposed into

$$\mathbf{T} = T_n \mathbf{n} + T_t \mathbf{t},$$

where $\mathbf{n}$ is the normal vector and $\mathbf{t}$ is the tangent vector. The equilibrium equation, boundary conditions and jump conditions for the body are

$$\begin{aligned} \operatorname{div} \boldsymbol{T} &= 0 \quad \text{on} \quad D & (3.1) \\ \boldsymbol{T} \cdot \mathbf{n}^b &= 0 \quad \text{on} \quad \partial D & (3.2) \\ [\mathbf{u}]_-^+ &= \boldsymbol{U}(s) \quad \text{on} \quad L & (3.3) \end{aligned}$$

where $\mathbf{u} = (u, v)$ is the displacement for the body D, and $[u]_L = U(s)$ and $[v]_L = V(s)$, where $U(s)$ and $V(s)$ are components of $\boldsymbol{U}(s)$. There is also continuity of traction across the crack $[\mathbf{T} \cdot \mathbf{n}]_L = 0$ where $\mathbf{n}$ is normal to crack face.

Let $\boldsymbol{\sigma}^n$ be the solution to the following problem

$$\operatorname{div} \boldsymbol{\sigma}^n = 0 \tag{3.4}$$

in D and $\boldsymbol{\sigma}^n \mathbf{n}^b = 0$ on ∂D with $\mathbf{u}^n = (u^n, v^n)$ and

$$[u^n]_L = \delta(S - s) \tag{3.5}$$

along L with arclength coordinate S, and s is variable. And $\boldsymbol{\sigma}^t$ be the solution to the following problem

$$\text{div}\boldsymbol{\sigma}^t = 0 \tag{3.6}$$

in D and $\boldsymbol{\sigma}^t \mathbf{n}^b = 0$ on ∂D, with $\mathbf{u}^t = (u^t, v^t)$ and

$$[v^t]_L = \delta(S - s). \tag{3.7}$$

We can construct the solution with a prescribed jump in displacement across the crack by superposition of the Green's function solution weighted appropriately. By using Green's function methods we can write the traction components at the crack faces and displacement components on the crack faces as integrals of Green's functions weighted by displacement discontinuity along the crack. The traction components, decomposed into normal and tangential directions, are

$$T_n = \int \sigma_n^n U(s)\, ds + \int \sigma_n^t V(s)\, ds, \tag{3.8}$$

$$T_t = \int \sigma_t^n U(s)\, ds + \int \sigma_t^t V(s)\, ds. \tag{3.9}$$

The displacement components, decomposed into normal direction and tangential direction, are

$$u = \int u^n U(s) ds + \int u^t V(s) ds, \tag{3.10}$$

$$v = \int v^n U(s) ds + \int v^t V(s) ds. \tag{3.11}$$

The Green's functions σ_n^n, σ_n^t, σ_t^n, σ_t^t and u^n, u^t, v^n, v^t are solved from equations 3.1-3.3. Hence when the traction (T_n, T_t) is given, the displacement (u, v) will be solved.

3.2 Crack problem on infinite plane

A tear problem in an infinite plane is illustrated and solved analytically in this section. The plane strain problem has been described by the Airy stress function, and the displacements have been given by Slaughter [2002]. We use Fourier transform on the compatibility condition of the Airy stress function, then get the general solution of the ODEs. With

the boundary conditions and jump conditions we get the solutions of the ODEs for the specific crack problems. After we invert the Fourier transform, the Green's function for the integral equations, which describe the traction and displacement of the crack, are expressed. The tear problem is then solved. We will get the displacement as the traction is given.

3.2.1 Basic equations

Slaughter [2002] uses the the Airy stress function $\chi(x, y)$ to describe plane strain problems. The stress components are written in terms of χ via

$$\sigma_{xx} = \chi_{,yy} + \Omega, \quad \sigma_{yy} = \chi_{,xx} + \Omega \quad \text{and} \quad \sigma_{xy} = -\chi_{,xy}\,. \tag{3.12}$$

where Ω is the potential function for the body force. If the body force is homogeneous, the compatibility condition gives

$$\nabla^4 \chi \;\; = \;\; 0, \tag{3.13}$$

and the displacement components will be

$$2\mu u = -\chi_{,x} + \alpha\psi_{,y}\,, \quad 2\mu v = -\chi_{,y} + \alpha\psi_{,x}\,, \tag{3.14}$$

where $\psi(x, y)$ is a potential function that satisfies the conditions

$$\nabla^2 \psi = 0 \quad \text{and} \quad \psi_{,xy} = \nabla^2 \chi, \tag{3.15}$$

and $\alpha = 1 - \nu$ for plane strain, and $\alpha = \dfrac{1}{1+\nu}$ for plane stress.
Define the Fourier trasform $\mathcal{F}[f] = \hat{f}(g, y) = \int_{-\infty}^{\infty} f(x, y)e^{-igx}dx$ and inverse Fourier transform $f(x, y) = \frac{1}{2\pi}\int_{-\infty}^{\infty} \hat{f}(g, y)e^{igx}dg$. After applying the Fourier transform, the equation (3.13) changes to

$$\hat{\chi}_{yyyy} - 2g^2\hat{\chi}_{yy} + g^4\hat{\chi} = 0. \tag{3.16}$$

The general solution is

$$\hat{\chi}(y, g) = Ae^{gy} + Be^{-gy} + Cye^{gy} + Dye^{-gy}, \tag{3.17}$$

where A, B, C, D are constants connected with boundary conditions and jump conditions. Now we define region 2 as the region where $y \geq 0$, and region 1 as the region where $y \leq 0$.

Using $\chi \to 0$ as $y \to +\infty$ in region 2 we get

$$\begin{aligned} \hat{\chi}(y,g) &= A_2 e^{gy} + B_2 e^{-gy} + C_2 y e^{gy} + D_2 y e^{-gy}, && (3.18)\\ A_2 &= C_2 = 0 \quad \text{for} \quad g > 0, && (3.19)\\ B_2 &= D_2 = 0 \quad \text{for} \quad g < 0. && (3.20) \end{aligned}$$

Using $\chi \to 0$ as $y \to -\infty$ in region 1 we get

$$\begin{aligned} \hat{\chi}(y,g) &= A_1 e^{gy} + B_1 e^{-gy} + C_1 y e^{gy} + D_1 y e^{-gy}, && (3.21)\\ B_1 &= D_1 = 0 \quad \text{for} \quad g > 0, && (3.22)\\ A_1 &= C_1 = 0 \quad \text{for} \quad g < 0. && (3.23) \end{aligned}$$

After appling the Fourier transform, equations (3.15) become

$$\begin{aligned} \hat{\psi}_{yy} - g^2 \hat{\psi} &= 0, && (3.24)\\ ig\hat{\psi}_{,y} &= \hat{\chi}_{,yy} - g^2 \hat{\chi}, && (3.25) \end{aligned}$$

and the general solution for equation (3.24) is

$$\hat{\psi} = E e^{gy} + F e^{-gy}. \tag{3.26}$$

Substituting $\hat{\chi}$ and $\hat{\psi}$ into equation (3.25), we get

$$ig(Ege^{gy} - Fge^{-gy}) = 2gCe^{gy} - 2gDe^{-gy}. \tag{3.27}$$

Hence

$$E = -\frac{2C}{g} i, \quad F = -\frac{2D}{g} i, \quad \hat{\psi} = -\frac{2C}{g} i e^{gy} - \frac{2D}{g} i e^{-gy}. \tag{3.28}$$

After Fourier transformation, equations (3.12) and equations (3.14) become

$$\begin{aligned} \hat{\sigma}_{xx} &= \hat{\chi}_{,yy} \ , \quad \hat{\sigma}_{yy} = -g^2 \hat{\chi} \ , \quad \hat{\sigma}_{xy} = -ig\hat{\chi}_{,y} \ , && (3.29)\\ 2\mu\hat{u} &= -ig\hat{\chi} + \alpha\hat{\psi}_{,y} \ , \quad 2\mu\hat{v} = -\hat{\chi}_{,y} + ig\alpha\hat{\psi} \ . && (3.30) \end{aligned}$$

Substituting (3.17) and (3.28) into above equations we get

$$\begin{aligned} \hat{\sigma}_{xx} &= Ag^2 e^{gy} + Bg^2 e^{-gy} + gCe^{gy}(2+yg) + gDe^{-gy}(-2+yg), && (3.31)\\ \hat{\sigma}_{yy} &= -Ag^2 e^{gy} - Bg^2 e^{-gy} - g^2 Cy e^{gy} - g^2 Dy e^{-gy},\\ \hat{\sigma}_{xy} &= -Ag^2 ie^{gy} + Bg^2 ie^{-gy} - igC(1+yg)e^{gy} - igD(1-yg)e^{-gy},\\ 2\mu\hat{u} &= -igAe^{gy} - igBe^{-gy} - igCye^{gy} - igDye^{-gy} + \alpha(-2iCe^{gy} + 2iDe^{-gy}),\\ 2\mu\hat{v} &= Age^{gy} - Bge^{-gy} + C(1+yg)e^{gy} + D(1-yg)e^{-gy} + \alpha(2Ce^{gy} + 2De^{-gy}). \end{aligned}$$

3.2.2 Jump in v

Now assume the displacement discontinuity is only in the normal direction v and the crack is at $y = 0$ as shown in Figure 3.2. The jump conditions at $y = 0$ are

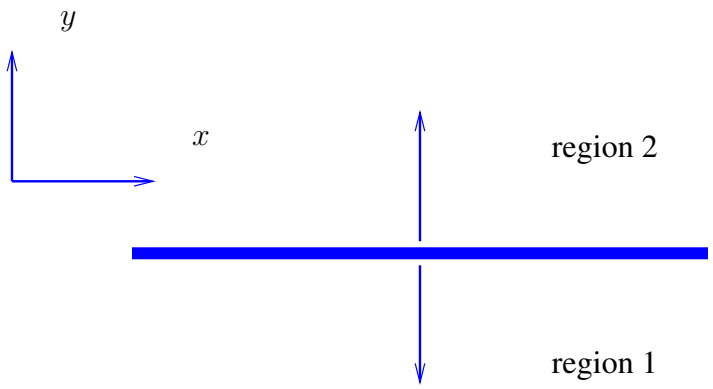

Figure 3.2: The displacement discontinuity in normal direction.

$$[v]^+_- = v_2 - v_1 = \delta(x), \quad [u]^+_- = u_2 - u_1 = 0, \quad [\sigma_{yy}]^+_- = \sigma^2_{yy} - \sigma^1_{yy} = 0, \quad [\sigma_{xy}]^+_- = \sigma^2_{xy} - \sigma^1_{xy} = 0, \tag{3.32}$$

and they are used to construct the Green's function referring to Lighthill [1958], which is used in (3.59) etc.. After Fourier transformation these equations become

$$[\hat{v}]^+_- = \hat{v}_2 - \hat{v}_1 = 1, \quad [\hat{u}]^+_- = \hat{u}_2 - \hat{u}_1 = 0, \quad [\hat{\sigma}_{yy}]^+_- = \hat{\sigma}^2_{yy} - \hat{\sigma}^1_{yy} = 0, \quad [\hat{\sigma}_{xy}]^+_- = \hat{\sigma}^2_{xy} - \hat{\sigma}^1_{xy} = 0. \tag{3.33}$$

By using (3.19), (3.22) and (3.31) in jump conditions (3.33), when $g > 0$ we have

$$\begin{aligned}
[-B_2 g + D_2 + 2\alpha D] - [A_1 g + C_1 + 2\alpha C_1] &= 2\mu, && (3.34)\\
[-igB_2 + 2\alpha i D_2] - [-igA_1 - 2\alpha i C_1] &= 0, && (3.35)\\
\left[-B_2 g^2\right] - \left[-A_1 g^2\right] &= 0, && (3.36)\\
\left[iB_2 g^2 - igD_2\right] - \left[-iA_1 g^2 - igC_1\right] &= 0. && (3.37)
\end{aligned}$$

Hence we obtain

$$\begin{aligned}
A_1 = \frac{2\mu}{4\alpha g}\ ,\ B_1 = 0\ ,\ C_1 = -\frac{2\mu}{4\alpha}\ ,\ D_1 = 0; \qquad (3.38)\\
A_2 = 0\ ,\ B_2 = \frac{2\mu}{4\alpha g}\ ,\ C_2 = 0\ ,\ D_2 = \frac{2\mu}{4\alpha}.
\end{aligned}$$

When $g < 0$ we have

$$A_1 = 0\ ,\ B_1 = -\frac{2\mu}{4\alpha g}\ ,\ C_1 = 0\ ,\ D_1 = -\frac{2\mu}{4\alpha}; \tag{3.39}$$
$$A_2 = -\frac{2\mu}{4\alpha g}\ ,\ B_2 = 0\ ,\ C_2 = \frac{2\mu}{4\alpha}\ ,\ D_2 = 0.$$

Put (3.38) and (3.39) into equations (3.31), and when $y \geq 0$ the inverse Fourier transform of σ^v_{yy} is

$$\begin{aligned}
\sigma^v_{yy} &= \frac{1}{2\pi}\int_{-\infty}^{\infty} e^{igx}\hat{\sigma}_{yy}(g,y)\,dg \\
&= \frac{1}{2\pi}\left[\int_{-\infty}^{0} e^{igx}\hat{\sigma}_{yy}(g,y)\,dg + \int_{0}^{\infty} e^{igx}\hat{\sigma}_{yy}(g,y)\,dg\right] \\
&= \frac{2\mu}{2\pi}\left[\int_{-\infty}^{0} e^{igx}\left(\frac{g}{4\alpha}e^{gy} - \frac{g^2y}{4\alpha}e^{gy}\right)dg - \int_{0}^{\infty} e^{igx}\left(\frac{g}{4\alpha}e^{-gy} + \frac{g^2y}{4\alpha}e^{-gy}\right)dg\right] \\
&= \frac{\mu}{4\pi\alpha}\left[\int_{-\infty}^{0} e^{g(ix+y)}(g - g^2y)dg - \int_{0}^{\infty} e^{g(ix-y)}(g + g^2y)dg\right] \\
&= \frac{1}{2}\frac{\mu\left(-x^4 - 6x^2y^2 + 3y^4\right)}{\pi\alpha\left(-ix^3 - 3yx^2 + 3iy^2x + y^3\right)\left(-ix^3 + 3yx^2 + 3ixy^2 - y^3\right)} \\
&= \frac{\mu(x^4 + 6x^2y^2 - 3y^4)}{2\pi\alpha(x^2+y^2)^3}
\end{aligned}$$

where the superscript 'v' means 'Jump in v'. When $y \leq 0$, $\sigma^v_{yy} = \dfrac{\mu(x^4 + 6x^2y^2 - 3y^4)}{2\pi\alpha(x^2+y^2)^3}$, and when $y = 0$, $\sigma^v_{yy} = \dfrac{\mu}{2\pi\alpha x^2}$.

When $y \geq 0$ the inverse Fourier transform of σ^v_{xy} is

$$\begin{aligned}
\sigma^v_{xy} &= \frac{1}{2\pi}\int_{-\infty}^{\infty} e^{igx}\hat{\sigma}_{xy}(g,y)\,dg \\
&= \frac{1}{2\pi}\left[\int_{-\infty}^{0} e^{igx}\hat{\sigma}_{xy}(g,y)\,dg + \int_{0}^{\infty} e^{igx}\hat{\sigma}_{xy}(g,y)\,dg\right] \\
&= \frac{2\mu}{2\pi}\left[\int_{-\infty}^{0} e^{igx}\left(\frac{ig}{4\alpha}e^{gy} - \frac{ig}{4\alpha}(1+yg)e^{gy}\right)dg + \int_{0}^{\infty} e^{igx}\left(\frac{ig}{4\alpha}e^{-gy} - \frac{ig}{4\alpha}(1-gy)e^{-gy}\right)dg\right] \\
&= -\frac{\mu yx\left(-x^2 + 3y^2\right)}{\pi\alpha\left(-ix^3 - 3yx^2 + 3iy^2x + y^3\right)\left(ix^3 - 3yx^2 - 3ixy^2 + y^3\right)} \\
&= \frac{\mu xy(x^2 - 3y)}{\pi\alpha(x^2+y^2)^3}
\end{aligned}$$

When $y \leq 0$ the inverse Fourier transform is

$$\sigma^v_{xy} = \frac{1}{2\pi}\int_{-\infty}^{\infty} e^{igx}\hat{\sigma}_{xy}(g,y)\,dg \tag{3.40}$$
$$= -\frac{\mu yx\left(x^2 - 3y^2\right)}{\pi\alpha\left(ix^3 - 3yx^2 - 3iy^2x + y^3\right)\left(ix^3 + 3yx^2 - 3ixy^2 - y^3\right)} \tag{3.41}$$
$$= -\frac{\mu xy(x^2 - 3y)}{\pi\alpha(x^2+y^2)^3} \tag{3.42}$$

and when $y = 0$, $\sigma^v_{xy} = 0$. It's straightforward to get u^v and v^v by the same way, and the superscript u means 'Jump in u'.

3.2.3 Jump in u

Now assume the displacement discontinuity is only in tangential direction and the crack is at $y = 0$. Jump conditions at $y = 0$ are

$$[v]^+_- = v_2 - v_1 = 0, \quad [u]^+_- = u_2 - u_1 = \delta(x), \quad [\sigma_{yy}]^+_- = \sigma^2_{yy} - \sigma^1_{yy} = 0, \quad [\sigma_{xy}]^+_- = \sigma^2_{xy} - \sigma^1_{xy} = 0. \tag{3.43}$$

After Fourier transform these equations become

$$[\hat{v}]^+_- = \hat{v}_2 - \hat{v}_1 = 0, \quad [\hat{u}]^+_- = \hat{u}_2 - \hat{u}_1 = 1, \quad [\hat{\sigma}_{yy}]^+_- = \hat{\sigma}^2_{yy} - \hat{\sigma}^1_{yy} = 0, \quad [\hat{\sigma}_{xy}]^+_- = \hat{\sigma}^2_{xy} - \hat{\sigma}^1_{xy} = 0. \tag{3.44}$$

We use (3.19), (3.22) and (3.31) in these jump condtions (3.33), when $g > 0$ we have

$$\begin{aligned}
[-B_2 g + D_2 + 2\alpha D] - [A_1 g + C_1 + 2\alpha C_1] &= 0, && (3.45)\\
[-igB_2 + 2\alpha i D_2] - [-igA_1 - 2\alpha i C_1] &= 2\mu, && (3.46)\\
\left[-B_2 g^2\right] - \left[-A_1 g^2\right] &= 0, && (3.47)\\
\left[iB_2 g^2 - igD_2\right] - \left[-iA_1 g^2 - igC_1\right] &= 0. && (3.48)
\end{aligned}$$

Hence we obtain

$$\begin{aligned}
A_1 = 0\ ,\ B_1 = 0\ ,\ C_1 = -\frac{i\mu}{2\alpha}\ ,\ D_1 = 0; \qquad (3.49)\\
A_2 = 0\ ,\ B_2 = 0\ ,\ C_2 = 0\ ,\ D_2 = -\frac{i\mu}{2\alpha}.
\end{aligned}$$

When $g < 0$ we have

$$\begin{aligned}
A_1 = 0\ ,\ B_1 = 0\ ,\ C_1 = 0\ ,\ D_1 = \frac{i\mu}{2\alpha}; \qquad (3.50)\\
A_2 = -0\ ,\ B_2 = 0\ ,\ C_2 = \frac{i\mu}{2\alpha}\ ,\ D_2 = 0.
\end{aligned}$$

Put (3.49) and (3.50) into equations (3.31), when $y \geq 0$ the inverse Fourier transform of $\hat{\sigma}^u_{yy}$ is

$$\begin{aligned}
\sigma^u_{yy} &= \frac{1}{2\pi}\int_{-\infty}^{\infty} e^{igx}\hat{\sigma}_{yy}(g,y)\,dg && (3.51)\\
&= \frac{1}{2\pi}\left[\int_{-\infty}^{0} e^{igx}\hat{\sigma}_{yy}(g,y)\,dg + \int_{0}^{\infty} e^{igx}\hat{\sigma}_{yy}(g,y)\,dg\right] && (3.52)\\
&= -\frac{\mu y x\left(-x^2+3y^2\right)}{\pi\alpha\left(-ix^3-3yx^2+3iy^2x+y^3\right)\left(ix^3-3yx^2-3ixy^2+y^3\right)} && (3.53)\\
&= \frac{\mu x y(x^2-3y)}{\pi\alpha(x^2+y^2)^3}. && (3.54)
\end{aligned}$$

When $y \leq 0$ the inverse Fourier transform of σ^u_{yy} is

$$\begin{aligned} \sigma^u_{yy} &= \frac{1}{2\pi}\int_{-\infty}^{\infty} e^{igx}\hat{\sigma}_{yy}(g,y)\,dg & (3.55)\\ &= -\frac{\mu yx\left(x^2-3y^2\right)}{\pi\alpha\left(ix^3-3yx^2-3iy^2x+y^3\right)\left(ix^3+3yx^2-3ixy^2-y^3\right)} & (3.56)\\ &= -\frac{\mu xy(x^2-3y)}{\pi\alpha(x^2+y^2)^3}. & (3.57)\end{aligned}$$

When $y=0$ the stress component $\sigma^u_{yy}=0$. For all y the inverse Fourier transform of σ^u_{xy} is

$$\sigma^u_{xy} = \frac{\mu(x^4+6x^2y^2-3y^4)}{2\pi\alpha(x^2+y^2)^3}. \quad (3.58)$$

When $y=0$ the stress component $\sigma^u_{xy}=\dfrac{\mu}{2\pi\alpha x^2}$. It's straightforward to get u^u and v^u by the same way.

3.2.4 Integral equation

The traction components, decomposed into normal and tangential direction, are

$$\begin{aligned} T_y &= \int \sigma^u_{yy}(x-s,y)U(s)\,ds + \int \sigma^v_{yy}(x-s,y)V(s)\,ds,\\ T_x &= \int \sigma^u_{xy}(x-s,y)U(s)\,ds + \int \sigma^v_{xy}(x-s,y)V(s)\,ds. \quad (3.59)\end{aligned}$$

The displacement components, decomposed into normal and tangential direction, are

$$\begin{aligned} u &= \int u^u(x-s,r)U(s)ds + \int u^v(x-s,r)V(s)ds\\ v &= \int v^u(x-s,r)U(s)ds + \int v^v(x-s,r)V(s)ds \quad (3.60)\end{aligned}$$

The value of $\sigma^u_{yy},\sigma^v_{yy},\sigma^u_{xy},\sigma^v_{xy}$ and u^u,u^v,v^u,v^v are known. Hence if the traction (T_x,T_y) along the crack is given, we can calculate the displacement (u,v).

When $y=0$ and we assume the crack is along the interval $-\frac{L}{2}\leq x\leq\frac{L}{2}$,

$$\begin{aligned} \mathrm{T}_y &= 0+\int_{-\frac{L}{2}}^{\frac{L}{2}} \frac{\mu V(s)}{2\pi\alpha(x-s)^2}ds & (3.61)\\ \mathrm{T}_x &= \int_{-\frac{L}{2}}^{\frac{L}{2}} \frac{\mu U(s)}{2\pi\alpha(x-s)^2}ds+0, & (3.62)\end{aligned}$$

for the plane strain problem

$$\int_{-\frac{L}{2}}^{\frac{L}{2}} \frac{\mu U(s)}{2\pi\alpha(x-s)^2}ds = \frac{\mu}{2\pi\,(1-v)}\int_{-\frac{L}{2}}^{\frac{L}{2}} \frac{U(s)}{(x-s)^2}ds \tag{3.63}$$

$$= \frac{E}{4\pi\,(1-v^2)}\int_{-\frac{L}{2}}^{\frac{L}{2}} \frac{U(s)}{(x-s)^2}ds, \tag{3.64}$$

$$\int_{-\frac{L}{2}}^{\frac{L}{2}} \frac{\mu V(s)}{2\pi\alpha(x-s)^2}ds = \frac{E}{4\pi\,(1-v^2)}\int_{-\frac{L}{2}}^{\frac{L}{2}} \frac{V(s)}{(x-s)^2}ds \tag{3.65}$$

where the integral $\int_{-\frac{L}{2}}^{\frac{L}{2}} \frac{V(s)}{(x-s)^2}ds$ is Hadamard integral, and

$$E = \frac{\mu(3\lambda+2\mu)}{\lambda+\mu}, \nu = \frac{\lambda}{2(\lambda+\mu)}, 1+\nu = \frac{3\lambda+2\mu}{2(\lambda+\mu)}, \mu = \frac{E}{2(1+\nu)}. \tag{3.66}$$

Hence when (T_x, T_y) in (3.59) along the crack is given, the value of $(U(s), V(s))$ is solved by inversion of the integral equation. Then the displacement (u, v) in (3.60) will be obtained.

3.3 Static tears in 2D strip—linear elasticity for 2D plane cracks

We illustrate the crack problem in a 2D strip, which is closer than the crack problem in an infinite plane to our aim to solve the crack problem in an elastic tube. We try to use analytical approach to solve it in this section, but find that the Fourier inversions can not be performed analytically. Then we use numerical approach to solve it in next section.

3.3.1 Method for crack problem in a 2D strip

The crack is decomposed into normal direction (jump in u) and tangential direction (jump in v) as shown in Figure 3.3 .

The jump conditions on the crack surface are

$$u_2 - u_1 = 0, \quad v_2 - v_1 = \delta(x), \quad \sigma^2_{xy} - \sigma^1_{xy} = 0, \quad \sigma^2_{yy} - \sigma^1_{yy} = 0 \quad \text{for jump in } v \tag{3.67}$$

$$u_2 - u_1 = \delta(x), \quad v_2 - v_1 = 0, \quad \sigma^2_{xy} - \sigma^1_{xy} = 0, \quad \sigma^2_{yy} - \sigma^1_{yy} = 0 \quad \text{for jump in } u \tag{3.68}$$

with boundary condition (3.2) on $y = \pm h$ and equilibrium equation (3.1).

Following are the details of the methods to solve the equilibrium equations with boundary and jump conditions. Firstly, the strain tensor $\boldsymbol{\varepsilon}$ and stress tensor $\boldsymbol{\sigma}$ are the functions

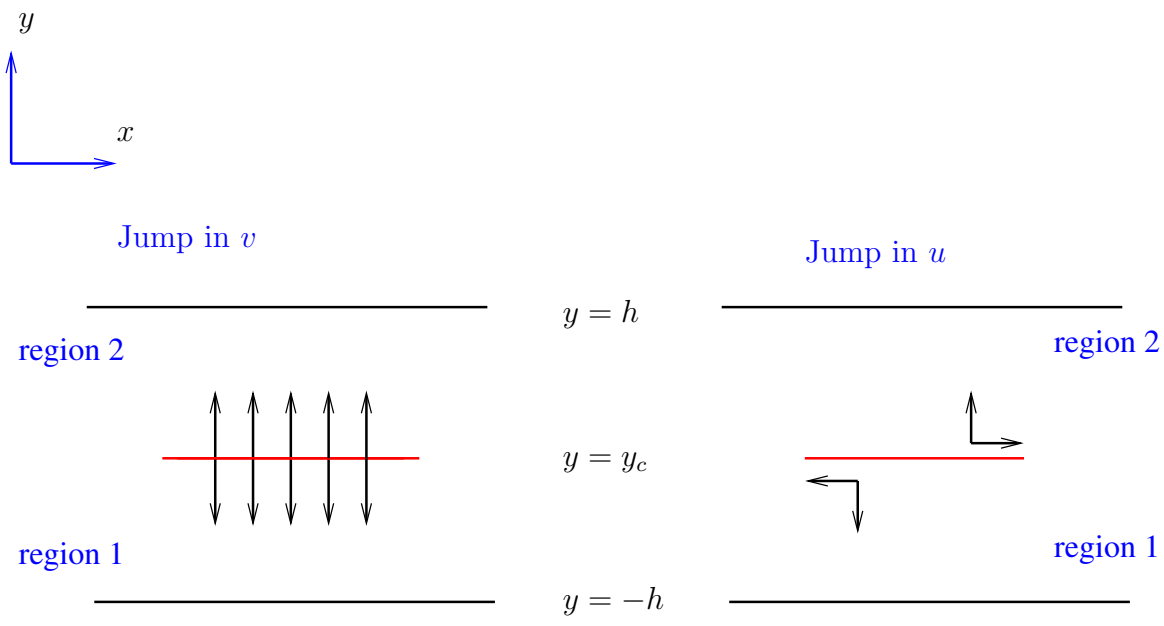

Figure 3.3: The crack is decomposed into normal and tangential direction.

of displacements u^u, w^u or u^w, w^w. Write the equilibrium equations $\operatorname{div} \boldsymbol{\sigma} = 0$ into components to obtain two partial differentiation equations with variables u^u, w^u or u^w, w^w; secondly, taking the Fourier transform to change these PDEs to ODEs with the wave number g and the variables are $\hat{u}^u, \hat{w}^u$ or $\hat{u}^w, \hat{w}^w$; thirdly, solving these ODEs with boundary conditions and jump conditions by using analytical way or numerical way; finally, taking the inverse Fourier transform to obtain the solution for PDEs. The Cauchy stress $\boldsymbol{\sigma}$ is the functions of displacements u^u, w^u or u^w, w^w, hence when u^u, w^u and u^w, w^w are solved σ^u_{rz}, σ^w_{rr} and σ^u_{rz}, σ^w_{rr} will be obtained.

By solving these equations for 'Jump in u' we get σ^u_{yy}, σ^u_{xy}, u^u, v^u, and solving them for 'Jump in v' we obtain σ^v_{yy}, σ^v_{xy}, u^v, v^v. Where the superscript 'u' means 'Jump in u', and 'v' means 'Jump in v'.

In the 2D strip the traction components are described as

$$T_y = \int \sigma^u_{yy}(x-s,y)U(s)\,ds + \int \sigma^v_{yy}(x-s,y)V(s)\,ds, \tag{3.69}$$

$$T_x = \int \sigma^u_{xy}(x-s,y)U(s)\,ds + \int \sigma^v_{xy}(x-s,y)V(s)\,ds. \tag{3.70}$$

Displacements, decomposed into normal and tangential direction, are

$$u = \int u^u(x-s,y)U(s)ds + \int u^v(x-s,y)V(s)ds \tag{3.71}$$

$$v = \int v^u(x-s,y)U(s)ds + \int v^v(x-s,y)V(s)ds \tag{3.72}$$

Hence if the traction $(\mathrm{T}_y, \mathrm{T}_x)$ along the crack is given $(U(s), V(s))$ will be calculated, then the displacement (u, v) will be obtained. We use this method to calculate the displacements for the upper crack face, lower crack face, outer boundary layer and inner boundary layer. Then plot them on one figure to get the crack profile.

3.3.2 Basic 2D plane crack problem

Consider the 2D problem of a crack in a linear elastic material occupying a strip $-h \leq y \leq h$ in plane strain. The coordinate system is (x, y) and the displacements in the coordinate directions are (u, v). The components of the Cauchy stress are σ_{yy} and σ_{xy}. The crack is located along the line $y = y_c$. The strain tensor is

$$\boldsymbol{\varepsilon} = \begin{bmatrix} \dfrac{\partial u(x,y)}{\partial x} & \dfrac{1}{2}\dfrac{\partial u(x,y)}{\partial y} + \dfrac{1}{2}\dfrac{\partial v(x,y)}{\partial x} \\ \frac{1}{2}\dfrac{\partial u(x,y)}{\partial y} + \dfrac{1}{2}\dfrac{\partial v(x,y)}{\partial x} & \dfrac{\partial v(x,y)}{\partial y} \end{bmatrix}, \tag{3.73}$$

The constitutive law is

$$\boldsymbol{\sigma} = \lambda \mathrm{tr}\left(\boldsymbol{\varepsilon}\right) \boldsymbol{I} + 2\mu\boldsymbol{\varepsilon}. \tag{3.74}$$

The stress tensor is

$$\boldsymbol{\sigma} = \begin{bmatrix} \left(\lambda + 2\mu\right) \dfrac{\partial u(x,y)}{\partial x} + \lambda \dfrac{\partial v(x,y)}{\partial y} & \mu \dfrac{\partial u(x,y)}{\partial y} + \mu \dfrac{\partial v(x,y)}{\partial x} \\ \mu \dfrac{\partial u(x,y)}{\partial y} + \mu \dfrac{\partial v(x,y)}{\partial x} & \left(\lambda + 2\mu\right) \dfrac{\partial v(x,y)}{\partial y} + \lambda \dfrac{\partial v(x,y)}{\partial y} \end{bmatrix}. \tag{3.75}$$

The Poisson's ratio

$$\nu = \frac{\lambda}{2\left(\lambda + \mu\right)} \tag{3.76}$$

so that $\lambda = \frac{2\nu}{1-2\nu}\mu$ and $\lambda + 2\mu = \frac{2-2\nu}{1-2\nu}\mu$. Hence (λ, μ) are replaced by (λ, ν)

$$\sigma_{xx} = \left(\lambda + 2\mu\right) u_{,x} + \lambda v_{,y} = \frac{2\mu}{1-2\nu}\left[\left(1-\nu\right) u_{,x} + \nu v_{,y}\right] \tag{3.77}$$

$$\sigma_{xy} = 2\mu\left(\frac{v_{,x} + u_{,y}}{2}\right) \tag{3.78}$$

$$\sigma_{yy} = \left(\lambda + 2\mu\right) v_{,y} + \lambda u_{,y} = \frac{2\mu}{1-2\nu}\left[\left(1-\nu\right) v_{,y} + \nu u_{,x}\right] \tag{3.79}$$

The equilibrium for Cauchy stress is

$$\mathrm{div}\boldsymbol{\sigma} = 0, \tag{3.80}$$

and the boundary conditions are

$$\sigma_{yy} = 0 \quad \text{at} \quad y = \pm h, \tag{3.81}$$

$$\sigma_{xy} = 0 \quad \text{at} \quad y = \pm h. \tag{3.82}$$

The jump conditions on crack surface $y = y_c$ are (3.68) and (3.67). Write the equilibrium equation (3.80) into components and use Fourier transformation on these equations

$$ig\frac{d\hat{v}(y)}{dy} + (1-2\nu)\frac{d^2\hat{u}(y)}{dy^2} - 2g^2(1-\nu)\hat{u}(y) = 0, \tag{3.83}$$

$$ig\frac{d\hat{u}(y)}{dy} + 2(1-\nu)\frac{d^2\hat{v}(y)}{dy^2} - \hat{v}(y)g^2(1-2\nu) = 0. \tag{3.84}$$

where $\hat{u}(y) = \int_{-\infty}^{\infty} u(x,y)e^{-igx}dx$ and $\hat{v}(y) = \int_{-\infty}^{\infty} v(x,y)e^{-igx}dx$. The general solution for these two equations is

$$\hat{v}(y) = Ae^{-gy} + Be^{-gy}y + Ce^{gy} + De^{gy}y \tag{3.85}$$

and

$$\hat{u}(y) = -\frac{i}{g}\left(4\nu Be^{-gy} + 4\nu De^{gy} + Age^{-gy} + Bge^{-gy}y - 3Be^{-gy} - Cge^{gy} - Dge^{gy}y - 3De^{gy}\right), \tag{3.86}$$

where A, B, C, D are constants connected to boundary conditions and jump conditions.

Now assume the traction is in normal direction, which is the 'Jump in v' in Figure 3.3 and $h = 1$ and $y_c = 0$ are given. The boundary conditions (3.81) and (3.82) after transform are

$$\hat{\sigma}_{yy} = 0 \quad \text{at} \quad y = \pm 1, \tag{3.87}$$

$$\hat{\sigma}_{xy} = 0 \quad \text{at} \quad y = \pm 1. \tag{3.88}$$

where $\hat{\sigma}_{yy} = \int_{-\infty}^{\infty} \sigma_{yy}(x,y)e^{-igx}dx$ and $\hat{\sigma}_{xy} = \int_{-\infty}^{\infty} \sigma_{xy}(x,y)e^{-igx}dx$.
The jump conditions (3.67) after Fourier transformation are

$$\hat{u}_2 - \hat{u}_1 = 0, \quad \hat{v}_2 - \hat{v}_1 = 1, \quad \hat{\sigma}^2_{yy} - \hat{\sigma}^1_{yy} = 0, \quad \hat{\sigma}^2_{xy} - \hat{\sigma}^1_{xy} = 0 \quad \text{at} \quad y = 0 \tag{3.89}$$

where subscript or superscript '1' means region 1, and '2' means region 2.

Put the solutions (3.164) and (5.82) into these boundary conditions and jump conditions

we obtain the constants $A_1, A_2, B_1, B_2, C_1, C_2, D_1, D_2$.

$$A_1 = \frac{1}{2}\frac{\left(g^2e^g - 2\,\nu\,ge^g + 2\,ge^g + e^g - \nu\,e^g - e^{-g} + \nu\,e^{-g}\right)e^{-g}}{\nu\,\left(e^g\right)^2 - \left(e^g\right)^2 + 4\,e^{-g}ge^g\nu - 4\,e^{-g}ge^g + \left(e^{-g}\right)^2 - \left(e^{-g}\right)^2\nu}, \tag{3.90}$$

$$B_1 = \frac{1}{4}\frac{\left(2\,ge^g + e^g - e^{-g}\right)ge^{-g}}{\nu\,\left(e^g\right)^2 - \left(e^g\right)^2 + 4\,e^{-g}ge^g\nu - 4\,e^{-g}ge^g + \left(e^{-g}\right)^2 - \left(e^{-g}\right)^2\nu}, \tag{3.91}$$

$$C_1 = -\frac{1}{2}\frac{e^g\left(2\,\nu\,ge^{-g} + \nu\,e^g - \nu\,e^{-g} + g^2e^{-g} - 2\,ge^{-g} - e^g + e^{-g}\right)}{\nu\,\left(e^g\right)^2 - \left(e^g\right)^2 + 4\,e^{-g}ge^g\nu - 4\,e^{-g}ge^g + \left(e^{-g}\right)^2 - \left(e^{-g}\right)^2\nu}, \tag{3.92}$$

$$D_1 = -1/4\,\frac{ge^g\left(2\,ge^{-g} + e^g - e^{-g}\right)}{\nu\,\left(e^g\right)^2 - \left(e^g\right)^2 + 4\,e^{-g}ge^g\nu - 4\,e^{-g}ge^g + \left(e^{-g}\right)^2 - \left(e^{-g}\right)^2\nu}, \tag{3.93}$$

$$A_2 = \frac{1}{2}\frac{e^g\left(2\,\nu\,ge^{-g} + \nu\,e^g - \nu\,e^{-g} + g^2e^{-g} - 2\,ge^{-g} - e^g + e^{-g}\right)}{\nu\,\left(e^g\right)^2 - \left(e^g\right)^2 + 4\,e^{-g}ge^g\nu - 4\,e^{-g}ge^g + \left(e^{-g}\right)^2 - \left(e^{-g}\right)^2\nu}, \tag{3.94}$$

$$B_2 = -\frac{1}{4}\frac{ge^g\left(2\,ge^{-g} + e^g - e^{-g}\right)}{\nu\,\left(e^g\right)^2 - \left(e^g\right)^2 + 4\,e^{-g}ge^g\nu - 4\,e^{-g}ge^g + \left(e^{-g}\right)^2 - \left(e^{-g}\right)^2\nu}, \tag{3.95}$$

$$C_2 = -\frac{1}{2}\frac{\left(g^2e^g - 2\,\nu\,ge^g + 2\,ge^g + e^g - \nu\,e^g - e^{-g} + \nu\,e^{-g}\right)e^{-g}}{\nu\,\left(e^g\right)^2 - \left(e^g\right)^2 + 4\,e^{-g}ge^g\nu - 4\,e^{-g}ge^g + \left(e^{-g}\right)^2 - \left(e^{-g}\right)^2\nu}, \tag{3.96}$$

$$D_2 = \frac{1}{4}\frac{\left(2\,ge^g + e^g - e^{-g}\right)ge^{-g}}{\nu\,\left(e^g\right)^2 - \left(e^g\right)^2 + 4\,e^{-g}ge^g\nu - 4\,e^{-g}ge^g + \left(e^{-g}\right)^2 - \left(e^{-g}\right)^2\nu}. \tag{3.97}$$

3.3.3 The Fourier transform is unbounded as g increasing

In region 2

$$\begin{aligned}\hat{\sigma}_{yy}\left(g,y\right) &= \frac{1}{4}\frac{\left(2\,g^2e^{-gy}y + 2\,g^2e^{gy}y + 2\,e^{-gy}g - 2\,e^{gy}g - 2\,e^{-gy}g^2 - 2\,e^{gy}g^2 + e^{-g(-2+y)}\right)g}{\nu\,e^{2\,g} - e^{2\,g} + 4\,\nu\,g - 4\,g + e^{-2\,g} - e^{-2\,g}\nu} \\ &+ \frac{1}{4}\frac{\left(-e^{-gy} - e^{gy} + e^{g(-2+y)} + ge^{-g(-2+y)}y - ge^{-gy}y + ge^{gy}y - ge^{g(-2+y)}y\right)g}{\nu\,e^{2\,g} - e^{2\,g} + 4\,\nu\,g - 4\,g + e^{-2\,g} - e^{-2\,g}\nu}\end{aligned}$$

If we let y tends to 0, we find $\hat{\sigma}_{yy}$ is divergent when g increases, which means this can not be inverted by inverse Fourier transform $\frac{1}{2\pi}\int_{-\infty}^{\infty}\hat{\sigma}_{yy}e^{igx}dg$.

The behaviours of $\hat{\sigma}_{yy}\left(g,y\right)$ and $\hat{\sigma}_{xy}\left(g,y\right)$ as g gets large lead us to consider a decomposition of the form

$$\hat{\sigma}_{yy}\left(g,y\right) = \sigma^1_{yy}g + \sigma^0_{yy} + \tilde{\sigma}_{yy}, \tag{3.98}$$

which makes $\left(\hat{\sigma}_{yy}\left(g,y\right) - \sigma^1_{yy}g\right) \to 0$ or $\left(\hat{\sigma}_{yy}\left(g,y\right) - \sigma^1_{yy}g - \sigma^0_{yy}\right) \to 0$ invertible.

In the future section, we will introduce a numerical approach to solve these equilibrium equations, and we will use the decomposition and invert them numerically.

3.3.4 Useful results

The following results

$$\lim_{y\to 0^+}\frac{1}{\pi}\int_0^\infty ge^{-gy}\cos gx\,dg = -\frac{1}{\pi x^2}, \tag{3.99}$$

$$\lim_{y\to 0^+}\frac{1}{\pi}\int_0^\infty e^{-gy}\cos gx\,dg = \delta(x), \tag{3.100}$$

$$\lim_{y\to 0^+}\frac{1}{\pi}\int_0^\infty ge^{-gy}\sin gx\,dg = -\delta'(x), \tag{3.101}$$

$$\lim_{y\to 0^+}\frac{1}{\pi}\int_0^\infty e^{-gy}\sin gx\,dg = \frac{1}{\pi x}, \tag{3.102}$$

are useful for the calculation in the future sections.

3.4 Solution for the compressible plane crack problem in a 2D strip

In this section we are going to solve the plane crack problem in a compressible 2D strip numerically. We consider the crack decomposed into normal and tangential direction as shown in Figure 3.3.

3.4.1 Fourier transformation

The Fourier transform and inverse Fourier transform in the x direction are defined as

$$\mathcal{F}[f] = \hat{f}(g,y) = \int_{-\infty}^{\infty} f(x,y)e^{-igx}dx, \tag{3.103}$$

$$\mathcal{F}^{-1}[\hat{f}] = f(x,y) = \frac{1}{2\pi}\int_{-\infty}^{\infty}\hat{f}(g,y)e^{igx}dg. \tag{3.104}$$

If $f(-x,y) = -f(x,y)$

$$\mathcal{F}_s[f] = \hat{f}(g,y) = -2i\int_0^\infty f(x,y)\sin(gx)dx, \tag{3.105}$$

and $\hat{f}(-g,y) = -\hat{f}(g,y)$ leads to

$$\mathcal{F}_s^{-1}[\hat{f}] = f(x,y) = \frac{i}{\pi}\int_0^\infty \hat{f}(g,y)\sin(gx)dg. \tag{3.106}$$

If $f(-x,y) = f(x,y)$

$$\mathcal{F}_c[f] = \hat{f}(g,y) = 2\int_0^\infty f(x,y)\cos(gx)dx, \tag{3.107}$$

and $\hat{f}(-g,y) = -\hat{f}(g,y)$ leads to

$$\mathcal{F}_c^{-1}[\hat{f}] = f(x,y) = \frac{1}{\pi}\int_0^\infty \hat{f}(g,y)\cos(gx)dg. \tag{3.108}$$

The derivative of these equations are

$$\mathcal{F}[f_{,x}] = \int_{-\infty}^{\infty} f(x,y)_{,x}\, e^{-igx}dx = ig\mathcal{F}[f(x,y)] = ig\hat{f}(g,y) \tag{3.109}$$

$$\mathcal{F}[f_{,y}] = \int_{-\infty}^{\infty} f(x,y)_{,y}\, e^{-igx}dx = \hat{f}(g,y)_{,y} \tag{3.110}$$

$$\mathcal{F}[f_{,xy}] = \int_{-\infty}^{\infty} f(x,y)_{,xy}\, e^{-igx}dx = ig\hat{f}(g,y)_{,y} \tag{3.111}$$

$$\mathcal{F}[f_{,xx}] = \int_{-\infty}^{\infty} f(x,y)_{,xx}\, e^{-igx}dx = -g^2\mathcal{F}[f(x,y)] = -g^2\hat{f}(g,y) \tag{3.112}$$

$$\mathcal{F}[f_{,yy}] = \int_{-\infty}^{\infty} f(x,y)_{,yy}\, e^{-igx}dx = \hat{f}(g,y)_{,yy} \tag{3.113}$$

3.4.2 Jump in v across the crack

The symmetry of the problem gives $u(-x,y) = -u(x,y)$, then the Fourier and inverse transformation for the displacement u are

$$\hat{u}(g,y) = \mathcal{F}_s[u] = -2i\int_0^\infty u(x,y)\sin(gx)dx, \tag{3.114}$$

$$u(x,y) = \mathcal{F}_s^{-1}[\hat{u}] = \frac{i}{\pi}\int_0^\infty \hat{u}(g,y)\sin(gx)dg. \tag{3.115}$$

Since $v(-x,y) = v(x,y)$ the Fourier and inverse transformation for displacement v are

$$\hat{v}(g,y) = \mathcal{F}_c[v] = 2\int_0^\infty v(x,y)\cos(gx)dx, \tag{3.116}$$

$$v(x,y) = \mathcal{F}_c^{-1}[\hat{v}] = \frac{1}{\pi}\int_0^\infty \hat{v}(g,y)\cos(gx)dg. \tag{3.117}$$

The stress σ_{xx} is given by

$$\sigma_{xx} = \frac{2\mu}{1-2\nu}\left[(1-\nu)\,u_{,x} + \nu v_{,y}\right], \tag{3.118}$$

where

$$u_{,x}(x,y) = \frac{i}{\pi}\int_0^\infty \hat{u}(g,y)g\cos(gx)dg \quad \text{and} \quad v_{,y}(x,y) = \frac{1}{\pi}\int_0^\infty \hat{v}_{,y}(g,y)\cos(gx)dg. \tag{3.119}$$

Hence

$$\sigma_{xx} = \frac{2\mu}{1-2\nu}\frac{1}{\pi}\int_0^\infty \left((1-\nu)\,ig\hat{u} + \nu\hat{v}_{,y}\right)\cos(gx)dg \tag{3.120}$$

$$= \frac{2\mu}{1-2\nu}\frac{1}{\pi}\int_0^\infty \left((1-\nu)\,\mathcal{F}[u_{,x}] + \nu\mathcal{F}[v_{,y}]\right)\cos(gx)dg \tag{3.121}$$

$$= \frac{1}{\pi}\int_0^\infty \mathcal{F}[\sigma_{xx}]\cos(gx)dg = \frac{1}{\pi}\int_0^\infty \hat{\sigma}_{xx}(g,y)\cos(gx)dg. \tag{3.122}$$

The stress σ_{xy} is the function

$$\sigma_{xy} \quad = \quad \mu\left(v_{,x}+u_{,y}\right), \tag{3.123}$$

where

$$v_{,x}\left(x,y\right)=-\frac{1}{\pi}\int_0^\infty \hat{v}(g,y)g\sin(gx)dg \quad \text{and} \quad u_{,y}\left(x,y\right)=\frac{i}{\pi}\int_0^\infty \hat{u}_{,y}\left(g,y\right)\sin(gx)dg. \tag{3.124}$$

Hence

$$\begin{aligned}
\sigma_{xy} &= \frac{\mu}{\pi}\int_0^\infty \left(-\hat{v}(g,y)g+i\hat{u}_{,y}\left(g,y\right)\right)\sin(gx)dg && (3.125)\\
&= \frac{\mu}{\pi}\int_0^\infty \left(i\mathcal{F}[v_{,x}\,]+i\mathcal{F}[u_{,y}\,]\right)\sin(gx)dg && (3.126)\\
&= \frac{i}{\pi}\int_0^\infty \mathcal{F}[\sigma_{xy}]\sin(gx)dg=\frac{i}{\pi}\int_0^\infty \hat{\sigma}_{xy}\left(g,y\right)\sin(gx)dg. && (3.127)
\end{aligned}$$

Using the symmetry of the domain in x, we express the displacements and the stresses as

$$\begin{aligned}
u\left(x,y\right)&=\frac{i}{\pi}\int_0^\infty \hat{u}\left(g,y\right)\sin(gx)\,dg=\frac{1}{\pi}\int_0^\infty \hat{U}^v\left(g,y\right)\sin(gx)\,dg,\\
v\left(x,y\right)&=\frac{1}{\pi}\int_0^\infty \hat{v}\left(g,y\right)\cos(gx)\,dg=\frac{1}{\pi}\int_0^\infty \hat{V}^v\left(g,y\right)\cos(gx)\,dg,\\
\sigma_{yy}\left(x,y\right)&=\frac{1}{\pi}\int_0^\infty \hat{\sigma}_{yy}\left(g,y\right)\cos(gx)\,dg=\frac{1}{\pi}\int_0^\infty \hat{\sigma}^v_{yy}\left(g,y\right)\cos(gx)\,dg,\\
\sigma_{xx}\left(x,y\right)&=\frac{1}{\pi}\int_0^\infty \hat{\sigma}_{xx}\left(g,y\right)\cos(gx)\,dg=\frac{1}{\pi}\int_0^\infty \hat{\sigma}^v_{xx}\left(g,y\right)\cos(gx)\,dg,\\
\sigma_{xy}\left(x,y\right)&=\frac{i}{\pi}\int_0^\infty \hat{\sigma}_{xy}\left(g,y\right)\sin(gx)\,dg=\frac{1}{\pi}\int_0^\infty \hat{\sigma}^v_{xy}\left(g,y\right)\sin(gx)\,dg,
\end{aligned} \tag{3.128}$$

with the definition

$$\hat{U}^v=i\hat{u},\quad \hat{V}^v=\hat{v},\quad \hat{\sigma}^v_{xx}=\hat{\sigma}_{xx},\quad \hat{\sigma}^v_{yy}=\hat{\sigma}_{yy},\quad \hat{\sigma}^v_{xy}=i\hat{\sigma}_{xy}. \tag{3.129}$$

Fourier transform on the equilibrium equation $\mathrm{div}\boldsymbol{\sigma}=0$ are

$$\mathcal{F}[\sigma_{xx,x}]+\mathcal{F}[\sigma_{xy,y}]=0, \tag{3.130}$$

$$\mathcal{F}[\sigma_{xy,x}]+\mathcal{F}[\sigma_{yy,y}]=0. \tag{3.131}$$

Using the relations (3.77-3.79) between the stresses and the displacements we get the equilibrium equations in terms of $\hat{U}^v$ and $\hat{V}^v$

$$\left(1-2\nu\right)\left(\hat{U}^v\right)''-2g^2\left(1-\nu\right)\hat{U}^v-g\left(\hat{V}^v\right)'=0, \tag{3.132}$$

$$2\left(1-\nu\right)\left(\hat{V}^v\right)''-g^2\left(1-2\nu\right)\hat{V}^v+g\left(\hat{U}^v\right)'=0. \tag{3.133}$$

The boundary conditions at $y = \pm h$ are $\hat{\sigma}^v_{yy} = 0$ and $\hat{\sigma}^v_{xy} = 0$, which translate to

$$\left(\hat{U}^v\right)' - g\hat{V}^v = 0 \qquad (1-\nu)\left(\hat{V}^v\right)' + \nu g\hat{U}^v = 0. \tag{3.134}$$

The jump conditions across the crack at $y = y_c$ are

$$\left[\hat{U}^v\right]^+_- = 0, \qquad \left[\hat{V}^v\right]^+_- = 1, \qquad \left[\hat{\sigma}^v_{yy}\right]^+_- = \left[\hat{\sigma}^v_{xy}\right]^+_- = 0. \tag{3.135}$$

3.4.3 Jump in u across the crack

The symmetry of the problem gives $v(-x, y) = -v(x, y)$, then the Fourier and inverse transformation for displacement v are

$$\hat{v}(g, y) = \mathcal{F}_s[v] = -2i\int_0^\infty v(x, y)\sin(gx)dx, \tag{3.136}$$

$$v(x, y) = \mathcal{F}_s^{-1}[\hat{v}] = \frac{i}{\pi}\int_0^\infty \hat{v}(g, y)\sin(gx)dg. \tag{3.137}$$

Since $u(-x, y) = u(x, y)$ the Fourier and inverse transformation for displacement u are

$$\hat{u}(g, y) = \mathcal{F}_c[u] = 2\int_0^\infty u(x, y)\cos(gx)dx, \tag{3.138}$$

$$u(x, y) = \mathcal{F}_c^{-1}[\hat{u}] = \frac{1}{\pi}\int_0^\infty \hat{u}(g, y)\cos(gx)dg. \tag{3.139}$$

The stress σ_{xx} is the function of displacements

$$\sigma_{xx} = \frac{2\mu}{1-2\nu}\left[(1-\nu)\,u_{,x} + \nu v_{,y}\right], \tag{3.140}$$

where

$$u_{,x}(x, y) = -\frac{1}{\pi}\int_0^\infty \hat{u}(g, y)g\sin(gx)dg \quad \text{and} \quad v_{,y}(x, y) = \frac{i}{\pi}\int_0^\infty \hat{v}_{,y}(g, y)\sin(gx)dg.$$

Hence

$$\sigma_{xx} = \frac{2\mu}{1-2\nu}\frac{1}{\pi}\int_0^\infty \left[-(1-\nu)\,g\hat{u} + i\nu\hat{v}_{,y}\right]\sin(gx)dg \tag{3.141}$$

$$= \frac{2\mu}{1-2\nu}\frac{1}{\pi}\int_0^\infty \left[(1-\nu)\,i\mathcal{F}[u_{,x}] + \nu i\mathcal{F}[v_{,y}]\right]\sin(gx)dg \tag{3.142}$$

$$= \frac{i}{\pi}\int_0^\infty \mathcal{F}[\sigma_{xx}]\sin(gx)dg = \frac{i}{\pi}\int_0^\infty \hat{\sigma}_{xx}\sin(gx)dg. \tag{3.143}$$

Using the symmetry of the domain in x, express the displacements and the stress as

$$\begin{aligned}
u(x,y) &= \frac{1}{\pi}\int_0^\infty \hat{u}(g,y)\cos(gx)\,dg = \frac{1}{\pi}\int_0^\infty \hat{U}^u(g,y)\cos(gx)\,dg,\\
v(x,y) &= \frac{i}{\pi}\int_0^\infty \hat{v}(g,y)\sin(gx)\,dg = \frac{1}{\pi}\int_0^\infty \hat{V}^u(g,y)\sin(gx)\,dg,\\
\sigma_{yy}(x,y) &= \frac{i}{\pi}\int_0^\infty \hat{\sigma}_{yy}(g,y)\sin(gx)\,dg = \frac{1}{\pi}\int_0^\infty \hat{\sigma}^u_{yy}(g,y)\sin(gx)\,dg,\\
\sigma_{xx}(x,y) &= \frac{i}{\pi}\int_0^\infty \hat{\sigma}_{xx}(g,y)\sin(gx)\,dg = \frac{1}{\pi}\int_0^\infty \hat{\sigma}^u_{xx}(g,y)\sin(gx)\,dg,\\
\sigma_{xy}(x,y) &= \frac{1}{\pi}\int_0^\infty \hat{\sigma}_{xy}(g,y)\cos(gx)\,dg = \frac{1}{\pi}\int_0^\infty \hat{\sigma}^u_{xy}(g,y)\cos(gx)\,dg.
\end{aligned} \tag{3.144}$$

where define

$$\hat{U}^u = \hat{u}^u, \quad \hat{V}^u = i\hat{v}^u, \quad \hat{\sigma}^u_{yy} = i\hat{\sigma}_{yy}, \quad \hat{\sigma}^u_{xx} = i\hat{\sigma}_{xx}, \quad \hat{\sigma}^u_{xy} = \hat{\sigma}_{xy}. \tag{3.145}$$

The equilibrium equations 3.130 and 3.131 in terms of $\hat{U}^u$ and $\hat{V}^u$ are

$$(1-2\nu)\left(\hat{U}^u\right)'' - 2g^2(1-\nu)\hat{U}^u + g\left(\hat{V}^u\right)' = 0, \tag{3.146}$$

$$2(1-\nu)\left(\hat{V}^u\right)'' - g^2(1-2\nu)\hat{V}^u - g\left(\hat{U}^u\right)' = 0. \tag{3.147}$$

The boundary conditions at $y = \pm h$ are $\hat{\sigma}^u_{yy} = 0$ and $\hat{\sigma}^u_{xy} = 0$, which translate to

$$\left(\hat{U}^u\right)' + g\hat{V}^u = 0 \qquad (1-\nu)\left(\hat{V}^u\right)' - \nu g\hat{U}^u = 0. \tag{3.148}$$

The jump conditions across the crack at $y = y_c$ are

$$\left[\hat{U}^u\right]^+_- = 1, \qquad \left[\hat{V}^u\right]^+_- = 0, \qquad \left[\hat{\sigma}^u_{yy}\right]^+_- = \left[\hat{\sigma}^u_{xy}\right]^+_- = 0. \tag{3.149}$$

3.4.4 Numerical solution

In this section we are going to solve $\hat{U}^v, \hat{V}^v, \hat{U}^u, \hat{V}^u$ and $\hat{\sigma}^v_{yy}, \hat{\sigma}^v_{xy}, \hat{\sigma}^u_{yy}, \hat{\sigma}^u_{xy}$ numerically. Now we assume $h = 1$. We consider $g = 0$ separately, which will give singularity if we use the following collocation method.

Collocation method

As shown in Figure 3.3, region 1 is $-1 \le y \le y_c$ and region 2 is $y_c \le y \le 1$.
Now we change the variable y to Y. In region 1, $y = -1 + Y(y_c+1)$ and $\dfrac{d}{dy} = \dfrac{1}{y_c+1}\dfrac{d}{dY}$; in region 2, $y = 1 + Y(y_c-1)$ and $\dfrac{d}{dy} = \dfrac{1}{y_c-1}\dfrac{d}{dY}$. The range of Y is $[0,1]$.
The boundary in each region is represented by $Y = 0$, and $Y = 1$ represents the crack face.

Jump in v

Define Y_1, Y_2, Y_3, Y_4 to be $\hat{U}^v, (\hat{U}^v)', \hat{V}^v, (\hat{V}^v)'$ respectively in region 1, and Y_5, Y_6, Y_7, Y_8 to be $\hat{U}^v, (\hat{U}^v)', \hat{V}^v, (\hat{V}^v)'$ respectively in region 2.

Referring to equations (3.132)

$$
\begin{aligned}
(\hat{U}^v)'' &= \frac{1}{1-2\nu}\left[2g^2(1-\nu)\hat{U}^v + g\hat{(\hat{V}^v)'}\right], && (3.150)\\
(\hat{V}^v)'' &= \frac{1}{2(1-\nu)}\left[g^2(1-2\nu)\hat{V}^v - g\hat{(\hat{U}^v)'}\right]. && (3.151)
\end{aligned}
$$

$$
\begin{aligned}
\frac{dY_1}{dY} &= Y_2\\
\frac{dY_2}{dY} &= \frac{1}{1-2\nu}\left[2g^2(1-\nu)(y_c+1)^2 Y_1 + g(y_c+1)Y_4\right]\\
\frac{dY_3}{dY} &= Y_4\\
\frac{dY_4}{dY} &= \frac{1}{2(1-\nu)}\left[g^2(1-2\nu)(y_c+1)^2 Y_3 - g(y_c+1)Y_2\right]\\
\frac{dY_5}{dY} &= Y_6\\
\frac{dY_6}{dY} &= \frac{1}{1-2\nu}\left[2g^2(1-\nu)(y_c-1)^2 Y_5 + g(y_c-1)Y_8\right]\\
\frac{dY_7}{dY} &= Y_8\\
\frac{dY_8}{dY} &= \frac{1}{2(1-\nu)}\left[g^2(1-2\nu)(y_c-1)^2 Y_7 - g(y_c-1)Y_6\right] && (3.152)
\end{aligned}
$$

The boundary conditions (3.134) on the boundary, and the jump conditions (3.135) on the upper and lower crack faces are

$$
\begin{aligned}
Y_2 - g(y_c+1)Y_3 &= 0\\
(1-\nu)Y_4 + \nu g(y_c+1)Y_1 &= 0\\
Y_6 - g(y_c-1)Y_7 &= 0\\
(1-\nu)Y_8 + \nu g(y_c-1)Y_5 &= 0\\
Y_5 - Y_1 &= 0\\
Y_7 - Y_3 - 1 &= 0\\
\frac{Y_2}{y_c+1} - gY_3 - \left(\frac{Y_6}{y_c-1} - gY_7\right) &= 0\\
\frac{1-\nu}{y_c+1}Y_4 - \frac{1-\nu}{y_c-1}Y_8 + \nu g Y_1 - \nu g Y_5 &= 0. \qquad (3.153)
\end{aligned}
$$

We use the Matlab routine '`bvp4c`', which solves boundary value problems for ODEs by collocation, to calculate the values of $Y_1, Y_2, Y_3, Y_4, Y_5, Y_6, Y_7, Y_8$, hence $\hat{U}^v, \hat{V}^v$ are obtained. The stress components $\hat{\sigma}^v_{yy}, \hat{\sigma}^v_{xy}$ are functions of $\hat{U}^v, \hat{V}^v$.

Jump in u

Define Y_1, Y_2, Y_3, Y_4 to be $\hat{U}^u, (\hat{U}^u)', \hat{V}^u, (\hat{V}^u)'$ respectively in region 1, and Y_5, Y_6, Y_7, Y_8 to be $\hat{U}^u, (\hat{U}^u)', \hat{V}^u, (\hat{V}^u)'$ respectively in region 2.

Referring to equations (3.146)

$$
\begin{aligned}
(\hat{U}^u)'' &= \frac{1}{1-2\nu}\left[2g^2(1-\nu)\hat{U}^u - g(\hat{V}^u)'\right], && (3.154)\\
(\hat{V}^u)'' &= \frac{1}{2(1-\nu)}\left[g^2(1-2\nu)\hat{V}^u + g(\hat{U}^u)'\right]. && (3.155)
\end{aligned}
$$

$$
\begin{aligned}
\frac{dY_1}{dY} &= Y_2\\
\frac{dY_2}{dY} &= \frac{1}{1-2\nu}\left[2g^2(1-\nu)(y_c+1)^2 Y_1 - g(y_c+1)Y_4\right]\\
\frac{dY_3}{dY} &= Y_4\\
\frac{dY_4}{dY} &= \frac{1}{2(1-\nu)}\left[g^2(1-2\nu)(y_c+1)^2 Y_3 + g(y_c+1)Y_2\right]\\
\frac{dY_5}{dY} &= Y_6\\
\frac{dY_6}{dY} &= \frac{1}{1-2\nu}\left[2g^2(1-\nu)(y_c-1)^2 Y_5 - g(y_c-1)Y_8\right]\\
\frac{dY_7}{dY} &= Y_8\\
\frac{dY_8}{dY} &= \frac{1}{2(1-\nu)}\left[g^2(1-2\nu)(y_c-1)^2 Y_7 + g(y_c-1)Y_6\right] && (3.156)
\end{aligned}
$$

The boundary conditions (3.148) on the boundary, and the jump conditions (3.149) on the upper and lower crack faces are

$$
\begin{aligned}
Y_2 + g(y_c+1)Y_3 &= 0\\
(1-\nu)Y_4 - \nu g(y_c+1)Y_1 &= 0\\
Y_6 + g(y_c-1)Y_7 &= 0\\
(1-\nu)Y_8 - \nu g(y_c-1)Y_5 &= 0\\
Y_5 - Y_1 + 1 &= 0\\
Y_7 - Y_3 &= 0\\
\frac{Y_2}{y_c+1} + gY_3 - \left(\frac{Y_6}{y_c-1} + gY_7\right) &= 0\\
\frac{1-\nu}{y_c+1}Y_4 - \frac{1-\nu}{y_c-1}Y_8 - \nu g Y_1 + \nu g Y_5 &= 0. && (3.157)
\end{aligned}
$$

We use the Matlab routine '`bvp4c`' to calculate the values of $Y_1, Y_2, Y_3, Y_4, Y_5, Y_6, Y_7, Y_8$, hence $\hat{U}^u, \hat{V}^u$ are obtained. The stress components $\hat{\sigma}^u_{yy}, \hat{\sigma}^u_{xy}$ are functions of $\hat{U}^u, \hat{V}^u$.

3.4.5 The case $g = 0$

The calculation of $\hat{U}^v, \hat{V}^v, \hat{\sigma}^v_{yy}, \hat{\sigma}^v_{xy}$ and $\hat{U}^u, \hat{V}^u, \hat{\sigma}^u_{yy}, \hat{\sigma}^u_{xy}$ when $g = 0$ must be solved separately.

Jump in v when $g = 0$

Equations (3.132) become

$$(1-2\nu)\left(\hat{U}^v\right)'' = 0 \quad \text{and} \quad 2(1-\nu)\left(\hat{V}^v\right)'' = 0. \tag{3.158}$$

Hence the solution for $\hat{U}^v$ and $\hat{V}^v$ are

$$\hat{U}^v = Ay + B \quad \text{and} \quad \hat{V}^v = Cy + D.$$

By using the boundary conditions (3.134) on lower and upper boundaries and the jump conditions (3.135) we get

$$A_1 = 0 \quad B_1 = 0 \quad C_1 = 0 \quad D_1 = -\frac{1}{2} \quad A_2 = 0 \quad B_2 = 0 \quad C_2 = 0 \quad D_2 = \frac{1}{2}$$

where subscript '1' means region '1', and subscript '1' means region '2'.
Hence the displacements on the upper crack face are $\hat{U}^v = 0$ and $\hat{V}^v = \frac{1}{2}$; the displacements on the lower crack face are $\hat{U}^v = 0$ and $\hat{V}^v = -\frac{1}{2}$; the displacements on the top boundary are $\hat{U}^v = 0$ and $\hat{V}^v = \frac{1}{2}$; the displacements on the bottom boundary are $\hat{U}^v = 0$ and $\hat{V}^v = -\frac{1}{2}$; on the crack face $\hat{\sigma}^v_{yy} = 0$ and $\hat{\sigma}^v_{xy} = 0$.

Jump in u when $g = 0$

Equations 3.146 change to

$$(1-2\nu)\left(\hat{U}^u\right)'' = 0, \tag{3.159}$$

$$2(1-\nu)\left(\hat{V}^u\right)'' = 0. \tag{3.160}$$

Hence the solution for $\hat{U}^u$ and $\hat{V}^u$ are

$$\begin{aligned} \hat{U}^u &= Ay + B, \\ \hat{V}^u &= Cy + D. \end{aligned}$$

Put the solutions into the boundary conditions (3.148) on inner and outer layers and the jump conditions (3.149) we get

$$A_1 = 0 \quad B_1 = -\frac{1}{2} \quad C_1 = 0 \quad D_1 = 0 \quad A_2 = 0 \quad B_2 = \frac{1}{2} \quad C_2 = 0 \quad D_2 = 0$$

where subscript '1' means region '1', and subscript '1' means region '2'.

Hence the displacements on the upper crack face are $\hat{U}^u = \frac{1}{2}$ and $\hat{W}^u = 0$; the displacements on the lower crack face are $\hat{U}^u = -\frac{1}{2}$ and $\hat{W}^u = 0$; the displacements on the top boundary are $\hat{U}^u = \frac{1}{2}$ and $\hat{W}^u = 0$; the displacements on the bottom boundary are $\hat{U}^u = -\frac{1}{2}$ and $\hat{W}^u = 0$; on the crack face $\hat{\sigma}^u_{yy} = 0$ and $\hat{\sigma}^u_{xy} = 0$.

3.4.6 Matrix equations

We obtain $\hat{U}^v(g,y), \hat{V}^v(g,y), \hat{U}^u(g,y), \hat{V}^u(g,y)$ and $\hat{\sigma}^v_{yy}(g,y), \hat{\sigma}^v_{xy}(g,y), \hat{\sigma}^u_{yy}(g,y), \hat{\sigma}^u_{xy}(g,y)$ for each g from above numerical approach. Now we assume the length of the crack is L, and the length of the strip is $3L$. The traction and displacement components, decomposed into normal and tangential direction, are

$$T_y = \int \sigma^u_{yy}(x-s,y)U(s)\,ds + \int \sigma^v_{yy}(x-s,y)V(s)\,ds, \tag{3.161}$$

$$T_x = \int \sigma^u_{xy}(x-s,y)U(s)\,ds + \int \sigma^v_{xy}(x-s,y)V(s)\,ds. \tag{3.162}$$

$$u = \int u^u(x-s,y)U(s)ds + \int u^v(x-s,y)V(s)ds \tag{3.163}$$

$$v = \int v^u(x-s,y)U(s)ds + \int v^v(x-s,y)V(s)ds \tag{3.164}$$

We discretize the integral equations (3.161) and (3.162) assuming piecewise constant openings along a crack of length L. We evaluate the integral equation at a discrete set of points $x_i, i = 1, ..., N$.

Useful results

The following results will be used in future sections

$$\int_{x_j-\Delta}^{x_j+\Delta} U_j\left(-\frac{1}{\pi(x_i-s)^2}\right)ds = U_j\left[-\frac{2\Delta}{\pi\left((x_i-x_j)^2-\Delta^2\right)}\right], \tag{3.165}$$

$$\int_{x_j-\Delta}^{x_j+\Delta} U_j\left(\delta(x_i-s)\right)ds = U_j I_{x_i\in(x_j-\Delta,x_j+\Delta)}, \tag{3.166}$$

$$\int_{x_j-\Delta}^{x_j+\Delta} U_j\left(\delta'(x_i-s)\right)ds = 0, \tag{3.167}$$

$$\int_{x_j-\Delta}^{x_j+\Delta} U_j\left(\frac{1}{\pi(x_i-s)}\right)ds = \frac{1}{\pi}\log\left|\frac{x_i-x_j+\Delta}{x_i-x_j-\Delta}\right|U_j, \tag{3.168}$$

in which $\Delta = \frac{L}{N}$, $i = 1, ..., N$, and $j = 1, ..., N$.

For the first term in the RHS of equation (3.161)

$$\begin{aligned}
\int \sigma^u_{yy}(x_i - s, y)U(s)\,ds &= \int \left[\frac{1}{\pi}\int_0^\infty \hat{\sigma}^u_{yy}(g, y)\sin g(x_i - s)\,dg\right] U(s)\,ds \\
&= \frac{1}{\pi}\sum_j \int_j \left[\int_0^\infty \hat{\sigma}^u_{yy}(g, y)\sin g(x_i - s)\,dg\right] U_j\,ds \\
&= \frac{1}{\pi}\sum_j \int_j \left[\int_0^\infty \left(\hat{\sigma}^u_{yy}(g, y) - g\sigma^{u1}_{yy}\right)\sin g(x_i - s)\,dg\right] U_j\,ds \\
&+ \frac{1}{\pi}\sum_j \int_j \left[\int_0^\infty g\sigma^{u1}_{yy}\sin g(x_i - s)\,dg\right] U_j\,ds,
\end{aligned}$$

where

$$\int_j \left[\int_0^\infty (\hat{\sigma}^u_{yy}(g, y) - g\sigma^{u1}_{yy})\sin g(x_i - s)\,dg\right] U_j\,ds = U_j \int_0^\infty (\hat{\sigma}^u_{yy} - g\sigma^{u1}_{yy})\left[\int_j \sin g(x_i - s)\,ds\right] dg,$$

and

$$\int_j \sin g(x_i - s)\,ds = \int_{x_j - \Delta}^{x_j + \Delta} \sin g(x_i - s)\,ds = 2\frac{\sin g\Delta}{g}\sin g(x_i - x_j).$$

Then using equation (3.101) we have

$$\frac{1}{\pi}\int_0^\infty g\sigma^{u1}_{yy}\sin g(x_i - s)\,dg = \frac{\sigma^{u1}_{yy}}{\pi}\lim_{y\to 0^+}\int_0^\infty ge^{-gy}\sin g(x_i - s)\,dg = \sigma^{u1}_{yy}\delta'(x_i - s),$$

and using equation (3.167) we have

$$\int \sigma^u_{yy}(x_i - s, y)U(s)\,ds = 2\frac{1}{\pi}\sum_j U_j \int_0^\infty \left(\hat{\sigma}^u_{yy}(g, y) - g\sigma^{u1}_{yy}\right)\frac{\sin g\Delta}{g}\sin g(x_i - x_j)\,dg,$$

which is the form of $\sum_j \sigma^u_{yy}[i, j]U_j$ and

$$\sigma^u_{yy}[i, j] = 2\frac{1}{\pi}\int_0^\infty \left(\hat{\sigma}^u_{yy}(g, y) - g\sigma^{u1}_{yy}\right)\frac{\sin g\Delta}{g}\sin g(x_i - x_j)\,dg.$$

For the second term in the RHS of equation (3.161), in which we use equations (3.99) and (3.165), we have

$$\begin{aligned}
\int \sigma^v_{yy}(x_i - s, y)V(s)\,ds &= \int \left[\frac{1}{\pi}\int_0^\infty \hat{\sigma}^v_{yy}(g, y)\cos g(x_i - s)\,dg\right] V(s)\,ds \\
&= \frac{1}{\pi}\sum_j \int_j \left[\int_0^\infty \left(\hat{\sigma}^v_{yy}(g, y) - g\sigma^{v1}_{yy}\right)\cos g(x_i - s)\,dg\right] V_j\,ds \\
&+ \frac{1}{\pi}\sum_j \int_j \left[\int_0^\infty g\sigma^{v1}_{yy}\cos g(x_i - s)\,dg\right] V_j\,ds \\
&= 2\frac{1}{\pi}\sum_j V_j \int_0^\infty \left(\hat{\sigma}^v_{yy}(g, y) - g\sigma^{v1}_{yy}\right)\frac{\sin g\Delta}{g}\cos g(x_i - x_j)\,dg \\
&- \sigma^{v1}_{yy}\sum_j V_j \left[\frac{2\Delta}{\pi\left((x_i - x_j)^2 - \Delta^2\right)}\right],
\end{aligned}$$

which is the form of $\sum_j \sigma^v_{yy}[i,j]V_j$ and

$$\begin{aligned}\sigma^v_{yy}[i,j] &= 2\frac{1}{\pi}\int_0^\infty \left(\hat{\sigma}^v_{yy}(g,y) - g\sigma^{v1}_{yy}\right)\frac{\sin g\Delta}{g}\cos g(x_i - x_j)\,dg \\ &- \sigma^{v1}_{yy}\left[\frac{2\Delta}{\pi\left((x_i-x_j)^2-\Delta^2\right)}\right]\end{aligned}$$

For the first term in the RHS of equation (3.162), in which we use (3.99) and (3.165), we have

$$\begin{aligned}\int \sigma^u_{xy}(x_i - s, y)U(s)\,ds &= \int\left[\frac{1}{\pi}\int_0^\infty \hat{\sigma}^u_{xy}(g,y)\cos g(x_i - s)\,dg\right]U(s)\,ds \\ &= \frac{1}{\pi}\sum_j\int_j\left[\int_0^\infty\left(\hat{\sigma}^u_{xy}(g,y) - g\sigma^{u1}_{xy}\right)\cos g(x_i-s)\,dg\right]U_j\,ds \\ &+ \frac{1}{\pi}\sum_j\int_j\left[\int_0^\infty g\sigma^{u1}_{xy}\cos g(x_i-s)\,dg\right]U_j\,ds \\ &= 2\frac{1}{\pi}\sum_j U_j\int_0^\infty\left(\hat{\sigma}^u_{xy}(g,y) - g\sigma^{u1}_{xy}\right)\frac{\sin g\Delta}{g}\cos g(x_i-x_j)\,dg \\ &- \sigma^{u1}_{xy}\sum_j U_j\left[\frac{2\Delta}{\pi\left((x_i-x_j)^2-\Delta^2\right)}\right],\end{aligned}$$

which is the form of $\sum_j \sigma^u_{xy}[i,j]U_j$ and

$$\begin{aligned}\sigma^u_{xy}[i,j] &= 2\frac{1}{\pi}\int_0^\infty\left(\hat{\sigma}^u_{xy}(g,y) - g\sigma^{u1}_{xy}\right)\frac{\sin g\Delta}{g}\cos g(x_i-x_j)\,dg \\ &- \sigma^{u1}_{xy}\left[\frac{2\Delta}{\pi\left((x_i-x_j)^2-\Delta^2\right)}\right]\end{aligned}$$

For the second term in the RHS of equation (3.162), in which we use (3.101) and (3.167), we have

$$\int \sigma^v_{xy}(x_i - s, y)V(s)\,ds = 2\frac{1}{\pi}\sum_j V_j\int_0^\infty\left(\hat{\sigma}^v_{xy}(g,y) - g\sigma^{v1}_{xy}\right)\frac{\sin g\Delta}{g}\sin g(x_i-x_j)\,dg.$$

which is the form of $\sum_j \sigma^v_{xy}[i,j]V_j$ and

$$\sigma^v_{xy}[i,j] = = 2\frac{1}{\pi}\int_0^\infty\left(\hat{\sigma}^v_{xy}(g,y) - g\sigma^{v1}_{xy}\right)\frac{\sin g\Delta}{g}\sin g(x_i-x_j)\,dg.$$

We write these integral equations (3.161) and (3.162) into the form of matrix equation

$$\begin{bmatrix} T_{y_i} \\ T_{xi}\end{bmatrix} = \begin{bmatrix}\sigma^u_{yy}[i,j] & \sigma^v_{yy}[i,j] \\ \sigma^u_{xy}[i,j] & \sigma^v_{xy}[i,j]\end{bmatrix}\begin{bmatrix} U_j \\ V_j\end{bmatrix} \tag{3.169}$$

where $j = 1, ..., N$.

We discretize the integral equations (5.82) and (3.164) assuming piecewise constant openings along length L for upper, and lower crack faces and $3L$ for top and bottom boundaries. We evaluate the integral equation at a discrete set of points $x_i, i = 1, ..., N$ for upper and lower crack faces, and $x_i, i = 1, ..., 3N$ for top and bottom boundaries. For the first term in the RHS of equation (5.82), in which we use (3.100) and (3.166), we have

$$\begin{aligned}
\int u^u(x_i - s, y)U(s)ds &= \frac{1}{\pi}\int\int_0^\infty \left(\hat{U}^u - u^{1u}\right)\cos g\,(x_i - s)\; dg\,U\,ds \\
&+ \frac{1}{\pi}\int\int_0^\infty u^{1u}\cos g\,(x_i - s)\; dg\,U\,ds \\
&= \frac{2}{\pi}\sum_j U_j \int_0^\infty (\hat{U}^u - u^{1u})\frac{\sin g\Delta}{g}\cos\left(gx_i - gx_j\right)dg \\
&+ u^{1u}\sum_j \int_j \lim_{y\to 0^+}\int_0^\infty e^{-gy}\cos g\,(x_i - s)\; dg\,U_j\,ds \\
&= \frac{2}{\pi}\sum_j U_j \int_0^\infty (\hat{U}^u - u^{1u})\frac{\sin g\Delta}{g}\cos\left(gx_i - gx_j\right)dg \\
&+ u^{1u}\sum_j U_j I_{x_i\in(x_j-\Delta,x_j+\Delta)},
\end{aligned}$$

which is the form of $\sum_j u^u[i,j]U_j$ and

$$\begin{aligned}
u^u[i,j] &= \frac{2}{\pi}\int_0^\infty (\hat{U}^u - u^{1u})\frac{\sin g\Delta}{g}\cos\left(gx_i - gx_j\right)dg \\
&+ u^{1u}I_{x_i\in(x_j-\Delta,x_j+\Delta)}.
\end{aligned}$$

For the second term in the RHS of equation (5.82), in which we use (3.102) and (3.168), we have

$$\begin{aligned}
\int u^v(x_i - s, y)V(s)ds &= \frac{1}{\pi}\int\int_0^\infty \left(\hat{U}^v - u^{1v}\right)\sin g\,(x_i - s)\; dg\,V\,ds \\
&+ \frac{1}{\pi}\int\int_0^\infty u^{1v}\sin g\,(x_i - s)\; dg\,V\,ds \\
&= \frac{2}{\pi}\sum_j V_j \int_0^\infty (\hat{U}^v - u^{1v})\frac{\sin g\Delta}{g}\sin\left(gx_i - gx_j\right)dg \\
&+ u^{1v}\sum_j \int_j \lim_{y\to 0^+}\int_0^\infty e^{-gy}\sin g\,(x_i - s)\; dg\,V_j\,ds \\
&= \frac{2}{\pi}\sum_j V_j \int_0^\infty (\hat{U}^v - u^{1v})\frac{\sin g\Delta}{g}\sin\left(gx_i - gx_j\right)dg \\
&+ \frac{u^{1v}}{\pi}\sum_j V_j \log\left|\frac{x_i - x_j + \Delta}{x_i - x_j - \Delta}\right|,
\end{aligned}$$

which is the form of $\sum_j u^v[i,j]V_j$ and

$$\begin{aligned} u^v[i,j] &= \frac{2}{\pi}\int_0^\infty (\hat{U}^v - u^{1v})\frac{\sin g\Delta}{g}\sin\left(gx_i - gx_j\right)dg \\ &+ \frac{u^{1v}}{\pi}\log\left|\frac{x_i - x_j + \Delta}{x_i - x_j - \Delta}\right|. \end{aligned}$$

For the first term in the RHS of equation (3.164), in which we use (3.102) and (3.168), we have

$$\begin{aligned} \int v^u(x_i - s, y)U(s)ds &= \frac{1}{\pi}\int\int_0^\infty \left(\hat{V}^u - v^{1u}\right)\sin g\left(x_i - s\right)\, dg\, U\, ds \\ &+ \frac{1}{\pi}\int\int_0^\infty v^{1u}\sin g\left(x_i - s\right)\, dg\, U\, ds \\ &= \frac{2}{\pi}\sum_j U_j\int_0^\infty (\hat{V}^u - v^{1u})\frac{\sin g\Delta}{g}\sin\left(gx_i - gx_j\right)dg \\ &+ v^{1u}\sum_j\int_j \lim_{y\to 0^+}\int_0^\infty e^{-gy}\sin g\left(x_i - s\right)\, dg\, U_j\, ds \\ &= \frac{2}{\pi}\sum_j U_j\int_0^\infty (\hat{V}^u - v^{1u})\frac{\sin g\Delta}{g}\sin\left(gx_i - gx_j\right)dg \\ &+ \frac{v^{1u}}{\pi}\sum_j U_j\log\left|\frac{x_i - x_j + \Delta}{x_i - x_j - \Delta}\right|, \end{aligned}$$

which is the form of $\sum_j v^u[i,j]U_j$ and

$$\begin{aligned} v^u[i,j] &= \frac{2}{\pi}\int_0^\infty (\hat{V}^u - v^{1u})\frac{\sin g\Delta}{g}\sin\left(gx_i - gx_j\right)dg \\ &+ \frac{v^{1u}}{\pi}\log\left|\frac{x_i - x_j + \Delta}{x_i - x_j - \Delta}\right|. \end{aligned}$$

For the second term in the RHS of equation (3.164), in which we use (3.100) and (3.166), we have

$$\begin{aligned} \int v^v(x_i - s, y)V(s)ds &= \frac{1}{\pi}\int\int_0^\infty \left(\hat{V}^v - v^{1v}\right)\cos g\left(x_i - s\right)\, dg\, V\, ds \\ &+ \frac{1}{\pi}\int\int_0^\infty v^{1v}\cos g\left(x_i - s\right)\, dg\, V\, ds \\ &= \frac{2}{\pi}\sum_j V_j\int_0^\infty (\hat{V}^v - v^{1v})\frac{\sin g\Delta}{g}\cos\left(gx_i - gx_j\right)dg \\ &+ v^{1v}\sum_j\int_j \lim_{y\to 0^+}\int_0^\infty e^{-gy}\cos g\left(x_i - s\right)\, dg\, V_j\, ds \\ &= \frac{2}{\pi}\sum_j V_j\int_0^\infty (\hat{V}^v - v^{1v})\frac{\sin g\Delta}{g}\cos\left(gx_i - gx_j\right)dg \\ &+ v^{1v}\sum_j V_j I_{x_i\in(x_j-\Delta,x_j+\Delta)}, \end{aligned}$$

which is the form of $\sum_j v^v[i,j]U_j$ and

$$\begin{aligned} v^v[i,j] &= \frac{2}{\pi}\int_0^\infty (\hat{V}^v - v^{1v})\frac{\sin g\Delta}{g}\cos(gx_i - gx_j)\,dg \\ &+ v^{1v} I_{x_i \in (x_j-\Delta, x_j+\Delta)}. \end{aligned}$$

We write these integral equations (5.82) and (3.164) into the form of matrix equation

$$\begin{bmatrix} u_i \\ v_i \end{bmatrix} = \begin{bmatrix} u^u[i,j] & u^v[i,j] \\ v^u[i,j] & v^v[i,j] \end{bmatrix} \begin{bmatrix} U_j \\ V_j \end{bmatrix}. \tag{3.170}$$

3.4.7 Results

Assuming $T_{y_i} = 10^{-2}$ and $T_{xi} = 0$ in equation (3.169) we could solve U_j and V_j. When U_j and V_j have been obtained, the displacements u_i and v_i in (3.170) for upper and lower crack face, and for top and bottom boundaries are obtained as shown in Figure 3.4, 3.5 and 3.6. The crack is symmetric in Figure 3.4, since it is in the middle of the strip. When the tear location moves towards to the boundary, the opening is not symmetric. The upper tear face, that is closer to the boundary, becomes much higher and the lower tear face changes less in 3.5 and 3.6. The reason is that the elastic material between the top boundary and upper tear face is thinner, which makes it easier to change.

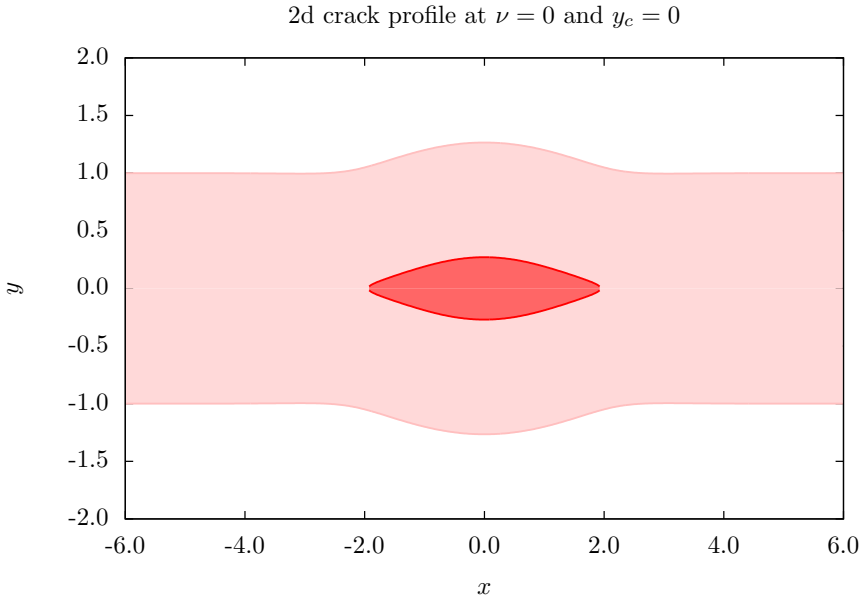

Figure 3.4: Plot of crack profile in compressible 2d strip with $T_{y_i} = 10^{-2}$, $T_{xi} = 0$, $\nu = 0$ and $y_c = 0.2$.

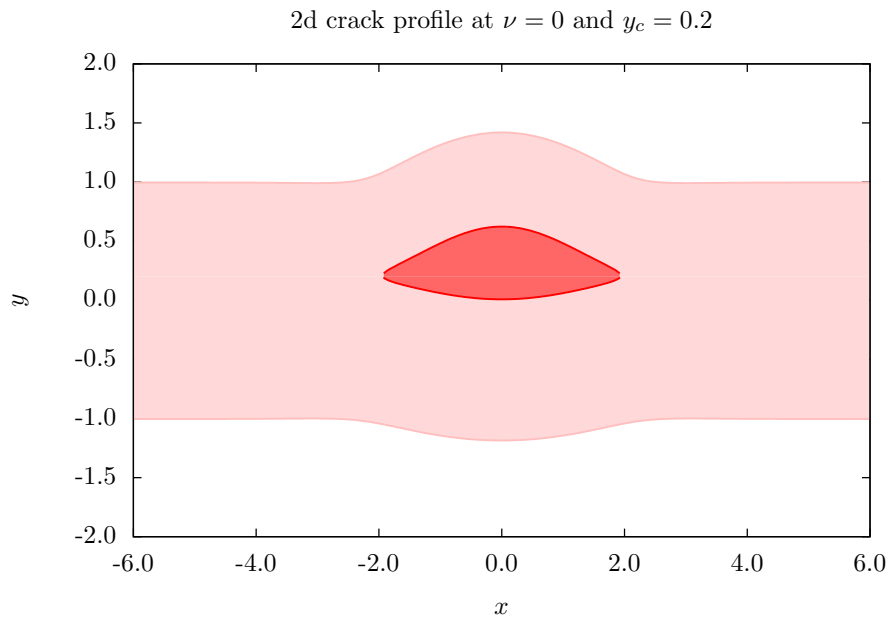

Figure 3.5: Plot of crack profile in compressible 2d strip with $T_{y_i} = 10^{-2}$, $T_{xi} = 0$, $\nu = 0$ and $y_c = 0.2$.

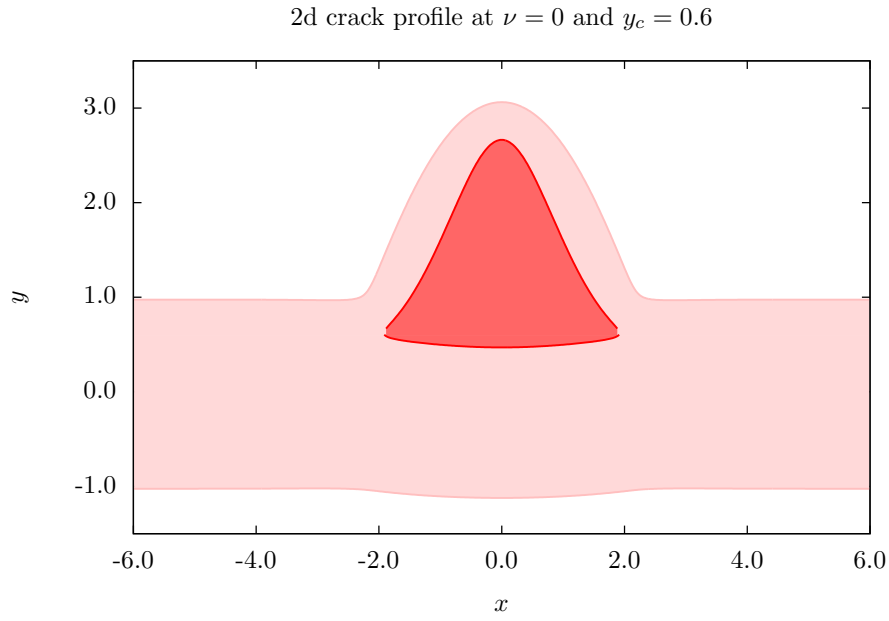

Figure 3.6: Plot of crack profile in compressible 2d strip with $T_{y_i} = 10^{-2}$, $T_{xi} = 0$, $\nu = 0$ and $y_c = 0.2$.

3.5 Solution for 2D incompressible plane crack problem

Now we assume that the 2D strip is incompressible. The strain tensor is still the same as equation (3.73). But the stress tensor changes to

$$\boldsymbol{\sigma} = \lambda \mathrm{tr}\,(\boldsymbol{\varepsilon})\,\mathbf{I} + 2\mu\boldsymbol{\varepsilon} - p\mu\mathbf{I} = 2\mu\boldsymbol{\varepsilon} - p\mu\mathbf{I} \tag{3.171}$$

due to incompressibility

$$\mathrm{tr}\,(\boldsymbol{\varepsilon}) = \nabla \cdot \mathbf{u} = 0. \tag{3.172}$$

Hence

$$\sigma_{xx} = \mu\,(2u_{,x} - p)\,, \tag{3.173}$$

$$\sigma_{xy} = \mu\,(v_{,x} + u_{,y}\,)\,, \tag{3.174}$$

$$\sigma_{yy} = \mu\,(2v_{,y} - p)\,. \tag{3.175}$$

The equilibrium equations and incompressibility are

$$\mathrm{div}\,\boldsymbol{\sigma} = 0 \quad \text{and} \quad \nabla \cdot \mathbf{u} = 0, \tag{3.176}$$

which are written into components

$$\sigma_{xx,x} + \sigma_{xy,y} = 0, \tag{3.177}$$

$$\sigma_{xy,x} + \sigma_{yy,y} = 0, \tag{3.178}$$

$$u_{,x} + v_{,y} = 0. \tag{3.179}$$

Put equations (3.173)-(3.175) in we obtain

$$u_{,xx} - p_{,x} + u_{,yy} + v_{,xy} = 0, \tag{3.180}$$

$$u_{,xy} + v_{,xx} + v_{,yy} - p_{,y} = 0, \tag{3.181}$$

$$u_{,x} + v_{,y} = 0. \tag{3.182}$$

The boundary conditions are the same as equations (3.81) and (3.82), and the jump conditions are the same as equations (3.67) and (3.68).

3.5.1 Jump in v

Fourier transform for components of displacement and stress are same as (3.128) and (3.129), besides we have one more term transformed

$$p\,(x,y) = \frac{1}{\pi}\int_0^\infty \hat{p}\,(g,y)\cos gx\,dg = \frac{1}{\pi}\int_0^\infty \hat{P}^v\,(g,y)\cos gx\,dg \quad \text{and define} \quad \hat{P}^v = \hat{p}. \tag{3.183}$$

Equilibrium equations and incompressible equation after Fourier transform are

$$\begin{aligned}\left(\hat{U}^v\right)'' - 2g^2\left(\hat{U}^v\right) + g\left(\hat{P}^v\right) - g\left(\hat{V}^v\right)' &= 0,\\ -\left(\hat{P}^v\right)' + g\left(\hat{U}^v\right)' - g^2\left(\hat{V}^v\right) + 2\left(\hat{V}^v\right)'' &= 0,\\ g\left(\hat{U}^v\right) + \left(\hat{V}^v\right)' &= 0. \end{aligned} \tag{3.184}$$

Replace $\left(\hat{V}^u\right)' = -g\hat{U}^u$ into these equilibrium equations we have

$$\left(\hat{V}^v\right)''' = g^2\left(\left(\hat{V}^v\right)' + \hat{P}^v\right), \tag{3.185}$$

$$\left(\hat{P}^v\right)' = \left(\hat{V}^v\right)'' - g^2\hat{V}^v. \tag{3.186}$$

Boundary conditions at $y = \pm h$ are $\hat{\sigma}^v_{yy} = 0$ and $\hat{\sigma}^v_{xy} = 0$ which translate to

$$\left(\hat{V}^v\right)' - \hat{P}^v = 0, \tag{3.187}$$

$$-g^2\hat{V}^v + \left(\hat{V}^v\right)'' = 0. \tag{3.188}$$

The jump conditions across the crack at $y = y_c$ are

$$\left[\hat{U}^v\right]^+_- = 0, \qquad \left[\hat{V}^v\right]^+_- = 1 \qquad \text{and} \qquad \left[\hat{\sigma}^v_{yy}\right]^+_- = \left[\hat{\sigma}^v_{xy}\right]^+_- = 0. \tag{3.189}$$

Write into components

$$\left[\left(\hat{V}^v\right)'\right]^+_- = 0, \qquad \left[\hat{V}^v\right]^+_- = 1, \qquad \left[\left(\hat{V}^v\right)' - \hat{P}^v\right]^+_- = 0 \qquad \text{and} \qquad \left[-g^2\hat{V}^v + \left(\hat{V}^v\right)''\right]^+_- = 0.$$

3.5.2 Jump in u

Fourier transform for components of displacement and stress are same as (3.144) and (3.145), besides we have one more term transformed

$$p(x,y) = \frac{i}{\pi}\int_0^\infty \hat{p}(g,y)\sin gx\, dg = \frac{1}{\pi}\int_0^\infty \hat{P}^u(g,y)\sin gx\, dg \quad \text{and define} \quad \hat{P}^v = i\hat{p}. \tag{3.190}$$

Equilibrium equations and incompressible equation after Fourier transform are

$$\begin{aligned} -\left(\hat{U}^u\right)'' + 2g^2\left(\hat{U}^u\right) + g\left(\hat{P}^u\right) - g\left(\hat{V}^u\right)' &= 0,\\ \left(\hat{P}^u\right)' + g\left(\hat{U}^u\right)' + g^2\left(\hat{V}^u\right) + 2\left(\hat{V}^u\right)'' &= 0,\\ -g\left(\hat{U}^u\right) + \left(\hat{V}^u\right)' &= 0. \end{aligned} \tag{3.191}$$

Replace $\left(\hat{V}^u\right)' = g\hat{U}^u$ into these equilibrium equations we have

$$\left(\hat{V}^u\right)''' = g^2\left(\left(\hat{V}^u\right)' + \hat{P}^u\right), \tag{3.192}$$

$$\left(\hat{P}^u\right)' = \left(\hat{V}^u\right)'' - g^2\hat{V}^u. \tag{3.193}$$

Boundary conditions at $y = \pm h$ are $\hat{\sigma}^u_{yy} = 0$ and $\hat{\sigma}^u_{xy} = 0$ which translate to

$$\left(\hat{V}^u\right)' - \hat{P}^u = 0, \tag{3.194}$$

$$g^2\hat{V}^u + \left(\hat{V}^u\right)'' = 0. \tag{3.195}$$

The jump conditions across the crack at $y = y_c$ are

$$\left[\hat{U}^u\right]^+_- = 1, \qquad \left[\hat{V}^u\right]^+_- = 0 \qquad \text{and} \qquad \left[\hat{\sigma}^u_{yy}\right]^+_- = \left[\hat{\sigma}^u_{xy}\right]^+_- = 0. \tag{3.196}$$

Write into components

$$\left[\left(\hat{V}^u\right)'\right]^+_- = g, \qquad \left[\hat{V}^u\right]^+_- = 0, \qquad \left[\left(\hat{V}^u\right)' - \hat{P}^u\right]^+_- = 0 \qquad \text{and} \qquad \left[g^2\hat{V}^u + \left(\hat{V}^u\right)''\right]^+_- = 0.$$

3.5.3 Numerical solution

Now we assume $h = 1$. We consider $g = 0$ separately, which will give singularity if we use the following collocation method.

Collocation method

As shown in Figure 3.3, region 1 is $-1 \le y \le y_c$ and region 2 is $y_c \le y \le 1$.
In region 1, $y = -1 + Y(y_c + 1)$ and $\dfrac{d}{dy} = \dfrac{1}{y_c + 1}\dfrac{d}{dY}$; in region 2, $y = 1 + Y(y_c - 1)$ and $\dfrac{d}{dy} = \dfrac{1}{y_c - 1}\dfrac{d}{dY}$. The range of Y is $[0, 1]$.

Jump in v

Define Y_1, Y_2, Y_3, Y_4 to $\hat{U}^v, (\hat{U}^v)', \hat{V}^v, (\hat{V}^v)'$ respectively in region 1, and Y_5, Y_6, Y_7, Y_8 to $\hat{U}^v, (\hat{U}^v)', \hat{V}^v, (\hat{V}^v)'$ respectively in region 2.

Referring to equations (3.185)

$$\begin{aligned}
\frac{dY_1}{dY} &= Y_2 \\
\frac{dY_2}{dY} &= Y_3 \\
\frac{dY_3}{dY} &= g^2(y_c+1)^2 Y_2 + g^2(y_c+1)^3 Y_4 \\
\frac{dY_4}{dY} &= \frac{Y_3}{y_c+1} - g^2(y_c+1)Y_1 \\
\frac{dY_5}{dY} &= Y_6 \\
\frac{dY_6}{dY} &= Y_7 \\
\frac{dY_7}{dY} &= g^2(y_c-1)^2 Y_6 + g^2(y_c-1)^3 Y_8 \\
\frac{dY_8}{dY} &= \frac{Y_7}{y_c-1} - g^2(y_c-1)Y_5
\end{aligned} \tag{3.197}$$

The boundary conditions (3.187) on outer and inner boundaries, and jump conditions (3.189) on upper and lower crack faces are

$$\begin{aligned}
gY_1 + \frac{1}{g}\frac{Y_3}{(y_c+1)^2} &= 0 \\
\frac{2Y_2}{y_c+1} - Y_4 &= 0 \\
gY_5 + \frac{1}{g}\frac{Y_7}{(y_c-1)^2} &= 0 \\
\frac{2Y_6}{y_c-1} - Y_8 &= 0 \\
\frac{Y_6}{g(y_c-1)} - \frac{Y_2}{g(y_c+1)} &= 0 \\
Y_5 - Y_1 - 1 &= 0 \\
gY_5 + \frac{1}{g}\frac{Y_7}{(y_c-1)^2} - (gY_1 + \frac{1}{g}\frac{Y_3}{(y_c+1)^2}) &= 0 \\
\frac{2Y_6}{y_c-1} - Y_8 - (\frac{2Y_2}{y_c+1} - Y_4) &= 0.
\end{aligned} \tag{3.198}$$

We use the Matlab routine '`bvp4c`' to calculate the values of $Y_1, Y_2, Y_3, Y_4, Y_5, Y_6, Y_7, Y_8$, hence $\hat{U}^v, \hat{V}^v, \hat{\sigma}^v_{yy}, \hat{\sigma}^v_{xy}$ are obtained.

Jump in u

Define Y_1, Y_2, Y_3, Y_4 to $\hat{U}^u, (\hat{U}^u)', \hat{V}^u, (\hat{V}^u)'$ respectively in region 1, and Y_5, Y_6, Y_7, Y_8 to $\hat{U}^u, (\hat{U}^u)', \hat{V}^u, (\hat{V}^u)'$ respectively in region 2.

Referring to equations (3.192)

$$\begin{aligned}
\frac{dY_1}{dY} &= Y_2 \\
\frac{dY_2}{dY} &= Y_3 \\
\frac{dY_3}{dY} &= g^2(y_c+1)^2 Y_2 + g^2(y_c+1)^3 Y_4 \\
\frac{dY_4}{dY} &= \frac{Y_3}{y_c+1} - g^2(y_c+1)Y_1 \\
\frac{dY_5}{dY} &= Y_6 \\
\frac{dY_6}{dY} &= Y_7 \\
\frac{dY_7}{dY} &= g^2(y_c-1)^2 Y_6 + g^2(y_c-1)^3 Y_8 \\
\frac{dY_8}{dY} &= \frac{Y_7}{y_c-1} - g^2(y_c-1)Y_5
\end{aligned} \tag{3.199}$$

The boundary conditions (3.194) on outer and inner boundaries, and jump consitions (3.196) on upper and lower crack faces are

$$\begin{aligned}
gY_1 + \frac{1}{g}\frac{Y_3}{(y_c+1)^2} &= 0 \\
\frac{2Y_2}{y_c+1} - Y_4 &= 0 \\
gY_5 + \frac{1}{g}\frac{Y_7}{(y_c-1)^2} &= 0 \\
\frac{2Y_6}{y_c-1} - Y_8 &= 0 \\
\frac{Y_6}{g(y_c-1)} - \frac{Y_2}{g(y_c+1)} - 1 &= 0 \\
Y_5 - Y_1 &= 0 \\
gY_5 + \frac{1}{g}\frac{Y_7}{(y_c-1)^2} - (gY_1 + \frac{1}{g}\frac{Y_3}{(y_c+1)^2}) &= 0 \\
\frac{2Y_6}{y_c-1} - Y_8 - (\frac{2Y_2}{y_c+1} - Y_4) &= 0.
\end{aligned} \tag{3.200}$$

We use the Matlab routine '`bvp4c`' to calculate the values of $Y_1, Y_2, Y_3, Y_4, Y_5, Y_6, Y_7, Y_8$, hence $\hat{U}^u, \hat{V}^u, \hat{\sigma}^u_{yy}, \hat{\sigma}^u_{xy}$ are obtained.

3.5.4 The case $g = 0$

The calculation of $\hat{U}^v, \hat{V}^v, \hat{\sigma}^v_{yy}, \hat{\sigma}^v_{xy}$ and $\hat{U}^u, \hat{V}^u, \hat{\sigma}^u_{yy}, \hat{\sigma}^u_{xy}$ when $g = 0$ must be solved separately.

Jump in v when $g = 0$

Equations (3.184) become

$$\left(\hat{U}^v\right)'' = 0, \quad -\left(\hat{P}^v\right)' + 2\left(\hat{V}^v\right)'' = 0 \quad \text{and} \quad \left(\hat{V}^v\right)' = 0. \tag{3.201}$$

Hence the solution for $\hat{U}^v$, $\hat{V}^v$ and $\hat{P}^v$ are

$$\hat{U}^v = Ay + B, \quad \hat{V}^v = C \quad \text{and} \quad \hat{P}^v = D. \tag{3.202}$$

Put the solutions into the boundary conditions (3.187) and the jump conditions (3.189) we get

$$A_1 = 0, \quad B_1 = 0, \quad C_1 = -\frac{1}{2}, \quad D_1 = 0, \quad A_2 = 0, \quad B_2 = 0, \quad C_2 = \frac{1}{2}, \quad D_2 = 0,$$

where subscript '1' means region one, and region subscript '2' means region 2.
Hence the displacements on the upper crack face are $\hat{U}^v = 0$ and $\hat{V}^v = \frac{1}{2}$; the displacements on the lower crack face are $\hat{U}^v = 0$ and $\hat{V}^v = -\frac{1}{2}$; the displacements on the top boundary are $\hat{U}^v = 0$ and $\hat{V}^v = \frac{1}{2}$; the displacements on the bottom boundary are $\hat{U}^v = 0$ and $\hat{V}^v = -\frac{1}{2}$; on the crack face $\hat{\sigma}^v_{yy} = 0$ and $\hat{\sigma}^v_{xy} = 0$.

Jump in u when $g = 0$

Equations (3.191) become

$$-\left(\hat{U}^u\right)'' = 0, \quad \left(\hat{P}^u\right)' + 2\left(\hat{V}^u\right)'' = 0 \quad \text{and} \quad \left(\hat{V}^u\right)' = 0. \tag{3.203}$$

Hence the solution for $\hat{U}^u$ and $\hat{V}^u$ are

$$\hat{U}^u = Ay + B, \quad \hat{V}^u = C \quad \text{and} \quad \hat{P}^u = D$$

Put the solutions into the boundary conditions 3.194 and the jump conditions 3.196 we get

$$A_1 = 0, \quad B_1 = -\frac{1}{2}, \quad C_1 = 0, \quad D_1 = 0, \quad A_2 = 0, \quad B_2 = \frac{1}{2}, \quad C_2 = 0, \quad D_2 = 0,$$

where subscript '1' means region one, and subscript '2' means region 2.
Hence the displacements on the upper crack face are $\hat{U}^u = \frac{1}{2}$ and $\hat{W}^u = 0$; the displacements on the lower crack face are $\hat{U}^u = -\frac{1}{2}$ and $\hat{W}^u = 0$; the displacements on the top boundary are $\hat{U}^u = \frac{1}{2}$ and $\hat{W}^u = 0$; the displacements on the bottom boundary are $\hat{U}^u = -\frac{1}{2}$ and $\hat{W}^u = 0$; on the crack face $\hat{\sigma}^u_{yy} = 0$ and $\hat{\sigma}^u_{xy} = 0$.

3.5.5 Matrix equations and results

This part for the incompressible strip are same as the compressible one. Assuming $T_{y_i} = 10^{-2}$ and $T_{xi} = 0$ in equation (3.169) we could solve U_j and V_j. When (U_j, V_j) have been obtained, the displacements (u_i, v_i) in (3.170) for upper and lower crack face, and for top and bottom boundaries are obtained as shown in Figure 3.7, 3.8 and 3.9. The Figure 3.7

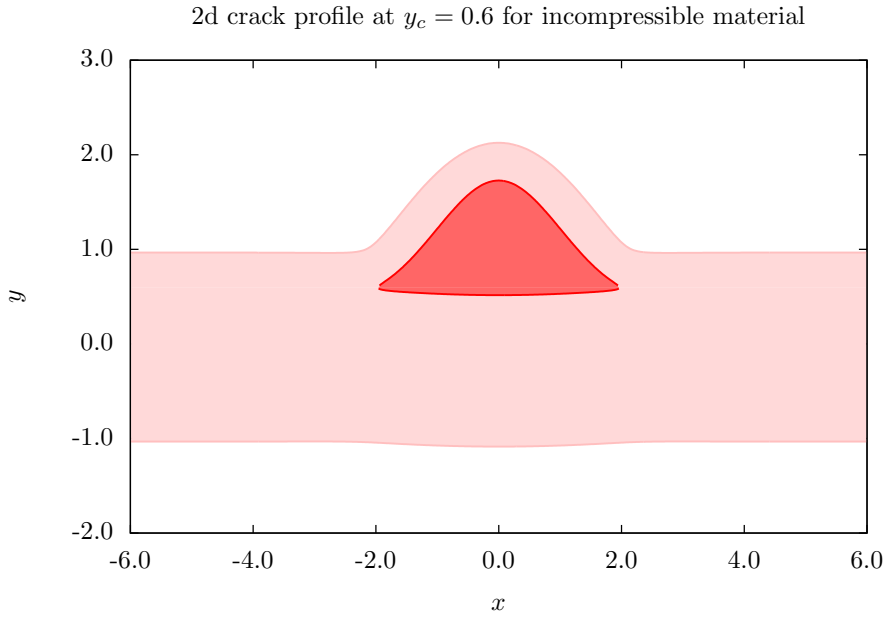

Figure 3.7: Plot of crack profile in incompressible 2D strip with $T_{y_i} = 10^{-2}$, $T_{xi} = 0$ and $y_c = 0.6$.

shows that when the crack location is close to the top boundary, the upper crack face and top boundary change significantly. In Figure 3.8 the crack location is in the middle of the strip, and the boundary condition on eack boundary layer is same. Therefore the crack is symmetric. The Figure 3.9 shows that when the crack location is close to the bottom boundary, the lower crack face and bottom boundary change more significantly than the upper crack face and top boundary.

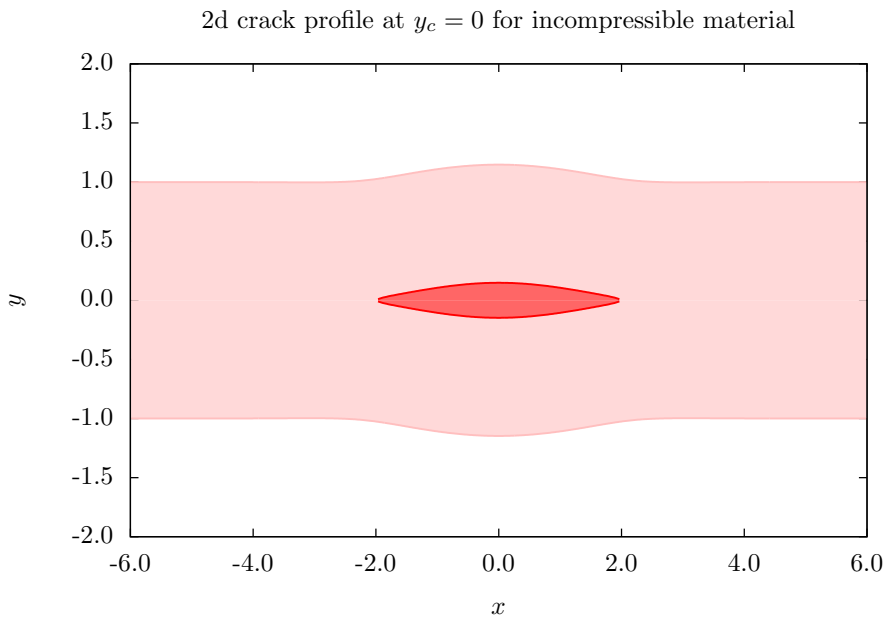

Figure 3.8: Plot of crack profile in incompressible 2D strip with $T_{y_i} = 10^{-2}$, $T_{xi} = 0$ and $y_c = 0.6$.

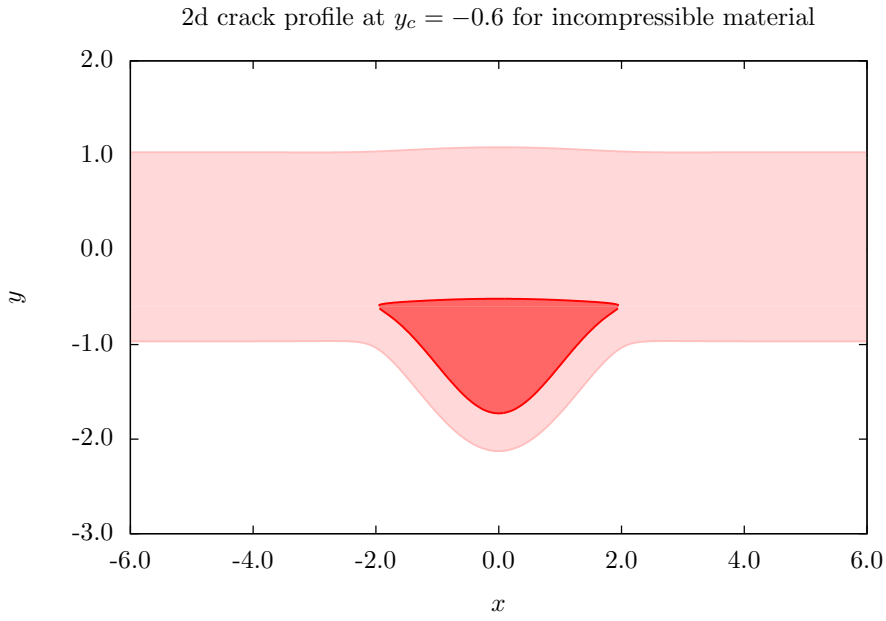

Figure 3.9: Plot of crack profile in incompressible 2D strip with $T_{y_i} = 10^{-2}$, $T_{xi} = 0$ and $y_c = 0.6$.

3.6 Comparison between compressible and incompressible solutions

In compressible 2D strip when $\nu = 0.5$ the material is incompressible. Although we can not make $\nu = 0.5$ exactly in the code due to singularity in numerical, $\nu = 0.4999$ is close to the incompressible material. When $\nu = 0.4999$ we compare the results for compressible and incompressible we find out they match well as shown in Figure 3.10 and 3.11, where the difference is of the order $0.5 - \nu = 0.0001$.

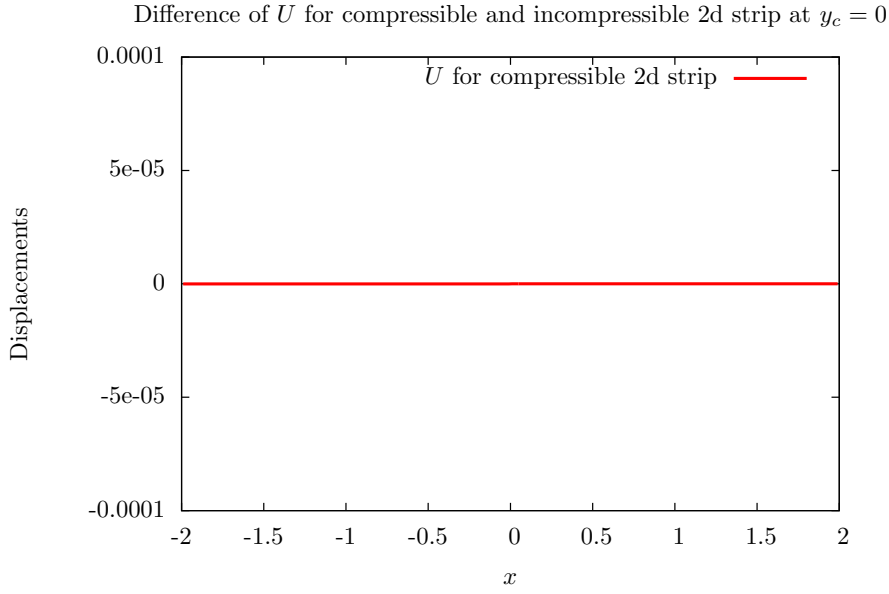

Figure 3.10: Difference of U for compressible and incompressible 2D strip, when the stresses on crack face are $T_{y_i} = 10^{-2}$, $T_{xi} = 0$ at $y_c = 0$. For incompressible one the Poisson's ratio is $\nu = 0.4999$

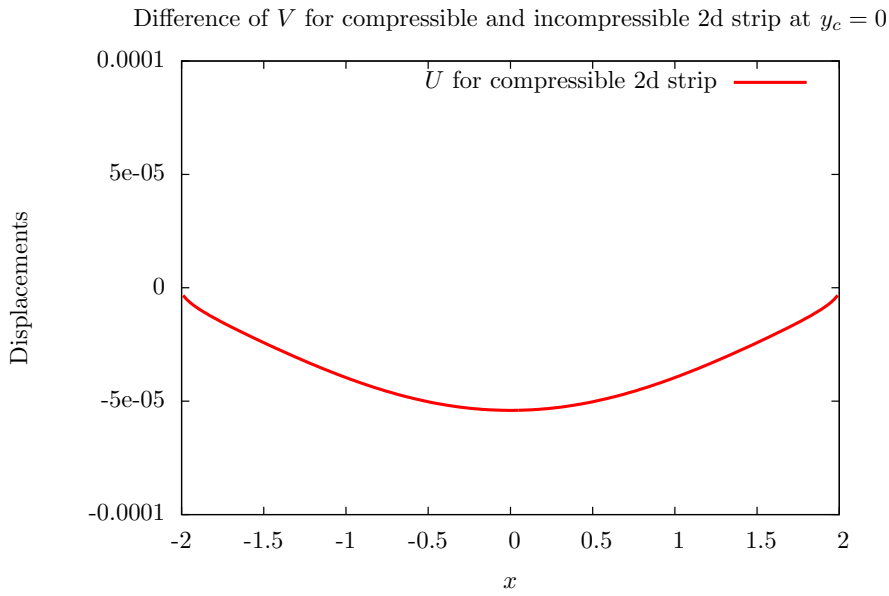

Figure 3.11: Difference of V for compressible and incompressible 2d strip, when the stresses on crack face are $T_{yi} = 10^{-2}$, $T_{xi} = 0$ at $y_c = 0$. For incompressible one the Poisson's ratio is $\nu = 0.4999$

3.7 Conclusions

In this chapter, we introduced the approaches to solve the linear elastic crack problem for 2D plane strain. Moreover, we solve the tear problems in compressible and incompressible 2D strips numerically, and the crack problem in infinite plane analytically. We will use similar methods to solve the linear elastic crack problem in axisymmetric cylindrical tube in next chapter, which is closer to our aim than the 2D crack problem.

Chapter 4

Static axisymmetric tears in compressible and incompressible linear elastic cylindrical annulus

Our aim in this chapter is to take one step closer to a model of a tear in the aorta. The methods of Chapter 3 will be used in this chapter to analyse an axisymmetric crack in a linearly elastic tube. We will show that the numerical method works well and use the same approach in Chapter 5 to study a tear in the aorta.

4.1 Introduction-Method for axisymmetric crack problem

Now we consider an axisymmetric elastic tube with inner radius r_{in} and outer radius r_{out}. We assume the crack, which locates at r_c, is axisymmetric in the wall of the annulus as shown in Figure 4.1. The coordinate system is (r, θ, z) and the displacements in the coordinate directions are (u, v, w). The components of the Cauchy stress are σ_{rr}, $\sigma_{\theta\theta}$, σ_{rz} and σ_{zz}. Due to the axisymmetric crack we don't consider the circumferential displacement v. The jump conditions at $r = r_c$ are

$$[u]^+_- = \delta(z), [w]^+_- = 0, [\sigma_{rr}]^+_- = 0, [\sigma_{rz}]^+_- = 0 \quad \text{for jump in } u \tag{4.1}$$

$$[u]^+_- = 0, [w]^+_- = \delta(z), [\sigma_{rr}]^+_- = 0, [\sigma_{rz}]^+_- = 0 \quad \text{for jump in } w \tag{4.2}$$

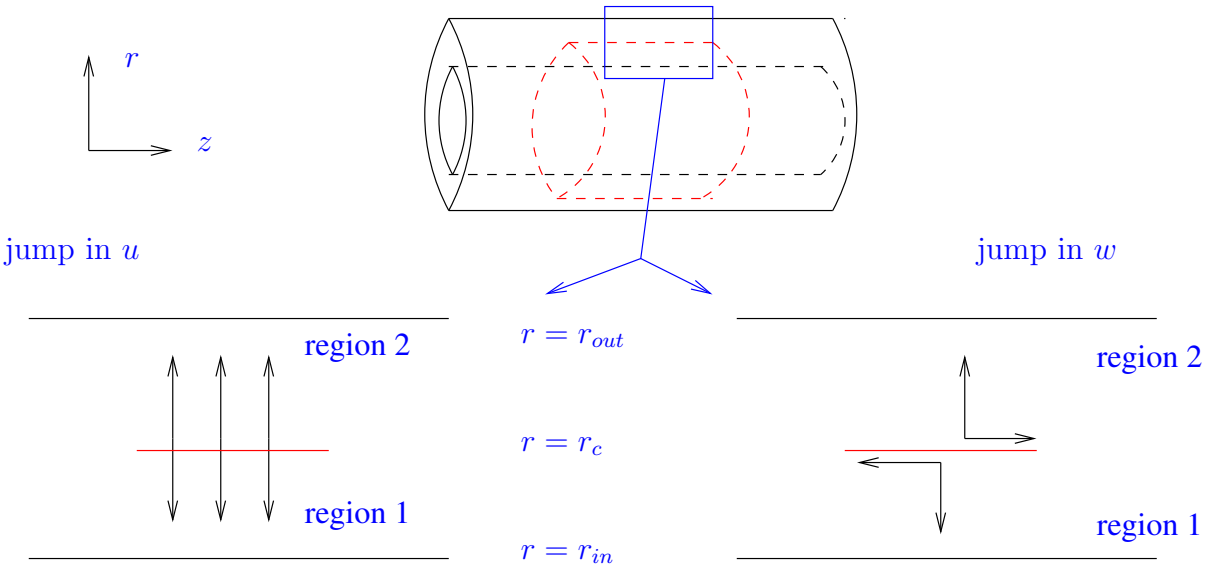

Figure 4.1: Displacement is decomposed into normal and tangential directions.

with boundary condition and equilibrium equation

$$\boldsymbol{\sigma} \cdot \mathbf{n} = 0 \quad \text{at} \quad r = r_{out} \quad \text{and} \quad r = r_{in} \tag{4.3}$$

$$\text{div}\boldsymbol{\sigma} = 0 \tag{4.4}$$

where u is the displacement in radial direction, w is the displacement in axial direction, and $\mathbf{n}$ is the normal to the boundary.

Following are the details of the methods to solve the equilibrium equations with boundary and jump conditions. The strain tensor $\boldsymbol{\varepsilon}$ and stress tensor $\boldsymbol{\sigma}$ are functions of displacements u^u, w^u or u^w, w^w. Write the equilibrium equations $\text{div}\boldsymbol{\sigma} = 0$ in components to obtain 2 partial differential equations with variables u^u, w^u or u^w, w^w; secondly, we take the Fourier transform to change these PDE to ODE with the wave number g, and the variables are $\hat{u}^u, \hat{w}^u$ or $\hat{u}^w, \hat{w}^w$; thirdly, we solve these ODEs with boundary conditions and jump conditions by using analytical way or numerical way; finally, taking the inverse Fourier transform we obtain the solution for PDEs. The stress components are the functions of displacements u^u, w^u or u^w, w^w, hence when u^u, w^u and u^w, w^w are solved σ^u_{rz}, σ^w_{rr} and σ^u_{rz}, σ^w_{rr} will be calculated.

By solving these equations for 'jump in u' we get σ^u_{rr}, σ^u_{rz}, u^u, w^u, and solving them for 'jump in w' we obtain σ^w_{rr}, σ^w_{rz}, u^w, w^w.

Similar as last chapter we define $T = (T_r, T_z)$ as the traction on the crack, which is

decomposed into normal and tangential direction,

$$T_r = \int \sigma^u_{rr}(z-s,r)U(s)\,ds + \int \sigma^w_{rr}(z-s,r)W(s)\,ds, \tag{4.5}$$

$$T_z = \int \sigma^u_{rz}(z-s,r)U(s)\,ds + \int \sigma^w_{rz}(z-s,r)W(s)\,ds. \tag{4.6}$$

The displacement is decomposed into normal and tangential direction as

$$u = \int u^u(z-s,r)U(s)ds + \int u^w(z-s,r)W(s)ds, \tag{4.7}$$

$$w = \int w^u(z-s,r)U(s)ds + \int w^w(z-s,r)W(s)ds. \tag{4.8}$$

Hence if the traction (T_r, T_z) along the crack is given, the displacement (u, w) will be obtained. We use this method to calculate the displacements for the upper crack face, lower crack face, outer boundary and inner boundary. Then we plot them on one figure to get the crack profile.

4.2 Static tears for an axisymmetric crack problem in a linear compressible cylindrical tube

The strain tensor is

$$\boldsymbol{\varepsilon} = \begin{bmatrix} u_{,r} & 0 & \frac{u_{,z}+w_{,r}}{2} \\ 0 & \frac{u}{r} & 0 \\ \frac{u_{,z}+w_{,r}}{2} & 0 & w_{,z} \end{bmatrix}. \tag{4.9}$$

And the stress tensor is

$$\boldsymbol{\sigma} = \begin{bmatrix} (\lambda+2\mu)\,u_{,r} + \lambda\left(\frac{u}{r}+w_{,z}\right) & 0 & \mu\,(u_{,z}+w_{,r}) \\ 0 & (\lambda+2\mu)\,\frac{u}{r} + \lambda\,(u_{,r}+w_{,z}) & 0 \\ \mu\,(u_{,z}+w_{,r}) & 0 & (\lambda+2\mu)\,w_{,z} + \lambda\left(u_{,r}+\frac{u}{r}\right) \end{bmatrix} \tag{4.10}$$

Define the Poisson's ratio

$$\nu = \frac{\lambda}{2\,(\lambda+\mu)} \tag{4.11}$$

so that $\lambda = 2\mu\nu/(1-2\nu)$.

$$\begin{aligned}
\sigma_{rr} &= (\lambda+2\mu)\,u_{,r} + \lambda\left(\frac{u}{r}+w_{,z}\right) = \frac{2\mu}{1-2\nu}\left[(1-\nu)\,u_{,r} + \nu\left(\frac{u}{r}+w_{,z}\right)\right] \\
\sigma_{rz} &= 2\mu\frac{u_{,z}+w_{,r}}{2} \\
\sigma_{\theta\theta} &= (\lambda+2\mu)\,\frac{u}{r} + \lambda\,(u_{,r}+w_{,z}) = \frac{2\mu}{1-2\nu}\left[(1-\nu)\,\frac{u}{r} + \nu\,(u_{,r}+w_{,z})\right] \\
\sigma_{zr} &= 2\mu\frac{u_{,z}+w_{,r}}{2} \\
\sigma_{zz} &= (\lambda+2\mu)\,w_{,z} + \lambda\left(\frac{u}{r}+u_{,r}\right) = \frac{2\mu}{1-2\nu}\left[(1-\nu)\,w_{,z} + \nu\left(\frac{u}{r}+u_{,r}\right)\right] \qquad (4.12)
\end{aligned}$$

The equilibrium for Cauchy stress is (4.4) and the boundary conditions (4.3) are

$$\sigma_{rr} = 0 \quad \text{and} \quad \sigma_{rz} = 0 \quad \text{at} r = r_{\text{in}},$$
$$\sigma_{rr} = 0 \quad \text{and} \quad \sigma_{rz} = 0 \quad \text{at} r = r_{\text{out}}.$$

The jump conditions on the crack faces are (4.1) and (4.2).

4.2.1 Jump in w across the crack

The symmetry of the problem gives $u(r,-z) = -u(r,z)$, hence the Fourier and inverse transformation for the displacement u are

$$\hat{u}(g,r) = \mathcal{F}_s[u] = -2i\int_0^\infty u(r,z)\sin gz dz, \qquad (4.13)$$
$$u(r,z) = \mathcal{F}_s^{-1}[\hat{u}] = \frac{i}{\pi}\int_0^\infty \hat{u}(g,z)\sin gz dg. \qquad (4.14)$$

Since $w(-r,z) = w(r,z)$ the Fourier and inverse transformation for displacement w are

$$\hat{w}(g,r) = \mathcal{F}_c[w] = 2\int_0^\infty w(r,z)\cos gz dz, \qquad (4.15)$$
$$w(r,z) = \mathcal{F}_c^{-1}[\hat{w}] = \frac{1}{\pi}\int_0^\infty \hat{w}(g,r)\cos gz dg. \qquad (4.16)$$

The stress σ_{rr} is given by

$$\sigma_{rr} = \frac{2\mu}{1-2\nu}\left[(1-\nu)\,u_{,r} + \nu\left(\frac{u}{r}+w_{,z}\right)\right], \qquad (4.17)$$

where

$$u_{,r}(r,z) = \frac{i}{\pi}\int_0^\infty \hat{u}_{,r}(g,r)\sin gz dg, \quad u(r,z) = \frac{i}{\pi}\int_0^\infty \hat{u}(g,r)\sin gz dg, \qquad (4.18)$$
$$w_{,z}(r,z) = -\frac{1}{\pi}\int_0^\infty \hat{w}(g,r) g \sin gz dg. \qquad (4.19)$$

Hence

$$\begin{aligned}\sigma_{rr} &= \frac{2\mu}{1-2\nu}\frac{1}{\pi}\int_0^\infty \left[(1-\nu)\, i\hat{u}_{,r} + \nu\left(\frac{i\hat{u}}{r} - g\hat{w}\right)\right]\sin gz dg \\ &= \frac{2\mu}{1-2\nu}\frac{1}{\pi}\int_0^\infty \left[(1-\nu)\, i\mathcal{F}[u_{,r}] + \nu\left(\frac{i\mathcal{F}[u]}{r} + i\mathcal{F}[w_{,z}]\right)\right]\sin gz dg \\ &= \frac{i}{\pi}\int_0^\infty \mathcal{F}[\sigma_{rr}]\sin gz dg = \frac{i}{\pi}\int_0^\infty \hat{\sigma}_{rr}(g,r)\sin gz dg. \end{aligned} \tag{4.20}$$

Using the symmetry of the domain in z, we express the displacements and the stresses as

$$\begin{aligned} u(r,z) &= \frac{i}{\pi}\int_0^\infty \hat{u}(g,r)\sin gz\, dg = \frac{1}{\pi}\int_0^\infty \hat{U}^w(g,r)\sin gz\, dg, \\ w(r,z) &= \frac{1}{\pi}\int_0^\infty \hat{w}(g,r)\cos gz\, dg = \frac{1}{\pi}\int_0^\infty \hat{W}^w(g,r)\cos gz\, dg, \\ \sigma_{rr}(r,z) &= \frac{i}{\pi}\int_0^\infty \hat{\sigma}_{rr}(g,r)\sin gz\, dg = \frac{1}{\pi}\int_0^\infty \hat{\sigma}^w_{rr}(g,r)\sin gz\, dg, \\ \sigma_{rz}(r,z) &= \frac{1}{\pi}\int_0^\infty \hat{\sigma}_{rz}(g,r)\cos gz\, dg = \frac{1}{\pi}\int_0^\infty \hat{\sigma}^w_{rz}(g,r)\cos gz\, dg, \\ \sigma_{\theta\theta}(r,z) &= \frac{i}{\pi}\int_0^\infty \hat{\sigma}_{\theta\theta}(g,r)\sin gz\, dg = \frac{1}{\pi}\int_0^\infty \hat{\sigma}^w_{\theta\theta}(g,r)\sin gz\, dg, \\ \sigma_{zr}(r,z) &= \frac{1}{\pi}\int_0^\infty \hat{\sigma}_{zr}(g,r)\cos gz\, dg = \frac{1}{\pi}\int_0^\infty \hat{\sigma}^w_{zr}(g,r)\cos gz\, dg, \\ \sigma_{zz}(r,z) &= \frac{i}{\pi}\int_0^\infty \hat{\sigma}_{zz}(g,r)\sin gz\, dg = \frac{1}{\pi}\int_0^\infty \hat{\sigma}^w_{zz}(g,r)\sin gz\, dg, \end{aligned} \tag{4.21}$$

where

$$\hat{U}^w = i\hat{u}, \quad \hat{W}^w = \hat{w}, \quad \hat{\sigma}^w_{rr} = i\hat{\sigma}_{rr}, \quad \hat{\sigma}^w_{rz} = \hat{\sigma}_{rz}, \quad \hat{\sigma}^w_{\theta\theta} = i\hat{\sigma}_{\theta\theta}, \quad \hat{\sigma}^w_{zr} = \hat{\sigma}_{zr}, \quad \hat{\sigma}^w_{zz} = i\hat{\sigma}_{zz}. \tag{4.22}$$

The stress components (4.12) after Fourier transform are

$$\frac{\mathcal{F}[\sigma_{rr,r}]}{2\mu} = \frac{1}{1-2\nu}\left[(1-\nu)\,\mathcal{F}[u_{,rr}] + \nu\left(\frac{\mathcal{F}[u_{,r}]}{r} - \frac{\mathcal{F}[u]}{r^2} + \mathcal{F}[w_{,rz}]\right)\right], \tag{4.23}$$

$$\frac{\mathcal{F}[\sigma_{zr,z}]}{2\mu} = \frac{1}{2}\left(\mathcal{F}[u_{,zz}] + \mathcal{F}[w_{,rz}]\right), \tag{4.24}$$

$$\frac{\mathcal{F}[\sigma_{rz,r}]}{2\mu} = \frac{1}{2}\left(\mathcal{F}[u_{,zr}] + \mathcal{F}[w_{,rr}]\right), \tag{4.25}$$

$$\frac{\mathcal{F}[\sigma_{zz,z}]}{2\mu} = \frac{1}{1-2\nu}\left[(1-\nu)\,\mathcal{F}[w_{,zz}] + \nu\left(\frac{\mathcal{F}[u_{,z}]}{r} + \mathcal{F}[u_{,rz}]\right)\right]. \tag{4.26}$$

Write the equilibrium equation (4.4) into components

$$\mathcal{F}[\sigma_{rr,r}] + \mathcal{F}[\sigma_{zr,z}] + \frac{\mathcal{F}[\sigma_{rr}] - \mathcal{F}[\sigma_{\theta\theta}]}{r} = 0, \tag{4.27}$$

$$\mathcal{F}[\sigma_{rz,r}] + \mathcal{F}[\sigma_{zz,z}] + \frac{\mathcal{F}[\sigma_{rz}]}{r} = 0. \tag{4.28}$$

Replace them in terms of $\hat{U}^w$ and $\hat{W}^w$

$$2(1-\nu)\left(\hat{U}^w\right)'' + 2(1-\nu)\frac{\left(\hat{U}^w\right)'}{r} - g^2(1-2\nu)\hat{U}^w - 2(1-\nu)\frac{\hat{U}^w}{r^2} - g\left(\hat{W}^w\right)' = 0,$$

$$(1-2\nu)\left(\hat{W}^w\right)'' + (1-2\nu)\frac{\left(\hat{W}^w\right)'}{r} - 2(1-\nu)g^2\hat{W}^w + g\left(\hat{U}^w\right)' + g\frac{\hat{U}^w}{r} = 0.$$

The boundary conditions (4.3) translate to

$$(1-\nu)\left(\hat{U}^w\right)' + \nu\left(\frac{\hat{U}^w}{r} - gW^w\right) = 0 \quad and \quad gU^w + \left(\hat{W}^w\right)' = 0. \tag{4.29}$$

The jump conditions (4.1) and (4.2) are

$$\left[\hat{U}^w\right]_-^+ = 0, \qquad \left[\hat{W}^w\right]_-^+ = 1, \qquad [\hat{\sigma}^w_{rr}]_-^+ = [\hat{\sigma}^w_{rz}]_-^+ = 0. \tag{4.30}$$

4.2.2 Jump in u across the crack

Symmetry of the problem gives $w(-r,z) = -w(r,z)$, hence the Fourier and inverse transformation for the displacement w are

$$\hat{w}(g,r) = \mathcal{F}_s[w] = -2i\int_0^\infty w(r,z)\sin gz dz, \tag{4.31}$$

$$w(r,z) = \mathcal{F}_s^{-1}[\hat{w}] = \frac{i}{\pi}\int_0^\infty \hat{w}(g,r)\sin gz dg. \tag{4.32}$$

Since $u(-r,z) = u(r,z)$ the Fourier and inverse transformation for the displacement u are

$$\hat{u}(g,r) = \mathcal{F}_c[u] = 2\int_0^\infty u(r,z)\cos gz dz, \tag{4.33}$$

$$u(r,z) = \mathcal{F}_c^{-1}[\hat{u}] = \frac{1}{\pi}\int_0^\infty \hat{u}(g,r)\cos gz dg. \tag{4.34}$$

The stress σ_{rr} is

$$\sigma_{rr} = \frac{2\mu}{1-2\nu}\left[(1-\nu)u_{,r} + \nu\left(\frac{u}{r} + w_{,z}\right)\right], \tag{4.35}$$

where

$$u_{,r}(r,z) = \frac{1}{\pi}\int_0^\infty \hat{u}_{,r}(g,r)\cos gz dg, \quad u(r,z) = \frac{1}{\pi}\int_0^\infty \hat{u}(g,r)\cos gz dg, \tag{4.36}$$

$$w_{,z}(r,z) = \frac{i}{\pi}\int_0^\infty \hat{w}(g,r)g\cos gz dg. \tag{4.37}$$

Hence

$$\sigma_{rr} = \frac{2\mu}{1-2\nu}\frac{1}{\pi}\int_0^\infty \left[(1-\nu)\hat{u}_{,r} + \nu\left(\frac{\hat{u}}{r} + ig\hat{w}\right)\right]\cos gz dg \tag{4.38}$$

$$= \frac{2\mu}{1-2\nu}\frac{1}{\pi}\int_0^\infty \left[(1-\nu)\mathcal{F}[u_{,r}] + \nu\left(\frac{\mathcal{F}[u]}{r} + \mathcal{F}[w_{,z}]\right)\right]\cos gz dg \tag{4.39}$$

$$= \frac{1}{\pi}\int_0^\infty \mathcal{F}[\sigma_{rr}]\cos gz dg = \frac{1}{\pi}\int_0^\infty \hat{\sigma}_{rr}\cos gz dg. \tag{4.40}$$

Using the symmetry of the domain in z, we express the displacements and the stresses as

$$\begin{aligned}
u(r,z) &= \frac{1}{\pi}\int_0^\infty \hat{u}(g,r)\cos gz\,dg = \frac{1}{\pi}\int_0^\infty \hat{U}^u(g,r)\cos gz\,dg,\\
w(r,z) &= \frac{i}{\pi}\int_0^\infty \hat{w}(g,r)\sin gz\,dg = \frac{1}{\pi}\int_0^\infty \hat{W}^u(g,r)\sin gz\,dg,\\
\sigma_{rr}(r,z) &= \frac{1}{\pi}\int_0^\infty \hat{\sigma}_{rr}(g,r)\cos gz\,dg = \frac{1}{\pi}\int_0^\infty \hat{\sigma}^u_{rr}(g,r)\cos gz\,dg,\\
\sigma_{rz}(r,z) &= \frac{i}{\pi}\int_0^\infty \hat{\sigma}_{rz}(g,r)\sin gz\,dg = \frac{1}{\pi}\int_0^\infty \hat{\sigma}^u_{rz}(g,r)\sin gz\,dg,\\
\sigma_{\theta\theta}(r,z) &= \frac{1}{\pi}\int_0^\infty \hat{\sigma}_{\theta\theta}(g,r)\cos gz\,dg = \frac{1}{\pi}\int_0^\infty \hat{\sigma}^u_{\theta\theta}(g,r)\cos gz\,dg,\\
\sigma_{zr}(r,z) &= \frac{i}{\pi}\int_0^\infty \hat{\sigma}_{zr}(g,r)\sin gz\,dg = \frac{1}{\pi}\int_0^\infty \hat{\sigma}^u_{zr}(g,r)\sin gz\,dg,\\
\sigma_{zz}(r,z) &= \frac{1}{\pi}\int_0^\infty \hat{\sigma}_{zz}(g,r)\cos gz\,dg = \frac{1}{\pi}\int_0^\infty \hat{\sigma}^u_{zz}(g,r)\cos gz\,dg,
\end{aligned} \tag{4.41}$$

where we define

$$\hat{U}^u = \hat{u},\quad \hat{W}^u = i\hat{w},\quad \hat{\sigma}^u_{rr} = \hat{\sigma}_{rr},\quad \hat{\sigma}^u_{rz} = i\hat{\sigma}_{rz},\quad \hat{\sigma}^u_{\theta\theta} = \hat{\sigma}_{\theta\theta},\quad \hat{\sigma}^u_{zr} = i\hat{\sigma}_{zr},\quad \hat{\sigma}^u_{zz} = \hat{\sigma}_{zz}. \tag{4.42}$$

The stress components (4.12) after Fourier transform are

$$\frac{\mathcal{F}[\sigma_{rr,r}]}{2\mu} = \frac{1}{1-2\nu}\left[(1-\nu)\,\mathcal{F}[u_{,rr}] + \nu\left(\frac{\mathcal{F}[u_{,r}]}{r} - \frac{\mathcal{F}[u]}{r^2} + \mathcal{F}[w_{,rz}]\right)\right], \tag{4.43}$$

$$\frac{\mathcal{F}[\sigma_{zr,z}]}{2\mu} = \frac{1}{2}\left(\mathcal{F}[u_{,zz}] + \mathcal{F}[w_{,rz}]\right), \tag{4.44}$$

$$\frac{\mathcal{F}[\sigma_{rz,r}]}{2\mu} = \frac{1}{2}\left(\mathcal{F}[u_{,zr}] + \mathcal{F}[w_{,rr}]\right), \tag{4.45}$$

$$\frac{\mathcal{F}[\sigma_{zz,z}]}{2\mu} = \frac{1}{1-2\nu}\left[(1-\nu)\,\mathcal{F}[w_{,zz}] + \nu\left(\frac{\mathcal{F}[u_{,z}]}{r} + \mathcal{F}[u_{,rz}]\right)\right], \tag{4.46}$$

and the equilibrium equation (4.4) written into components are

$$\mathcal{F}[\sigma_{rr,r}] + \mathcal{F}[\sigma_{zr,z}] + \frac{\mathcal{F}[\sigma_{rr}] - \mathcal{F}[\sigma_{\theta\theta}]}{r} = 0, \tag{4.47}$$

$$\mathcal{F}[\sigma_{rz,r}] + \mathcal{F}[\sigma_{zz,z}] + \frac{\mathcal{F}[\sigma_{rz}]}{r} = 0. \tag{4.48}$$

These equations in terms of $\hat{U}^u$ and $\hat{W}^u$ are

$$2(1-\nu)\left(\hat{U}^u\right)'' + 2(1-\nu)\frac{\left(\hat{U}^u\right)'}{r} - g^2(1-2\nu)\hat{U}^u - 2(1-\nu)\frac{\hat{U}^u}{r^2} + g\left(\hat{W}^u\right)' = 0,$$

$$(1-2\nu)\left(\hat{W}^u\right)'' + (1-2\nu)\frac{\left(\hat{W}^u\right)'}{r} - 2(1-\nu)g^2\hat{W}^u - g\left(\hat{U}^u\right)' - g\frac{\hat{U}^u}{r} = 0.$$

The boundary conditions (4.3) translate to

$$(1-\nu)\left(\hat{U}^u\right)' + \nu\left(\frac{\hat{U}^u}{r} + gW^u\right) = 0 \quad \text{and} \quad gU^u - \left(\hat{W}^u\right)' = 0 \tag{4.49}$$

The jump conditions (4.1) and (4.2) are

$$\left[\hat{U}^u\right]_-^+ = 1, \qquad \left[\hat{W}^u\right]_-^+ = 0, \qquad [\hat{\sigma}^u_{rr}]_-^+ = [\hat{\sigma}^u_{rz}]_-^+ = 0. \tag{4.50}$$

4.2.3 Numerical solution—Collocation method

In this section we are going to solve $\hat{U}^w, \hat{W}^w, \hat{U}^u, \hat{W}^u$ and $\hat{\sigma}^w_{rr}, \hat{\sigma}^w_{rz}, \hat{\sigma}^u_{rr}, \hat{\sigma}^u_{rz}$ numerically. Now we assume $r_{in} = 1, r_{out} = 3$. We consider $g = 0$ separately, which will give singularity if we use the following collocation method.

As shown in Figure 4.1, region 1 is $r_{in} \le r \le r_c$ and region 2 is $r_c \le r \le r_{out}$.
In region 1, $r = r_{in} + R(r_c - r_{in})$ and $\dfrac{d}{dr} = \dfrac{1}{r_c - r_{in}} \dfrac{d}{dR}$; in region 2, $r = r_{out} + R(r_c - r_{out})$ and $\dfrac{d}{dr} = \dfrac{1}{r_c - r_{out}} \dfrac{d}{dR}$. The range of R is $[0, 1]$. The boundary in each region is represented by $R = 0$, and $R = 1$ represents the crack face.

Jump in w

Define Y_1, Y_2, Y_3, Y_4 to be $\hat{U}^w, (\hat{U}^w)', \hat{W}^w, (\hat{W}^w)'$ respectively in region 1, and Y_5, Y_6, Y_7, Y_8 to be $\hat{U}^w, (\hat{U}^w)', \hat{W}^w, (\hat{W}^w)'$ respectively in region 2. Referring to the equilibrium equations (4.29)

$$\begin{aligned}
\frac{dY_1}{dR} &= Y_2 \\
\frac{dY_2}{dR} &= -\frac{(r_c - r_{in})\, Y_2}{r_1} + \frac{g^2 (r_c - r_{in})^2 (1 - 2\nu)\, Y_1}{2(1 - \nu)} + \frac{(r_c - r_{in})^2 Y_1}{r_1^2} + \frac{g (r_c - r_{in})\, Y_4}{2(1 - \nu)} \\
\frac{dY_3}{dR} &= Y_4 \\
\frac{dY_4}{dR} &= -\frac{(r_c - r_{in})\, Y_4}{r_1} + \frac{2(1 - \nu)(r_c - r_{in})^2 g^2 Y_3}{(1 - 2\nu)} - \frac{g (r_c - r_{in})\, Y_2}{1 - 2\nu} - \frac{g (r_c - r_{in})^2 Y_1}{(1 - 2\nu)\, r_1} \\
\frac{dY_5}{dR} &= Y_6 \\
\frac{dY_6}{dR} &= -\frac{(r_c - r_{out})\, Y_6}{r_2} + \frac{g^2 (r_c - r_{out})^2 (1 - 2\nu)\, Y_5}{2(1 - \nu)} + \frac{(r_c - r_{out})^2 Y_5}{r_2^2} + \frac{g (r_c - r_{out})\, Y_8}{2(1 - \nu)} \\
\frac{dY_7}{dR} &= Y_8 \\
\frac{dY_8}{dR} &= -\frac{(r_c - r_{out})\, Y_8}{r_2} + \frac{2(1 - \nu)(r_c - r_{out})^2 g^2 Y_7}{(1 - 2\nu)} - \frac{g (r_c - r_{out})\, Y_6}{1 - 2\nu} - \frac{g (r_c - r_{out})^2 Y_5}{(1 - 2\nu)\, r_2}
\end{aligned}$$

The boundary conditions (4.29) on outer and inner boundaries, and jump conditions (4.30) on upper and lower crack faces are

$$\begin{aligned}
(1-\nu)\,Y_2+\nu\,(r_c-r_{in})\left(\frac{Y_1}{r_{in}}-gY_3\right)&=0\\
gY_1\,(r_c-r_{in})+Y_4&=0\\
(1-\nu)\,Y_6+\nu\,(r_c-r_{out})\left(\frac{Y_5}{r_{out}}-gY_7\right)&=0\\
gY_5\,(r_c-r_{out})+Y_8&=0\\
Y_5-Y_1&=0\\
Y_7-Y_3-1&=0\\
(1-\nu)\,Y_6+\nu\,(r_c-r_{out})\left(\frac{Y_5}{r_{out}}-gY_7\right)-\left[(1-\nu)\,Y_2+\nu\,(r_c-r_{in})\left(\frac{Y_1}{r_{in}}-gY_3\right)\right]&=0\\
gY_5\,(r_c-r_{out})+Y_8-\left[gY_1\,(r_c-r_{in})+Y_4\right]&=0.
\end{aligned}$$

We use the Matlab routine '`bvp4c`' to calculate the values of $Y_1, Y_2, Y_3, Y_4, Y_5, Y_6, Y_7, Y_8$, hence $\hat{U}^w, \hat{W}^w$ are obtained and $\hat{\sigma}^w_{rr}, \hat{\sigma}^w_{rz}$ are functions of $\hat{U}^w, \hat{W}^w$.

Jump in u

Define Y_1, Y_2, Y_3, Y_4 to be $\hat{U}^u, (\hat{U}^u)', \hat{W}^u, (\hat{W}^u)'$ respectively in region 1, and Y_5, Y_6, Y_7, Y_8 to be $\hat{U}^u, (\hat{U}^u)', \hat{W}^u, (\hat{W}^u)'$ respectively in region 2. Referring to the equilibrium equations (4.49)

$$\begin{aligned}
\frac{dY_1}{dR} &= Y_2\\
\frac{dY_2}{dR} &= -\frac{(r_c-r_{in})\,Y_2}{r_1}+\frac{g^2\,(r_c-r_{in})^2\,(1-2\nu)\,Y_1}{2(1-\nu)}+\frac{(r_c-r_{in})^2\,Y_1}{r_1^2}-\frac{g\,(r_c-r_{in})\,Y_4}{2(1-\nu)}\\
\frac{dY_3}{dR} &= Y_4\\
\frac{dY_4}{dR} &= -\frac{(r_c-r_{in})\,Y_4}{r_1}+\frac{2(1-\nu)\,(r_c-r_{in})^2\,g^2Y_3}{(1-2\nu)}+\frac{g\,(r_c-r_{in})\,Y_2}{1-2\nu}+\frac{g\,(r_c-r_{in})^2\,Y_1}{(1-2\nu)\,r_1}\\
\frac{dY_5}{dR} &= Y_6\\
\frac{dY_6}{dR} &= -\frac{(r_c-r_{out})\,Y_6}{r_2}+\frac{g^2\,(r_c-r_{out})^2\,(1-2\nu)\,Y_5}{2(1-\nu)}+\frac{(r_c-r_{out})^2\,Y_5}{r_2^2}-\frac{g\,(r_c-r_{out})\,Y_8}{2(1-\nu)}\\
\frac{dY_7}{dR} &= Y_8\\
\frac{dY_8}{dR} &= -\frac{(r_c-r_{out})\,Y_8}{r_2}+\frac{2(1-\nu)\,(r_c-r_{out})^2\,g^2Y_7}{(1-2\nu)}+\frac{g\,(r_c-r_{out})\,Y_6}{1-2\nu}+\frac{g\,(r_c-r_{out})^2\,Y_5}{(1-2\nu)\,r_2}
\end{aligned}$$

The boundary conditions (4.49) on outer and inner boundaries, and jump conditions (4.50) on upper and lower crack faces are

$$\begin{aligned}
(1-\nu)\,Y_2+\nu\,(r_c-r_{in})\left(\frac{Y_1}{r_{in}}+gY_3\right)&=0\\
gY_1\,(r_c-r_{in})-Y_4&=0\\
(1-\nu)\,Y_6+\nu\,(r_c-r_{out})\left(\frac{Y_5}{r_{out}}+gY_7\right)&=0\\
gY_5\,(r_c-r_{out})-Y_8&=0\\
Y_5-Y_1-1&=0\\
Y_7-Y_3&=0\\
(1-\nu)\,Y_6+\nu\,(r_c-r_{out})\left(\frac{Y_5}{r_{out}}+gY_7\right)-\left[(1-\nu)\,Y_2+\nu\,(r_c-r_{in})\left(\frac{Y_1}{r_{in}}+gY_3\right)\right]&=0\\
-gY_5\,(r_c-r_{out})+Y_8-\left[-gY_1\,(r_c-r_{in})+Y_4\right]&=0.
\end{aligned}$$

We use the Matlab routine '`bvp4c`' to calculate the values of $Y_1, Y_2, Y_3, Y_4, Y_5, Y_6, Y_7, Y_8$, hence $\hat{U}^u, \hat{W}^u$ are obtained, and $\hat{\sigma}^u_{rr}, \hat{\sigma}^u_{rz}$ are functions of $\hat{U}^u, \hat{W}^u$.

4.2.4 The case when $g = 0$

The calculation of $\hat{U}^w, \hat{W}^w, \hat{\sigma}^w_{rr}, \hat{\sigma}^w_{rz}$ and $\hat{U}^u, \hat{W}^u, \hat{\sigma}^u_{rr}, \hat{\sigma}^u_{rz}$ when $g = 0$ must be solved separately.

Jump in w when $g = 0$

Equations (4.29) become

$$2\,(1-\nu)\left(\hat{U}^w\right)''+2\,(1-\nu)\,\frac{\left(\hat{U}^w\right)'}{r}-2\,(1-\nu)\,\frac{\hat{U}^w}{r^2}=0, \tag{4.51}$$

$$(1-2\nu)\left(\hat{W}^w\right)''+(1-2\nu)\,\frac{\left(\hat{W}^w\right)'}{r}=0. \tag{4.52}$$

Hence the solution for $\hat{U}^w$ and $\hat{W}^w$ are

$$\hat{U}^w=Ar+\frac{B}{r},\quad \text{and}\quad \hat{W}^w=C\log(r)+D.$$

Put the solutions into the boundary conditions (4.29) on inner and outer layers and the jump conditions (4.30) we get

$$A_1=0,\quad B_1=0,\quad C_1=0,\quad D_1=-\frac{1}{2},\quad A_2=0,\quad B_2=0,\quad C_2=0,\quad D_2=\frac{1}{2},$$

where subscript '1' means region '1', and subscript '1' means region '2'.
Hence the displacements on the upper crack face are $\hat{U}=0$ and $\hat{W}=\frac{1}{2}$; the displacements

on the lower crack face are $\hat{U} = 0$ and $\hat{W} = -\frac{1}{2}$; the displacements on the outside boundary are $\hat{U} = 0$ and $\hat{W} = \frac{1}{2}$; the displacements on the inside boundary are $\hat{U} = 0$ and $\hat{W} = -\frac{1}{2}$; on the crack face $\hat{\sigma}_{rr} = 0$ and $\hat{\sigma}_{rz} = 0$.

Jump in u when $g = 0$

Equations (4.49) become

$$2(1-\nu)\left(\hat{U}^u\right)'' + 2(1-\nu)\frac{\left(\hat{U}^u\right)'}{r} - 2(1-\nu)\frac{\hat{U}^u}{r^2} = 0, \tag{4.53}$$

$$(1-2\nu)\left(\hat{W}^u\right)'' + (1-2\nu)\frac{\left(\hat{W}^u\right)'}{r} = 0. \tag{4.54}$$

Hence the solution for $\hat{U}^u$ and $\hat{W}^u$ are

$$\begin{aligned} \hat{U}^u &= Ar + \frac{B}{r}, \\ \hat{W}^u &= C\log(r) + D. \end{aligned}$$

Put the solutions into the boundary conditions (4.49) on inner and outer layers and the jump conditions (4.50) we get

$$\begin{aligned} A_1 &= -\frac{1}{2}\frac{(r_{out}^2 - r_{in}^2)(-1+2\nu)}{r_c(r_{out}^2 - r_{in}^2)(\nu-1)}, \quad B_1 = \frac{1}{2}\frac{r_{in}^2(r_{out}^2 - r_c^2)}{r_c(r_{out}^2 - r_{in}^2)(\nu-1)}, \quad C_1 = 0, \quad D_1 = 0, \\ A_2 &= -\frac{1}{2}\frac{(r_{in}^2 - r_c^2)(-1+2\nu)}{r_c(r_{out}^2 - r_{in}^2)(\nu-1)}, \quad B_2 = \frac{1}{2}\frac{r_{out}^2(r_{in}^2 - r_c^2)}{r_c(r_{out}^2 - r_{in}^2)(\nu-1)}, \quad C_2 = 0, \quad D_2 = 0. \end{aligned}$$

Hence the displacements on the upper crack face are

$$\hat{U} = \frac{1}{2}\frac{(r_{in}^2 - r_c^2)(r_c^2 - 2r_c^2\nu + r_{out}^2)}{r_c^2(r_{out}^2 - r_{in}^2)(\nu-1)}, \quad \hat{W} = 0, \tag{4.55}$$

the displacements on the lower crack face are

$$\hat{U} = \frac{1}{2}\frac{(r_{out}^2 - r_c^2)(r_c^2 - 2r_c^2\nu + r_{in}^2)}{r_c^2(r_{out}^2 - r_{in}^2)(\nu-1)}, \quad \hat{W} = 0, \tag{4.56}$$

the displacements on the outside boundary are

$$\hat{U} = -\frac{(r_{in}^2 - r_c^2)r_{out}}{(r_{out}^2 - r_{in}^2)r_c}, \quad \hat{W} = 0, \tag{4.57}$$

the displacements on the inside boundary are

$$\hat{U} = -\frac{(r_{out}^2 - r_c^2)r_{in}}{(r_{out}^2 - r_{in}^2)r_c}, \quad \hat{W} = 0, \tag{4.58}$$

on the crack face

$$\hat{\sigma}_{rr} = \frac{1}{2}\frac{(r_{out}^2 - r_c^2)(r_c^2 - r_{in}^2)(1-2\nu)}{r_c^3(r_{out}^2 - r_{in}^2)(\nu-1)}, \quad \hat{\sigma}_{rz} = 0. \tag{4.59}$$

4.2.5 Matrix equations

We obtain $\hat{U}^w(g,r), \hat{W}^w(g,r), \hat{U}^u(g,r), \hat{W}^u(g,r)$ and $\hat{\sigma}^w_{rr}(g,r), \hat{\sigma}^w_{rz}(g,r), \hat{\sigma}^u_{rr}(g,r), \hat{\sigma}^u_{rz}(g,r)$ for each g from above numerical approach. Now we assume the length of the crack is L, and the length of the strip is $3L$. The traction and displacement components, decomposed into normal and tangential direction, are

$$T_r = \int \sigma^u_{rr}(z_i - s, r)U(s)\,ds + \int \sigma^w_{rr}(z_i - s, r)W(s)\,ds, \tag{4.60}$$

$$T_z = \int \sigma^u_{rz}(z_i - s, r)U(s)\,ds + \int \sigma^w_{rz}(z_i - s, r)W(s)\,ds. \tag{4.61}$$

$$u = \int u^u(z_i - s, r)U(s)ds + \int u^w(z_i - s, r)W(s)ds \tag{4.62}$$

$$w = \int w^u(z_i - s, r)U(s)ds + \int w^w(z_i - s, r)W(s)ds \tag{4.63}$$

We discretize the integral equations (4.60) and (4.61) assuming piecewise constant openings along a crack of length L. We evaluate the integral equation at a discrete set of points $z_i, i = 1, ..., N$.

For the second term in the RHS of equation (4.60) we have

$$\begin{aligned}
\int \sigma^w_{rr}(z_i - s, r)W(s)\,ds &= \int \left[\frac{1}{\pi}\int_0^\infty \hat{\sigma}^w_{rr}(g,r)\sin g(z_i - s)\,dg\right] W(s)\,ds \\
&= \frac{1}{\pi}\sum_j \int_j \left[\int_0^\infty \hat{\sigma}^w_{rr}(g,r)\sin g(z_i - s)\,dg\right] W_j\,ds \\
&= \frac{1}{\pi}\sum_j \int_j \left[\int_0^\infty \left(\hat{\sigma}^w_{rr}(g,r) - g\sigma^{w1}_{rr} - \sigma^{w0}_{rr}\right)\sin g(z_i - s)\,dg\right] W_j\,ds \\
&+ \frac{1}{\pi}\sum_j \int_j \left[\int_0^\infty g\sigma^{w1}_{rr}\sin g(z_i - s)\,dg\right] W_j\,ds \\
&+ \frac{1}{\pi}\sum_j \int_j \left[\int_0^\infty \sigma^{w0}_{rr}\sin g(z_i - s)\,dg\right] W_j\,ds,
\end{aligned}$$

where

$$\begin{aligned}
&\int_j \left[\int_0^\infty (\hat{\sigma}^w_{rr}(g,r) - g\sigma^{w1}_{rr} - \dot{S}^{w0}_{rr})\sin g(z_i - s)\,dg\right] W_j\,ds \\
&= W_j \int_0^\infty (\hat{\sigma}^w_{rr} - g\sigma^{w1}_{rr} - \sigma^{w0}_{rr})\left[\int_j \sin g(z_i - s)\,ds\right] dg
\end{aligned}$$

and

$$\int_j \sin g(z_i - s)\,ds = \int_{z_j - \Delta}^{z_j + \Delta} \sin g(z_i - s)\,ds = 2\frac{\sin g\Delta}{g}\sin g(z_i - z_j),$$

in which $\Delta = \frac{L}{N}$. Then using equation (3.101) we have

$$\frac{1}{\pi}\int_0^\infty g\sigma_{rr}^{w1}\sin g\,(z_i-s)\,dg = \frac{\sigma_{rr}^{w1}}{\pi}\lim_{r\to 0^+}\int_0^\infty ge^{-gr}\sin g\,(z_i-s)\,dg \quad = \sigma_{rr}^{w1}\delta'(z_i-s),$$

and using equation (3.102) we have

$$\frac{1}{\pi}\int_0^\infty \sigma_{rr}^{w0}\sin g\,(z_i-s)\,dg = \frac{\sigma_{rr}^{w0}}{\pi}\lim_{r\to 0^+}\int_0^\infty e^{-gr}\sin g\,(z_i-s)\,dg \quad = \frac{\sigma_{rr}^{w0}}{\pi(z_i-s)}.$$

Then using (3.167) and (3.168)

$$\begin{aligned}\int \sigma_{rr}^{w}\,(z_i-s,r)W\,(s)\,ds &= 2\frac{1}{\pi}\sum_j W_j\int_0^\infty\left(\hat{\sigma}_{rr}^{w}\,(g,r)-g\sigma_{rr}^{w1}-\sigma_{rr}^{w0}\right)\frac{\sin g\Delta}{g}\sin g(z_i-z_j)\,dg\\ &+ \sigma_{rr}^{w0}\sum_j W_j\frac{1}{\pi}\log|\frac{z_i-z_j+\Delta}{z_i-z_j-\Delta}|,\end{aligned}$$

which is the form of $\sum_j \sigma_{rr}^{w}[i,j]W_j$ and

$$\sigma_{rr}^{w}[i,j] = 2\frac{1}{\pi}\int_0^\infty\left(\hat{\sigma}_{rr}^{w}\,(g,r)-g\sigma_{rr}^{w1}-\sigma_{rr}^{w0}\right)\frac{\sin g\Delta}{g}\sin g(z_i-z_j)\,dg+\sigma_{rr}^{w0}\frac{1}{\pi}\log|\frac{z_i-z_j+\Delta}{z_i-z_j-\Delta}|.$$

For the first term in the RHS of equation (4.60), in which we use (3.99), (3.100), (3.165) and (3.166), we have

$$\begin{aligned}\int \sigma_{rr}^{u}\,(z_i-s,r)U\,(s)\,ds &= \int\left[\frac{1}{\pi}\int_0^\infty\hat{\sigma}_{rr}^{u}\,(g,r)\cos g\,(z_i-s)\,dg\right]U\,(s)\;ds\\ &= \frac{1}{\pi}\sum_j\int_j\left[\int_0^\infty\left(\hat{\sigma}_{rr}^{u}\,(g,r)-g\sigma_{rr}^{u1}-\sigma_{rr}^{u0}\right)\cos g\,(z_i-s)\,dg\right]U_j\,ds\\ &+ \frac{1}{\pi}\sum_j\int_j\left[\int_0^\infty g\sigma_{rr}^{u1}\cos g\,(z_i-s)\,dg\right]U_j\,ds\\ &+ \frac{1}{\pi}\sum_j\int_j\left[\int_0^\infty\sigma_{rr}^{u0}\cos g\,(z_i-s)\,dg\right]U_j\,ds\\ &= 2\frac{1}{\pi}\sum_j U_j\int_0^\infty\left(\hat{\sigma}_{rr}^{u}\,(g,r)-g\sigma_{rr}^{u1}-\sigma_{rr}^{u0}\right)\frac{\sin g\Delta}{g}\cos g(z_i-z_j)\,dg\\ &- \sigma_{rr}^{u1}\sum_j U_j\left[\frac{2\Delta}{\pi\left((z_i-z_j)^2-\Delta^2\right)}\right]\\ &+ \sigma_{rr}^{u0}\sum_j U_j I_{z_i\in(z_j-\Delta,z_j+\Delta)},\end{aligned}$$

which is the form of $\sum_j \sigma_{rr}^{u}[i,j]U_j$ and

$$\begin{aligned}\sigma_{rr}^{u}[i,j] &= 2\frac{1}{\pi}\int_0^\infty\left(\hat{\sigma}_{rr}^{u}\,(g,r)-g\sigma_{rr}^{u1}-\sigma_{rr}^{u0}\right)\frac{\sin g\Delta}{g}\cos g(z_i-z_j)\,dg\\ &- \sigma_{rr}^{u1}\left[\frac{2\Delta}{\pi\left((z_i-z_j)^2-\Delta^2\right)}\right]+\sigma_{rr}^{u0}\mathbf{I}_{z_i\in(z_j-\Delta,z_j+\Delta)}.\end{aligned}$$

For the second term in the RHS of equation (4.61), in which we use (3.99), (3.100), (3.165) and (3.166), we have

$$\begin{aligned}
\int \sigma_{rz}^{w}\left(z_i - s, r\right) W\left(s\right) ds &= \int \left[\frac{1}{\pi}\int_0^{\infty} \hat{\sigma}_{rz}^{w}\left(g, r\right) \cos g\left(z_i - s\right) dg\right] W\left(s\right)\, ds \\
&= \frac{1}{\pi}\sum_j \int_j \left[\int_0^{\infty} \left(\hat{\sigma}_{rz}^{w}\left(g, r\right) - g\sigma_{rz}^{w1} - \sigma_{rz}^{w0}\right) \cos g\left(z_i - s\right) dg\right] W_j\, ds \\
&+ \frac{1}{\pi}\sum_j \int_j \left[\int_0^{\infty} g\sigma_{rz}^{w1} \cos g\left(z_i - s\right) dg\right] W_j\, ds \\
&+ \frac{1}{\pi}\sum_j \int_j \left[\int_0^{\infty} \sigma_{rz}^{w0} \cos g\left(z_i - s\right) dg\right] W_j\, ds \\
&= 2\frac{1}{\pi}\sum_j W_j \int_0^{\infty} \left(\hat{\sigma}_{rz}^{w}\left(g, r\right) - g\sigma_{rz}^{w1} - g\sigma_{rz}^{w0}\right) \frac{\sin g\Delta}{g} \cos g(z_i - z_j)\, dg \\
&- \sigma_{rz}^{w1}\sum_j W_j \left[\frac{2\Delta}{\pi\left(\left(z_i - z_j\right)^2 - \Delta^2\right)}\right] \\
&+ \sigma_{rz}^{w0}\sum_j W_j \mathbf{I}_{z_i \in (z_j - \Delta, z_j + \Delta)},
\end{aligned}$$

which is the form of $\sum_j \sigma_{rz}^{w}[i,j] W_j$ and

$$\begin{aligned}
\sigma_{rz}^{w}[i,j] &= 2\frac{1}{\pi}\int_0^{\infty} \left(\hat{\sigma}_{rz}^{w}\left(g, r\right) - g\sigma_{rz}^{w1} - g\sigma_{rz}^{w0}\right) \frac{\sin g\Delta}{g} \cos g(z_i - z_j)\, dg \\
&- \sigma_{rz}^{w1}\left[\frac{2\Delta}{\pi\left(\left(z_i - z_j\right)^2 - \Delta^2\right)}\right] \\
&+ \sigma_{rz}^{w0} I_{z_i \in (z_j - \Delta, z_j + \Delta)}.
\end{aligned}$$

For the first term in the RHS of of equation (4.61), in which we use (3.101), (3.102), (3.167) and (3.168), we have

$$\begin{aligned}
\int \sigma_{rz}^{u}\left(z_i - s, r\right) U\left(s\right) ds &= 2\frac{1}{\pi}\sum_j U_j \int_0^{\infty} \left(\hat{\sigma}_{rz}^{u}\left(g, r\right) - g\sigma^{u1} - \sigma_{rz}^{u0}\right) \frac{\sin g\Delta}{g} \sin g(z_i - z_j)\, dg \\
&+ \sigma_{rz}^{u0}\sum_j U_j \frac{1}{\pi} \log\left|\frac{z_i - z_j + \Delta}{z_i - z_j - \Delta}\right|,
\end{aligned}$$

which is the form of $\sum_j \sigma_{rz}^{u}[i,j] U_j$ and

$$\begin{aligned}
\sigma_{rz}^{u}[i,j] &= 2\frac{1}{\pi}\int_0^{\infty} \left(\hat{\sigma}_{rz}^{u}\left(g, r\right) - g\sigma^{u1} - \sigma_{rz}^{u0}\right) \frac{\sin g\Delta}{g} \sin g(z_i - z_j)\, dg \\
&+ \sigma_{rz}^{u0}\frac{1}{\pi} \log\left|\frac{z_i - z_j + \Delta}{z_i - z_j - \Delta}\right|.
\end{aligned}$$

We write these integral equations (4.60) and (4.61) into the form of matrix equation

$$\begin{bmatrix} \mathrm{T}_{rj} \\ \mathrm{T}_{zj} \end{bmatrix} = \begin{bmatrix} \sigma^u_{rr}[i,j] & \sigma^w_{rr}[i,j] \\ \sigma^u_{rz}[i,j] & \sigma^w_{rz}[i,j] \end{bmatrix} \begin{bmatrix} U_j \\ W_j \end{bmatrix} \tag{4.64}$$

where $j = 1, ..., N$.

We discretize the integral equations (4.62) and (4.63) assuming piecewise constant openings along length L for upper, and lower crack faces and $3L$ for top and bottom boundaries. We evaluate the integral equation at a discrete set of points $z_i, i = 1, ..., N$ for upper and lower crack faces, and $z_i, i = 1, ..., 3N$ for top and bottom boundaries.

For the first term in the RHS of equation (4.62), in which we use (3.100) and (3.166), we have

$$\begin{aligned}
\int u^u(z_i - s, r)U(s)ds &= \frac{1}{\pi}\int\int_0^\infty \left(\hat{U}^u - u^{1u}\right)\cos g\,(z_i - s)\; dg\,U\,ds \\
&+ \frac{1}{\pi}\int\int_0^\infty u^{1u}\cos g\,(z_i - s)\; dg\,U\,ds \\
&= \frac{2}{\pi}\sum_j U_j \int_0^\infty (\hat{U}^u - u^{1u})\frac{\sin g\Delta}{g}\cos\left(gz_i - gz_j\right)dg \\
&+ u^{1u}\sum_j \int_j \lim_{r\to 0^+}\int_0^\infty e^{-gr}\cos g\,(z_i - s)\; dg\,U_j\,ds \\
&= \frac{2}{\pi}\sum_j U_j \int_0^\infty (\hat{U}^u - u^{1u})\frac{\sin g\Delta}{g}\cos\left(gz_i - gz_j\right)dg \\
&+ u^{1u}\sum_j U_j I_{z_i\in(z_j-\Delta, z_j+\Delta)}
\end{aligned}$$

which is the form of $\sum_j u^u[i,j]U_j$ and

$$\begin{aligned}
u^u[i,j] &= \frac{2}{\pi}\int_0^\infty (\hat{U}^u - u^{1u})\frac{\sin g\Delta}{g}\cos\left(gz_i - gz_j\right)dg \\
&+ u^{1u}I_{z_i\in(z_j-\Delta, z_j+\Delta)}.
\end{aligned}$$

For the first term in the RHS of equation (4.62), in which we use (3.102) and (3.168), we have

$$\begin{aligned}
\int u^w(z_i-s,r)W(s)ds &= \frac{1}{\pi}\int\int_0^\infty \left(\hat{U}^w - u^{1w}\right)\sin g\,(z_i-s)\;dg\,W\,ds \\
&+ \frac{1}{\pi}\int\int_0^\infty u^{1w}\sin g\,(z_i-s)\;dg\,W\,ds \\
&= \frac{2}{\pi}\sum_j W_j\int_0^\infty (\hat{U}^w - u^{1w})\frac{\sin g\Delta}{g}\sin\left(gz_i-gz_j\right)dg \\
&+ u^{1w}\sum_j\int_j \lim_{r\to 0^+}\int_0^\infty e^{-gr}\sin g\,(z_i-s)\;dg\,W_j\,ds \\
&= \frac{2}{\pi}\sum_j W_j\int_0^\infty (\hat{U}^w - u^{1w})\frac{\sin g\Delta}{g}\sin\left(gz_i-gz_j\right)dg \\
&+ \frac{u^{1w}}{\pi}\sum_j W_j\log\left|\frac{z_i-z_j+\Delta}{z_i-z_j-\Delta}\right|
\end{aligned}$$

which is the form of $\sum_j u^w[i,j]W_j$ and

$$\begin{aligned}
u^w[i,j] = &= \frac{2}{\pi}\int_0^\infty (\hat{U}^w - u^{1w})\frac{\sin g\Delta}{g}\sin\left(gz_i-gz_j\right)dg \\
&+ \frac{u^{1w}}{\pi}\log\left|\frac{z_i-z_j+\Delta}{z_i-z_j-\Delta}\right|
\end{aligned}$$

For the first term in the RHS of equation (4.63), in which we use (3.102) and (3.168), we have

$$\begin{aligned}
\int w^u(z_i-s,r)U(s)ds &= \frac{1}{\pi}\int\int_0^\infty \left(\hat{W}^u - w^{1u}\right)\sin g\,(z_i-s)\;dg\,U\,ds \\
&+ \frac{1}{\pi}\int\int_0^\infty w^{1u}\sin g\,(z_i-s)\;dg\,U\,ds \\
&= \frac{2}{\pi}\sum_j U_j\int_0^\infty (\hat{W}^u - w^{1u})\frac{\sin g\Delta}{g}\sin\left(gz_i-gz_j\right)dg \\
&+ w^{1u}\sum_j\int_j \lim_{r\to 0^+}\int_0^\infty e^{-gr}\sin g\,(z_i-s)\;dg\,U_j\,ds \\
&= \frac{2}{\pi}\sum_j U_j\int_0^\infty (\hat{W}^u - w^{1u})\frac{\sin g\Delta}{g}\sin\left(gz_i-gz_j\right)dg \\
&+ \frac{w^{1u}}{\pi}\sum_j U_j\log\left|\frac{z_i-z_j+\Delta}{z_i-z_j-\Delta}\right|
\end{aligned}$$

which is the form of $\sum_j w^u[i,j]U_j$ and

$$\begin{aligned}
w^u[i,j] &= \frac{2}{\pi}\int_0^\infty (\hat{W}^u - w^{1u})\frac{\sin g\Delta}{g}\sin\left(gz_i-gz_j\right)dg \\
&+ \frac{w^{1u}}{\pi}\log\left|\frac{z_i-z_j+\Delta}{z_i-z_j-\Delta}\right|.
\end{aligned}$$

For the first term in the RHS of equation (4.63), in which we use (3.100) and (3.166), we have

$$\begin{aligned}
\int w^w(z_i-s,r)W(s)ds &= \frac{1}{\pi}\int\int_0^\infty \left(\hat{W}^w - w^{1w}\right)\cos g\,(z_i-s)\;dg\,W\,ds \\
&+ \frac{1}{\pi}\int\int_0^\infty w^{1w}\cos g\,(z_i-s)\;dg\,W\,ds \\
&= \frac{2}{\pi}\sum_j W_j\int_0^\infty (\hat{W}^w - w^{1w})\frac{\sin g\Delta}{g}\cos\left(gz_i - gz_j\right)dg \\
&+ w^{1w}\sum_j\int_j \lim_{r\to 0^+}\int_0^\infty e^{-gr}\cos g\,(z_i-s)\;dg\,W_j\,ds \\
&= \frac{2}{\pi}\sum_j W_j\int_0^\infty (\hat{W}^w - w^{1w})\frac{\sin g\Delta}{g}\cos\left(gz_i - gz_j\right)dg \\
&+ w^{1w}\sum_j W_j I_{z_i\in(z_j-\Delta,z_j+\Delta)}
\end{aligned}$$

which is the form of $\sum_j w^w[i,j]W_j$ and

$$\begin{aligned}
w^w[i,j] = &= \frac{2}{\pi}\int_0^\infty (\hat{W}^w - w^{1w})\frac{\sin g\Delta}{g}\cos\left(gz_i - gz_j\right)dg \\
&+ w^{1w}I_{z_i\in(z_j-\Delta,z_j+\Delta)}.
\end{aligned}$$

We write these integral equations (4.62) and (4.63) into the form of matrix equation

$$\begin{bmatrix} u_i \\ w_i \end{bmatrix} = \begin{bmatrix} u^u[i,j] & u^w[i,j] \\ w^u[i,j] & w^w[i,j] \end{bmatrix}\begin{bmatrix} U_j \\ W_j \end{bmatrix}. \tag{4.65}$$

4.2.6 Results

Assuming $T_{ri} = 10^{-1}$ and $T_{zi} = 0$ in equation (5.84) we could solve U_j and W_j. When U_j and V_j have been obtained, the displacements u_i and w_i in (5.85) for upper and lower crack face, and for top and bottom boundaries are obtained as shown in Figure 4.2, 4.3 and 4.4.

In Figure 4.3 although the tear is in the middle of the wall, the displacement is not symmetric due to the pressure on the inner boundary and outer boundary not same. In Figure 4.2 the tear location is close to the inner boundary. That the elastic material between the inner boundary and the crack face is thinner than it between the outer boundary and the crack leads to more change on the inner face. We can see that the introduction of a tear in the elastic tube has led to a narrowing of the interior. This could have physiological implications for fluid inside the wall. Comparing Figure 4.3 and Figure 4.4 we find the

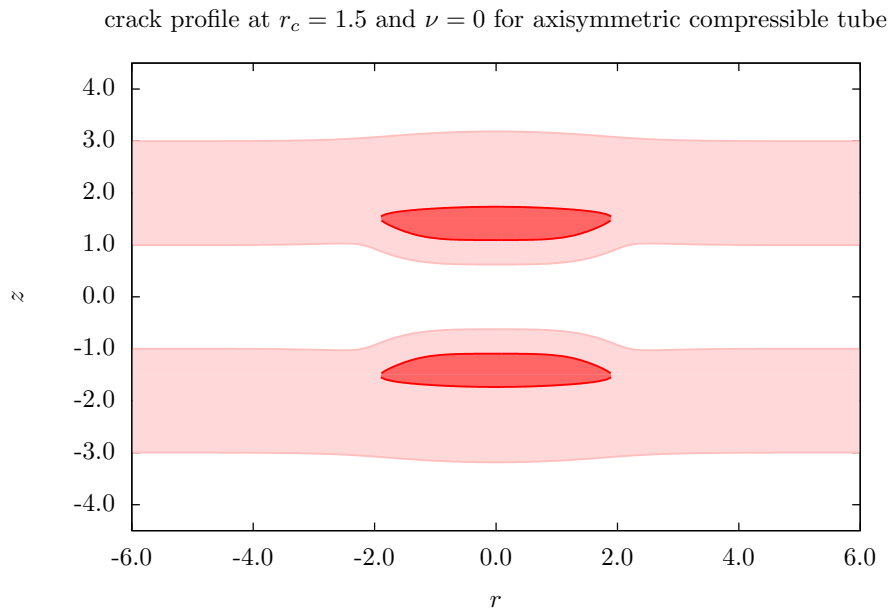

Figure 4.2: Plot of crack profile for compressible axisymmetric elastic tube with $T_{ri} = 10^{-1}$, $T_{zi} = 0$, Poisson's ratio $\nu = 0$, $r_{in} = 1$, $r_{out} = 3$ and $r_c = 1.5$.

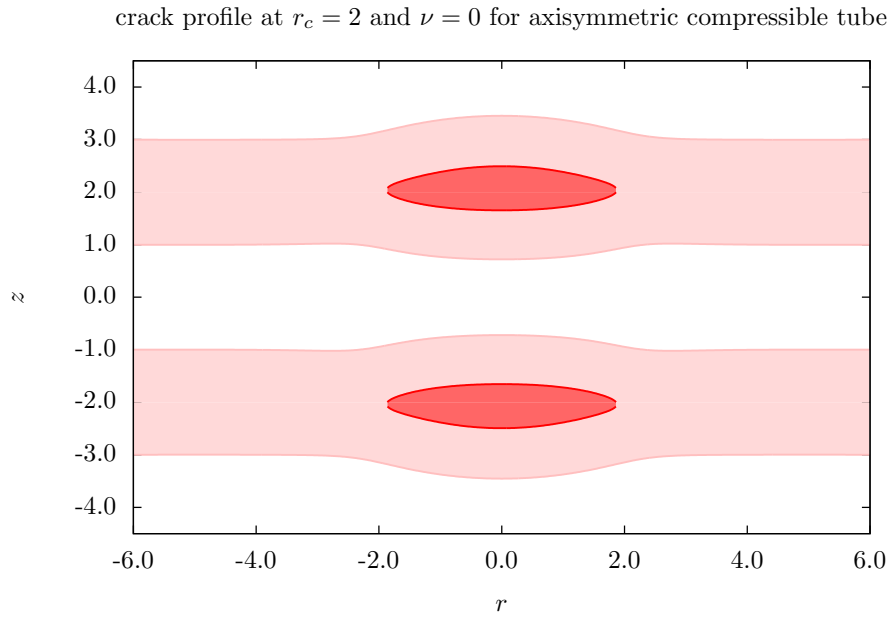

Figure 4.3: Plot of crack profile for compressible axisymmetric elastic tube with $T_{ri} = 10^{-1}$, $T_{zi} = 0$, Poisson's ratio $\nu = 0$, $r_{in} = 1$, $r_{out} = 3$ and $r_c = 1.5$.

opening of the tear is wider in the latter, since the pressure on the outer boundary is set as zero, and is non-zero on inner boundary.

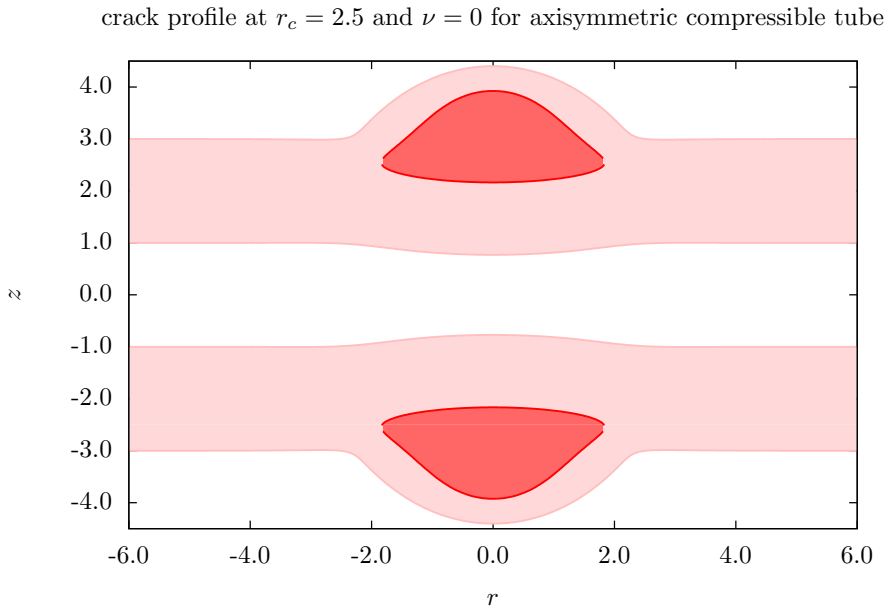

Figure 4.4: Plot of crack profile for compressible axisymmetric elastic tube with $T_{ri} = 10^{-1}$, $T_{zi} = 0$, Poisson's ratio $\nu = 0$, $r_{in} = 1$, $r_{out} = 3$ and $r_c = 1.5$.

4.3 Static tears for axisymmetric crack problem in an incompressible linear elastic annulus

Now we assume the elastic tube is incompressible. The strain tensor is still the same as (4.9). But the stress tensor changes to

$$\sigma = \lambda \mathrm{tr}\,(\boldsymbol{\varepsilon})\,\mathbf{I} + 2\mu\boldsymbol{\varepsilon} - \mu p\mathbf{I} \tag{4.66}$$

$$= 2\mu\boldsymbol{\varepsilon} - \mu p\mathbf{I} \tag{4.67}$$

due to incompressibility $\mathrm{tr}\,(\boldsymbol{\varepsilon}) = \nabla \cdot \mathbf{u} = 0$.

Hence

$$\sigma = \mu \begin{bmatrix} 2u_{,r} - p & 0 & u_{,z} + w_{,r} \\ 0 & 2\frac{u}{r} - p & 0 \\ u_{,z} + w_{,r} & 0 & 2w_{,z} - p \end{bmatrix}. \tag{4.68}$$

Write the equilibrium equations $\mathrm{div}\sigma = 0$ and incompressibility into components

$$\frac{\partial \sigma_{rr}}{\partial r} + \frac{\partial \sigma_{zr}}{\partial z} + \frac{1}{r}\left(\sigma_{rr} - \sigma_{\theta\theta}\right) = 0, \tag{4.69}$$

$$\frac{\partial \sigma_{rz}}{\partial r} + \frac{\partial \sigma_{zz}}{\partial z} + \frac{1}{r}\sigma_{rz} = 0, \tag{4.70}$$

$$\frac{1}{r}\frac{\partial (ru)}{\partial r} + \frac{\partial w}{\partial z} = 0. \tag{4.71}$$

Equations (4.69) and (4.70) become

$$2u_{,rr} - p_{,r} + u_{,zz} + w_{,rz} + \frac{2}{r}\left(u_{,r} - \frac{u}{r}\right) = 0, \tag{4.72}$$

$$u_{,zr} + w_{,rr} + 2w_{,zz} - p_{,z} + \frac{2}{r}\left(u_{,z} + w_{,r}\right) = 0. \tag{4.73}$$

4.3.1 Jump in w

Fourier transform for components of displacement and stress are the same as (4.21) and (4.22), moreover, we have one more term transformed

$$p(r,z) = \frac{i}{\pi}\int_0^\infty \hat{p}(g,r)\sin gz\, dg = \frac{1}{\pi}\int_0^\infty \hat{P}^w(g,r)\sin gz\, dg \quad \text{and define} \quad \hat{P}^w = i\hat{p}. \tag{4.74}$$

Equilibrium equations and incompressible equation after Fourier transform are

$$2\left(\hat{U}^w\right)'' + \frac{2}{r}\left(\hat{U}^w\right)' - g^2\hat{U}^w - \frac{2}{r^2}\hat{U}^w - g\left(\hat{W}^w\right)' - \left(\hat{P}^w\right)' = 0, \tag{4.75}$$

$$\left(\hat{W}^w\right)'' + \frac{\left(\hat{W}^w\right)'}{r} - 2g^2\hat{W}^w + g\left(\hat{U}^w\right)' + \frac{g}{r}\hat{U}^w - g\left(\hat{P}^w\right) = 0, \tag{4.76}$$

$$\frac{1}{g}\left(\frac{\hat{U}^w}{r} + \hat{U}^w\right) - \hat{W}^w = 0. \tag{4.77}$$

Replace $\hat{W}^w = \frac{1}{g}\left(\frac{\hat{U}^w}{r} + \left(\hat{U}^w\right)'\right)$, $\left(\hat{W}^w\right)' = \frac{1}{g}\left(\frac{(\hat{U}^w)'}{r} - \frac{(\hat{U}^w)}{r^2} + \left(\hat{U}^w\right)''\right)$ and $\left(\hat{W}^w\right)'' = \frac{1}{g}\left(\left(\hat{U}^w\right)''' + \frac{(\hat{U}^w)''}{r} - 2\frac{(\hat{U}^w)'}{r^2} + 2\frac{(\hat{U}^w)}{r^3}\right)$ into these equilibrium equations we can present $\left(\hat{U}^w\right)'''$ and $\left(\hat{P}^w\right)'$.

$$\left(\hat{U}^w\right)''' = -2\frac{\left(\hat{U}^w\right)''}{r} + \frac{\left(\hat{U}^w\right)'}{r^2} - \frac{\left(\hat{U}^w\right)}{r^3} + g^2\frac{\left(\hat{U}^w\right)}{r} + g^2\left(\hat{P}^w\right) + g^2\left(\hat{U}^w\right)' \tag{4.78}$$

$$\left(\hat{P}^w\right)' = \left(\hat{U}^w\right)'' + \frac{\left(\hat{U}^w\right)'}{r} - \left(g^2 + \frac{1}{r^2}\right)\hat{U}^w \tag{4.79}$$

The boundary conditions at $r = r_{in}$ and $r = r_{out}$ are $\hat{\sigma}^w_{rr} = 0$ and $\hat{\sigma}^w_{rz} = 0$ which translate to

$$2\left(\hat{U}^w\right)' - \hat{P}^w = 0, \tag{4.80}$$

$$g\hat{U}^w - \frac{1}{g}\frac{\hat{U}^w}{r^2} + \frac{1}{g}\frac{\left(\hat{U}^w\right)'}{r} + \frac{1}{g}\left(\hat{U}^w\right)'' = 0. \tag{4.81}$$

The jump conditions at $r = r_c$ are

$$\left[\hat{U}^w\right]^+_- = 0, \qquad \left[\hat{W}^w\right]^+_- = 1, \qquad [\hat{\sigma}^w_{rr}]^+_- = [\hat{\sigma}^w_{rz}]^+_- = 0. \tag{4.82}$$

4.3.2 Jump in u

Fourier transform for components of displacement and stress are the same as (4.41) and (4.42), besides we have one more term transformed

$$p(r,z) = \frac{1}{\pi}\int_0^\infty \hat{p}(g,r)\cos gz\, dg = \frac{1}{\pi}\int_0^\infty \hat{P}^u(g,r)\cos gz\, dg \quad \text{and define} \quad \hat{P}^u = \hat{p} \tag{4.83}$$

Equilibrium equations and incompressible equation after Fourier transform are

$$2\left(\hat{U}^u\right)'' + \frac{2}{r}\left(\hat{U}^u\right)' - g^2\hat{U}^u - \frac{2}{r^2}\hat{U}^u + g\left(\hat{W}^u\right)' - \left(\hat{P}^u\right)' = 0, \tag{4.84}$$

$$\left(\hat{W}^u\right)'' + \frac{\left(\hat{W}^u\right)'}{r} - 2g^2\hat{W}^u - g\left(\hat{U}^u\right)' - \frac{g}{r}\hat{U}^u + g\left(\hat{P}^u\right) = 0, \tag{4.85}$$

$$\frac{1}{g}\left(\frac{\hat{U}^u}{r} + \hat{U}^u\right) + \hat{W}^u = 0. \tag{4.86}$$

Replace $\hat{W}^u = -\frac{1}{g}\left(\frac{\hat{U}^u}{r} + \left(\hat{U}^u\right)'\right)$, $\left(\hat{W}^u\right)' = -\frac{1}{g}\left(\frac{(\hat{U}^u)'}{r} - \frac{(\hat{U}^u)}{r^2} + \left(\hat{U}^u\right)''\right)$ and $\left(\hat{W}^u\right)'' = -\frac{1}{g}\left(\left(\hat{U}^u\right)''' + \frac{(\hat{U}^u)''}{r} - 2\frac{(\hat{U}^u)'}{r^2} + 2\frac{(\hat{U}^u)}{r^3}\right)$ into these equilibrium equations.

$$\left(\hat{U}^u\right)''' = -2\frac{\left(\hat{U}^u\right)''}{r} + \frac{\left(\hat{U}^u\right)'}{r^2} - \frac{\left(\hat{U}^u\right)}{r^3} + g^2\frac{\left(\hat{U}^u\right)}{r} + g^2\left(\hat{P}^u\right) + g^2\left(\hat{U}^u\right)' \tag{4.87}$$

$$\left(\hat{P}^u\right)' = \left(\hat{U}^u\right)'' + \frac{\left(\hat{U}^u\right)'}{r} - \left(g^2 + \frac{1}{r^2}\right)\hat{U}^u \tag{4.88}$$

The boundary conditions at $r = r_{in}$ and $r = r_{out}$ are $\hat{\sigma}^u_{rr} = 0$ and $\hat{\sigma}^u_{rz} = 0$, which translate to

$$2\left(\hat{U}^u\right)' - \hat{P}^u = 0, \tag{4.89}$$

$$g\hat{U}^u - \frac{1}{g}\frac{\hat{U}^u}{r^2} + \frac{1}{g}\frac{\left(\hat{U}^u\right)'}{r} + \frac{1}{g}\left(\hat{U}^u\right)'' = 0. \tag{4.90}$$

The jump conditions at $r = r_c$ are

$$\left[\hat{U}^u\right]^+_- = 1, \qquad \left[\hat{W}^u\right]^+_- = 0, \qquad [\hat{\sigma}^u_{rr}]^+_- = [\hat{\sigma}^u_{rz}]^+_- = 0. \tag{4.91}$$

4.3.3 Numerical solution—Collocation method

In this section we are going to solve $\hat{U}^w, \hat{W}^w, \hat{U}^u, \hat{W}^u$ and $\hat{\sigma}^w_{yy}, \hat{\sigma}^w_{xy}, \hat{\sigma}^u_{yy}, \hat{\sigma}^u_{xy}$ numerically. Now we assume $r_{in} = 1, r_{out} = 3, r_c = 2$. We consider $g = 0$ separately, which will give singularity if we use the following collocation method.

As shown in Figure 4.1, region 1 is $r_{in} \le r \le r_c$ and region 2 is $r_c \le r \le r_{out}$. In

region 1, $r = r_{in} + R(r_c - r_{in})$ and $\dfrac{d}{dr} = \dfrac{1}{r_c - r_{in}} \dfrac{d}{dR}$; in region 2, $r = r_{out} + R(r_c - r_{out})$ and $\dfrac{d}{dr} = \dfrac{1}{r_c - r_{out}} \dfrac{d}{dR}$. The range of R is $[0, 1]$. The boundary layer in each region is represented by $R = 0$, and $R = 1$ represents the crack face.

Jump in w

Define Y_1, Y_2, Y_3, Y_4 to be $\hat{U}^w, (\hat{U}^w)', \hat{W}^w, (\hat{W}^w)'$ respectively in region 1, and Y_5, Y_6, Y_7, Y_8 to be $\hat{U}^w, (\hat{U}^w)', \hat{W}^w, (\hat{W}^w)'$ respectively in region 2. Referring to the equilibrium equations (4.75)

$$
\begin{aligned}
\frac{dY_1}{dR} &= Y_2 \\
\frac{dY_2}{dR} &= Y_3 \\
\frac{dY_3}{dR} &= -2\frac{Y_3 (r_c - r_{in})}{r_1} + \frac{Y_2 (r_c - r_{in})^2}{r_1^2} + g^2 Y_2 (r_c - r_{in})^2 \\
&- \frac{Y_1 (r_c - r_{in})^3}{r_1^3} + g^2 \frac{Y_1 (r_c - r_{in})^3}{r_1} + g^2 Y_4 (r_c - r_{in})^3 \\
\frac{dY_4}{dR} &= \frac{Y_3}{r_c - r_{in}} + \frac{Y_2}{r_1} - \left(g^2 + \frac{1}{r_1^2} \right) Y_1 (r_c - r_{in}) \\
\frac{dY_5}{dR} &= Y_6 \\
\frac{dY_6}{dR} &= Y_7 \\
\frac{dY_7}{dR} &= -2\frac{Y_7 (r_c - r_{out})}{r_2} + \frac{Y_6 (r_c - r_{out})^2}{r_2^2} + g^2 Y_6 (r_c - r_{out})^2 - \frac{Y_5 (r_c - r_{out})^3}{r_2^3} \\
&+ g^2 \frac{Y_2 (r_c - r_{out})^3}{r_2} + g^2 Y_8 (r_c - r_{out})^3 \\
\frac{dY_8}{dR} &= \frac{Y_7}{r_c - r_{out}} + \frac{Y_6}{r_2} - \left(g^2 + \frac{1}{r_2^2} \right) Y_5 (r_c - r_{out})
\end{aligned}
$$

The boundary conditions (4.80) on outer and inner boundaries, and jump conditions (4.82) for upper and lower crack faces are

$$\begin{aligned}
2\frac{Y_2}{(r_c - r_{in})} - Y_4 &= 0 \\
gY_1 - \frac{Y_1}{gr_{in}^2} + \frac{Y_2}{gr_{in}(r_c - r_{in})} + \frac{Y_3}{g(r_c - r_{in})^2} &= 0 \\
2\frac{Y_6}{(r_c - r_{out})} - Y_8 &= 0 \\
gY_5 - \frac{Y_5}{gr_{out}^2} + \frac{Y_6}{gr_{out}(r_c - r_{out})} + \frac{Y_7}{g(r_c - r_{out})^2} &= 0 \\
Y_5 - Y_1 &= 0 \\
\frac{Y_5}{r_c} + \frac{Y_6}{(r_c - r_{out})} - \frac{Y_1}{r_c} - \frac{Y_2}{(r_c - r_{in})} - g &= 0 \\
2\frac{Y_6}{(r_c - r_{out})} - Y_8 - \left(2\frac{Y_2}{(r_c - r_{in})} - Y_4\right) &= 0 \\
gY_5 - \frac{Y_5}{gr_{out}^2} + \frac{Y_6}{gr_{out}(r_c - r_{out})} + \frac{Y_7}{g(r_c - r_{out})^2} & - \\
\left(gY_1 - \frac{Y_1}{gr_{in}^2} + \frac{Y_2}{gr_{in}(r_c - r_{in})} + \frac{Y_3}{g(r_c - r_{in})^2}\right) &= 0.
\end{aligned}$$

We use the Matlab routine '`bvp4c`' to calculate the values of $Y_1, Y_2, Y_3, Y_4, Y_5, Y_6, Y_7, Y_8$, hence $\hat{U}^w, \hat{W}^w$ are obtained. $\hat{\sigma}^w_{yy}, \hat{\sigma}^w_{xy}$ are functions of $\hat{U}^w, \hat{W}^w$.

Jump in u

Define Y_1, Y_2, Y_3, Y_4 to be $\hat{U}^u, (\hat{U}^u)', \hat{W}^u, (\hat{W}^u)'$ respectively in region 1, and Y_5, Y_6, Y_7, Y_8 to be $\hat{U}^u, (\hat{U}^u)', \hat{W}^u, (\hat{W}^u)'$ respectively in region 2. Referring to the equilibrium equations

(4.84)

$$
\begin{aligned}
\frac{dY_1}{dR} &= Y_2 \\
\frac{dY_2}{dR} &= Y_3 \\
\frac{dY_3}{dR} &= -2\frac{Y_3\left(r_c-r_{in}\right)}{r_1}+\frac{Y_2\left(r_c-r_{in}\right)^2}{r_1^2}+g^2Y_2\left(r_c-r_{in}\right)^2 \\
&- \frac{Y_1\left(r_c-r_{in}\right)^3}{r_1^3}+g^2\frac{Y_1\left(r_c-r_{in}\right)^3}{r_1}+g^2Y_4\left(r_c-r_{in}\right)^3 \\
\frac{dY_4}{dR} &= \frac{Y_3}{r_c-r_{in}}+\frac{Y_2}{r_1}-\left(g^2+\frac{1}{r_1^2}\right)Y_1\left(r_c-r_{in}\right) \\
\frac{dY_6}{dR} &= Y_7 \\
\frac{dY_7}{dR} &= -2\frac{Y_7\left(r_c-r_{out}\right)}{r_2}+\frac{Y_6\left(r_c-r_{out}\right)^2}{r_2^2}+g^2Y_6\left(r_c-r_{out}\right)^2-\frac{Y_5\left(r_c-r_{out}\right)^3}{r_2^3} \\
&+ g^2\frac{Y_2\left(r_c-r_{out}\right)^3}{r_2}+g^2Y_8\left(r_c-r_{out}\right)^3 \\
\frac{dY_8}{dR} &= \frac{Y_7}{r_c-r_{out}}+\frac{Y_6}{r_2}-\left(g^2+\frac{1}{r_2^2}\right)Y_5\left(r_c-r_{out}\right)
\end{aligned}
$$

The boundary conditions (4.89) on outer and inner boundaries, and jump conditions (4.91) for upper and lower crack faces are

$$
\begin{aligned}
2\frac{Y_2}{r_1\left(r_c-r_{in}\right)}-Y_4 &= 0 \\
gY_1-\frac{Y_1}{gr_{in}^2}+\frac{Y_2}{gr_{in}\left(r_c-r_{in}\right)}+\frac{Y_3}{g\left(r_c-r_{in}\right)^2} &= 0 \\
2\frac{Y_6}{r_1\left(r_c-r_{out}\right)}-Y_8 &= 0 \\
gY_5-\frac{Y_5}{gr_{in}^2}+\frac{Y_6}{gr_{in}\left(r_c-r_{out}\right)}+\frac{Y_7}{g\left(r_c-r_{out}\right)^2} &= 0 \\
Y_5-Y_1-1 &= 0 \\
\frac{Y_5}{r_c}+\frac{Y_6}{\left(r_c-r_{out}\right)}-\frac{Y_1}{r_c}-\frac{Y_2}{\left(r_c-r_{in}\right)} &= 0 \\
2\frac{Y_6}{r_1\left(r_c-r_{out}\right)}-Y_8-\left(2\frac{Y_2}{r_1\left(r_c-r_{in}\right)}-Y_4\right) &= 0 \\
gY_5-\frac{Y_5}{gr_{in}^2}+\frac{Y_6}{gr_{in}\left(r_c-r_{out}\right)}+\frac{Y_7}{g\left(r_c-r_{out}\right)^2} &- \\
\left(gY_1-\frac{Y_1}{gr_{in}^2}+\frac{Y_2}{gr_{in}\left(r_c-r_{in}\right)}+\frac{Y_3}{g\left(r_c-r_{in}\right)^2}\right) &= 0.
\end{aligned}
$$

We use the Matlab routine '`bvp4c`' to calculate the values of $Y_1, Y_2, Y_3, Y_4, Y_5, Y_6, Y_7, Y_8$, hence $\hat{U}^u, \hat{W}^u$ are obtained. $\hat{\sigma}^u_{yy}, \hat{\sigma}^u_{xy}$ are functions of $\hat{U}^u, \hat{W}^u$.

4.3.4 The case $g = 0$

Jump in w when $g = 0$

Equations (4.75) change to

$$2\left(\hat{U}^w\right)'' + \frac{2}{r}\left(\hat{U}^w\right)' - \frac{2}{r^2}\hat{U}^w - \left(\hat{P}^w\right)' = 0, \tag{4.92}$$

$$\left(\hat{W}^w\right)'' + \frac{\left(\hat{W}^w\right)'}{r} = 0, \tag{4.93}$$

$$\left(\frac{\hat{U}^w}{r} + \hat{U}^w\right) = 0. \tag{4.94}$$

Hence the solution for $\hat{U}^w$ and $\hat{W}^w$ are

$$\begin{aligned} \hat{U}^w &= \frac{A}{r}, \\ \hat{P}^w &= B, \\ \hat{W}^w &= C\log(r) + D. \end{aligned}$$

Put the solutions into the boundary conditions (4.80) on inner and outer layers and the jump conditions (4.82) we get

$$A_1 = 0, \quad B_1 = 0, \quad C_1 = 0, \quad D_1 = -\frac{1}{2}, \quad A_2 = 0, \quad B_2 = 0, \quad C_2 = 0, \quad D_2 = \frac{1}{2}.$$

where subscript '1' is means region 1, and subscript '2' is above the crack means region '2'. Hence the displacements on the upper crack face are $\hat{U} = 0$ and $\hat{W} = \frac{1}{2}$; the displacements on the lower crack face are $\hat{U} = 0$ and $\hat{W} = -\frac{1}{2}$; the displacements on the outside boundary are $\hat{U} = 0$ and $\hat{W} = \frac{1}{2}$; the displacements on the inside boundary are $\hat{U} = 0$ and $\hat{W} = -\frac{1}{2}$; on the crack face $\hat{\sigma}_{rr} = 0$ and $\hat{\sigma}_{rz} = 0$.

Jump in u when $g = 0$

Equations (4.84) change to

$$2\left(\hat{U}^u\right)'' + \frac{2}{r}\left(\hat{U}^u\right)' - \frac{2}{r^2}\hat{U}^u - \left(\hat{P}^u\right)' = 0, \tag{4.95}$$

$$\left(\hat{W}^u\right)'' + \frac{\left(\hat{W}^u\right)'}{r} = 0, \tag{4.96}$$

$$\left(\frac{\hat{U}^u}{r} + \hat{U}^u\right) = 0. \tag{4.97}$$

Hence the solution for $\hat{U}^u$ and $\hat{W}^u$ are

$$\begin{aligned}\hat{U}^u &= \frac{A}{r},\\ \hat{P}^w &= B,\\ \hat{W}^u &= C\log(r)+D.\end{aligned}$$

Put the solutions into the boundary conditions (4.89) on inner and outer layers and the jump conditions (4.91) we get

$$\begin{aligned}A_1 &= \frac{r_{in}^2(r_c^2-r_{out}^2)}{r_c(-r_{out}^2+r_{in}^2)}, \quad B_1 = 2\frac{(r_{out}^2-r_c^2)}{r_c(r_{out}^2-r_{in}^2)}, \quad C_1=0, \quad D_1=0,\\ A_2 &= \frac{(r_{in}^2-r_c^2)r_{out}^2}{r_c(r_{out}^2-r_{in}^2)}, \quad B_2 = 2\frac{(r_{in}^2-r_c^2)}{r_c(r_{out}^2-r_{in}^2)}, \quad C_2=0, \quad D_2=0.\end{aligned}$$

Hence the displacements on the upper crack face are $\hat{U} = -\frac{r_{out}^2(r_{in}^2-r_c^2)}{r_c^2(r_{out}^2-r_{in}^2)}$ and $\hat{W}=0$; the displacements on the lower crack face are $\hat{U} = -\frac{r_{in}^2(r_{out}^2-r_c^2)}{r_c^2(r_{out}^2-r_{in}^2)}$ and $\hat{W}=0$; the displacements on the outside boundary are $\hat{U} = -\frac{r_{out}(r_{in}^2-r_c^2)}{r_c(r_{out}^2-r_{in}^2)}$ and $\hat{W}=0$; the displacements on the inside boundary are $\hat{U} = -\frac{r_{in}(r_{out}^2-r_c^2)}{r_c(r_{out}^2-r_{in}^2)}$ and $\hat{W}=0$; on the crack face $\hat{\sigma}_{rr} = -2\frac{(r_{out}^2-r_c^2)(r_c^2-r_{in}^2)}{r_c^3(r_{out}^2-r_{in}^2)}$ and $\hat{\sigma}_{rz}=0$.

4.3.5 Comparison between compressible and incompressible solutions

In compressible axisymmetric artery when $\nu = 0.5$ the material is incompressible. Although we can not make $\nu = 0.5$ exactly in the code due to singularity in numerical , when $\nu = 0.4999$ it is close to the incompressible material. When $\nu = 0.4999$ we compare the results for compressible and incompressible, we find out they match well as shown in Figure 4.5 and Figure 4.6, where the difference is 10^{-4} which is the order of $0.5-\nu = 0.0001$.

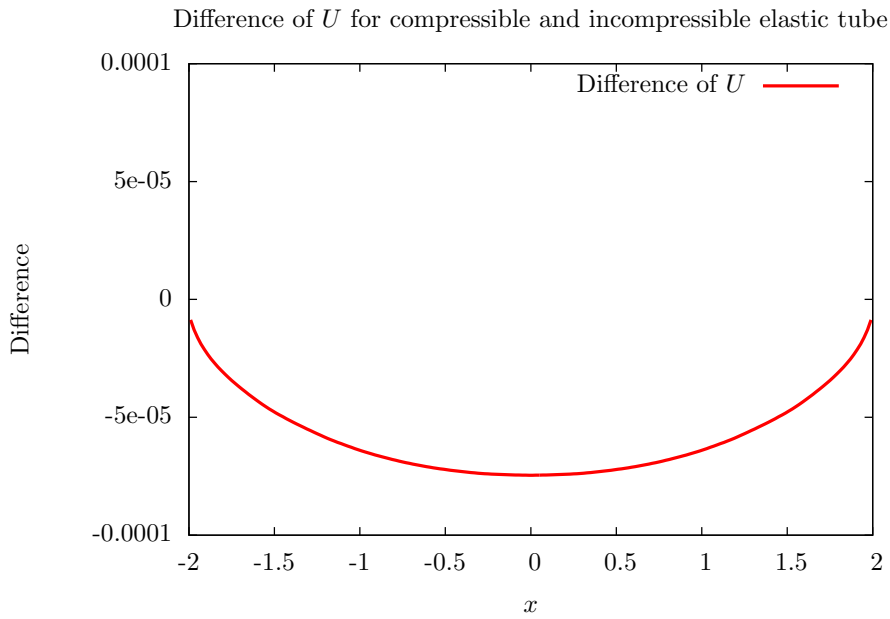

Figure 4.5: Difference of U for compressible and incompressible axisymmetric elastic tube with $T_{rj} = 10^{-1}$, $T_{zj} = 0$, $r_{in} = 1$, $r_{out} = 3$ and $r_c = 1.5$.

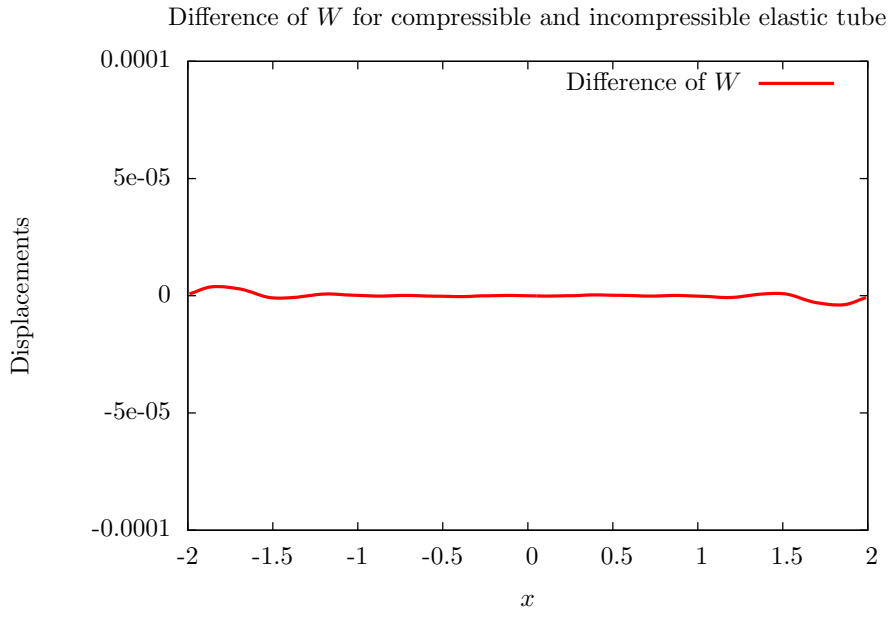

Figure 4.6: Difference of W for compressible and incompressible axisymmetric elastic tube with $T_{rj} = 10^{-1}$, $T_{zj} = 0$, $r_{in} = 1$, $r_{out} = 3$ and $r_c = 1.5$.

4.4 Conclusions

In this chapter, we have solved the axisymmetric crack problems in the compressible and incompressible linear elastic axisymmetric tube. And we have compared the displacement of the tear in the compressible tube with $\nu = 0.4999$, which is almost incompressible, with the displacement of the tear in the incompressible tube. The results match very well.

Chapter 5

Static axisymmetric tears based on Holzapfel's energy function

In this chapter we model an axisymmetric tear in the aorta.We use the strain energy function for a thick-walled non-linear elastic tube with residual stress and two families of fibres in the wall given by Holzapfel et al. [2000] to deduce the stresses, then construct the equilibrium equations with boundary conditions and jump conditions to describe the tear. The dissection is linearized as an incremental deformation, whose traction and displacement on the dissection faces and boundaries are presented as the integral of the Green's function weighted by the displacement discontinuity. The tear changes with the parameters in the strain energy function, which is shown in our results. In addition, a change in blood pressure inside the lumen treated as the incremental inner pressure, and its effect on the tear are found.

5.1 Axisymmetric dissection using Holzapfel et al.'s strain energy function

Now we consider an axisymmetric elastic tube with inner radius r_{in} and outer radius r_{out}. We assume the tear, which is located at r_c, is axisymmetric in the wall of tube as shown in Figure 4.1. The coordinate system is (r, θ, z) and the displacements in the coordinate directions are (u, v, w). Due to axisymmetry, we do not need consider the displacement v in circumferential direction.

5.1.1 Introduction—Methods for axisymmetric crack problem on aorta

We take the stress-free artery with specified opening angle as the reference configuration, and the closed artery with residual stress as the current configuration. The dissection of the artery is idealised as the incremental elastic deformation on the configuration with residual stress.

In vivo the residual stress and axial stretch, which are included into the Cauchy stress, have important effects on the aorta. The governing equations in the current configuration are

$$\begin{aligned} \operatorname{div}\boldsymbol{\sigma} &= 0, \\ \sigma_{rr} &= -P_{\text{ext}} \quad \text{at} \quad r = r_{\text{out}}, \end{aligned} \tag{5.1}$$

where P_{ext} is the pressure on the outer boundary of the aorta.

The dissection of the artery is idealized as an incremental elastic deformation,

$$\begin{aligned} \operatorname{div}\dot{\boldsymbol{S}}_0 &= 0, \\ \dot{\boldsymbol{S}}_0^T\mathbf{n} &= -\dot{P}\mathbf{n} - P\operatorname{tr}(\delta\mathbf{A}_0)\,\mathbf{n} + P\delta\mathbf{A}_0^T\mathbf{n} \quad \text{at} \quad r = r_{\text{in}} \quad \text{and} \quad r = r_{\text{out}}, \end{aligned} \tag{5.2}$$

where $\dot{\boldsymbol{S}}_0$ (the same tensor as $\delta\boldsymbol{S}_0$ in chapter 2) is the incremental nominal stress in the configuration in which the dissection happens, P is the pressure on the aorta, which is written as P_{ext} at outer boundary and P_{in} at inner boundary, and $\dot{P}$ is the incremental pressure which describes the change of P.

Similarly to the axisymmetric tear problem in Chapter 4, the tear is decomposed into normal and tangential direction as shown in Figure 4.1. The jump conditions at $r = r_c$ are

$$[u]_-^+ = \delta(z), [w]_-^+ = 0, [\dot{S}_{0rr}]_-^+ = 0, [\dot{S}_{0rz}]_-^+ = 0 \quad \text{for the jump in } u, \tag{5.3}$$

$$[u]_-^+ = 0, [w]_-^+ = \delta(z), [\dot{S}_{0rr}]_-^+ = 0, [\dot{S}_{0rz}]_-^+ = 0 \quad \text{for the jump in } w. \tag{5.4}$$

We calculate $\dot{S}^u_{0rr}$, $\dot{S}^u_{0rz}$, u^u and w^u for the 'jump in u' and $\dot{S}^w_{0rr}$, $\dot{S}^w_{0rz}$, u^w and w^w for the 'jump in w' separately by same methods.

Firstly, we obtain the nominal stress $\boldsymbol{S}$ (2.54) and the Cauchy stress from the strain-energy function Ψ. We calculate the incremental nominal stress $\dot{\boldsymbol{S}}_0$ by using the relation (2.44). The Cauchy stress $\boldsymbol{\sigma}$ and the incremental nominal stress $\dot{\boldsymbol{S}}_0$ are functions of the displacements $u^u(r,z), w^u(r,z)$ or $u^w(r,z), w^w(r,z)$. Writing the equilibrium equations $\operatorname{div}\boldsymbol{\sigma} = 0$ and $\operatorname{div}\dot{\boldsymbol{S}}_0 = 0$ in components, we obtain partial differential equations in the

variables $u^u(r,z), w^u(r,z)$ or $u^w(r,z), w^w(r,z)$. Secondly, we take a Fourier transform to change these PDEs to ODEs with wave number g and variables $\hat{u}^u(r,g), \hat{w}^u(r,g)$ or $\hat{u}^w(r,g), \hat{w}^w(r,g)$. Thirdly, we solve these ODEs with boundary conditions and jump conditions by using a collocation method. Finally, we take the inverse Fourier transform to obtain the solution for PDEs. $\dot{\boldsymbol{S}}_0$ is a function of $u^u(r,z), w^u(r,z)$ or $u^w(r,z), w^w(r,z)$. Thus when $u^u(r,z), w^u(r,z)$ or $u^w(r,z), w^w(r,z)$ are solved, $\dot{S}^u_{0rz}, \dot{S}^u_{0rr}$ or $\dot{S}^w_{0rz}, \dot{S}^w_{0rr}$ are obtained.

Define $T = (T_r, T_z)$ as the traction on the tear, which is decomposed into normal and tangential directions,

$$T_r = \int \dot{S}^u_{0rr}(z-s,r)U(s)\,ds + \int \dot{S}^w_{0rr}(z-s,r)W(s)\,ds, \tag{5.5}$$

$$T_z = \int \dot{S}^u_{0rz}(z-s,r)U(s)\,ds + \int \dot{S}^w_{0rz}(z-s,r)W(s)\,ds. \tag{5.6}$$

The displacement components are decomposed into normal and tangential direction

$$u = \int u^u(z-s,r)U(s)ds + \int u^w(z-s,r)W(s)ds \tag{5.7}$$

$$w = \int w^u(z-s,r)U(s)ds + \int w^w(z-s,r)W(s)ds \tag{5.8}$$

Hence if the traction (T_r, T_z) along the dissection is given, the displacement (u, w) can be found. We use this method to calculate the displacements for the upper tear face, lower tear face, outer boundary and inner boundary. These are plotted on one figure to get profile of the dissection.

5.1.2 Holzapfel-Gasser-Ogden strain-energy function

Equations (2.13) and (2.14) have been introduced as the strain-energy function

$$\Psi = U(J) + \frac{1}{2}c\left(\overline{I}_1 - 3\right) + \frac{k_1}{2k_2}\left[\Psi_f\left(\overline{I}_4\right) + \Psi_f\left(\overline{I}_6\right)\right], \tag{5.9}$$

and all the details about the equations have been introduced as equations (2.16), (2.17), (2.18).

5.1.3 Incremental Elastic Moduli

Following are some useful results for our calculation, We have

$$\frac{\partial}{\partial \mathbf{A}}\left[\operatorname{tr}\mathbf{A}^T\mathbf{A}\right] = 2\mathbf{A}^T \quad \text{and} \quad \frac{\partial}{\partial \mathbf{A}}\left[\det \mathbf{A}\right] = (\det \mathbf{A})\,\mathbf{A}^{-1}, \tag{5.10}$$

which in component form are (2.73) and (2.76). Any function of J can be differentiated easily

$$\frac{\partial}{\partial \mathbf{A}} F\left(\det \mathbf{A}\right) = \left(\det \mathbf{A}\right) F'\left(\det \mathbf{A}\right) \mathbf{A}^{-1}. \tag{5.11}$$

In addition, a useful result (2.81) has been introduced

$$\frac{\partial}{\partial A_{j\beta}} \left[\left(A^{-1}\right)_{\alpha i}\right] = -A^{-1}_{\alpha j} A^{-1}_{\beta i}. \tag{5.12}$$

Another useful result is

$$\frac{\partial}{\partial A_{i\alpha}} \left[M_{pq} A_{kq} A_{kp}\right] = M_{p\alpha} A_{ip} + A_{iq} M_{\alpha q} \tag{5.13}$$

so that

$$\frac{\partial}{\partial \mathbf{A}} \left[\mathrm{tr}\left(\mathbf{M}\mathbf{A}^T\mathbf{A}\right)\right] = \left(\mathbf{M}^T + \mathbf{M}\right)\mathbf{A}^T. \tag{5.14}$$

Combining the results above we have

$$\frac{\partial}{\partial \mathbf{A}} \overline{I}_1 = 2J^{-2/3}\left[\mathbf{A}^T - \frac{1}{3}\mathrm{tr}\left(\mathbf{A}^T\mathbf{A}\right)\mathbf{A}^{-1}\right] \tag{5.15}$$

$$\frac{\partial}{\partial \mathbf{A}} \overline{I}_4 = 2J^{-2/3}\left[\mathrm{Sym}\left(\mathbf{M}_+\right)\mathbf{A}^T - \frac{1}{3}\mathrm{tr}\left(\mathbf{M}_+\mathbf{A}^T\mathbf{A}\right)\mathbf{A}^{-1}\right] \tag{5.16}$$

$$\frac{\partial}{\partial \mathbf{A}} \overline{I}_6 = 2J^{-2/3}\left[\mathrm{Sym}\left(\mathbf{M}_-\right)\mathbf{A}^T - \frac{1}{3}\mathrm{tr}\left(\mathbf{M}_-\mathbf{A}^T\mathbf{A}\right)\mathbf{A}^{-1}\right]. \tag{5.17}$$

Then the stress $\mathbf{S}$ (2.27) is given by

$$\begin{aligned}\mathbf{S} = \frac{\partial \Psi}{\partial \mathbf{A}} &= JU'(J)\mathbf{A}^{-1} + cJ^{-2/3}\left[\mathbf{A}^T - \frac{1}{3}\mathrm{tr}\left(\mathbf{A}^T\mathbf{A}\right)\mathbf{A}^{-1}\right] \\ &+ 2k_1 J^{-2/3}\left(\overline{I}_4 - 1\right)\exp\left[k_2\left(\overline{I}_4 - 1\right)^2\right]\left[\mathrm{Sym}\left(\mathbf{M}_+\right)\mathbf{A}^T - \frac{1}{3}\mathrm{tr}\left(\mathbf{M}_+\mathbf{A}^T\mathbf{A}\right)\mathbf{A}^{-1}\right] \\ &+ 2k_1 J^{-2/3}\left(\overline{I}_6 - 1\right)\exp\left[k_2\left(\overline{I}_6 - 1\right)^2\right]\left[\mathrm{Sym}\left(\mathbf{M}_-\right)\mathbf{A}^T - \frac{1}{3}\mathrm{tr}\left(\mathbf{M}_-\mathbf{A}^T\mathbf{A}\right)\mathbf{A}^{-1}\right].\end{aligned} \tag{5.18}$$

The elastic moduli (2.37) are given as a function of deformation gradient $\mathbf{A}$ by

$$\mathcal{A}^1 = \frac{\partial \mathbf{S}}{\partial \mathbf{A}}. \tag{5.19}$$

In component form we have

$$\mathcal{A}^1_{\alpha i \beta j} = \frac{\partial S_{\alpha i}}{\partial A_{j\beta}}. \tag{5.20}$$

Now

$$\begin{aligned}\frac{\partial}{\partial A_{l\beta}}\left(JU'(J)\left(A^{-1}\right)_{\alpha j}\right) &= J^2U''(J)\left(A^{-1}\right)_{\beta l}\left(A^{-1}\right)_{\alpha j} \\ &+ JU'(J)\left[\left(A^{-1}\right)_{\beta l}\left(A^{-1}\right)_{\alpha j} - \left(A^{-1}\right)_{\alpha l}\left(A^{-1}\right)_{\beta j}\right].\end{aligned}$$

Let

$$F\left(\mathbf{M},\mathbf{A}\right)=\mathrm{Sym}\left(\mathbf{M}\right)\mathbf{A}^{T}-\frac{1}{3}\mathrm{tr}\left(\mathbf{M}\mathbf{A}^{T}\mathbf{A}\right)\mathbf{A}^{-1}, \tag{5.21}$$

then

$$\begin{aligned}\frac{\partial}{\partial A_{l\beta}}F\left(\mathbf{M},\mathbf{A}\right)_{\alpha j} &= \mathcal{F}_{\alpha j\beta l}\left(\mathbf{M}\right)\\ &= \mathrm{Sym}\left(\mathbf{M}\right)_{\alpha\beta}\delta_{jl}-\frac{1}{3}\left[M_{p\beta}A_{lp}+M_{\beta p}A_{lp}\right]\left(A^{-1}\right)_{\alpha j}\\ &+ \frac{1}{3}\mathrm{tr}\left(\mathbf{M}\mathbf{A}^{T}\mathbf{A}\right)\left(A^{-1}\right)_{\alpha l}\left(A^{-1}\right)_{\beta j}.\end{aligned}$$

$$\frac{\partial}{\partial A_{l\beta}}J^{-2/3}=-\frac{2}{3}J^{-2/3}\left(A^{-1}\right)_{\beta l}, \tag{5.22}$$

and

$$\frac{\partial}{\partial A_{l\beta}}f\left(\overline{I}_{4}\right)=2f'\left(\overline{I}_{4}\right)F\left(\mathbf{M}_{+},\mathbf{A}\right)_{\beta l}. \tag{5.23}$$

These results lead to

$$\begin{aligned}\mathcal{A}^{1}_{\alpha j\beta l} &= J^{2}U''(J)\left(A^{-1}\right)_{\beta l}\left(A^{-1}\right)_{\alpha j}+JU'(J)\left[\left(A^{-1}\right)_{\beta l}\left(A^{-1}\right)_{\alpha j}-\left(A^{-1}\right)_{\alpha l}\left(A^{-1}\right)_{\beta j}\right]\\
&- \frac{2c}{3}J^{-2/3}\left(A^{-1}\right)_{\beta l}F\left(\mathbf{I},\mathbf{A}\right)_{\alpha j}\\
&+ cJ^{-2/3}\left[\delta_{\alpha\beta}\delta_{jl}-\frac{2}{3}A_{l\beta}\left(A^{-1}\right)_{\alpha j}+\frac{1}{3}\mathrm{tr}\left(\mathbf{A}^{T}\mathbf{A}\right)\left(A^{-1}\right)_{\alpha l}\left(A^{-1}\right)_{\beta j}\right]\\
&- \frac{4}{3}k_{1}J^{-2/3}\left(\overline{I}_{4}-1\right)\exp\left[k_{2}\left(\overline{I}_{4}-1\right)^{2}\right]\left(A^{-1}\right)_{\beta l}F\left(\mathbf{M}_{+},\mathbf{A}\right)_{\alpha j}\\
&- \frac{4}{3}k_{1}J^{-2/3}\left(\overline{I}_{6}-1\right)\exp\left[k_{2}\left(\overline{I}_{6}-1\right)^{2}\right]\left(A^{-1}\right)_{\beta l}F\left(\mathbf{M}_{-},\mathbf{A}\right)_{\alpha j}\\
&+ 4k_{1}J^{-4/3}\left[1+2k_{2}\left(\overline{I}_{4}-1\right)^{2}\right]\exp\left[k_{2}\left(\overline{I}_{4}-1\right)^{2}\right]F\left(\mathbf{M}_{+},\mathbf{A}\right)_{\beta l}F\left(\mathbf{M}_{+},\mathbf{A}\right)_{\alpha j}\\
&+ 4k_{1}J^{-4/3}\left[1+2k_{2}\left(\overline{I}_{6}-1\right)^{2}\right]\exp\left[k_{2}\left(\overline{I}_{6}-1\right)^{2}\right]F\left(\mathbf{M}_{-},\mathbf{A}\right)_{\beta l}F\left(\mathbf{M}_{-},\mathbf{A}\right)_{\alpha j}\\
&+ 2k_{1}J^{-2/3}\left(\overline{I}_{4}-1\right)\exp\left[k_{2}\left(\overline{I}_{4}-1\right)^{2}\right]\mathcal{F}_{\alpha j\beta l}\left(\mathbf{M}_{+}\right)\\
&+ 2k_{1}J^{-2/3}\left(\overline{I}_{6}-1\right)\exp\left[k_{2}\left(\overline{I}_{6}-1\right)^{2}\right]\mathcal{F}_{\alpha j\beta l}\left(\mathbf{M}_{-}\right).\end{aligned} \tag{5.24}$$

The instantaneous moduli (2.43) defined by R.W.Ogden [1997] is

$$\mathcal{A}^{1}_{0ijkl}=J^{-1}A_{i\alpha}A_{k\beta}\mathcal{A}^{1}_{\alpha j\beta l}. \tag{5.25}$$

For this problem

$$\begin{aligned}
\mathcal{A}^1_{0ijkl} &= JU''(J)\delta_{ij}\delta_{kl} + U'(J)\left[\delta_{ij}\delta_{kl} - \delta_{il}\delta_{kj}\right] \\
&- \frac{2c}{3}J^{-5/3}A_{i\alpha}A_{j\alpha}\delta_{kl} + \frac{2c}{9}J^{-5/3}\mathrm{tr}\left(\mathbf{A}^T\mathbf{A}\right)\delta_{ij}\delta_{kl} \\
&+ cJ^{-5/3}\left[A_{i\alpha}A_{k\alpha}\delta_{jl} - \frac{2}{3}A_{k\alpha}A_{l\alpha}\delta_{ij} + \frac{1}{3}\mathrm{tr}\left(\mathbf{A}^T\mathbf{A}\right)\delta_{il}\delta_{jk}\right] \\
&- \frac{4}{3}k_1J^{-5/3}\left(\overline{I}_4 - 1\right)\exp\left[k_2\left(\overline{I}_4 - 1\right)^2\right]\delta_{kl}Q_+ \\
&- \frac{4}{3}k_1J^{-5/3}\left(\overline{I}_6 - 1\right)\exp\left[k_2\left(\overline{I}_6 - 1\right)^2\right]\delta_{kl}Q_- \\
&+ 4k_1J^{-7/3}\left[1 + 2k_2\left(\overline{I}_4 - 1\right)^2\right]\exp\left[k_2\left(\overline{I}_4 - 1\right)^2\right]P_+ \\
&+ 4k_1J^{-7/3}\left[1 + 2k_2\left(\overline{I}_6 - 1\right)^2\right]\exp\left[k_2\left(\overline{I}_6 - 1\right)^2\right]P_- \\
&+ 2k_1J^{-5/3}\left(\overline{I}_4 - 1\right)\exp\left[k_2\left(\overline{I}_4 - 1\right)^2\right]\mathcal{T}_{ijkl}\left(\mathbf{M}_+\right) \\
&+ 2k_1J^{-5/3}\left(\overline{I}_6 - 1\right)\exp\left[k_2\left(\overline{I}_6 - 1\right)^2\right]\mathcal{T}_{ijkl}\left(\mathbf{M}_-\right). \qquad (5.26)
\end{aligned}$$

where

$$\begin{aligned}
Q_+ &= \left[\left(\mathbf{A}\mathrm{Sym}\left(\mathbf{M}_+\right)\mathbf{A}^T\right)_{ij} - \frac{1}{3}\mathrm{tr}\left(\mathbf{A}\mathrm{Sym}\left(\mathbf{M}_+\right)\mathbf{A}^T\right)\delta_{ij}\right], \\
Q_- &= \left[\left(\mathbf{A}\mathrm{Sym}\left(\mathbf{M}_-\right)\mathbf{A}^T\right)_{ij} - \frac{1}{3}\mathrm{tr}\left(\mathbf{A}\mathrm{Sym}\left(\mathbf{M}_-\right)\mathbf{A}^T\right)\delta_{ij}\right], \\
P_+ &= T\left(\mathbf{A}\mathrm{Sym}\left(\mathbf{M}_+\right)\mathbf{A}^T\right)_{ij}T\left(\mathbf{A}\mathrm{Sym}\left(\mathbf{M}_+\right)\mathbf{A}^T\right)_{kl}, \\
P_- &= T\left(\mathbf{A}\mathrm{Sym}\left(\mathbf{M}_-\right)\mathbf{A}^T\right)_{ij}T\left(\mathbf{A}\mathrm{Sym}\left(\mathbf{M}_-\right)\mathbf{A}^T\right)_{kl}, \\
\mathcal{T}_{ijkl}\left(\mathbf{M}\right) &= \left(\mathbf{A}\mathrm{Sym}\left(\mathbf{M}\right)\mathbf{A}^T\right)_{ik}\delta_{jl} - \frac{2}{3}\left(\mathbf{A}\mathrm{Sym}\left(\mathbf{M}\right)\mathbf{A}^T\right)_{kl}\delta_{ij} \\
&+ \frac{1}{3}\delta_{il}\delta_{jk}\mathrm{tr}\left(\mathbf{A}\mathrm{Sym}\left(\mathbf{M}\right)\mathbf{A}^T\right),
\end{aligned}$$

in which

$$T\left(\mathbf{G}\right) = \mathbf{G} - \frac{1}{3}\mathrm{tr}\left(\mathbf{G}\right)\mathbf{I}. \qquad (5.27)$$

5.1.4 Stress

Unconstrained–compressible

We have the incremental nominal stress (2.44) in the form of

$$\dot{S}_{0ij} = \mathcal{A}^1_{0ijkl}\delta A_{0lk}. \qquad (5.28)$$

Using the results above gives

$$\begin{aligned}
\dot{S}_{0ij} &= \left[JU''(J)+U'(J)\right]\mathrm{tr}\left(\delta\mathbf{A}_0\right)\delta_{ij}-U'(J)\delta A_{0ij}\\
&- \frac{2c}{3}J^{-5/3}\mathrm{tr}\left(\delta\mathbf{A}_0\right)T\left(\mathbf{A}\mathbf{A}^T\right)_{ij}\\
&+ cJ^{-5/3}\left[T\left(\mathbf{A}\mathbf{A}^T\left(\delta\mathbf{A}_0\right)^T\right)_{ij}+\frac{1}{3}\left(\mathrm{tr}\left(\mathbf{A}\mathbf{A}^T\right)\delta A_{0ij}-\mathrm{tr}\left(\mathbf{A}\mathbf{A}^T\delta\mathbf{A}_0^T\right)\delta_{ij}\right)\right]\\
&- \frac{4k_1}{3}J^{-5/3}\left(\overline{I}_4-1\right)\exp\left[k_2\left(\overline{I}_4-1\right)^2\right]\mathrm{tr}\left(\delta\mathbf{A}_0\right)T\left(\mathbf{A}\mathrm{Sym}\left(\mathbf{M}_+\right)\mathbf{A}^T\right)_{ij}\\
&- \frac{4k_1}{3}J^{-5/3}\left(\overline{I}_6-1\right)\exp\left[k_2\left(\overline{I}_6-1\right)^2\right]\mathrm{tr}\left(\delta\mathbf{A}_0\right)T\left(\mathbf{A}\mathrm{Sym}\left(\mathbf{M}_-\right)\mathbf{A}^T\right)_{ij}\\
&+ 4k_1J^{-7/3}\left[1+2k_2\left(\overline{I}_4-1\right)^2\right]\exp\left[k_2\left(\overline{I}_4-1\right)^2\right](T_+)_{ij}\\
&+ 4k_1J^{-7/3}\left[1+2k_2\left(\overline{I}_6-1\right)^2\right]\exp\left[k_2\left(\overline{I}_6-1\right)^2\right](T_-)_{ij}\\
&+ 2k_1J^{-5/3}\left(\overline{I}_4-1\right)\exp\left[k_2\left(\overline{I}_4-1\right)^2\right]\mathcal{T}_{ijkl}\left(\mathbf{M}_+\right)\delta A_{0lk}\\
&+ 2k_1J^{-5/3}\left(\overline{I}_6-1\right)\exp\left[k_2\left(\overline{I}_6-1\right)^2\right]\mathcal{T}_{ijkl}\left(\mathbf{M}_-\right)\delta A_{0lk} \qquad (5.29)
\end{aligned}$$

where

$$\begin{aligned}
(T_+)_{ij} &= T\left(\mathbf{A}\mathrm{Sym}\left(\mathbf{M}_+\right)\mathbf{A}^T\right)_{ij}\mathrm{tr}\left(T\left(\mathbf{A}\mathrm{Sym}\left(\mathbf{M}_+\right)\mathbf{A}^T\right)\delta\mathbf{A}_0\right)\\
(T_-)_{ij} &= T\left(\mathbf{A}\mathrm{Sym}\left(\mathbf{M}_-\right)\mathbf{A}^T\right)_{ij}\mathrm{tr}\left(T\left(\mathbf{A}\mathrm{Sym}\left(\mathbf{M}_-\right)\mathbf{A}^T\right)\delta\mathbf{A}_0\right)\\
\mathcal{T}_{ijkl}\left(\mathbf{M}\right)\delta A_{0lk} &= \left(\mathbf{A}\mathrm{Sym}\left(\mathbf{M}\right)\mathbf{A}^T\delta\mathbf{A}_0^T\right)_{ij}\\
&+ \frac{1}{3}\mathrm{tr}\left(\mathbf{A}\mathrm{Sym}\left(\mathbf{M}\right)\mathbf{A}^T\right)\delta A_{0ij}-\frac{2}{3}\mathrm{tr}\left(\mathbf{A}\mathrm{Sym}\left(\mathbf{M}\right)\mathbf{A}^T\delta\mathbf{A}_0\right)\delta_{ij}.
\end{aligned}$$

The equilibrium equation and boundary conditions for the incremental nominal stress are equations (5.2), which are written in components as

$$\frac{\partial\dot{S}_{0rr}}{\partial r}+\frac{\partial\dot{S}_{0zr}}{\partial z}+\frac{1}{r}(\dot{S}_{0rr}-\dot{S}_{0\theta\theta})=0, \qquad (5.30)$$

$$\frac{\partial\dot{S}_{0rz}}{\partial r}+\frac{\partial\dot{S}_{0zz}}{\partial z}+\frac{1}{r}\dot{S}_{0rz}=0, \qquad (5.31)$$

and setting $\dot{P}=0$ in (5.2) we have

$$\begin{bmatrix}\dot{S}_{0rr}&0&\dot{S}_{0zr}\\0&\dot{S}_{0\theta\theta}&0\\\dot{S}_{0rz}&0&\dot{S}_{0zz}\end{bmatrix}\begin{bmatrix}1\\0\\0\end{bmatrix}=-P\mathrm{tr}\left(\delta\mathbf{A}_0\right)\begin{bmatrix}1\\0\\0\end{bmatrix}+P\begin{bmatrix}u_{,r}&0&w_{,r}\\0&\frac{u}{r}&0\\u_{,z}&0&w_{,z}\end{bmatrix}\begin{bmatrix}1\\0\\0\end{bmatrix} \qquad (5.32)$$

on $r=r_{\mathrm{out}}$ and $r=r_{\mathrm{in}}$. On the outer boundary $r=r_{\mathrm{out}}$,

$$\dot{S}_{0rr} = -P_{\mathrm{ext}}\left(u_{,r}+\frac{u}{r}+w_{,z}\right)+P_{\mathrm{ext}}u_{,r}=-P_{\mathrm{ext}}\left(\frac{u}{r}+w_z\right) \qquad (5.33)$$

$$\dot{S}_{0rz} = P_{\mathrm{ext}}u_{,z} \qquad (5.34)$$

and on the inner boundary $r = r_{\text{in}}$

$$\dot{S}_{0rr} = -P_{\text{in}}\left(u_{,r} + \frac{u}{r} + w_{,z}\right) + P_{\text{in}}u_{,r} = -P_{\text{in}}\left(\frac{u}{r} + w_{,z}\right) \tag{5.35}$$

$$\dot{S}_{0rz} = P_{\text{in}}u_{,z}\,. \tag{5.36}$$

The boundary conditions on the interface $r = r_c$ are given by (5.3) and (5.4).

Constrained–incompressible

Consider the artery to be incompressible, in which $J = 1$, $U'(J) = 0$, $U''(J) = 1$ and $\text{tr}\,(\delta\mathbf{A}_0) = 0$. The form of the nominal stress is slightly different from the unconstrained equation (5.18), in that

$$\mathbf{S} = \frac{\partial\Psi}{\partial\mathbf{A}} - cp\mathbf{A}^{-1}, \tag{5.37}$$

where cp is a Lagrange multiplier and

$$\begin{aligned}\frac{\partial\Psi}{\partial\mathbf{A}} &= c\left[\mathbf{A}^T - \frac{1}{3}\text{tr}\left(\mathbf{A}^T\mathbf{A}\right)\mathbf{A}^{-1}\right]\\ &+ 2k_1\left(\overline{I}_4 - 1\right)\exp\left[k_2\left(\overline{I}_4 - 1\right)^2\right]\left[\text{Sym}\left(\mathbf{M}_+\right)\mathbf{A}^T - \frac{1}{3}\text{tr}\left(\mathbf{M}_+\mathbf{A}^T\mathbf{A}\right)\mathbf{A}^{-1}\right]\\ &+ 2k_1\left(\overline{I}_6 - 1\right)\exp\left[k_2\left(\overline{I}_6 - 1\right)^2\right]\left[\text{Sym}\left(\mathbf{M}_-\right)\mathbf{A}^T - \frac{1}{3}\text{tr}\left(\mathbf{M}_-\mathbf{A}^T\mathbf{A}\right)\mathbf{A}^{-1}\right]\end{aligned} \tag{5.38}$$

hence the nominal stress is

$$\begin{aligned}\mathbf{S} &= c\left[\mathbf{A}^T - \frac{1}{3}\text{tr}\left(\mathbf{A}^T\mathbf{A}\right)\mathbf{A}^{-1} - p\mathbf{A}^{-1}\right]\\ &+ 2k_1\left(\overline{I}_4 - 1\right)\exp\left[k_2\left(\overline{I}_4 - 1\right)^2\right]\left[\text{Sym}\left(\mathbf{M}_+\right)\mathbf{A}^T - \frac{1}{3}\text{tr}\left(\mathbf{M}_+\mathbf{A}^T\mathbf{A}\right)\mathbf{A}^{-1}\right]\\ &+ 2k_1\left(\overline{I}_6 - 1\right)\exp\left[k_2\left(\overline{I}_6 - 1\right)^2\right]\left[\text{Sym}\left(\mathbf{M}_-\right)\mathbf{A}^T - \frac{1}{3}\text{tr}\left(\mathbf{M}_-\mathbf{A}^T\mathbf{A}\right)\mathbf{A}^{-1}\right]\end{aligned} \tag{5.39}$$

The Cauchy stress has the relation $\boldsymbol{\sigma} = \text{J}^{-1}\mathbf{AS}$ with the nominal stress, hence

$$\begin{aligned}\boldsymbol{\sigma} &= J^{-1}\mathbf{A}\frac{\partial\Psi}{\partial\mathbf{A}} - cp\mathbf{I}\\ &= c\left[\mathbf{A}\mathbf{A}^T - \frac{1}{3}\text{tr}\left(\mathbf{A}^T\mathbf{A}\right) - p\mathbf{I}\right]\\ &+ 2k_1\left(\overline{I}_4 - 1\right)\exp\left[k_2\left(\overline{I}_4 - 1\right)^2\right]\left[\text{Sym}\left(\mathbf{M}_+\right)\mathbf{A}\mathbf{A}^T - \frac{1}{3}\text{tr}\left(\mathbf{M}_+\mathbf{A}^T\mathbf{A}\right)\mathbf{I}\right]\\ &+ 2k_1\left(\overline{I}_6 - 1\right)\exp\left[k_2\left(\overline{I}_6 - 1\right)^2\right]\left[\text{Sym}\left(\mathbf{M}_-\right)\mathbf{A}\mathbf{A}^T - \frac{1}{3}\text{tr}\left(\mathbf{M}_-\mathbf{A}^T\mathbf{A}\right)\mathbf{I}\right]\\ &= c\left[\mathbf{A}\mathbf{A}^T - q\mathbf{I}\right]\\ &+ 2F_1(r)\left[\text{Sym}\left(\mathbf{M}_+\right)\mathbf{A}\mathbf{A}^T - \frac{1}{3}\text{tr}\left(\mathbf{M}_+\mathbf{A}^T\mathbf{A}\right)\mathbf{I}\right]\\ &+ 2F_2(r)\left[\text{Sym}\left(\mathbf{M}_-\right)\mathbf{A}\mathbf{A}^T - \frac{1}{3}\text{tr}\left(\mathbf{M}_-\mathbf{A}^T\mathbf{A}\right)\mathbf{I}\right]\end{aligned} \tag{5.40}$$

where $q = p + \frac{1}{3}\mathrm{tr}\left(\mathbf{A}\mathbf{A}^T\right)$. From equations (2.44), the incremental nominal stress is

$$\begin{aligned}
\dot{S}_{0ij} &= c\left[\left(\mathbf{A}\mathbf{A}^T\left(\delta\mathbf{A}_0\right)^T\right)_{ij} + \frac{1}{3}\mathrm{tr}\left(\mathbf{A}\mathbf{A}^T\right)\delta A_{0ij} - \frac{2}{3}\mathrm{tr}\left(\mathbf{A}\mathbf{A}^T\delta\mathbf{A}_0^T\right)\delta_{ij} - \dot{p}\delta_{ij} + p\delta A_{0lk}\right] \\
&+ 4P1(r)T\left(\mathbf{A}\mathrm{Sym}\left(\mathbf{M}_+\right)\mathbf{A}^T\right)_{ij}\mathrm{tr}\left(T\left(\mathbf{A}\mathrm{Sym}\left(\mathbf{M}_+\right)\mathbf{A}^T\right)\delta\mathbf{A}_0\right) \\
&+ 4P2(r)T\left(\mathbf{A}\mathrm{Sym}\left(\mathbf{M}_-\right)\mathbf{A}^T\right)_{ij}\mathrm{tr}\left(T\left(\mathbf{A}\mathrm{Sym}\left(\mathbf{M}_-\right)\mathbf{A}^T\right)\delta\mathbf{A}_0\right) \\
&+ 2F1(r)\mathcal{T}_{ijkl}\left(\mathbf{M}_+\right)\delta A_{0lk} \\
&+ 2F2(r)\mathcal{T}_{ijkl}\left(\mathbf{M}_-\right)\delta A_{0lk} \\
&= c\left[\left(\mathbf{A}\mathbf{A}^T\left(\delta\mathbf{A}_0\right)^T\right)_{ij} - \dot{q}\delta_{ij} + q\delta A_{0lk}\right], \\
&+ 4P1(r)(T_+)_{ij} + 4P2(r)(T_-)_{ij} \\
&+ 2F1(r)\mathcal{T}_{ijkl}\left(\mathbf{M}_+\right)\delta A_{0lk} + 2F2(r)\mathcal{T}_{ijkl}\left(\mathbf{M}_-\right)\delta A_{0lk}
\end{aligned} \tag{5.41}$$

where

$$\begin{aligned}
P_1(r) &= k_1\left[1 + 2k_2\left(\overline{I}_4 - 1\right)^2\right]\exp\left[k_2\left(\overline{I}_4 - 1\right)^2\right], \\
P_2(r) &= k_1\left[1 + 2k_2\left(\overline{I}_6 - 1\right)^2\right]\exp\left[k_2\left(\overline{I}_6 - 1\right)^2\right], \\
F_1(r) &= k_1\left(\overline{I}_4 - 1\right)\exp\left[k_2\left(\overline{I}_4 - 1\right)^2\right], \\
F_2(r) &= k_1\left(\overline{I}_6 - 1\right)\exp\left[k_2\left(\overline{I}_6 - 1\right)^2\right], \\
\dot{q} &= \dot{p} + \frac{2}{3}\mathrm{tr}\left(\mathbf{A}\mathbf{A}^T\delta\mathbf{A}_0^T\right).
\end{aligned}$$

The deformation gradient is

$$\mathbf{A} = \begin{bmatrix} \frac{R(r)}{kr\lambda} & 0 & 0 \\ 0 & k\frac{r}{R(r)} & 0 \\ 0 & 0 & \lambda \end{bmatrix} = \begin{bmatrix} a_r(r) & 0 & 0 \\ 0 & a_\theta(r) & 0 \\ 0 & 0 & a_z(r) \end{bmatrix} \tag{5.42}$$

where $R(r) = \sqrt{k\lambda\left(r^2 - r_i^2\right) + R_i^2}$. The incremental deformation gradient is

$$\delta\mathbf{A_0} = \begin{bmatrix} u_{,r} & 0 & u_{,z} \\ 0 & \frac{u}{r} & 0 \\ w_{,r} & 0 & w_{,z} \end{bmatrix}. \tag{5.43}$$

The equilibrium equations and boundary conditions for the Cauchy stress are equations (5.1). Writing these in components, we have

$$\begin{aligned}
\frac{dq}{dr} &= 2\,a_r\left(r\right)\frac{d}{dr}a_r\left(r\right) - \frac{2}{3}\frac{\left(\frac{d}{dr}F_1\left(r\right)\right)I_4\left(r\right)}{\mu} - \frac{2}{3}\frac{F_1\left(r\right)\frac{d}{dr}I_4\left(r\right)}{\mu} - \frac{2}{3}\frac{\left(\frac{d}{dr}F_2\left(r\right)\right)I_6\left(r\right)}{\mu} \\
&- \frac{2}{3}\frac{F_2\left(r\right)\frac{d}{dr}I_6\left(r\right)}{\mu} + \frac{\left(a_r\left(r\right)\right)^2}{r} - \frac{\left(a_\theta\left(r\right)\right)^2}{r} - 2\frac{F_1\left(r\right)\left(\cos\left(\beta\right)\right)^2\left(a_\theta\left(r\right)\right)^2}{\mu\,r} \\
&- 2\frac{F_2\left(r\right)\left(\cos\left(\beta\right)\right)^2\left(a_\theta\left(r\right)\right)^2}{\mu\,r}
\end{aligned} \tag{5.44}$$

with

$$\mu a_r(r)^2 - \mu q(r) - \frac{2}{3}F_1(r)I_4(r) - \frac{2}{3}F_2(r)I_6(r) = -P_{\text{ext}} \quad \text{at} \quad r = r_{\text{out}}. \tag{5.45}$$

The equilibrium equations and boundary conditions for the incremental nominal stress are equations (5.2), which are written in components,

$$\begin{aligned} \frac{\partial \dot{S}_{0rr}}{\partial r} + \frac{\partial \dot{S}_{0zr}}{\partial z} + \frac{1}{r}(\dot{S}_{0rr} - \dot{S}_{0\theta\theta}) = 0, \\ \frac{\partial \dot{S}_{0rz}}{\partial r} + \frac{\partial \dot{S}_{0zz}}{\partial z} + \frac{1}{r}\dot{S}_{0rz} = 0, \end{aligned} \tag{5.46}$$

and since $\dot{P} = 0$ and $\text{tr}(\delta \mathbf{A}_0) = 0$ in (5.2) we have

$$\dot{S}_{0rr} = P_{\text{ext}} u_{,r} \quad \text{and} \quad \dot{S}_{0rz} = P_{\text{ext}} u_{,z} \quad \text{at} \quad r = r_{\text{out}}, \tag{5.47}$$

$$\dot{S}_{0rr} = P_{\text{in}} u_{,r} \quad \text{and} \quad \dot{S}_{0rz} = P_{\text{in}} u_{,z} \quad \text{at} \quad r = r_{\text{in}}. \tag{5.48}$$

The jump conditions on the interface at $r = r_c$ are (5.3) and (5.4).

5.1.5 Static tears for an axisymmetric incompressible aorta

Now consider one slice of crack section as shown in Figure 4.1, which is decomposed into the'jump in u' and the 'jump in w'. The jump conditions at $r = r_c$ are (5.3) and (5.4).

Jump in w across the crack

Similar to §4.2.1, using the symmetry of the domain in z, we express the displacements and the stresses as

$$u(r,z) = \frac{i}{\pi}\int_0^\infty \hat{u}(g,r)\sin gz\, dg = \frac{1}{\pi}\int_0^\infty \hat{U}^w(g,r)\sin gz\, dg \tag{5.49}$$

$$w(r,z) = \frac{1}{\pi}\int_0^\infty \hat{w}(g,r)\cos gz\, dg = \frac{1}{\pi}\int_0^\infty \hat{W}^w(g,r)\cos gz\, dg \tag{5.50}$$

$$\dot{S}_{0rr}(r,z) = \frac{i}{\pi}\int_0^\infty \hat{\dot{S}}_{0rr}(g,r)\sin gz\, dg = \frac{1}{\pi}\int_0^\infty \hat{\dot{S}}^w_{0rr}(g,r)\sin gz\, dg \tag{5.51}$$

$$\dot{S}_{0rz}(r,z) = \frac{1}{\pi}\int_0^\infty \hat{\dot{S}}_{0rz}(g,r)\cos gz\, dg = \frac{1}{\pi}\int_0^\infty \hat{\dot{S}}^w_{0rz}(g,r)\cos gz\, dg \tag{5.52}$$

$$\dot{S}_{0\theta\theta}(r,z) = \frac{i}{\pi}\int_0^\infty \hat{\dot{S}}_{0\theta\theta}(g,r)\sin gz\, dg = \frac{1}{\pi}\int_0^\infty \hat{\dot{S}}^w_{0\theta\theta}(g,r)\sin gz\, dg \tag{5.53}$$

$$\dot{S}_{0zr}(r,z) = \frac{1}{\pi}\int_0^\infty \hat{\dot{S}}_{0zr}(g,r)\cos gz\, dg = \frac{1}{\pi}\int_0^\infty \hat{\dot{S}}^w_{0zr}(g,r)\cos gz\, dg \tag{5.54}$$

$$\dot{S}_{0zz}(r,z) = \frac{i}{\pi}\int_0^\infty \hat{\dot{S}}_{0zz}(g,r)\sin gz\, dg = \frac{1}{\pi}\int_0^\infty \hat{\dot{S}}^w_{0zz}(g,r)\sin gz\, dg \tag{5.55}$$

$$\dot{q}(r,z) = \frac{i}{\pi}\int_0^\infty \hat{\dot{q}}(g,r)\sin gz dg = \frac{1}{\pi}\int_0^\infty \hat{\dot{q}}^w(g,r)\sin gz\, dg. \tag{5.56}$$

where we define

$$\hat{U}^w = i\hat{u}, \quad \hat{W}^w = \hat{w}, \quad \hat{\dot{S}}^w_{0rr} = i\hat{\dot{S}}_{0rr}, \quad \hat{\dot{S}}^w_{0rz} = \hat{\dot{S}}_{0rz}, \quad \hat{\dot{S}}^w_{0\theta\theta} = i\hat{\dot{S}}_{0\theta\theta} \tag{5.57}$$

$$\hat{\dot{S}}^w_{0zr} = \hat{\dot{S}}_{0zr}, \quad \hat{\dot{S}}^w_{0zz} = i\hat{\dot{S}}_{0zz}, \quad \hat{\dot{q}}^w = i\hat{\dot{q}}, \quad \hat{p}^w = i\hat{p}. \tag{5.58}$$

$$\tag{5.59}$$

The equilibrium equations (5.46) after Fourier transforming become

$$\begin{aligned} A_1\hat{U}^w + B_1(\hat{U}^w)' + C_1(\hat{U}^w)'' + D_1(\hat{U}^w)''' + E_1\hat{\dot{q}}^w &= 0 \\ A_2\hat{U}^w + B_2(\hat{U}^w)' + C_2(\hat{U}^w)'' + D_2(\hat{\dot{q}}^w)' &= 0. \end{aligned} \tag{5.60}$$

The boundary conditions (5.47) after Fourier transform are

$$\begin{aligned} a_1\hat{U}^w + a_2(\hat{U}^w)' + a_4\hat{\dot{q}}^w &= 0 \quad \text{at} \quad r = r_{\text{in}} \\ b_1\hat{U}^w + b_2(\hat{U}^w)' + b_3(\hat{U}^w)'' &= 0 \quad \text{at} \quad r = r_{\text{in}} \\ c_5\hat{U}^w + c_6(\hat{U}^w)' + c_8\hat{\dot{q}}^w &= 0 \quad \text{at} \quad r = r_{\text{out}} \\ d_5\hat{U}^w + d_6(\hat{U}^w)' + d_7(\hat{U}^w)'' &= 0 \quad \text{at} \quad r = r_{\text{out}}. \end{aligned} \tag{5.61}$$

Here $A_1, B_1, C_1, D_1, E_1, A_2, B_2, C_2, D_2, a_1, a_2, a_4, b_1, b_2, b_3, c_5, c_6, c_8, d_5, d_6, d_7$ are given in Appendix A.

The jump conditions after Fourier transformation are

$$\left[\hat{U}^w\right]^+_- = 0, \qquad \left[\hat{W}^w\right]^+_- = 1, \qquad \left[\hat{\dot{S}}^w_{0rr}\right]^+_- = \left[\hat{\dot{S}}^w_{0rz}\right]^+_- = 0, \qquad \left[\hat{\dot{q}}^w\right]^+_- = 0. \tag{5.62}$$

The stress components $\hat{\dot{S}}^w_{0rr}$ and $\hat{\dot{S}}^w_{0rz}$ are functions of $\hat{U}^w$, $\hat{W}^w$ and $\hat{\dot{q}}^w$:

$$\hat{\dot{S}}^w_{0rr} = s_{wr1}(r)\hat{U}^w(r) + s_{wr2}(r)\frac{d\hat{U}^w(r)}{dr} + \hat{\dot{q}}^w, \tag{5.63}$$

$$\hat{\dot{S}}^w_{0rz} = s_{wz1}(r)\hat{U}^w(r) + s_{wz2}(r)\frac{d\hat{U}^w(r)}{dr} + s_{wz3}(r)\frac{d\left[\hat{U}^w(r)\right]^2}{dr^2}, \tag{5.64}$$

where $s_{wr1}(r)$, $s_{wr2}(r)$, $s_{wz1}(r)$, $s_{wz2}(r)$ and $s_{wz3}(r)$ are in Appendix A.

Jump in u across the crack

Using the symmetry of the domain in z, we express the displacements and the stresses as

$$u(r,z) = \frac{1}{\pi}\int_0^\infty \hat{u}(g,r)\cos gz\,dg = \frac{1}{\pi}\int_0^\infty \hat{U}^u(g,r)\cos gz\,dg \tag{5.65}$$

$$w(r,z) = \frac{i}{\pi}\int_0^\infty \hat{w}(g,r)\sin gz\,dg = \frac{1}{\pi}\int_0^\infty \hat{W}^u(g,r)\sin gz\,dg \tag{5.66}$$

$$\dot{S}_{0rr}(r,z) = \frac{1}{\pi}\int_0^\infty \hat{\dot{S}}_{0rr}(g,r)\cos gz\,dg = \frac{1}{\pi}\int_0^\infty \hat{\dot{S}}^u_{0rr}(g,r)\cos gz\,dg \tag{5.67}$$

$$\dot{S}_{0rz}(r,z) = \frac{i}{\pi}\int_0^\infty \hat{\dot{S}}_{0rz}(g,r)\sin gz\,dg = \frac{1}{\pi}\int_0^\infty \hat{\dot{S}}^u_{0rz}(g,r)\sin gz\,dg \tag{5.68}$$

$$\dot{S}_{0\theta\theta}(r,z) = \frac{1}{\pi}\int_0^\infty \hat{\dot{S}}_{0\theta\theta}(g,r)\cos gz\,dg = \frac{1}{\pi}\int_0^\infty \hat{\dot{S}}^u_{0\theta\theta}(g,r)\cos gz\,dg \tag{5.69}$$

$$\dot{S}_{0zr}(r,z) = \frac{i}{\pi}\int_0^\infty \hat{\dot{S}}_{0zr}(g,r)\sin gz\,dg = \frac{1}{\pi}\int_0^\infty \hat{\dot{S}}^u_{0zr}(g,r)\sin gz\,dg \tag{5.70}$$

$$\dot{S}_{0zz}(r,z) = \frac{1}{\pi}\int_0^\infty \hat{\dot{S}}_{0zz}(g,r)\cos gz\,dg = \frac{1}{\pi}\int_0^\infty \hat{\dot{S}}^u_{0zz}(g,r)\cos gz\,dg \tag{5.71}$$

$$\dot{q}(r,z) = \frac{1}{\pi}\int_0^\infty \hat{\dot{q}}(g,r)\cos gz dg = \frac{1}{\pi}\int_0^\infty \hat{\dot{q}}(g,r)\cos gz dg, \tag{5.72}$$

where we define

$$\hat{U}^u = \hat{u}, \quad \hat{W}^u = i\hat{w}, \quad \hat{\dot{S}}^u_{0rr} = \hat{\dot{S}}_{0rr}, \quad \hat{\dot{S}}^u_{0rz} = i\hat{\dot{S}}_{0rz}, \quad \hat{\dot{S}}^u_{0\theta\theta} = \hat{\dot{S}}_{0\theta\theta}, \tag{5.73}$$

$$\hat{\dot{S}}^u_{0zr} = i\hat{\dot{S}}_{0zr}, \quad \hat{\dot{S}}^u_{0zz} = \hat{\dot{S}}_{0zz}, \quad \hat{p}^u = \hat{p}, \quad \hat{\dot{q}}^u = \hat{\dot{q}}. \tag{5.74}$$

The equilibrium equations (5.46) after Fourier transforming become

$$\begin{aligned} A_1\hat{U}^u + B_1(\hat{U}^u)' + C_1(\hat{U}^u)'' + D_1(\hat{U}^u)''' + E1\hat{\dot{q}}^u &= 0 \\ A_2\hat{U}^u + B_2(\hat{U}^u)' + C_2(\hat{U}^u)'' + D_2(\hat{\dot{q}}^u)' &= 0 \end{aligned} \tag{5.75}$$

The boundary condition (5.47) after Fourier transform are given

$$\begin{aligned} a_1\hat{U}^u + a_2(\hat{U}^u)' + a_4\hat{\dot{q}}^u &= 0 \quad \text{at} \quad r = r_{\text{in}} \\ b_1\hat{U}^u + b_2(\hat{U}^u)' + b_3(\hat{U}^u)'' &= 0 \quad \text{at} \quad r = r_{\text{in}} \\ c_5\hat{U}^u + c_6(\hat{U}^u)' + c_8\hat{\dot{q}}^u &= 0 \quad \text{at} \quad r = r_{\text{out}} \\ d_5\hat{U}^u + d_6(\hat{U}^u)' + d_7(\hat{U}^u)'' &= 0 \quad \text{at} \quad r = r_{\text{out}} \end{aligned} \tag{5.76}$$

where $A_1, B_1, C_1, D_1, E_1, A_2, B_2, C_2, D_2, a_1, a_2, a_4, b_1, b_2, b_3, c_5, c_6, c_8, d_5, d_6, d_7$ are in Appendix B.

The jump conditions after Fourier transform are

$$\left[\hat{U}^u\right]_-^+ = 1, \qquad \left[\hat{W}^u\right]_-^+ = 0, \qquad \left[\hat{\dot{S}}^u_{0rr}\right]_-^+ = \left[\hat{\dot{S}}^u_{0rz}\right]_-^+ = 0, \qquad \left[\hat{\dot{q}}^u\right]_-^+ = 0. \tag{5.77}$$

The stress components $\hat{\dot{S}}^u_{0rr}$ and $\hat{\dot{S}}^u_{0rz}$ are functions of $\hat{U}^u$, $\hat{W}^u$ and $\hat{\dot{q}}^u$:

$$\hat{\dot{S}}^u_{0rr} = s_{ur1}(r)\hat{U}^u(r) + s_{ur2}(r)\frac{d\hat{U}^u(r)}{dr} - \hat{\dot{q}}^u, \tag{5.78}$$

$$\hat{\dot{S}}^u_{0rz} = s_{uz1}(r)\hat{U}^u(r) + s_{uz2}(r)\frac{d\hat{U}^u(r)}{dr} + s_{uz3}(r)\frac{d\left[\hat{U}^u(r)\right]^2}{dr^2}, \tag{5.79}$$

where $s_{ur1}(r)$, $s_{ur2}(r)$, $s_{uz1}(r)$, $s_{uz2}(r)$ and $s_{uz3}(r)$ are given in Appendix B.

5.1.6 Numerical solution—Collocation method

In this section we are going to solve $\hat{U}^w, \hat{W}^w, \hat{U}^u, \hat{W}^u$ and $\hat{\dot{S}}^w_{0rr}, \hat{\dot{S}}^w_{0rz}, \hat{\dot{S}}^u_{0rr}, \hat{\dot{S}}^u_{0rz}$ numerically. we consider the special $g = 0$ separately, which will give singularity if we use the following collocation method.

BVP method

As shown in Figure 4.1, region 1 is $r_{\text{in}} \le r \le r_c$ and region 2 is $r_c \le r \le r_{\text{out}}$.
In region 1, $r = r_1 = r_{\text{in}} + R(r_c - r_{\text{in}})$ and $\dfrac{d}{dr} = \dfrac{1}{r_c - r_{\text{in}}}\dfrac{d}{dR}$; in region 2, $r = r_2 = r_{\text{out}} + R(r_c - r_{\text{out}})$ and $\dfrac{d}{dr} = \dfrac{1}{r_c - r_{\text{out}}}\dfrac{d}{dR}$. The range of R is $[0, 1]$. The boundary in each region is represented by $R = 0$, and $R = 1$ represents the crack face.

Jump in w

It's convenient to define Y_1, Y_2, Y_3, Y_4, Y_9 to be $\hat{U}^w, (\hat{U}^w)', (\hat{U}^w)'', \hat{\dot{q}}^w, \hat{q}^w$ respectively in region 1, and $Y_5, Y_6, Y_7, Y_8, Y_{10}$ to be $\hat{U}^w, (\hat{U}^w)', (\hat{U}^w)'', \hat{\dot{q}}^w, \hat{q}^w$ respectively in region 2.

From equations (5.44) and (5.60) we have the following system of fourth-order equations

$$\begin{aligned}
\frac{dY_1}{dR} &= Y_2 \\
\frac{dY_2}{dR} &= Y_3 \\
\frac{dY_3}{dR} &= -\frac{A_1}{D_1}Y_1\left(r_c - r_{\text{in}}\right)^3 - \frac{B_1}{D_1}Y_2\left(r_c - r_{\text{in}}\right)^2 - \frac{C_1}{D_1}Y_3\left(r_c - r_{\text{in}}\right) - \frac{E_1}{D_1}Y_4\left(r_c - r_{\text{in}}\right)^3 \\
\frac{dY_4}{dR} &= -\frac{A_2}{D_2}Y_1\left(r_c - r_{\text{in}}\right) - \frac{B_2}{D_2}Y_2 - \frac{C_2}{D_2}Y_3\frac{1}{\left(r_c - r_{\text{in}}\right)} \\
\frac{dY_9}{dR} &= \left(r_c - r_{\text{in}}\right)Q(r_1) \\
\frac{dY_5}{dR} &= Y_6 \\
\frac{dY_6}{dR} &= Y_7 \\
\frac{dY_7}{dR} &= -\frac{A_1}{D_1}Y_1\left(r_c - r_{\text{out}}\right)^3 - \frac{B_1}{D_1}Y_2\left(r_c - r_{\text{out}}\right)^2 - \frac{C_1}{D_1}Y_3\left(r_c - r_{\text{out}}\right) - \frac{E_1}{D_1}Y_4\left(r_c - r_{\text{out}}\right)^3 \\
\frac{dY_8}{dR} &= -\frac{A_2}{D_2}Y_1\left(r_c - r_{\text{out}}\right) - \frac{B_2}{D_2}Y_2 - \frac{C_2}{D_2}Y_3\frac{1}{\left(r_c - r_{\text{out}}\right)} \\
\frac{dY_{10}}{dR} &= \left(r_c - r_{\text{out}}\right)Q(r_2),
\end{aligned}$$

where

$$\begin{aligned}
Q(r) &= 2\,a_r\left(r\right)\frac{d}{dr}a_r\left(r\right) - \frac{2}{3}\frac{\left(\frac{d}{dr}F_1\left(r\right)\right)I_4\left(r\right)}{\mu} - \frac{2}{3}\frac{F_1\left(r\right)\frac{d}{dr}I_4\left(r\right)}{\mu} - \frac{2}{3}\frac{\left(\frac{d}{dr}F_2\left(r\right)\right)I_6\left(r\right)}{\mu} \\
&- \frac{2}{3}\frac{F_2\left(r\right)\frac{d}{dr}I_6\left(r\right)}{\mu} + \frac{\left(a_r\left(r\right)\right)^2}{r} - \frac{\left(a_t\left(r\right)\right)^2}{r} - 2\frac{F_1\left(r\right)\left(\cos\left(\beta\right)\right)^2\left(a_t\left(r\right)\right)^2}{\mu\, r} \\
&- 2\frac{F_2\left(r\right)\left(\cos\left(\beta\right)\right)^2\left(a_t\left(r\right)\right)^2}{\mu\, r}.
\end{aligned}$$

We define $Y_{a1}, Y_{a2}, Y_{a3}, Y_{a4}, Y_{a9}$ to be $\hat{U}^w, (\hat{U}^w)', (\hat{U}^w)'', \hat{\dot{q}}^w, \hat{q}^w$ respectively on the inner boundary; Y_{a5}, Y_{a6}, Y_{a7}, Y_{a8}, Y_{a10} to be $\hat{U}^w, (\hat{U}^w)', (\hat{U}^w)'', \hat{\dot{q}}^w, \hat{q}^w$ respectively on the outer boundary; Y_{b1}, Y_{b2}, Y_{b3}, Y_{b4}, Y_{b9} to be $\hat{U}^w, (\hat{U}^w)', (\hat{U}^w)'', \hat{\dot{q}}^w, \hat{q}^w$ respectively on the lower crack face; Y_{b5}, Y_{b6}, Y_{b7}, Y_{b8}, Y_{b10} to be $\hat{U}^w, (\hat{U}^w)', (\hat{U}^w)'', \hat{\dot{q}}^w, \hat{q}^w$ respectively on the upper crack face.

Referring to (5.45), (5.61) and (5.62), the conditions on the outer boundary and the jump

conditions on tear faces are

$$
\begin{aligned}
a_1 Y_{a1} + a_2 \frac{Y_{a2}}{r_c - r_{\text{in}}} + a_4 Y_{a4} &= 0 \\
b_1 Y_{a1} + b_2 \frac{Y_{a2}}{r_c - r_{\text{in}}} + b_3 \frac{Y_{a3}}{(r_c - r_{\text{in}})^2} &= 0 \\
c_5 Y_{a5} + c_6 \frac{Y_{a6}}{r_c - r_{\text{out}}} + c_8 Y_{a8} &= 0 \\
d_5 Y_{a5} + d_6 \frac{Y_{a6}}{r_c - r_{\text{out}}} + d_7 \frac{Y_{a7}}{(r_c - r_{\text{out}})^2} &= 0 \\
\mu a r (r_{\text{out}})^2 - \mu Y_{a10} - \frac{2}{3} F_1(r_{\text{out}}) I_4(r_{\text{out}}) - \frac{2}{3} F_2(r_{\text{out}}) I_6(r_{\text{out}}) - P_{\text{ext}} &= 0 \\
Y_{b5} - Y_{b1} &= 0 \\
-\frac{1}{g}\left(\frac{Y_{b6}}{r_c - r_{\text{out}}} + \frac{Y_{b5}}{r_c}\right) + \frac{1}{g}\left(\frac{Y_{b2}}{r_c - r_{\text{in}}} + \frac{Y_{b1}}{r_c}\right) - 1 &= 0 \\
e_5 Y_{b5} + e_6 \frac{Y_{b6}}{r_c - r_{\text{out}}} + e_8 Y_{b8} - \left(e_1 Y_{b1} + e_2 \frac{Y_{b2}}{r_c - r_{r_{\text{in}}}} + e_4 Y_{b4}\right) &= 0 \\
f_5 Y_{b5} + f_6 \frac{Y_{b6}}{r_c - r_{\text{out}}} + f_7 \frac{Y_{b7}}{(r_c - r_{\text{out}})^2} - \left(f_1 Y_{b1} + f_2 \frac{Y_{b2}}{r_c - r_{\text{in}}} + f_3 \frac{Y_{b3}}{(r_c - r_{\text{in}})^2}\right) &= 0 \\
Y_{b10} - Y_{b9} &= 0
\end{aligned}
$$

where $e_1, e_2, e_4, e_5, e_6, e_8$ and $f_1, f_2, f_3, f_5, f_6, f_7$ are in Appendix A. After we define the problem appropriately, we use the Matlab routine '`bvp4c`' to calculate the values of $Y_1, Y_2, Y_3, Y_4, Y_5, Y_6, Y_7, Y_8, Y_9, Y_{10}$, from which $\hat{U}^w, \hat{W}^w$ are obtained, and $\hat{\dot{S}}^w_{0rr}, \hat{\dot{S}}^w_{0rz}$ are functions of $\hat{U}^w, \hat{W}^w$.

Jump in u

It is convenient to define Y_1, Y_2, Y_3, Y_4, Y_9 to be $\hat{U}^u, (\hat{U}^u)', (\hat{U}^u)'', \hat{\dot{q}}^u, \hat{q}^u$ respectively in region 1, and $Y_5, Y_6, Y_7, Y_8, Y_{10}$ to be $\hat{U}^u, (\hat{U}^u)', (\hat{U}^u)'', \hat{\dot{q}}^u, \hat{q}^u$ respectively in region 2.

From equations (5.44) and (5.75) we have

$$\begin{aligned}
\frac{dY_1}{dR} &= Y_2 \\
\frac{dY_2}{dR} &= Y_3 \\
\frac{dY_3}{dR} &= -\frac{A_1}{D_1}Y_1\left(r_c - r_{\text{in}}\right)^3 - \frac{B_1}{D_1}Y_2\left(r_c - r_{\text{in}}\right)^2 - \frac{C_1}{D_1}Y_3\left(r_c - r_{\text{in}}\right) - \frac{E_1}{D_1}Y_4\left(r_c - r_{\text{in}}\right)^3 \\
\frac{dY_4}{dR} &= -\frac{A_2}{D_2}Y_1\left(r_c - r_{\text{in}}\right) - \frac{B_2}{D_2}Y_2 - \frac{C_2}{D_2}Y_3\frac{1}{\left(r_c - r_{\text{in}}\right)} \\
\frac{dY_9}{dR} &= \left(r_c - r_{\text{in}}\right)Q(r_1) \\
\frac{dY_5}{dR} &= Y_6 \\
\frac{dY_6}{dR} &= Y_7 \\
\frac{dY_7}{dR} &= -\frac{A_1}{D_1}Y_1\left(r_c - r_{\text{out}}\right)^3 - \frac{B_1}{D_1}Y_2\left(r_c - r_{\text{out}}\right)^2 - \frac{C_1}{D_1}Y_3\left(r_c - r_{\text{out}}\right) - \frac{E_1}{D_1}Y_4\left(r_c - r_{\text{out}}\right)^3 \\
\frac{dY_8}{dR} &= -\frac{A_2}{D_2}Y_1\left(r_c - r_{\text{out}}\right) - \frac{B_2}{D_2}Y_2 - \frac{C_2}{D_2}Y_3\frac{1}{\left(r_c - r_{\text{out}}\right)} \\
\frac{dY_{10}}{dR} &= \left(r_c - r_{\text{out}}\right)Q(r_2)
\end{aligned}$$

We define $Y_{a1}, Y_{a2}, Y_{a3}, Y_{a4}, Y_{a9}$ to be $\hat{U}^u, (\hat{U}^u)', (\hat{U}^u)'', \hat{\dot{q}}^u, \hat{q}^u$ respectively on the inner boundary; Y_{a5}, Y_{a6}, Y_{a7}, Y_{a8}, Y_{a10} to be $\hat{U}^u, (\hat{U}^u)', (\hat{U}^u)'', \hat{\dot{q}}^u, \hat{q}^u$ respectively on the outer boundary; Y_{b1}, Y_{b2}, Y_{b3}, Y_{b4}, Y_{b9} to be $\hat{U}^u, (\hat{U}^u)', (\hat{U}^u)'', \hat{\dot{q}}^u, \hat{q}^u$ respectively on the lower crack face; Y_{b5}, Y_{b6}, Y_{b7}, Y_{b8}, Y_{b10} to be $\hat{U}^u, (\hat{U}^u)', (\hat{U}^u)'', \hat{\dot{q}}^u, \hat{q}^u$ respectively on the upper crack face.

Refering to (5.45), (5.76) and (5.77), the conditions on the outer boundary and the jump

conditions on crack faces are

$$
\begin{aligned}
a_1 Y_{a1} + a_2 \frac{Y_{a2}}{r_c - r_{\text{in}}} + a_4 Y_{a4} &= 0 \\
b_1 Y_{a1} + b_2 \frac{Y_{a2}}{r_c - r_{\text{in}}} + b_3 \frac{Y_{a3}}{(r_c - r_{\text{in}})^2} &= 0 \\
c_5 Y_{a5} + c_6 \frac{Y_{a6}}{r_c - r_{\text{out}}} + c_8 Y_{a8} &= 0 \\
d_5 Y_{a5} + d_6 \frac{Y_{a6}}{r_c - r_{\text{out}}} + d_7 \frac{Y_{a7}}{(r_c - r_{\text{out}})^2} &= 0 \\
\mu a r(r_{\text{out}})^2 - \mu Y_{a10} - \frac{2}{3} F_1(r_{\text{out}}) I_4(r_{\text{out}}) - \frac{2}{3} F_2(r_{\text{out}}) I_6(r_{\text{out}}) - P_{\text{ext}} &= 0 \\
Y_{b5} - Y_{b1} - 1 &= 0 \\
\frac{1}{g}\left(\frac{Y_{b6}}{r_c - r_{\text{out}}} + \frac{Y_{b5}}{r_c}\right) - \frac{1}{g}\left(\frac{Y_{b2}}{r_c - r_{\text{in}}} + \frac{Y_{b1}}{r_c}\right) &= 0 \\
e_5 Y_{b5} + e_6 \frac{Y_{b6}}{r_c - r_{\text{out}}} + e_8 Y_{b8} - \left(e_1 Y_{b1} + e_2 \frac{Y_{b2}}{r_c - r_{r_{\text{in}}}} + e_4 Y_{b4}\right) &= 0 \\
f_5 Y_{b5} + f_6 \frac{Y_{b6}}{r_c - r_{\text{out}}} + f_7 \frac{Y_{b7}}{(r_c - r_{\text{out}})^2} - \left(f_1 Y_{b1} + f_2 \frac{Y_{b2}}{r_c - r_{\text{in}}} + f_3 \frac{Y_{b3}}{(r_c - r_{\text{in}})^2}\right) &= 0 \\
Y_{b10} - Y_{b9} &= 0
\end{aligned}
$$

where $e_1, e_2, e_4, e_5, e_6, e_8$ and $f_1, f_2, f_3, f_5, f_6, f_7$ are in Appendix B. Then we use the Matlab routine '`bvp4c`' to calculate the values of $Y_1, Y_2, Y_3, Y_4, Y_5, Y_6, Y_7, Y_8, Y_9, Y_{10}$, from which $\hat{U}^u, \hat{W}^u$ are obtained, and $\hat{\dot{S}}^u_{0rz}, \hat{\dot{S}}^u_{0rz}$ are functions of $\hat{U}^u, \hat{W}^u$.

5.1.7 The case $g = 0$

The calculation of $\hat{U}^w, \hat{W}^w, \hat{\dot{S}}^w_{0rr}, \hat{\dot{S}}^w_{0rz}$ and $\hat{U}^u, \hat{W}^u, \hat{\dot{S}}^u_{0rr}, \hat{\dot{S}}^u_{0rz}$ when $g = 0$ are solved separately.

Jump in w

We have exact solution for jump in w when $g = 0$

$$
\begin{aligned}
\hat{U}^w &= 0 \quad \text{at} \quad r = r_{\text{out}} \quad \text{and} \quad r = r_{in}, \\
\hat{W}^w &= \frac{1}{2} \quad \text{at} \quad r = r_{\text{out}}, \quad \hat{W}^w = -\frac{1}{2} \quad \text{at} \quad r = r_{\text{in}}, \\
\hat{U}^w &= 0 \quad \text{at upper crack face and lower crack face}, \\
\hat{W}^w &= \frac{1}{2} \quad \text{at upper crack face}, \quad \hat{W}^w = -\frac{1}{2} \quad \text{at lower crack face}.
\end{aligned}
$$

And $\hat{\dot{S}}^w_{0rr}, \hat{\dot{S}}^w_{0rz}$ are functions of $\hat{U}^w, \hat{W}^w$.

Jump in u

Define Y_1, Y_2, Y_5 to be $\hat{U}^u, \hat{\dot{q}}^u, \hat{q}^u$ respectively in region 1; Y_3, Y_4, Y_6 to be $\hat{U}^u, \hat{\dot{q}}^u, \hat{q}^u$ respectively in region 2; Y_{a1}, Y_{a2}, Y_{a5} to be $\hat{U}^u, \hat{\dot{q}}^u, \hat{q}^u$ respectively on the inner boundary; Y_{a3}, Y_{a4}, Y_{a6} to be $\hat{U}^u, \hat{\dot{q}}^u, \hat{q}^u$ respectivelyon the outer boundary; Y_{b1}, Y_{b2}, Y_{b5} to be $\hat{U}^u, \hat{\dot{q}}^u, \hat{q}^u$ respectively on the lower crack face; Y_{b3}, Y_{b4}, Y_{b6} to be $\hat{U}^u, \hat{\dot{q}}^u, \hat{q}^u$ respectively on the upper crack face.

When $g = 0$ the equations (5.44) and (5.60) simplify to

$$\begin{aligned}
\frac{dY_1}{dR} &= -\frac{Y_1}{r_1} \\
\frac{dY_2}{dR} &= Y_1(r_c - r_{\text{in}}) f_2(r_1) \\
\frac{dY_5}{dR} &= (r_c - r_{\text{in}}) f_5(r_1) \\
\frac{dY_3}{dR} &= -\frac{Y_3}{r_2} \\
\frac{dY_4}{dR} &= Y_3(r_c - r_{\text{in}}) f_2(r_2) \\
\frac{dY_5}{dR} &= (r_c - r_{\text{in}}) f_5(r_2)
\end{aligned}$$

where $f_2(r)$ and $f_5(r)$ are given in Appendix C.

Refering to (5.45), (5.76) and (5.77), the boundary conditions on outer layers and the jump conditions on crack faces are

$$\begin{aligned}
p_1(r_{\text{in}}) Y_{a1} - \mu Y_{a2} &= 0 \\
p_2(r_{\text{out}}) Y_{a3} - \mu Y_{a4} &= 0 \\
\mu \left(a_r\left(r_{\text{out}}\right)\right)^2 - \mu Y_{a6} - \frac{2}{3} F_1\left(r_{\text{out}}\right) I_4\left(r_{\text{out}}\right) - \frac{2}{3} F_2\left(r_{\text{out}}\right) I_6\left(r_{\text{out}}\right) - P_{\text{ext}} &= 0 \\
Y_{b5} - Y_{b1} - 1 &= 0 \\
(p_4(r_c) Y_{b3} - \mu Y_{b4}) - (p_3(r_c) Y_{b1} - \mu Y_{b2}) &= 0 \\
Y_{b6} - Y_{b5} &= 0
\end{aligned}$$

where $p_1(r_c), p_2(r_c), p_3(r_c), p_4(r_c)$ are defined in Appendix C.

We use the Matlab routine '`bvp4c`' to calculate the values of $Y_1, Y_2, Y_5, Y_3, Y_4, Y_6$. Hence $\hat{U}^u, \hat{W}^u$ $\hat{\dot{S}}^u_{0rr}, \hat{\dot{S}}^u_{0rz}$ which are functions of $\hat{U}^u, \hat{W}^u$ are all obtained.

5.1.8 Matrix equations

We obtain $\hat{U}^w(g,r), \hat{W}^w(g,r), \hat{U}^u(g,r), \hat{W}^u(g,r)$ and $\hat{\dot{S}}^w_{0rr}(g,r), \hat{\dot{S}}^w_{0rz}(g,r), \hat{\dot{S}}^u_{0rr}(g,r), \hat{\dot{S}}^u_{0rz}(g,r)$ for each value of g from above numerical approach. Now we assume the length of the crack

is $2L$, and we show a section of the tube whose length is $7L$. The traction and displacement components, decomposed into normal and tangential direction, are

$$T_r(z) = \int \dot{S}^u_{0rr}(z-s,r)U(s)\,ds + \int \dot{S}^w_{0rr}(z-s,r)W(s)\,ds, \tag{5.80}$$

$$T_z(z) = \int \dot{S}^u_{0rz}(z-s,r)U(s)\,ds + \int \dot{S}^w_{0rz}(z-s,r)W(s)\,ds, \tag{5.81}$$

$$u = \int u^u(z-s,r)U(s)ds + \int u^w(z-s,r)W(s)ds, \tag{5.82}$$

$$w = \int w^u(z-s,r)U(s)ds + \int w^w(z-s,r)W(s)ds. \tag{5.83}$$

We discretize the integral equations (5.80) and (5.81) assuming piecewise constant openings along the tear which is of length $2L$, and so we evaluate the integral equations at a discrete set of points $z_i, i = 1, ..., 2N$.

For the second term in the RHS of equation (5.80) we have

$$\begin{aligned}
\int \dot{S}^w_{0rr}(z_i-s,r)W(s)\,ds &= \int \left[\frac{1}{\pi}\int_0^\infty \hat{\dot{S}}^w_{0rr}(g,r)\sin g(z_i-s)\,dg\right] W(s)\,ds \\
&= \frac{1}{\pi}\sum_j \int_j \left[\int_0^\infty \hat{\dot{S}}^w_{0rr}(g,r)\sin g(z_i-s)\,dg\right] W_j\,ds \\
&= \frac{1}{\pi}\sum_j \int_j \left[\int_0^\infty \left(\hat{\dot{S}}^w_{0rr}(g,r) - g\dot{S}^{w1}_{0rr} - \dot{S}^{w0}_{0rr}\right)\sin g(z_i-s)\,dg\right] W_j\,ds \\
&+ \frac{1}{\pi}\sum_j \int_j \left[\int_0^\infty g\dot{S}^{w1}_{0rr}\sin g(z_i-s)\,dg\right] W_j\,ds \\
&+ \frac{1}{\pi}\sum_j \int_j \left[\int_0^\infty \dot{S}^{w0}_{0rr}\sin g(z_i-s)\,dg\right] W_j\,ds,
\end{aligned}$$

where

$$\begin{aligned}
&\textstyle\int_j \left[\int_0^\infty (\hat{\dot{S}}^w_{0rr}(g,r) - g\dot{S}^{w1}_{0rr} - \dot{S}^{w0}_{0rr})\sin g(z_i-s)\,dg\right] W_j\,ds \\
&= W_j \textstyle\int_0^\infty (\hat{\dot{S}}^w_{0rr} - g\dot{S}^{w1}_{0rr} - \dot{S}^{w0}_{0rr}) \left[\int_j \sin g(z_i-s)\,ds\right] dg
\end{aligned}$$

and

$$\int_j \sin g(z_i-s)\,ds = \int_{z_j-\Delta}^{z_j+\Delta} \sin g(z_i-s)\,ds = 2\frac{\sin(g\Delta)}{g}\sin g(z_i-z_j),$$

in which using equation (3.101)

$$\frac{1}{\pi}\int_0^\infty g\dot{S}^{w1}_{0rr}\sin g(z_i-s)\,dg = \frac{\dot{S}^{w1}_{0rr}}{\pi}\lim_{r\to 0^+}\int_0^\infty ge^{-gr}\sin g(z_i-s)\,dg \quad = \dot{S}^{w1}_{0rr}\delta'(z_i-s)$$

and using equation (3.102) we have

$$\frac{1}{\pi}\int_0^\infty \dot{S}^{w0}_{0rr}\sin g(z_i-s)\,dg = \frac{\dot{S}^{w0}_{0rr}}{\pi}\lim_{r\to 0^+}\int_0^\infty e^{-gr}\sin g(z_i-s)\,dg \quad = \frac{\dot{S}^{w0}_{0rr}}{\pi(z_i-s)}.$$

Hence

$$\begin{aligned}\int \dot{S}^{w}_{0rr}\left(z_i-s,r\right)W\left(s\right)ds &= 2\frac{1}{\pi}\sum_j W_j\int_0^{\infty}\left(\hat{\dot{S}}^{w}_{0rr}\left(g,r\right)-g\dot{S}^{w1}_{0rr}-\dot{S}^{w0}_{0rr}\right)\frac{\sin g\Delta}{g}\sin g(z_i-z_j)\,dg\\ &+ \dot{S}^{w0}_{0rr}\sum_j W_j\frac{1}{\pi}\log\left|\frac{z_i-z_j+\Delta}{z_i-z_j-\Delta}\right|\end{aligned}$$

which is of the form $\sum_j \dot{S}^{w}_{0rr}[i,j]W_j$ where

$$\begin{aligned}\dot{S}^{w}_{0rr}[i,j] &= 2\frac{1}{\pi}\int_0^{\infty}\left(\hat{\dot{S}}^{w}_{0rr}\left(g,r\right)-g\dot{S}^{w1}_{0rr}-\dot{S}^{w0}_{0rr}\right)\frac{\sin g\Delta}{g}\sin g(z_i-z_j)\,dg\\ &+ \dot{S}^{w0}_{0rr}\frac{1}{\pi}\log\left|\frac{z_i-z_j+\Delta}{z_i-z_j-\Delta}\right|.\end{aligned}$$

For the first term in the RHS of equation (5.80), in which we use (3.99), (3.100), (3.165) and (3.166), we have

$$\begin{aligned}\int \dot{S}^{u}_{0rr}\left(z_i-s,r\right)U\left(s\right)ds &= \int\left[\frac{1}{\pi}\int_0^{\infty}\hat{\dot{S}}^{u}_{0rr}\left(g,r\right)\cos g\left(z_i-s\right)dg\right]U\left(s\right)\,ds\\ &= \frac{1}{\pi}\sum_j\int_j\left[\int_0^{\infty}\left(\hat{\dot{S}}^{u}_{0rr}\left(g,r\right)-g\dot{S}^{u1}_{0rr}-\dot{S}^{u0}_{0rr}\right)\cos g\left(z_i-s\right)dg\right]U_j\,ds\\ &+ \frac{1}{\pi}\sum_j\int_j\left[\int_0^{\infty}g\dot{S}^{u1}_{0rr}\cos g\left(z_i-s\right)dg\right]U_j\,ds\\ &+ \frac{1}{\pi}\sum_j\int_j\left[\int_0^{\infty}\dot{S}^{u0}_{0rr}\cos g\left(z_i-s\right)dg\right]U_j\,ds\\ &= 2\frac{1}{\pi}\sum_j U_j\int_0^{\infty}\left(\hat{\dot{S}}^{u}_{0rr}\left(g,r\right)-g\dot{S}^{u1}_{0rr}-\dot{S}^{u0}_{0rr}\right)\frac{\sin g\Delta}{g}\cos g(z_i-z_j)\,dg\\ &- \dot{S}^{u1}_{0rr}\sum_j U_j\left[\frac{2\Delta}{\pi\left(\left(z_i-z_j\right)^2-\Delta^2\right)}\right]\\ &+ \dot{S}^{u0}_{0rr}\sum_j U_j I_{z_i\in(z_j-\Delta,z_j+\Delta)}\end{aligned}$$

which is of the form $\sum_j \dot{S}^{u}_{0rr}[i,j]U_j$ where

$$\begin{aligned}\dot{S}^{u}_{0rr}[i,j] &= 2\frac{1}{\pi}\int_0^{\infty}\left(\hat{\dot{S}}^{u}_{0rr}\left(g,r\right)-g\dot{S}^{u1}_{0rr}-\dot{S}^{u0}_{0rr}\right)\frac{\sin g\Delta}{g}\cos g(z_i-z_j)\,dg\\ &- \dot{S}^{u1}_{0rr}\left[\frac{2\Delta}{\pi\left(\left(z_i-z_j\right)^2-\Delta^2\right)}\right]\\ &+ \dot{S}^{u0}_{0rr}I_{z_i\in(z_j-\Delta,z_j+\Delta)}\end{aligned}$$

For the second term in the RHS of equation (5.81), in which we use (3.99), (3.100),

(3.165) and (3.166), we have

$$\begin{aligned}
\int \dot{S}^{w}_{0rz}\left(z_i-s,r\right)W\left(s\right)ds &= \int\left[\frac{1}{\pi}\int_0^{\infty}\hat{\dot{S}}^{w}_{0rz}\left(g,r\right)\cos g\left(z_i-s\right)dg\right]W\left(s\right)\,ds\\
&= \frac{1}{\pi}\sum_j\int_j\left[\int_0^{\infty}\left(\hat{\dot{S}}^{w}_{0rz}\left(g,r\right)-g\dot{S}^{w1}_{0rz}-\dot{S}^{w0}_{0rz}\right)\cos g\left(z_i-s\right)dg\right]W_j\,ds\\
&+ \frac{1}{\pi}\sum_j\int_j\left[\int_0^{\infty}g\dot{S}^{w1}_{0rz}\cos g\left(z_i-s\right)dg\right]W_j\,ds\\
&+ \frac{1}{\pi}\sum_j\int_j\left[\int_0^{\infty}\dot{S}^{w0}_{0rz}\cos g\left(z_i-s\right)dg\right]W_j\,ds\\
&= 2\frac{1}{\pi}\sum_j W_j\int_0^{\infty}\left(\hat{\dot{S}}^{w}_{0rz}\left(g,r\right)-g\dot{S}^{w1}_{0rz}-g\dot{S}^{w0}_{0rz}\right)\frac{\sin g\Delta}{g}\cos g(z_i-z_j)\,dg\\
&- \dot{S}^{w1}_{0rz}\sum_j W_j\left[\frac{2\Delta}{\pi\left(\left(z_i-z_j\right)^2-\Delta^2\right)}\right]\\
&+ \dot{S}^{w0}_{0rz}\sum_j W_j I_{z_i\in(z_j-\Delta,z_j+\Delta)}
\end{aligned}$$

which is of the form $\sum_j \dot{S}^{w}_{0rz}[i,j]W_j$ where

$$\begin{aligned}
\dot{S}^{w}_{0rz}[i,j] &= 2\frac{1}{\pi}\int_0^{\infty}\left(\hat{\dot{S}}^{w}_{0rz}\left(g,r\right)-g\dot{S}^{w1}_{0rz}-g\dot{S}^{w0}_{0rz}\right)\frac{\sin g\Delta}{g}\cos g(z_i-z_j)\,dg\\
&- \dot{S}^{w1}_{0rz}\left[\frac{2\Delta}{\pi\left(\left(z_i-z_j\right)^2-\Delta^2\right)}\right]\\
&+ \dot{S}^{w0}_{0rz}I_{z_i\in(z_j-\Delta,z_j+\Delta)}.
\end{aligned}$$

For the first term in the RHS of of equation (5.81), in which we use (3.101), (3.102), (3.167) and (3.168), we have

$$\begin{aligned}
\int \dot{S}^{u}_{0rz}\left(z_i-s,r\right)U\left(s\right)ds &= 2\frac{1}{\pi}\sum_j U_j\int_0^{\infty}\left(\hat{\dot{S}}^{u}_{0rz}\left(g,r\right)-g\dot{S}^{u1}_{0rz}-\dot{S}^{u0}_{0rz}\right)\frac{\sin g\Delta}{g}\sin g(z_i-z_j)\,dg\\
&+ \dot{S}^{u0}_{0rz}\sum_j U_j\frac{1}{\pi}\log\left|\frac{z_i-z_j+\Delta}{z_i-z_j-\Delta}\right|
\end{aligned}$$

which is of the form $\sum_j \dot{S}^{u}_{0rz}[i,j]U_j$ where

$$\begin{aligned}
\dot{S}^{u}_{0rz}[i,j] &= 2\frac{1}{\pi}\int_0^{\infty}\left(\hat{\dot{S}}^{u}_{0rz}\left(g,r\right)-g\dot{S}^{u1}_{0rz}-\dot{S}^{u0}_{0rz}\right)\frac{\sin g\Delta}{g}\sin g(z_i-z_j)\,dg\\
&+ \dot{S}^{u0}_{0rz}\frac{1}{\pi}\log\left|\frac{z_i-z_j+\Delta}{z_i-z_j-\Delta}\right|
\end{aligned}$$

We write these integral equations (5.80) and (5.81) as the matrix equation

$$\begin{bmatrix} T_{ri} \\ T_{zi} \end{bmatrix} = \begin{bmatrix} \dot{S}^{u}_{0rr}[i,j] & \dot{S}^{w}_{0rr}[i,j] \\ \dot{S}^{u}_{0rz}[i,j] & \dot{S}^{w}_{0rz}[i,j] \end{bmatrix} \begin{bmatrix} U_j \\ W_j \end{bmatrix} \tag{5.84}$$

where $j = 1, ..., 2N$.

We discretize the integral equations (5.82) and (5.83) assuming piecewise constant openings along length $2L$ for upper, and lower crack faces and $7L$ for top and bottom boundaries. We evaluate the integral equation at a discrete set of points $z_i, i = 1, ..., 2N$ for the upper and lower crack faces, and $z_i, i = 1, ..., 7N$ for the top and bottom boundaries.

For the first term in the RHS of equation (5.82), in which we use (3.100) and (3.166), we have

$$\begin{aligned}
\int u^u(z_i - s, r)U(s)ds &= \frac{1}{\pi}\int\int_0^\infty \left(\hat{U}^u - u^{1u}\right)\cos g\,(z_i - s)\; dg\,U\,ds \\
&+ \frac{1}{\pi}\int\int_0^\infty u^{1u}\cos g\,(z_i - s)\; dg\,U\,ds \\
&= \frac{2}{\pi}\sum_j U_j \int_0^\infty (\hat{U}^u - u^{1u})\frac{\sin g\Delta}{g}\cos\left(gz_i - gz_j\right)dg \\
&+ u^{1u}\sum_j \int_j \lim_{r\to 0^+}\int_0^\infty e^{-gr}\cos g\,(z_i - s)\; dg\,U_j\,ds \\
&= \frac{2}{\pi}\sum_j U_j \int_0^\infty (\hat{U}^u - u^{1u})\frac{\sin g\Delta}{g}\cos\left(gz_i - gz_j\right)dg \\
&+ u^{1u}\sum_j U_j I_{z_i\in(z_j-\Delta,z_j+\Delta)}
\end{aligned}$$

which is of the form $\sum_j u^u[i,j]U_j$ where

$$\begin{aligned}
u^u[i,j] &= \frac{2}{\pi}\int_0^\infty (\hat{U}^u - u^{1u})\frac{\sin g\Delta}{g}\cos\left(gz_i - gz_j\right)dg \\
&+ u^{1u}I_{z_i\in(z_j-\Delta,z_j+\Delta)}.
\end{aligned}$$

For the first term in the RHS of equation (5.82), in which we use (3.102) and (3.168),

we have

$$\begin{aligned}
\int u^w(z_i-s,r)W(s)ds &= \frac{1}{\pi}\int\int_0^\infty \left(\hat{U}^w - u^{1w}\right)\sin g\,(z_i-s)\;dg\,W\,ds \\
&+ \frac{1}{\pi}\int\int_0^\infty u^{1w}\sin g\,(z_i-s)\;dg\,W\,ds \\
&= \frac{2}{\pi}\sum_j W_j\int_0^\infty (\hat{U}^w - u^{1w})\frac{\sin g\Delta}{g}\sin\left(gz_i - gz_j\right)dg \\
&+ u^{1w}\sum_j\int_j \lim_{r\to 0^+}\int_0^\infty e^{-gr}\sin g\,(z_i-s)\;dg\,W_j\,ds \\
&= \frac{2}{\pi}\sum_j W_j\int_0^\infty (\hat{U}^w - u^{1w})\frac{\sin g\Delta}{g}\sin\left(gz_i - gz_j\right)dg \\
&+ \frac{u^{1w}}{\pi}\sum_j W_j\log\left|\frac{z_i-z_j+\Delta}{z_i-z_j-\Delta}\right|
\end{aligned}$$

which is of the form $\sum_j u^w[i,j]W_j$ where

$$\begin{aligned}
u^w[i,j] &= \frac{2}{\pi}\int_0^\infty (\hat{U}^w - u^{1w})\frac{\sin g\Delta}{g}\sin\left(gz_i - gz_j\right)dg \\
&+ \frac{u^{1w}}{\pi}\log\left|\frac{z_i-z_j+\Delta}{z_i-z_j-\Delta}\right|.
\end{aligned}$$

For the first term in the RHS of equation (5.83), in which we use (3.102) and (3.168), we have

$$\begin{aligned}
\int w^u(z_i-s,r)U(s)ds &= \frac{1}{\pi}\int\int_0^\infty \left(\hat{W}^u - w^{1u}\right)\sin g\,(z_i-s)\;dg\,U\,ds \\
&+ \frac{1}{\pi}\int\int_0^\infty w^{1u}\sin g\,(z_i-s)\;dg\,U\,ds \\
&= \frac{2}{\pi}\sum_j U_j\int_0^\infty (\hat{W}^u - w^{1u})\frac{\sin g\Delta}{g}\sin\left(gz_i - gz_j\right)dg \\
&+ w^{1u}\sum_j\int_j \lim_{r\to 0^+}\int_0^\infty e^{-gr}\sin g\,(z_i-s)\;dg\,U_j\,ds \\
&= \frac{2}{\pi}\sum_j U_j\int_0^\infty (\hat{W}^u - w^{1u})\frac{\sin g\Delta}{g}\sin\left(gz_i - gz_j\right)dg \\
&+ \frac{w^{1u}}{\pi}\sum_j U_j\log\left|\frac{z_i-z_j+\Delta}{z_i-z_j-\Delta}\right|
\end{aligned}$$

which is of the form $\sum_j w^u[i,j]U_j$ where

$$\begin{aligned}
w^u[i,j] &= \frac{2}{\pi}\int_0^\infty (\hat{W}^u - w^{1u})\frac{\sin g\Delta}{g}\sin\left(gz_i - gz_j\right)dg \\
&+ \frac{w^{1u}}{\pi}\log\left|\frac{z_i-z_j+\Delta}{z_i-z_j-\Delta}\right|.
\end{aligned}$$

For the first term in the RHS of equation (5.83), in which we use (3.100) and (3.166), we have

$$\begin{aligned}
\int w^w(z_i-s,r)W(s)ds &= \frac{1}{\pi}\int\int_0^\infty \left(\hat{W}^w - w^{1w}\right)\cos g\,(z_i-s)\;dg\,W\,ds \\
&+ \frac{1}{\pi}\int\int_0^\infty w^{1w}\cos g\,(z_i-s)\;dg\,W\,ds \\
&= \frac{2}{\pi}\sum_j W_j\int_0^\infty (\hat{W}^w - w^{1w})\frac{\sin g\Delta}{g}\cos\left(gz_i - gz_j\right)dg \\
&+ w^{1w}\sum_j\int_j \lim_{r\to 0^+}\int_0^\infty e^{-gr}\cos g\,(z_i-s)\;dg\,W_j\,ds \\
&= \frac{2}{\pi}\sum_j W_j\int_0^\infty (\hat{W}^w - w^{1w})\frac{\sin g\Delta}{g}\cos\left(gz_i - gz_j\right)dg \\
&+ w^{1w}\sum_j W_j I_{z_i\in(z_j-\Delta,z_j+\Delta)}
\end{aligned}$$

which is of the form $\sum_j w^w[i,j]W_j$ where

$$\begin{aligned}
w^w[i,j] &= \frac{2}{\pi}\int_0^\infty (\hat{W}^w - w^{1w})\frac{\sin g\Delta}{g}\cos\left(gz_i - gz_j\right)dg \\
&+ w^{1w}I_{z_i\in(z_j-\Delta,z_j+\Delta)}.
\end{aligned}$$

We write these integral equations (5.82) and (5.83) into the form of matrix equation

$$\begin{bmatrix} u_i \\ w_i \end{bmatrix} = \begin{bmatrix} u^u[i,j] & u^w[i,j] \\ w^u[i,j] & w^w[i,j] \end{bmatrix}\begin{bmatrix} U_j \\ W_j \end{bmatrix}. \tag{5.85}$$

5.1.9 Conditions at the crack face

In the static tear we use the following traction conditions at the crack face. The blood inside the tear is connecting with the blood in the aorta, and the blood pressure on the aorta wall is $-\sigma(r_{\text{in}})$ and the pressure on the tear face is $-\sigma(r_c)$. Therefore the traction on the tear is $T_{ri} = (-\sigma(r_c)) - (-\sigma(r_{\text{in}})) = \sigma(r_{\text{in}}) - \sigma(r_c)$ and $T_{zi} = 0$kPa. In order to calculate the opening of the tear we must solve equation (5.84) to get U_j and W_j. This requires the traction conditions at the crack face. When U_j and W_j have been obtained, the displacements u_i and w_i in (5.85) for upper and lower crack face, and for top and bottom boundaries are obtained.

5.1.10 Results

Following results are tear profiles with $r_{\text{in}} = 4\text{mm}$, $r_c = 5\text{mm}$, $r_{\text{out}} = 6\text{mm}$, $R_i = 3.9\text{mm}$, $P_{\text{ext}} = 0\text{kPa}$, $k_1 = 2.3632\text{kPa}$, $k_2 = 0.8393$, $c = 3\text{kPa}$, which are for a carotid artery from rabbit, refer to Holzapfel et al. [2000]. In Figure 5.1—5.8 we illustrate some tears for different choices of λ, k, and β. In Figure 5.9—5.20 we change one of these parameters and keep other parameters unchanged to compare the differences in order to test the effects of λ, k, β.

We choose the inner radius $r_{\text{in}} = 4\text{mm}$ and outer radius $r_{\text{out}} = 6\text{mm}$ instead of the inner radius $r_{\text{in}} = 1\text{mm}$ and outer radius $r_{\text{out}} = 3\text{mm}$. The reason is that unless the tube is sufficiently inflated when the open angle configurations is closed, it could lead to wrinkles on the inner boundary. Figures 5.7 and 5.8 show us the wrinkle on the inner boundary with $\alpha = 45^o$. In Figures 5.3 and 5.4 the open angle is $\alpha = 45^o$, however, there is no wrinkle on the inner boundary. The reason is that in Figures 5.7 and 5.8 the fibre angle with the circumferential direction $\beta = 30^o$ is smaller than the fibre angle $\beta = 60^o$ in Figures 5.3 and 5.4, which means the the fibre angle with the axial direction in Figures 5.7 and 5.8 is larger than the fibre angle in Figures 5.3 and 5.4, which contributes less to the axial direction to flatten the wrinkle. In additional, the opening of the tear is wider in Figures 5.7 and 5.8 than in Figures 5.3 and 5.4 since the fiber contributes less in axial direction. Comparing Figure 5.1 with 5.5, Figure 5.2 with 5.6, Figure 5.3 with 5.7, Figure 5.4 with 5.8 we find that larger axial stretch makes the tear narrower. We will discuss how will these parameters effect the opening in next part.

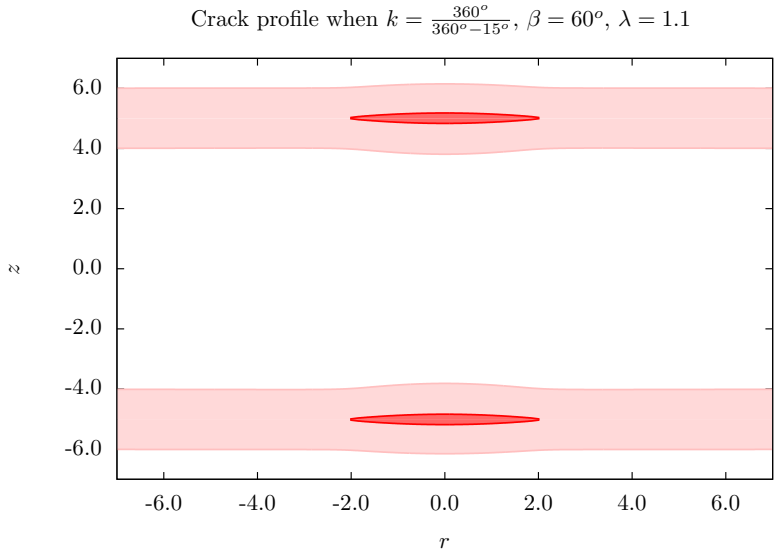

Figure 5.1: Plot of crack profile with $r_{\text{in}} = 4\text{mm}$, $r_c = 5\text{mm}$, $r_{\text{out}} = 6\text{mm}$, $R_i = 3.9\text{mm}$, $P_{\text{ext}} = 0\text{kPa}$, $k_1 = 2.3632\text{kPa}$, $k_2 = 0.8393$, $c = 3\text{kPa}$, $\lambda = 1.1$, $\beta = 60^o$, $k = \frac{360^o}{360^o - \alpha}$, $\alpha = 15^o$.

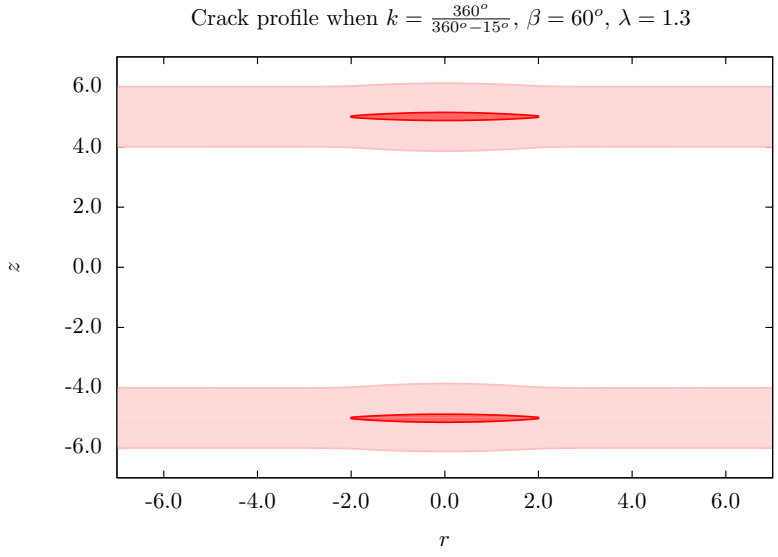

Figure 5.2: Plot of crack profile with $r_{\text{in}} = 4\text{mm}$, $r_c = 5\text{mm}$, $r_{\text{out}} = 6\text{mm}$, $R_i = 3.9\text{mm}$, $P_{\text{ext}} = 0\text{kPa}$, $k_1 = 2.3632\text{kPa}$, $k_2 = 0.8393$, $c = 3\text{kPa}$, $\lambda = 1.3$, $\beta = 60^o$, $k = \frac{360^o}{360^o - \alpha}$, $\alpha = 15^o$.

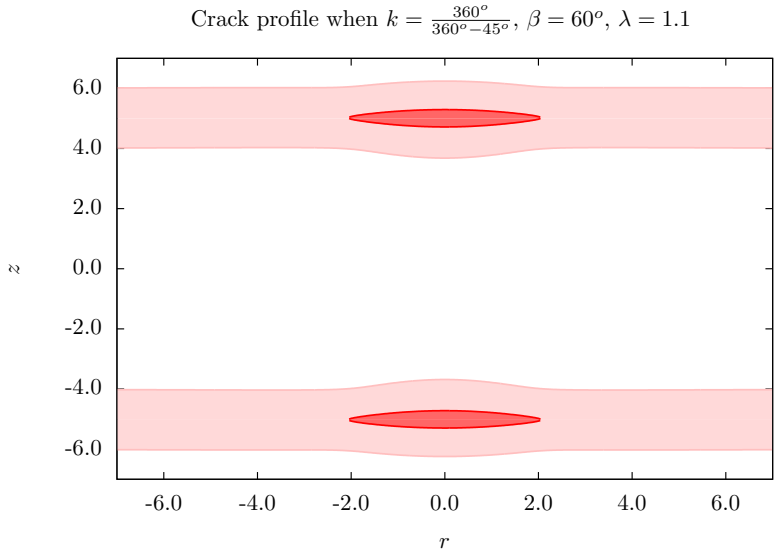

Figure 5.3: Plot of crack profile with $r_{\text{in}} = 4\text{mm}$, $r_c = 5\text{mm}$, $r_{\text{out}} = 6\text{mm}$, $R_i = 3.9\text{mm}$, $P_{\text{ext}} = 0\text{kPa}$, $k_1 = 2.3632\text{kPa}$, $k_2 = 0.8393$, $c = 3\text{kPa}$, $\lambda = 1.1$, $\beta = 60^o$, $k = \frac{360^o}{360^o - \alpha}$, $\alpha = 45^o$.

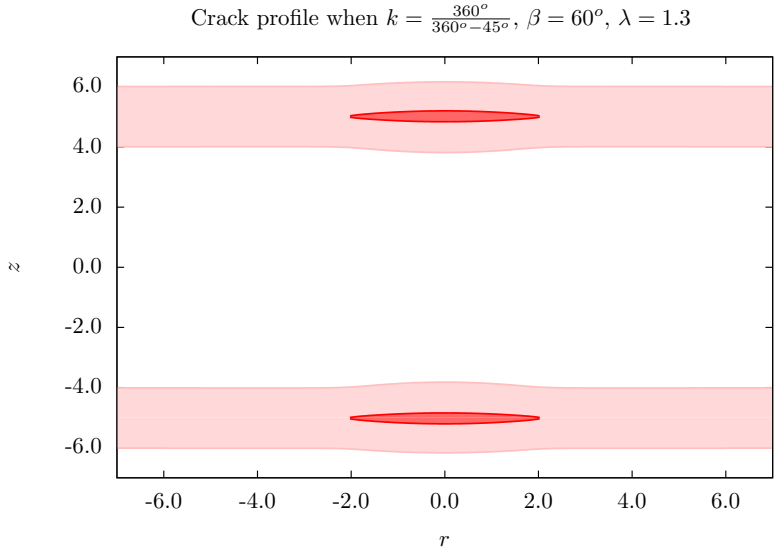

Figure 5.4: Plot of crack profile with $r_{\text{in}} = 4\text{mm}$, $r_c = 5\text{mm}$, $r_{\text{out}} = 6\text{mm}$, $R_i = 3.9\text{mm}$, $P_{\text{ext}} = 0\text{kPa}$, $k_1 = 2.3632\text{kPa}$, $k_2 = 0.8393$, $c = 3\text{kPa}$, $\lambda = 1.3$, $\beta = 60^o$, $k = \frac{360^o}{360^o - \alpha}$, $\alpha = 45^o$.

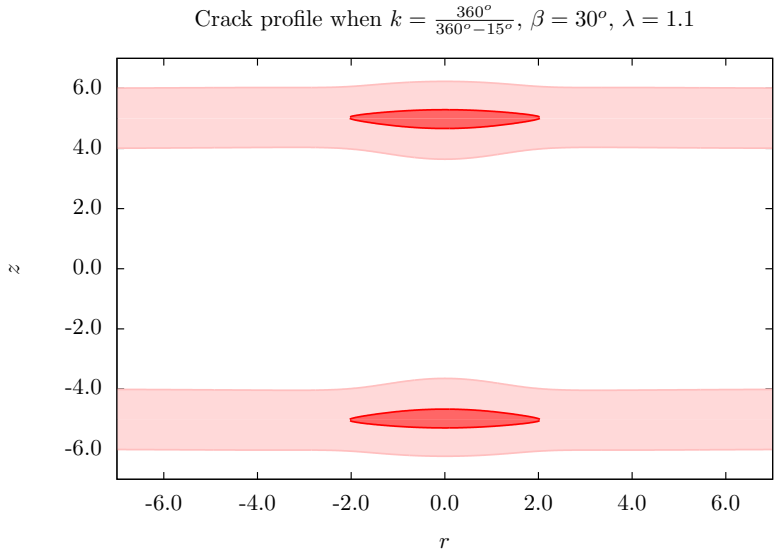

Figure 5.5: Plot of crack profile with $r_{\text{in}} = 4\text{mm}$, $r_c = 5\text{mm}$, $r_{\text{out}} = 6\text{mm}$, $R_i = 3.9\text{mm}$, $P_{\text{ext}} = 0\text{kPa}$, $k_1 = 2.3632\text{kPa}$, $k_2 = 0.8393$, $c = 3\text{kPa}$, $\lambda = 1.1$, $\beta = 30^o$, $k = \frac{360^o}{360^o - \alpha}$, $\alpha = 15^o$.

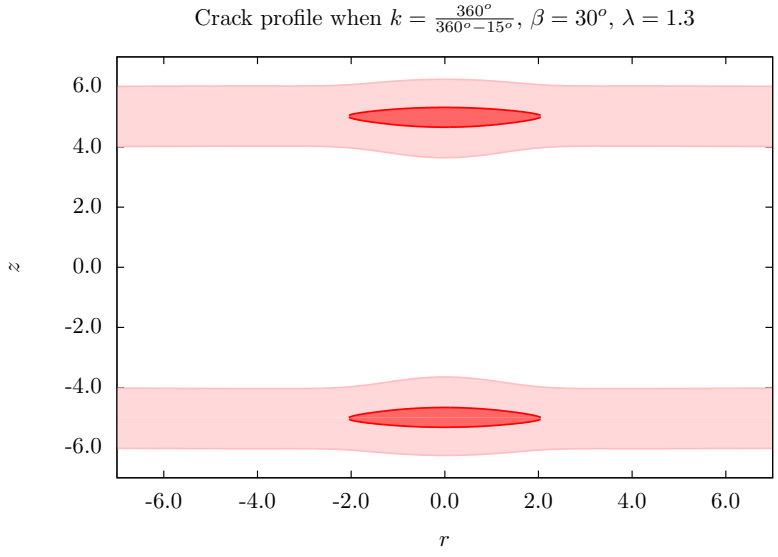

Figure 5.6: Plot of crack profile with $r_{\text{in}} = 4\text{mm}$, $r_c = 5\text{mm}$, $r_{\text{out}} = 6\text{mm}$, $R_i = 3.9\text{mm}$, $P_{\text{ext}} = 0\text{kPa}$, $k_1 = 2.3632\text{kPa}$, $k_2 = 0.8393$, $c = 3\text{kPa}$, $\lambda = 1.3$, $\beta = 30^o$, $k = \frac{360^o}{360^o - \alpha}$, $\alpha = 15^o$.

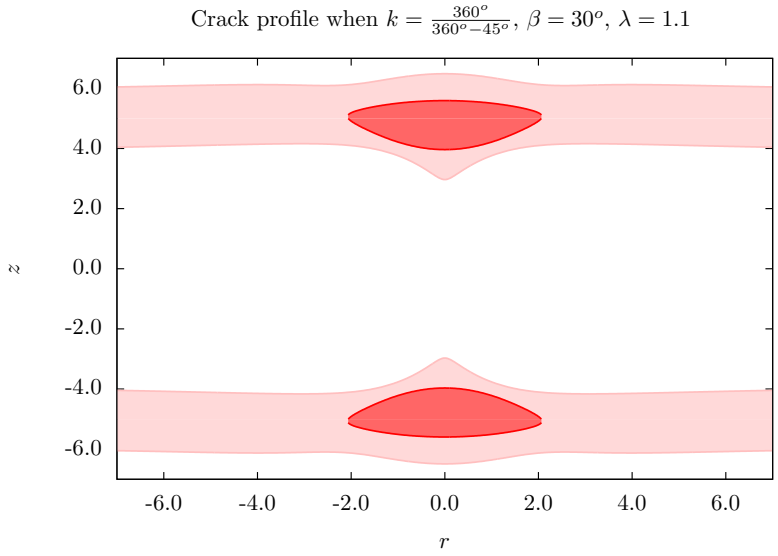

Figure 5.7: Plot of crack profile with $r_{\text{in}} = 4\text{mm}$, $r_c = 5\text{mm}$, $r_{\text{out}} = 6\text{mm}$, $R_i = 3.9\text{mm}$, $P_{\text{ext}} = 0\text{kPa}$, $k_1 = 2.3632\text{kPa}$, $k_2 = 0.8393$, $c = 3\text{kPa}$, $\lambda = 1.1$, $\beta = 30^o$, $k = \frac{360^o}{360^o - \alpha}$, $\alpha = 45^o$.

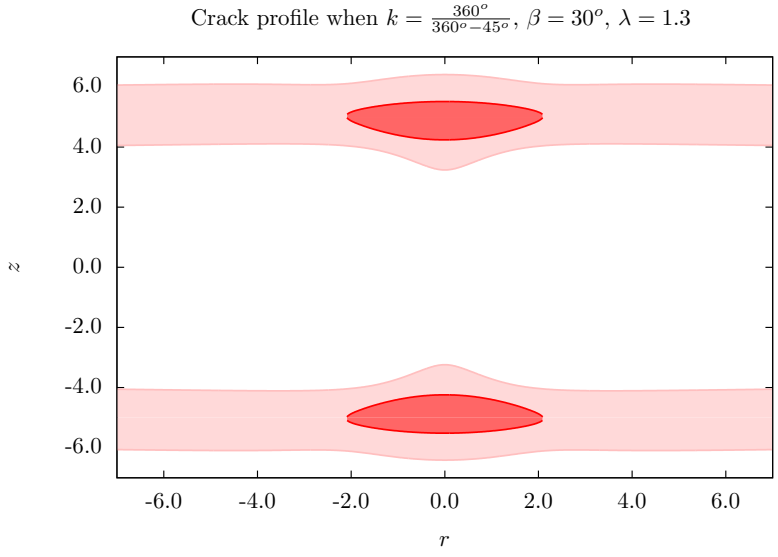

Figure 5.8: Plot of crack profile with $r_{\text{in}} = 4\text{mm}$, $r_c = 5\text{mm}$, $r_{\text{out}} = 6\text{mm}$, $R_i = 3.9\text{mm}$, $P_{\text{ext}} = 0\text{kPa}$, $k_1 = 2.3632\text{kPa}$, $k_2 = 0.8393$, $c = 3\text{kPa}$, $\lambda = 1.3$, $\beta = 30^o$, $k = \frac{360^o}{360^o - \alpha}$, $\alpha = 45^o$.

Comparison of λ

Figures 5.9—5.12 show us how the opening changes, when the axial stretch λ changes and other parameters are unchanged.

The results are as we expected: when the axial stretch λ increases, the tear becomes narrower, which means that a larger axial stretch makes the tear opening thinner.

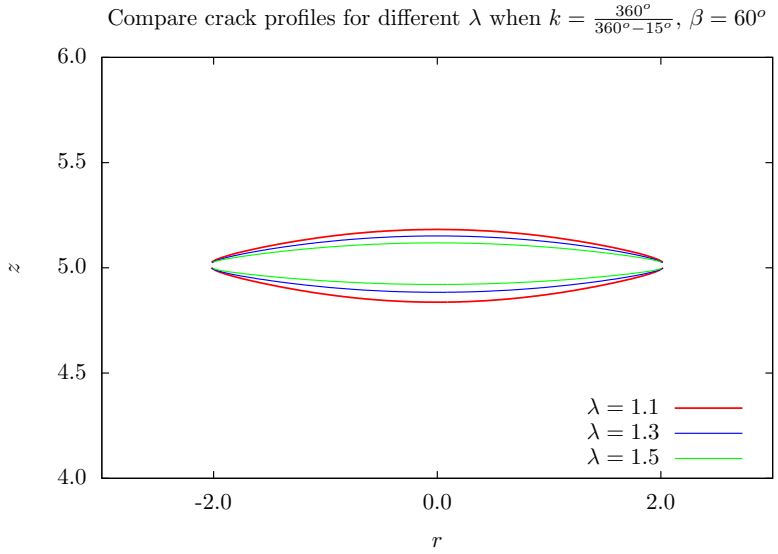

Figure 5.9: Comparison of the crack profiles for different values of λ with $r_{\text{in}} = 4\text{mm}$, $r_c = 5\text{mm}$, $r_{\text{out}} = 6\text{mm}$, $R_i = 3.9\text{mm}$, $P_{\text{ext}} = 0\text{kPa}$, $k_1 = 2.3632\text{kPa}$, $k_2 = 0.8393$, $c = 3\text{kPa}$, $\beta = 60^o$, $k = \frac{360^o}{360^o - \alpha}$, $\alpha = 15^o$.

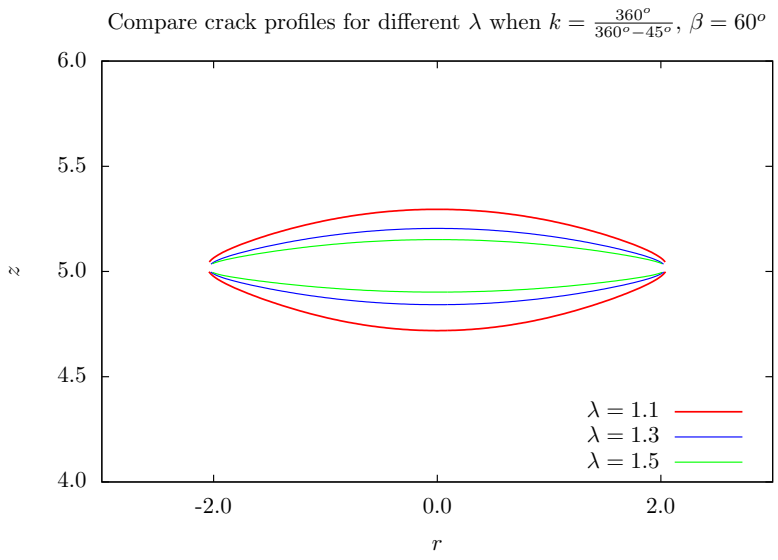

Figure 5.10: Comparison of the crack profiles for different values of λ with $r_{\text{in}} = 4\text{mm}$, $r_c = 5\text{mm}$, $r_{\text{out}} = 6\text{mm}$, $R_i = 3.9\text{mm}$, $P_{\text{ext}} = 0\text{kPa}$, $k_1 = 2.3632\text{kPa}$, $k_2 = 0.8393$, $c = 3\text{kPa}$, $\beta = 60^o$, $k = \frac{360^o}{360^o - \alpha}$, $\alpha = 45^o$.

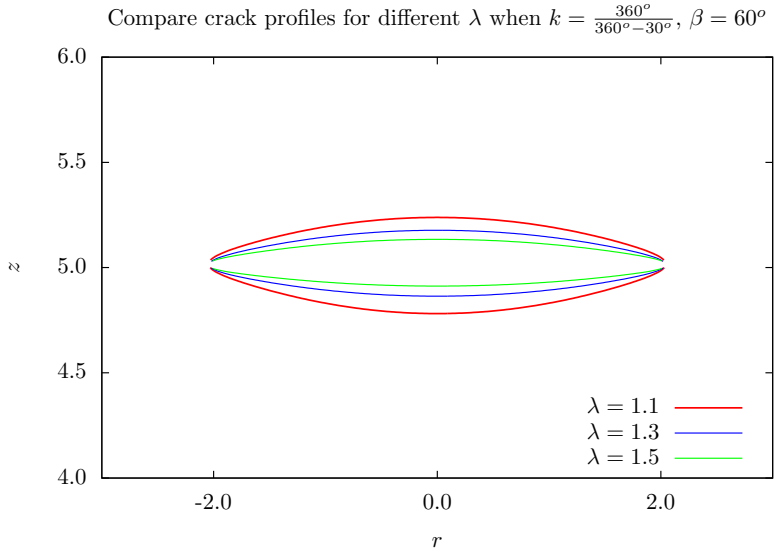

Figure 5.11: Comparison of the crack profiles for different values of λ with $r_{\text{in}} = 4\text{mm}$, $r_c = 5\text{mm}$, $r_{\text{out}} = 6\text{mm}$, $R_i = 3.9\text{mm}$, $P_{\text{ext}} = 0\text{kPa}$, $k_1 = 2.3632\text{kPa}$, $k_2 = 0.8393$, $c = 3\text{kPa}$, $\beta = 60^o$, $k = \frac{360^o}{360^o - \alpha}$, $\alpha = 30^o$.

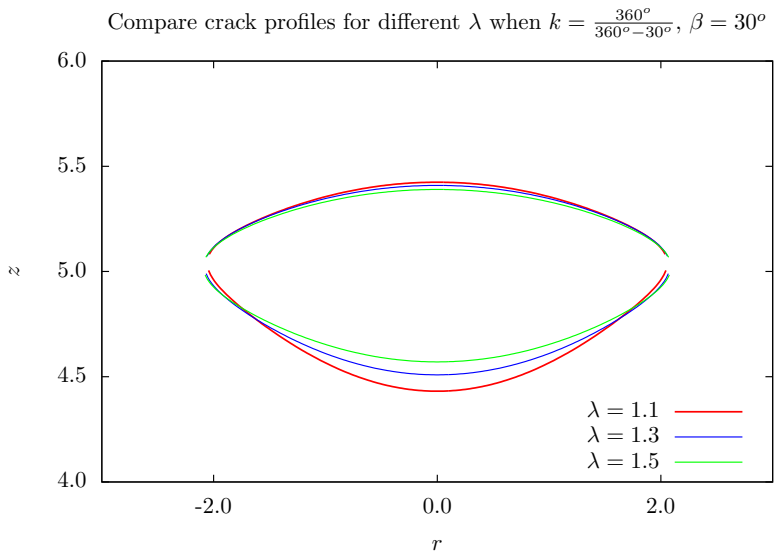

Figure 5.12: Comparison of the crack profiles for different values of λ with $r_{\text{in}} = 4\text{mm}$, $r_c = 5\text{mm}$, $r_{\text{out}} = 6\text{mm}$, $R_i = 3.9\text{mm}$, $P_{\text{ext}} = 0\text{kPa}$, $k_1 = 2.3632\text{kPa}$, $k_2 = 0.8393$, $c = 3\text{kPa}$, $\beta = 30^o$, $k = \frac{360^o}{360^o - \alpha}$, $\alpha = 30^o$.

Comparison of k

The parameter $k = \frac{2\pi}{2\pi - \alpha}$, where α is the open angle, is related to the residual stress. The Figures 5.13—5.16 show the effect of k on the opening of the tear.

The results are as we expected: when α increases (the residual stress parameter k increases), the opening of the tear becomes wider, which means that a larger residual stress in the circumferential direction makes the tear wider.

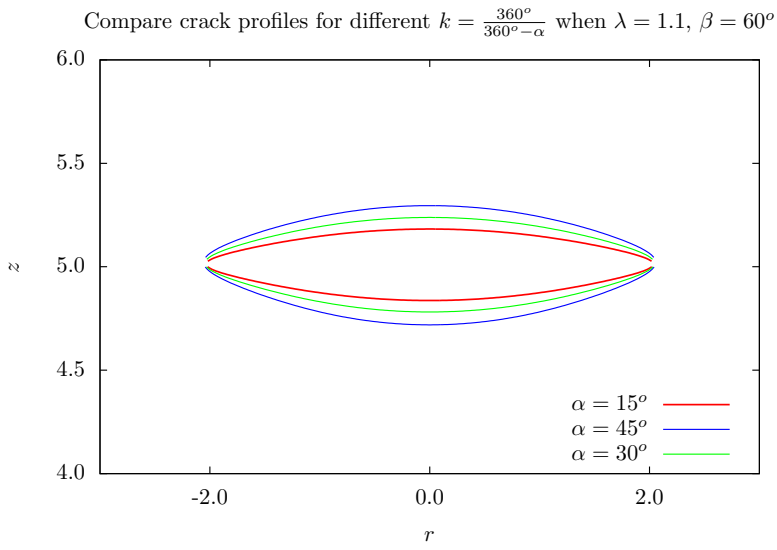

Figure 5.13: Comparison of the crack profiles for different k with $r_{\text{in}} = 4\text{mm}$, $r_c = 5\text{mm}$, $r_{\text{out}} = 6\text{mm}$, $R_i = 3.9\text{mm}$, $P_{\text{ext}} = 0\text{kPa}$, $k_1 = 2.3632\text{kPa}$, $k_2 = 0.8393$, $c = 3\text{kPa}$, $\lambda = 1.1$, $\beta = 60^o$.

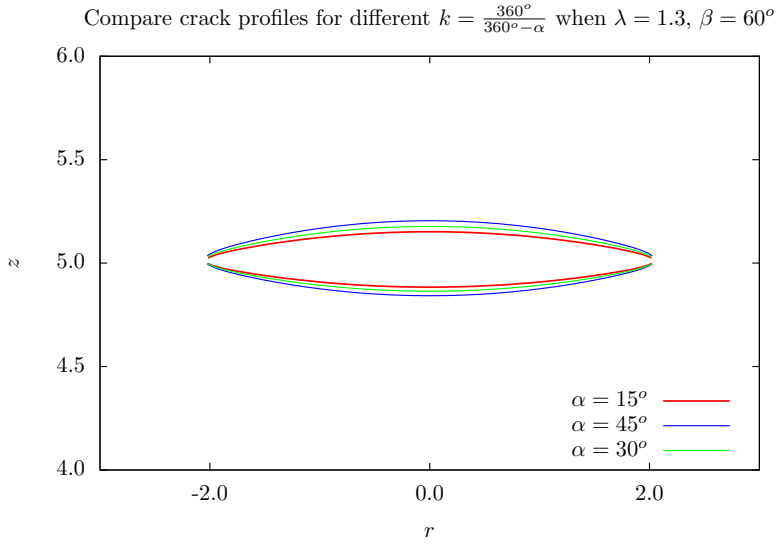

Figure 5.14: Comparison of the crack profiles for different k with $r_{\text{in}} = 4\text{mm}$, $r_c = 5\text{mm}$, $r_{\text{out}} = 6\text{mm}$, $R_i = 3.9\text{mm}$, $P_{\text{ext}} = 0\text{kPa}$, $k_1 = 2.3632\text{kPa}$, $k_2 = 0.8393$, $c = 3\text{kPa}$, $\lambda = 1.3$, $\beta = 60^o$.

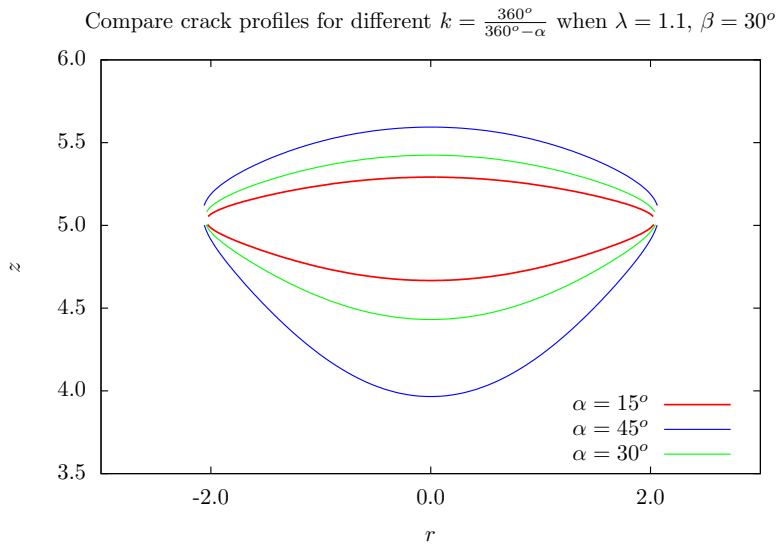

Figure 5.15: Comparison of the crack profiles for different k with $r_{\text{in}} = 4\text{mm}$, $r_c = 5\text{mm}$, $r_{\text{out}} = 6\text{mm}$, $R_i = 3.9\text{mm}$, $P_{\text{ext}} = 0\text{kPa}$, $k_1 = 2.3632\text{kPa}$, $k_2 = 0.8393$, $c = 3\text{kPa}$, $\lambda = 1.1$, $\beta = 30^o$.

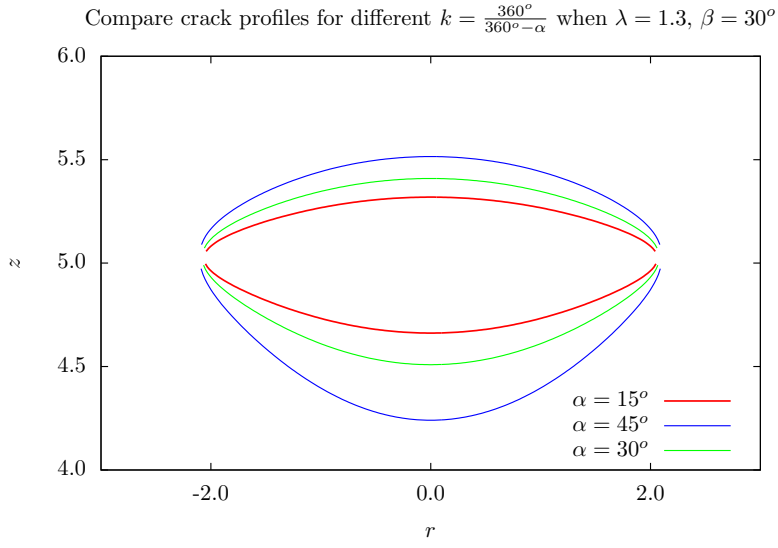

Figure 5.16: Comparison of the crack profiles for different k with $r_{\text{in}} = 4\text{mm}$, $r_c = 5\text{mm}$, $r_{\text{out}} = 6\text{mm}$, $R_i = 3.9\text{mm}$, $P_{\text{ext}} = 0\text{kPa}$, $k_1 = 2.3632\text{kPa}$, $k_2 = 0.8393$, $c = 3\text{kPa}$, $\lambda = 1.3$, $\beta = 30^o$.

Comparison of β

The parameter β is the fibre angle with respect to the circumferential direction. The Figures 5.18—5.20 show how the opening of the tear change when β varies.

As we expected, when the fibre angle with circumferential direction is larger (that is the angle with axial direction is small), then the fibre contributes more to the axial direction, which will make the opening of the tear narrower.

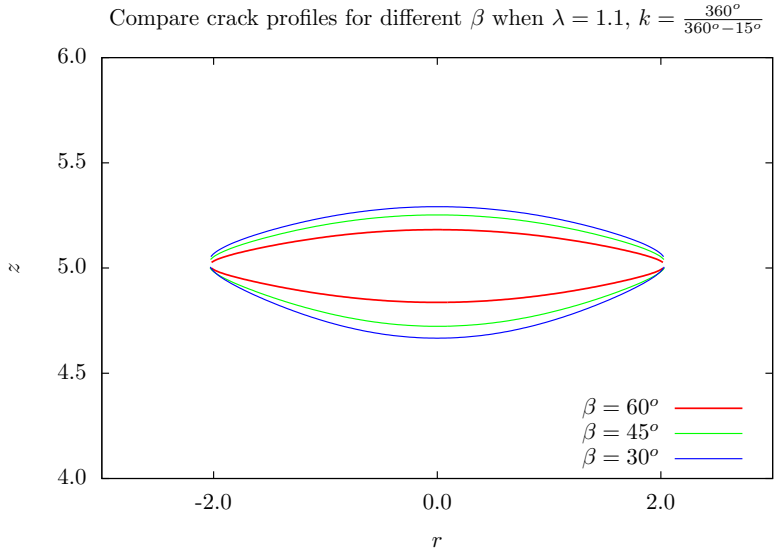

Figure 5.17: Comparison of the crack profiles for different β with $r_{\text{in}} = 4\text{mm}$, $r_c = 5\text{mm}$, $r_{\text{out}} = 6\text{mm}$, $R_i = 3.9\text{mm}$, $P_{\text{ext}} = 0\text{kPa}$, $k_1 = 2.3632\text{kPa}$, $k_2 = 0.8393$, $c = 3\text{kPa}$, $\lambda = 1.1$, $k = \frac{360^o}{360^o - \alpha}$, $\alpha = 15^o$.

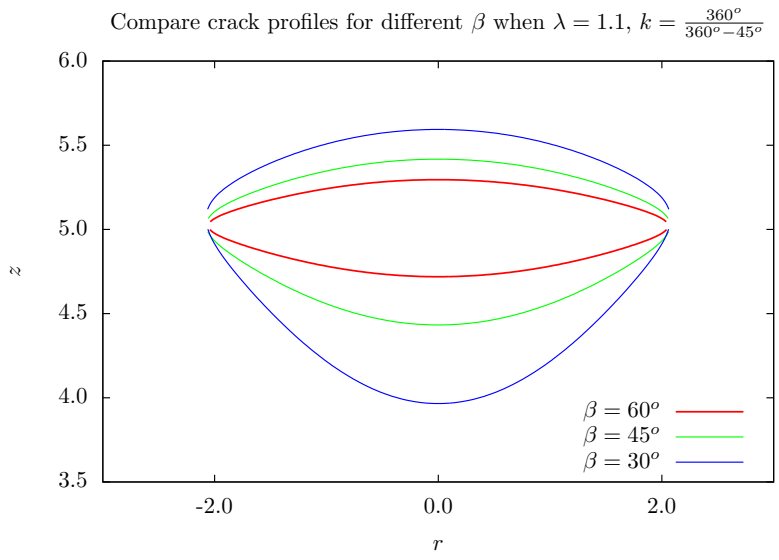

Figure 5.18: Comparison of the crack profiles for different β $r_{\text{in}} = 4\text{mm}$, $r_c = 5\text{mm}$, $r_{\text{out}} = 6\text{mm}$, $R_i = 3.9\text{mm}$, $P_{\text{ext}} = 0\text{kPa}$, $k_1 = 2.3632\text{kPa}$, $k_2 = 0.8393$, $c = 3\text{kPa}$, $\lambda = 1.1$, $k = \frac{360^o}{360^o - \alpha}$, $\alpha = 45^o$.

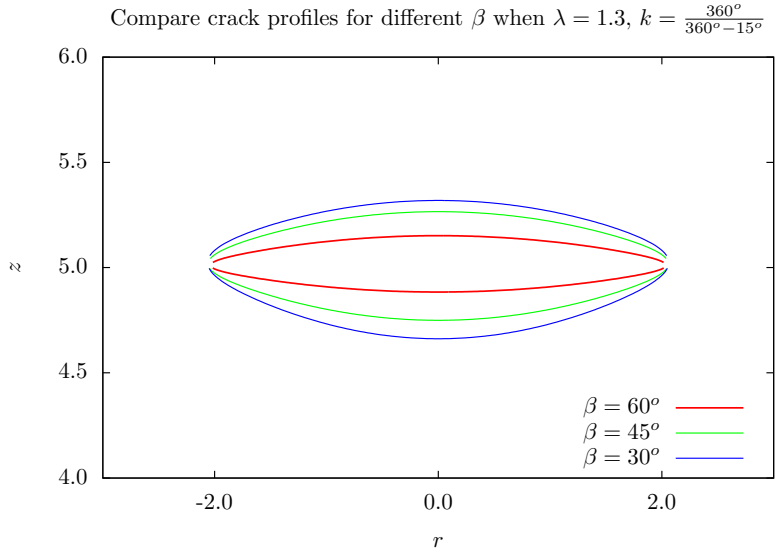

Figure 5.19: Comparison of the crack profiles for different β with $r_{\text{in}} = 4\text{mm}$, $r_c = 5\text{mm}$, $r_{\text{out}} = 6\text{mm}$, $R_i = 3.9\text{mm}$, $P_{\text{ext}} = 0\text{kPa}$, $k_1 = 2.3632\text{kPa}$, $k_2 = 0.8393$, $c = 3\text{kPa}$, $\lambda = 1.3$, $k = \frac{360^o}{360^o - \alpha}$, $\alpha = 15^o$.

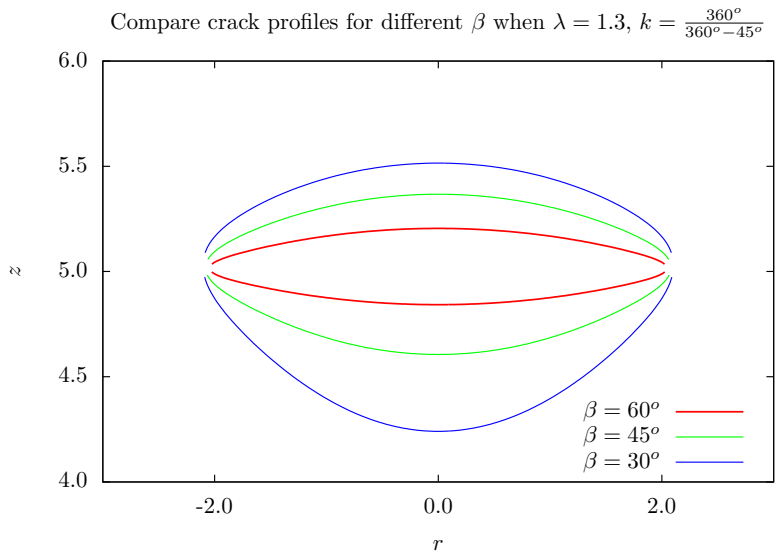

Figure 5.20: Comparison of the crack profiles for different β with $r_{\text{in}} = 4\text{mm}$, $r_c = 5\text{mm}$, $r_{\text{out}} = 6\text{mm}$, $R_i = 3.9\text{mm}$, $P_{\text{ext}} = 0\text{kPa}$, $k_1 = 2.3632\text{kPa}$, $k_2 = 0.8393$, $c = 3\text{kPa}$, $\lambda = 1.3$, $k = \frac{360^o}{360^o - \alpha}$, $\alpha = 45^o$.

Summary

From comparing these figures we know that larger axial stretch or larger fibre angle with circumferential direction makes the opening of the tear narrower, and larger residual stress in circumferential direction makes tear wider.

5.2 Incremental Inner Pressure

The blood pressure inside the aorta might change due to hypertension or other reasons. We consider the pressure change as the incremental inner pressure. The incremental inner pressure is presented as $\dot{P}$. Then the traction $(T_r(z), T_z(z))$ and displacement (u, w) are

$$T_r(z) = \int \dot{S}^u_{0rr}(z-s,r)U(s)\,ds + \int \dot{S}^w_{0rr}(z-s,r)W(s)\,ds + \dot{S}^P_{0rr}\dot{P} \quad (5.86)$$

$$T_z(z) = \int \dot{S}^u_{0rz}(z-s,r)U(s)\,ds + \int \dot{S}^w_{0rz}(z-s,r)W(s)\,ds, \quad (5.87)$$

$$u = \int u^u(z-s,r)U(s)ds + \int u^w(z-s,r)W(s)ds + u^P\dot{P} \quad (5.88)$$

$$w = \int w^u(z-s,r)U(s)ds + \int w^w(z-s,r)W(s)ds. \quad (5.89)$$

The displacement (u, w) is calculated as the previous section, and the values of $\dot{S}^u_{0rr}$, $\dot{S}^u_{0rz}$, $\dot{S}^w_{0rr}$, $\dot{S}^w_{0rz}$, and u^u, w^u, u^w, w^w are the same. The only difference is that we need to obtain $\dot{S}^P_{0rr}$ and u^P, which are calculated as follows. Once they have been found, and $(T_r(z), T_z(z))$ and $\dot{P}$ are given, we can get the displacement (u, w).

The equilibrium equations for Cauchy stress and incremental nominal stress are same as equations (5.1) and (5.2), where $\mathrm{tr}\,(\delta\mathbf{A}_0) = 0$ is due to incompressibility. The displacement of the incremental inner pressure is just in radial direction, which means $w = 0$. Using incompressibility $\nabla \cdot \boldsymbol{u} = \frac{1}{r}\frac{\partial(ru)}{\partial r} + \frac{\partial w}{\partial r} = 0$ we have $\frac{1}{r}\frac{\partial(ru)}{\partial r} = 0$, hence $\frac{du}{dr} = -\frac{u}{r}$. The equilibrium equations in (5.1), (5.2) and the incompressibility are written

$$\frac{dq}{dr} = A(r) \quad (5.90)$$

$$\frac{du}{dr} = -\frac{u}{r} \quad (5.91)$$

$$\frac{d\dot{q}}{dr} = \frac{B(r)}{\mu}u, \quad (5.92)$$

where $A(r)$ and $B(r)$ are in Appendix C. We define Y_1, Y_2, Y_3 to $q, u, \dot{q}$ respectively in region 1; Y_4, Y_5, Y_6 to $q, u, \dot{q}$ respectively in region 2. Y_{a1}, Y_{a2}, Y_{a3} to $q, u, \dot{q}$ respectively on inner boundary layer; Y_{a4}, Y_{a5}, Y_{a6} to $q, u, \dot{q}$ respectively on inner boundary layer; Y_{b1}, Y_{b2}, Y_{b3} to $q, u, \dot{q}$ respectively on lower crack face; Y_{b4}, Y_{b5}, Y_{b6} to $q, u, \dot{q}$ respectively on upper crack face.

In region 1, $r_1 = r_{\text{in}} + R(r_c - r_{\text{in}})$

$$\frac{dY_1}{dr_1} = A(r_1) \tag{5.93}$$
$$\frac{dY_2}{dr_1} = -\frac{u}{r_1} \tag{5.94}$$
$$\frac{dY_3}{dr_1} = \frac{B(r_1)}{\mu}u, \tag{5.95}$$

in region 2, $r_2 = r_{\text{out}} + R(r_c - r_{\text{out}})$

$$\frac{dY_4}{dr_2} = A(r_2) \tag{5.96}$$
$$\frac{dY_5}{dr_2} = -\frac{u}{r_2} \tag{5.97}$$
$$\frac{dY_6}{dr_2} = \frac{B(r_2)}{\mu}u. \tag{5.98}$$

Write the boundary conditions in (5.1) and (5.2) into components we have

$$\sigma_{rr} - P_{\text{ext}} = 0 \quad \text{at} \quad r = r_{\text{out}} \tag{5.99}$$
$$\dot{S}_{rr} - P_{\text{in}}\frac{du}{dr} + \dot{P} = 0 \quad \text{at} \quad r = r_{\text{in}} \tag{5.100}$$
$$\dot{S}_{rr} - P_{\text{ext}}\frac{du}{dr} = 0 \quad \text{at} \quad r = r_{\text{out}}. \tag{5.101}$$

which are

$$\begin{aligned} \mu\,(a_r(r_{\text{out}}))^2 - \mu\, Y_{a1} - \frac{2}{3}F_1(r_{\text{out}})\, I_4(r_{\text{out}}) - \frac{2}{3}F_2(r_{\text{out}})\, I_6(r_{\text{out}}) - P_{\text{ext}} &= 0 \\ a(r_{\text{in}})u(r_{\text{in}}) - \mu\dot{q}(r_{\text{in}}) + \dot{P} &= 0 \\ b(r_{\text{out}})u(r_{\text{out}}) - \mu\dot{q}(r_{\text{out}}) &= 0 \end{aligned}$$

where $a(r), b(r)$ are in Appendix C.

The jump conditions are

$$Y_{b4} - Y_{b1} = 0 \quad \text{at} \quad r = r_c \tag{5.102}$$
$$Y_{b5} - Y_{b2} = 0 \quad \text{at} \quad r = r_c \tag{5.103}$$
$$Y_{b6} - Y_{b3} = 0 \quad \text{at} \quad r = r_c, \tag{5.104}$$

We use the Matlab routine 'bvp4c' to calculate $q, u, \dot{q}$ in region 1 and 2 and $\dot{S}^P_{0rr} = S_1(r)u(r) - \dot{q}(r)$, in which $S_1(r)$ is in Appendix C. Hence when the traction (T_r, T_z) is given, we will get the displacement (u, v) for upper and lower crack faces, and top and bottom boundaries.

The traction on the tear is $T_r = \sigma(r_{\text{in}}) - \sigma(r_c) - \dot{P}$ and $T_z = 0$kPa. Figure 5.21—Figure 5.23 are our results, which show that the opening of the tear changes along with the incremental inner pressure.

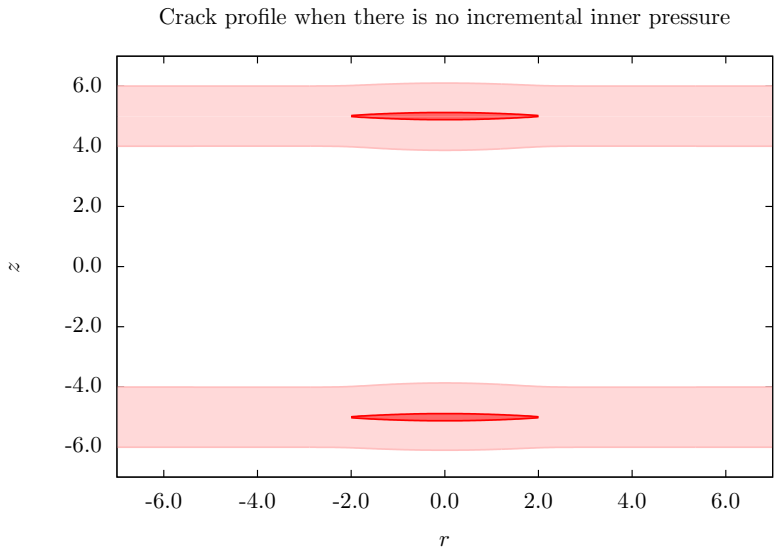

Figure 5.21: Plot of crack profile when there is no incremental inner pressure with $r_{\text{in}} = 4\text{mm}$, $r_c = 5\text{mm}$, $r_{\text{out}} = 6\text{mm}$, $R_i = 3.9\text{mm}$, $P_{\text{ext}} = 0\text{kPa}$, $k_1 = 2.3632\text{kPa}$, $k_2 = 0.8393$, $c = 3\text{kPa}$, $\beta = 60^o$, $k = 1$, $\lambda = 1.1$.

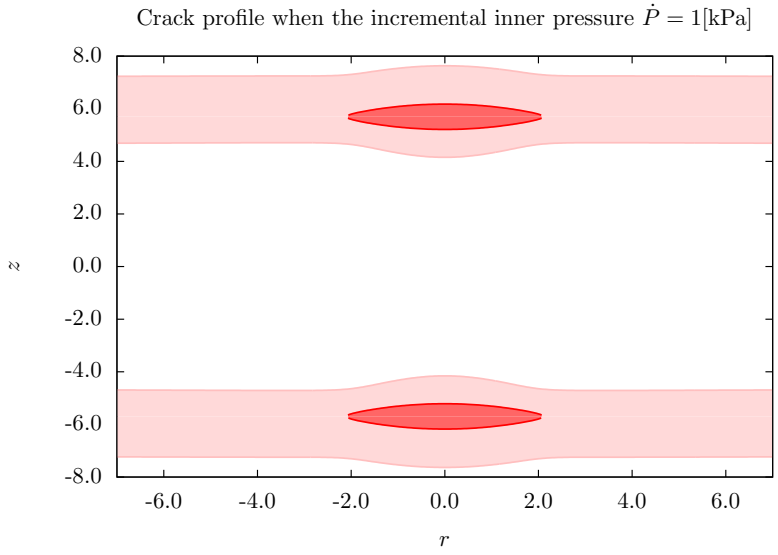

Figure 5.22: Plot of crack profile with incremental inner pressure $\dot{P} = 1kPa$ with $r_{\text{in}} = 4\text{mm}$, $r_c = 5\text{mm}$, $r_{\text{out}} = 6\text{mm}$, $R_i = 3.9\text{mm}$, $P_{\text{ext}} = 0\text{kPa}$, $k_1 = 2.3632\text{kPa}$, $k_2 = 0.8393$, $c = 3\text{kPa}$, $\beta = 60^o$, $k = 1$, $\lambda = 1.1$.

From Figure 5.21—Figure 5.23 we find that tear and the aorta wall are pushed away from the original location when the incremental inner pressure is $\dot{P} = 1kPa$. The fluid

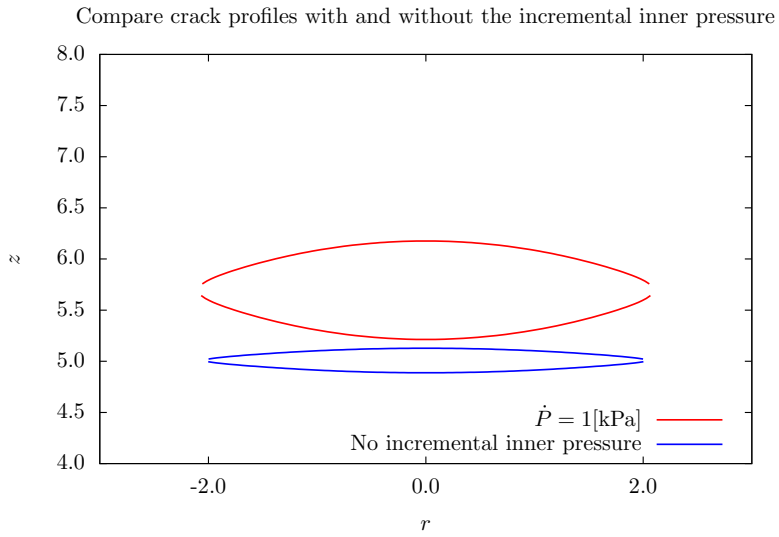

Figure 5.23: Different crack profiles for upper and lower crack face when the incremental inner pressure is $\dot{P} = 1kPa$ or there is no incremental inner pressure with $r_{\text{in}} = 4$mm, $r_c = 5$mm, $r_{\text{out}} = 6$mm, $R_i = 3.9$mm, $P_{\text{ext}} = 0$kPa, $k_1 = 2.3632$kPa, $k_2 = 0.8393$, $c = 3$kPa, $\beta = 60^o$, $k = 1$, $\lambda = 1.1$.

inside the tear is connecting with the fluid in the aorta, so the incremental inner pressure makes the tear wider in the case when $\dot{P} = 1$kPa.

5.3 Conclusions

In this chapter, we have modelled the tear on the idealized aorta, which is a thick-walled non-linear incompressible axisymmetric elastic annulus with residual stress and two family fibers and whose property is described by the strain energy function Holzapfel et al. [2000], as the incremental deformation. The parameters in the strain energy function has an effect the opening of the tear, which are compared and shown in our results. In addition, we have modelled the pressure change inside the aorta as the incremental inner pressure, which leads the change of the tear as well.

Chapter 6

Fluid dynamics in the tear

In an aortic dissection, blood penetrates the intima, and enters the media layer. The high pressure rips the tissue of the media apart. This can propagate along the length of the aorta for a variable distance forward and backwards, and the tear is filled with fluid.
In general terms, the fluid flow and tear opening are coupled, and an evolution equations for the tear opening must be found. In addition, a theory of propagation must include a criterion for tear extension and tear direction. We do not discuss these in this thesis, however it is an important direction for the development of a realistic tearing model that couples the elasticity of the artery and fluid flow.
In this chapter we get the equation, which is used to describe how the width of tear changs along time in the radial direction, from the Navier-Stokes equation.

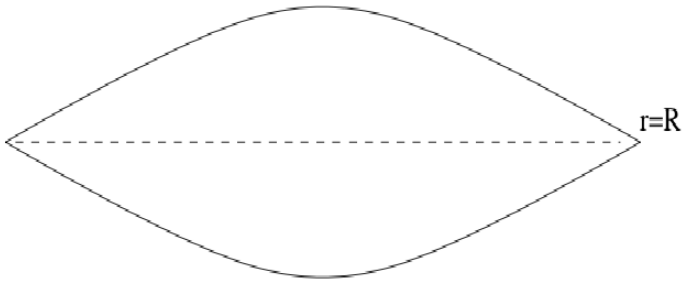

Figure 6.1: The distance from R to the upper tear face is $h_2(z,t)$, and $h_1(z,t)$ is the distance from R to the lower tear face.

6.1 Lubrication theory in Stokes flow

We assume a very thin tear in the aorta wall, which is in axisymmetric cylindrical polar coordinate, and blood, which is considered as the very viscous flow, filled in the tear. Define $h(z,t)$ as the width of the tear, L the length of the tear, R the location where tear happens, $h_2(z,t)$ the distance from R to the upper tear face, and $h_1(z,t)$ the distance from R to the lower tear face. Hence the location of the upper tear face is $R+h_2$, the location of the lower tear face is $R-h_1$, and $h=h_1+h_2$. The blood is considered to be a viscous fluid whose Reynolds number is very small, and the Navier-Stokes equations become

$$-\nabla p+\mu^v\nabla^2\boldsymbol{u}=0,\quad \nabla\cdot\boldsymbol{u}=0, \tag{6.1}$$

in which h is the opening distance between the upper face and the lower face, μ^v is the coefficient of viscosity, z is in the axial direction, t is time, p is the pressure on the tear face, and

$$\nabla^2\boldsymbol{u}=\left(\nabla^2u-\frac{u}{r^2}\right)\boldsymbol{e}_r+\left(\nabla^2w\right)\boldsymbol{e}_z, \tag{6.2}$$

where $\boldsymbol{e}_r$ is the unit vector in radius direction, $\boldsymbol{e}_z$ is the unit vector in axial direction, and $\boldsymbol{u}$ is the velocity which is $\boldsymbol{u}=u\boldsymbol{e}_r+w\boldsymbol{e}_z$.

Since $h\ll L$

$$\nabla^2u=\frac{1}{r}\frac{\partial}{\partial r}\left(r\frac{\partial u}{\partial r}\right)+\frac{\partial^2u}{\partial z^2}, \tag{6.3}$$

$$\frac{1}{r}\frac{\partial}{\partial r}\left(r\frac{\partial u}{\partial r}\right)\sim\frac{u}{h^2}, \tag{6.4}$$

$$\frac{\partial^2u}{\partial z^2}\sim\frac{u}{L^2}, \tag{6.5}$$

the dominant term is $\frac{1}{r}\frac{\partial}{\partial r}\left(r\frac{\partial u}{\partial r}\right)$. The equations in components are

$$-\frac{\partial p}{\partial r}+\mu^v\left[\frac{1}{r}\frac{\partial}{\partial r}\left(r\frac{\partial u}{\partial r}\right)-\frac{u}{r^2}\right]=0 \tag{6.6}$$

$$-\frac{dp}{dz}+\mu^v\frac{1}{r}\frac{\partial}{\partial r}\left(r\frac{\partial w}{\partial r}\right)=0. \tag{6.7}$$

In (6.7), $\frac{p}{L}\sim\frac{\mu^v w}{h^2}$. Hence in equation (6.6), $\frac{p}{h}\sim\frac{\mu^v wL}{h^3}$, $\frac{1}{r}\frac{\partial}{\partial r}\left(r\frac{\partial u}{\partial r}\right)\sim\frac{u}{h^2}$ and $\frac{u}{r^2}\sim\frac{u}{R^2}$. Since the crack width is much less than the radius $h\ll R$, the equation (6.6) becomes to

$$\frac{\partial p}{\partial r}=0, \tag{6.8}$$

so p is a function of z only.

Solve the equation (6.7) we have

$$w=\frac{1}{4\mu^v}\frac{dp}{dz}r^2+C\log r+D, \tag{6.9}$$

and since $\frac{r-R}{R}$ is small

$$\log r = \log(r-R+R) - \log R + \log R = \log\left(\frac{r-R}{R}+1\right) + \log R \quad (6.10)$$

$$= \frac{r}{R} - 1 + \log R + O\left(\left(\frac{r-R}{R}\right)^2\right). \quad (6.11)$$

Hence, approximately,

$$w = \frac{1}{4\mu^v}\frac{dp}{dz}r^2 + Ar + B + O\left(\left(\frac{r-R}{R}\right)^2\right). \quad (6.12)$$

The no slip boundary condition on the tear faces are

$$w = 0 \quad at \quad r = -h_1(z,t) + R \quad w = 0 \quad at \quad r = h_2(z,t) + R, \quad (6.13)$$

we get

$$A = -\frac{1}{4}\frac{dp}{dz}\frac{(-h_1 + 2R + h_2)}{\mu^v}, \quad (6.14)$$

$$B = \frac{1}{4}\frac{dp}{dz}\frac{(-Rh_1 + R^2 + Rh_2 - h_2h_1)}{\mu^v}. \quad (6.15)$$

The incompressibility condition gives

$$\nabla \cdot \boldsymbol{u} = 0, \quad (6.16)$$

$$\frac{1}{r}\frac{\partial(ru)}{\partial r} + \frac{\partial w}{\partial z} = 0. \quad (6.17)$$

Integrating the equation between $-h_1 + R$ and $R + h_2$ and multiplying 2π gives

$$2\pi\int_{R-h_1}^{R+h_2} r\left(\frac{1}{r}\frac{\partial(ru)}{\partial r} + \frac{\partial w}{\partial z}\right)dr = 0, \quad (6.18)$$

which is

$$\frac{\partial}{\partial z}\left[2\pi\int_{R-h_1}^{R+h_2} rwdr\right] + 2\pi\left[(R+h_2)\,u|_{R+h_2} - (R-h_1)\,u|_{R-h_1}\right]$$

$$+2\pi\left[(R-h_1)\,w|_{R-h_1}\frac{\partial(-h_1)}{\partial z} - (R+h_2)\,w|_{R+h_2}\frac{\partial h_2}{\partial z}\right] = 0.$$

Since $q = 2\pi\int_{R-h_1}^{R+h_2} rwdr$ and $\frac{d}{dz}\int_{f_1(z)}^{f_2(z)} q(r,z)dr = f_2'(z)q(f_2(z),z) - f_1'(z)q(f_1(z),z) + \int_{f_1(z)}^{f_2(z)}\frac{\partial q(r,z)}{\partial z}dr$, we have

$$\frac{\partial q}{\partial z} + 2\pi\left[(R+h_2)\,u|_{R+h_2} - (R-h_1)\,u|_{R-h_1}\right]$$
$$+2\pi\left[-(R+h_2)\,w|_{R+h_2}\frac{\partial h_2}{\partial z} + (R-h_1)\,w|_{R-h_1}\frac{\partial(-h_1)}{\partial z}\right] = 0. \quad (6.19)$$

The kinematic boundary conditions are

$$\frac{D}{Dt}\left(r-(R-h_1)\right)=0, \tag{6.20}$$

$$\frac{D}{Dt}\left(r-(R+h_2)\right)=0, \tag{6.21}$$

which are written out in full

$$\frac{\partial h_1}{\partial t}+u|_{R-h_1}+w|_{R-h_1}\frac{\partial h_1}{\partial z}=0, \tag{6.22}$$

$$-\frac{\partial h_2}{\partial t}+u|_{R+h_2}-w|_{R+h_2}\frac{\partial h_2}{\partial z}=0, \tag{6.23}$$

Put them in (6.19) we have

$$2\pi\left[(R+h_2)\frac{\partial h_2}{\partial t}+(R-h_1)\frac{\partial h_1}{\partial t}\right]-\frac{\partial q}{\partial z}=0, \tag{6.24}$$

$$\frac{\partial}{\partial t}(\pi[(R+h_2)^2-(R-h_1)^2])-\frac{\partial q}{\partial z}=0, \tag{6.25}$$

$$\pi\frac{\partial}{\partial t}[(h_2-h_1+2R)(h_2+h_1)]-\frac{\partial q}{\partial z}=0. \tag{6.26}$$

Since $h_1 \ll R$ and $h_2 \ll R$, it becomes

$$\pi\frac{\partial}{\partial t}[2R(h_2+h_1)]-\frac{\partial q}{\partial z}=0 \tag{6.27}$$

where

$$\begin{aligned} q &= 2\pi\int_{R-h_1}^{R+h_2} rw\,dr \\ &= 2\pi\int_{R-h_1}^{R+h_2} r\left(\frac{1}{4\mu^v}\frac{dp}{dz}r^2+Ar+B\right)dr \\ &= -\frac{1}{24}\frac{dp}{dz}\frac{\pi\left(6h_1R{h_2}^2+6h_2R{h_1}^2+{h_2}^4-{h_1}^4+2R{h_2}^3+2R{h_1}^3+2h_1{h_2}^3-2h_2{h_1}^3\right)}{\mu^v}, \end{aligned}$$

and it becomes

$$\begin{aligned} &\approx -\frac{1}{24}\frac{dp}{dz}\frac{\pi\left(6h_1R{h_2}^2+6h_2R{h_1}^2+2R{h_2}^3+2R{h_1}^3\right)}{\mu^v} \\ &= -\frac{1}{12}\frac{dp}{dz}\pi R(h_1+h_2)^3, \end{aligned} \tag{6.28}$$

since $h_1 \ll R$ and $h_2 \ll R$.

Combine (6.27) and (6.28) we have

$$\frac{\partial h}{\partial t}=\frac{1}{24\mu^v}\frac{\partial}{\partial z}\left(h^3\frac{dp}{dz}\right), \tag{6.29}$$

which is used to describe the flow inside the tear.

Non-dimensional equation

In this part the (6.29) is changed into non-dimension equation. From equation (5.5) the pressure on the tear face is written as

$$p = \int \dot{S}^u_{rr}(z-s,r)h(s)\,ds \tag{6.30}$$

The pressure p has the dimension $\frac{k_1 H_0}{L}$. We define $h = H_0 h^\star, z = Lz^\star, p = \frac{k_1 H_0}{L} p^\star, t = 8\frac{\mu^v L^3}{H_0^3 k_1} t^\star$, where $h^\star, z^\star, p^\star, t^\star$ are non-dimensional parameters. Hence we have $h \sim H_0, z \sim L, t \sim \frac{8\mu^v L^3}{H_0^3 k_1}$, $\dot{S}^u_{rr} \sim \frac{k_1}{L^2}$ and $p \sim \frac{k_1 H_0}{L}$. So the equation (6.29) changes to

$$\frac{\partial h^\star}{\partial t^\star} = \frac{1}{3}\frac{\partial}{\partial z^\star}\left(h^{\star 3}\frac{\partial p^\star}{\partial z^\star}\right). \tag{6.31}$$

In following sections we will drop '*' for simplicity and we use this non-dimension lubrication equation for our calculation.

Reynolds number

We can estimate Reynolds number as follows: typical length scale is the width of the dissection H_0, and typical time scale is given by $\frac{8\mu^v L^3}{H_0^3 k_1}$. Now we are considering a small width dissection, so for example we have $H_0 = 10^{-3}$m, and $L = 10^{-2}$m. The viscosity of blood μ^v is about 3×10^{-3}Pa $\cdot$ s, ν is about $3\times 10^{-6}\frac{m^2}{s}$, and k_1 in Chapter 5 is 2.3632kPa, hence the time scale is around 10s. If the time interval Δt is 1s, and ΔH_0 is $10^{-3}H_0$, which is close to our results in next section, the Reynolds number, which is expressed as $\frac{H_0}{\nu}\frac{\Delta H_0}{\Delta t}$, is $\frac{1}{3}\times 10^{-3} \ll 1$. Therefore the Reynolds number is very small, which satisfies our assumption.

6.2 Evolution of a fluid filled artery

We will discuss how the distance h between the upper tear face and lower tear face changes with time. By solving the equation (6.31) we find the opening of the tear changes in the radius direction with time, and finally stops. We use the explicit method to test the lubrication equation at first. For very small time interval this explicit method works, but when the time interval increases this method doesn't work anymore. Therefore an implicit method should be employed, which has been proved much better. To illustrate

the numerical method we use following expression

$$p = \int_{-L}^{L} \frac{h(s)}{(s-z)^2} ds, \tag{6.32}$$

which is similar as the result (3.61) in Chapter 3, to test our methods. Then we will use the p (6.30) to solve the problem.

6.2.1 Implicit method for time-dependent function

The lubrication equation can be written in the form

$$\begin{aligned} \frac{\partial h}{\partial t} &= \frac{1}{3}\frac{\partial}{\partial z}\left(h^3 \frac{\partial p}{\partial z}\right) \\ &= h^2 \frac{\partial h}{\partial z}\frac{\partial p}{\partial z} + \frac{1}{3}h^3 \frac{\partial^2 p}{\partial z^2} \end{aligned} \tag{6.33}$$

where $p = \int_{-L}^{L} \frac{h}{(s-z)^2} ds$. The initial condition is

$$h = h_0 \quad \text{at} \quad t = 0. \tag{6.34}$$

We discretize the integral equation p into N equal pieces

$$p_i = h_k \int_{L_k} \frac{1}{(s-z_i)^2} ds = M_{ik} h_k \tag{6.35}$$

where $k = 1, ..., N$ and $i = 1, ..., N$, and

$$M_{ik} = \int_{L_k} \frac{1}{(s-z_i)^2} ds = \int_{e_{k-1}}^{e_k} \frac{1}{(s-z_i)^2} ds = \left[-\frac{1}{s-z_i}\right]_{e_{k-1}}^{e_k} = -\frac{1}{e_k - z_i} + \frac{1}{e_{k-1} - z_i}. \tag{6.36}$$

Hence p can be written into the matrix form $p = Mh$.

The implicit difference method gives us

$$\frac{h_i^{n+1} - h_i^n}{\Delta t} = \left(h_i^{n+1}\right)^2 \frac{\partial h_i^{n+1}}{\partial z}\frac{\partial p_i^{n+1}}{\partial z} + \frac{1}{3}\left(h_i^{n+1}\right)^3 \frac{\partial^2 p_i^{n+1}}{\partial z^2} \tag{6.37}$$

where

$$h_i^{n+1} = \Delta h_i + h_i^n, \quad p_i^{n+1} = \Delta p_i + p_i^n, \quad \Delta p_i = M_{qi} \Delta h_i. \tag{6.38}$$

Hence the equation (6.33) is written as

$$\begin{aligned} \frac{\Delta h_i}{\Delta t} &= \left(\Delta h_i + h_i^n\right)^2 \frac{\partial\left(\Delta h_i + h_i^n\right)}{\partial z}\frac{\partial\left(\Delta p_i + p_i^n\right)}{\partial z} + \frac{1}{3}\left(\Delta h_i + h_i^n\right)^3 \frac{\partial^2\left(\Delta p_i + p_i^n\right)}{\partial z^2} \\ &= \left(\left(h_i^n\right)^2 \frac{\partial \Delta h_i}{\partial z}\frac{\partial p_i^n}{\partial z} + \left(h_i^n\right)^2 \frac{\partial h_i^n}{\partial z}\frac{\partial \Delta p_i}{\partial z} + 2h_i^n \frac{\partial h_i^n}{\partial z}\frac{\partial p_i^n}{\partial z}\Delta h_i + \left(h_i^n\right)^2 \frac{\partial^2 p_i^n}{\partial z^2}\Delta h_i\right) \\ &+ \left(\frac{1}{3}\left(h_i^n\right)^3 \frac{\partial^2 \Delta p_i^n}{\partial z^2} + \left(h_i^n\right)^2 \frac{\partial h_i^n}{\partial z}\frac{\partial p_i^n}{\partial z} + \frac{1}{3}\left(h_i^n\right)^3 \frac{\partial^2 p_i^n}{\partial z^2}\right) + O(\Delta^2). \end{aligned} \tag{6.39}$$

Define

$$\mathrm{H}_{ij} = \delta_{ij} h_i^n, \quad (\mathrm{H}_2)_{ij} = \delta_{ij}(h_i^n)^2, \quad (\mathrm{H}_3)_{ij} = \delta_{ij}(h_i^n)^3, \tag{6.40}$$

$$(\mathrm{D}_2 p)_{ij} = \delta_{ij}(\mathrm{D}_2 p)_i, \quad (\mathrm{D}p)_{ij} = \delta_{ij}(\mathrm{D}p)_i, \quad (\mathrm{D}h)_{ij} = \delta_{ij}(\mathrm{D}h)_i, \tag{6.41}$$

where $i = 1, ..., N$, $j = 1, ..., N$, $\delta_{ij} = 1$ for $i = j$, $\delta_{ij} = 0$ for $i \neq j$ and D, and D_2 are $N \times N$ matrixes

$$\mathrm{D} = \frac{\partial}{\partial z} = \begin{bmatrix} -3 & 4 & -1 & 0 & 0 & 0 & 0 \\ -1 & 0 & 1 & 0 & 0 & 0 & 0 \\ 0 & -1 & 0 & 1 & 0 & 0 & 0 \\ 0 & 0 & . & . & . & 0 & 0 \\ 0 & 0 & 0 & . & . & . & 0 \\ 0 & 0 & 0 & 0 & -1 & 0 & 1 \\ 0 & 0 & 0 & 0 & 1 & -4 & 3 \end{bmatrix} \tag{6.42}$$

$$\mathrm{D}_2 = \frac{\partial^2}{\partial z^2} = \begin{bmatrix} 2 & -5 & 4 & -1 & 0 & 0 & 0 \\ 1 & -2 & 1 & 0 & 0 & 0 & 0 \\ 0 & 1 & -2 & 1 & 0 & 0 & 0 \\ 0 & 0 & . & . & . & 0 & 0 \\ 0 & 0 & 0 & . & . & . & 0 \\ 0 & 0 & 0 & 0 & 1 & -2 & 1 \\ 0 & 0 & 0 & -1 & 4 & -5 & 2 \end{bmatrix}. \tag{6.43}$$

Write the equation (6.39) in the form of matrix we have

$$\mathrm{Q}\Delta\mathrm{h} = \mathrm{A}n \tag{6.44}$$

where

$$\begin{aligned} Q &= \mathrm{I} - \frac{\Delta t}{3}(\frac{\mathrm{H}_3}{3})\mathrm{D}_2\mathrm{M} - \Delta t(\mathrm{H}_2)(\mathrm{D}_2 p) - 2\Delta t(\mathrm{H})(\mathrm{D}h)(\mathrm{D}p) && (6.45) \\ &- \Delta t(\mathrm{H}_2)(\mathrm{D}p)\mathrm{D} - \Delta t(\mathrm{H}_2)(\mathrm{D}h)\mathrm{DM}, && (6.46) \\ \mathrm{A} &= \frac{\Delta t}{3}(\mathrm{H}_3)(\mathrm{D}_2 p) + \Delta t(\mathrm{H}_2)(\mathrm{D}h)(\mathrm{D}p), && (6.47) \\ n &= \begin{bmatrix} 1, 1, ..., 1 \end{bmatrix}^T. && (6.48) \end{aligned}$$

Figures 6.2 and 6.3 show that $h(z, t)$ changes with time, but finally stops.

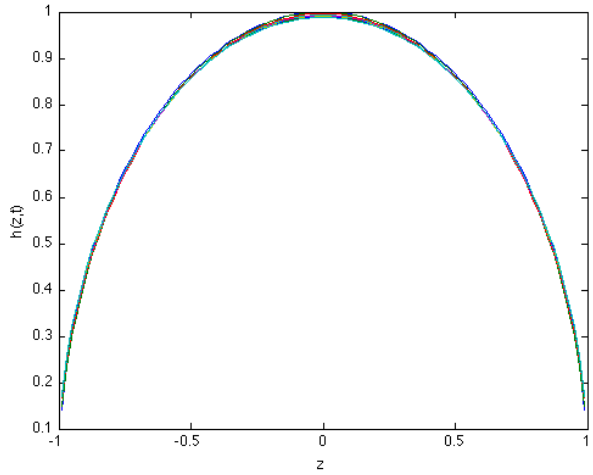

Figure 6.2: The profiles of $h(z,t)$ with the initial $h_0 = \sqrt{\left(1+\frac{z}{L}\right)\left(1-\frac{z}{L}\right)}$, $L = 1$, $N = 101$, and the final time 10.

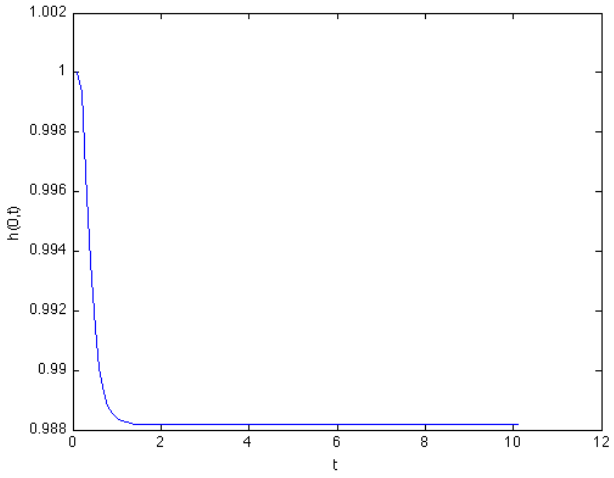

Figure 6.3: The profile of $h(0,t)$ changes with time with the initial $h_0 = \sqrt{\left(1+\frac{z}{L}\right)\left(1-\frac{z}{L}\right)}$, $L = 1$, $N = 101$, and the final time 10.

Figure 6.2 is the profiles of $h(z,t)$, which change along with time and finally stop. Figure 6.3 is the relation between $h(0,t)$ and time t, which shows that $h(0,t)$ stops changing before time t reaching 2.

Blood injection

The blood in the aorta interconnects with the blood in the tear. Now we assume the steady slow flow is injected from the middle of the crack, we use the condition below to replace the middle term of the matrix (6.44).

$$\Delta p|_{\frac{N+1}{2}} = p_{\text{injection}} - p^n|_{\frac{N+1}{2}} \tag{6.49}$$

Figures 6.4 and 6.5 show that $h(z,t)$ changes with time, but finally stops.

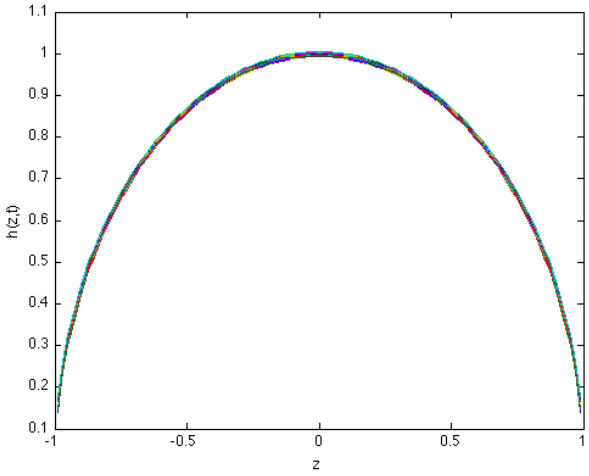

Figure 6.4: The profiles of $h(z,t)$ with the initial $h_0 = \sqrt{\left(1+\frac{z}{L}\right)\left(1-\frac{z}{L}\right)}$, $L = 1$, $N = 101$, and the final time 10.

Figure 6.4 is the profiles of $h(z,t)$, which change along with time and finally stop. Figure 6.5 is the relation between $h(0,t)$ and time t, which shows that $h(0,t)$ stops changing before time t reaching 6.

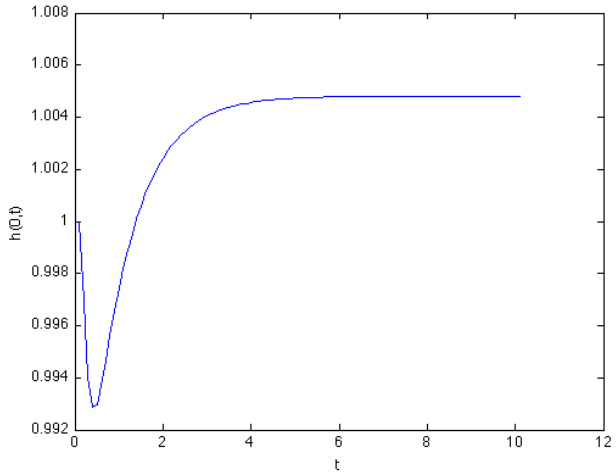

Figure 6.5: The profile of $h(0,t)$ changes with time with the initial $h_0 = \sqrt{\left(1+\frac{z}{L}\right)\left(1-\frac{z}{L}\right)}$, $L=1$, $N=101$, and the final time 10.

Tear on aorta based on Holzapfel Strain energy function

Now we use equation (6.30) to replace p, where $\dot{S}^u_{rr}(z-s,r)$ has been calculated in Chapter 5.

Without injection

If the injection is not considered and the initial tear is $h_0 = \sqrt{\left(1+\frac{z}{L}\right)\left(1-\frac{z}{L}\right)}$. We have the results shown in Figure 6.6 and 6.7.

Figure 6.6 shows profiles of $h(z,t)$, which change along with time and finally stop. Figure 6.7 shows the relation between $h(0,t)$ and time t, which shows that $h(0,t)$ stops changing before time t reaching 10.

With injection

If the injection is same as (6.49), and the initial tear is $h_0 = \sqrt{\left(1+\frac{z}{L}\right)\left(1-\frac{z}{L}\right)}$. We have the results shown in Figure 6.8 and 6.9.

Figure 6.8 is the profiles of $h(z,t)$, which change along with time and finally stop. Figure 6.9 is the relation between $h(0,t)$ and time t, which shows that $h(0,t)$ stops changing before time t reaching 30.

Comparing Figure 6.6 and 6.8 we find $h(0,t)$ stops at the place lower than 1 in Figure 6.6, however the parabola $h(t,z)$ becomes lower and wider. And $h(0,t)$ stops at the place

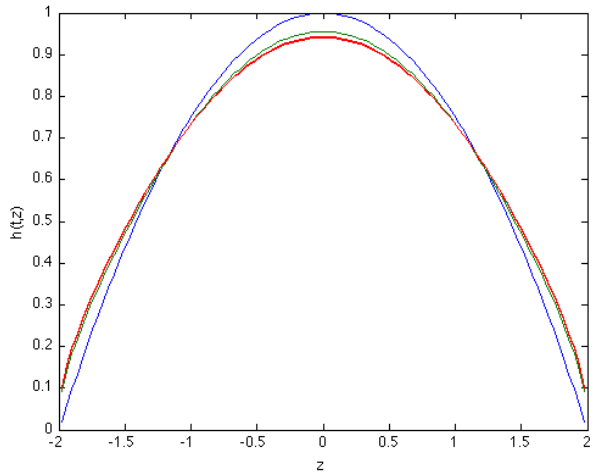

Figure 6.6: The profiles of $h(z,t)$ with the initial $h_0 = \sqrt{\left(1+\frac{z}{L}\right)\left(1-\frac{z}{L}\right)}$, $L = 2$, $N = 101$, and the final time 100.

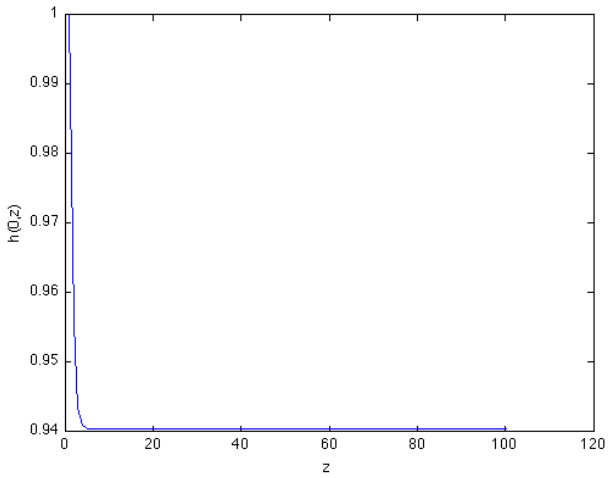

Figure 6.7: The profile of $h(0,t)$ changes with time with the initial $h_0 = \sqrt{\left(1+\frac{z}{L}\right)\left(1-\frac{z}{L}\right)}$, $L = 2$, $N = 101$, and the final time 100.

higher than 1 since the tear is inflated by the injection in Figure 6.8.

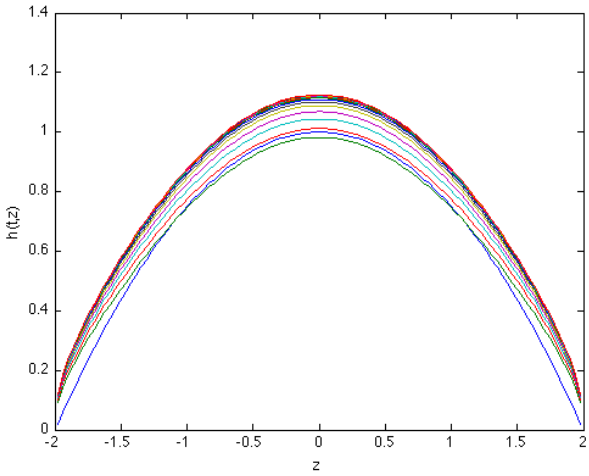

Figure 6.8: The profiles of $h(z,t)$ with the initial $h_0 = \sqrt{\left(1+\frac{z}{L}\right)\left(1-\frac{z}{L}\right)}$, $L = 2$, $N = 101$, and the final time 100.

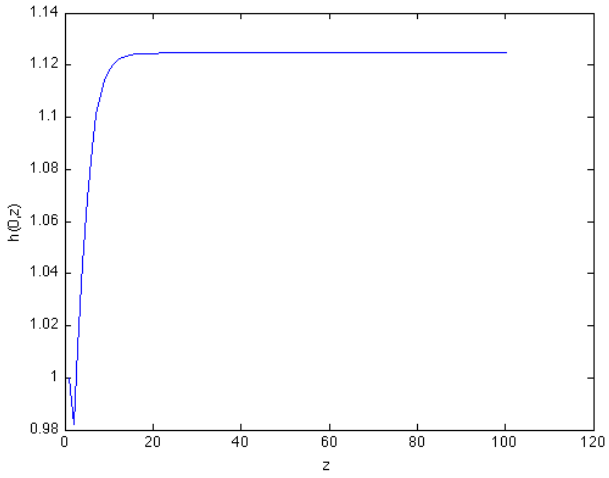

Figure 6.9: The profile of $h(0,t)$ changes with time with the initial $h_0 = \sqrt{\left(1+\frac{z}{L}\right)\left(1-\frac{z}{L}\right)}$, $L = 2$, $N = 101$, and the final time 100.

6.3 Conclusions

In this chapter we have obtained equations to model the thin steady flow inside the dissection. And we have modelled how the distance between the upper tear face and lower tear face along the tear changes with time. The work to couple fluid and elastic models, that the details in a real artery will depend on the viscosity, and flow regime in which the

fluid operates (low Reynolds number, high Reynolds number etc.) need to be considered in the future. The propagation of the tear in the axial direction should be learned, and it will be necessary to look at finite element methods.

Chapter 7

Conclusions

In this thesis we have analyzed and solved the 2D linear elastic plane crack problem for infinite plane and 2D compressible and incompressible strip in Chapter 3. The approach leads us to consider a numerical scheme to solve for the crack opening and displacements given the traction on the crack faces. The axisymmetric linear elastic crack problem in Chapter 4 for an elastic annulus has been studied. These crack problems are modelled mathematically with equilibrium equations, boundary conditions and jump conditions.

Chapter 5 illustrates the mathematical model of the axisymmetric tear on the idealized aorta, which is a thick-walled non-linear incompressible axisymmetric elastic tube with residual stress and two family fibers and whose properties are described by the strain energy function Holzapfel et al. [2000]. The tear problem is considered as the incremental deformation, and decomposed into normal and tangential direction. We use the integral of Green's function weighted by the displacement continuity to express the traction and displacement along the crack. The equilibrium equations of Cauchy stress and incremental nominal stress with boundary conditions, and jump conditions are solved to obtain the Green's function kernel, and the numerical methods are expressed in this paper. Given the traction along the crack the displacement along the crack is solved. We use the values of the parameters in Holzapfel et al. [2000] to test our model. The parameters in the strain energy function have effects on the opening of the tear, which are compared in our results. In addition, we consider the pressure change inside the aorta as the incremental inner pressure, and model the change caused by the incremental inner pressure.

The crack propagation is important and should be studied in the future. Referring to Benson et al. [1957] if there is a tear in the overlying media and intima, a column of blood under aortic pressure may then enter the false lumen and cause a more rapid and

complete dissection due to Bernoulli's law. The high pressure rips the tissue of the media apart. This can propagate along the length of the aorta for a variable distance forward and backwards. Hence the tear is filled with fluid. In general terms the fluid flow and tear opening are coupled, and an evolution equation for the tear opening must be found. In addition, a theory of propagation must include a criterion for tear extension and tear direction. We didn't discuss it in this thesis, however it is an important direction for the development of a realistic tearing model that couples the elasticity of the aorta and the fluid flow.

Appendix A

Coefficients for ODEs in the incremental crack problem of Chapter 5

Below equations are coefficients of ODEs for Jump in 'w' in Chapter 5.

$$
\begin{aligned}
A_1 &= \frac{\mu\,(a_z(r))^2\,g}{r} + 2/3\,\frac{F_1(r)\,g\,(\sin(\beta))^2\,(a_z(r))^2}{r} \\
&- 4\,\frac{P_1(r)\,(\cos(\beta))^2\,(a_\theta(r))^2\,g\,(\sin(\beta))^2\,(a_z(r))^2}{r} + 4/3\,\frac{P_1(r)\,(\cos(\beta))^4\,(a_\theta(r))^4\,g}{r} \\
&+ \frac{g\mu\,(a_\theta(r))^2}{r} - \frac{g\mu\,(a_r(r))^2}{r} - \frac{\mu\,(a_r(r))^2}{gr^3} + 10/3\,\frac{F_1(r)\,(\cos(\beta))^2\,(a_\theta(r))^2\,g}{r} \\
&+ 2/3\,\frac{F_2(r)\,g\,(\sin(\beta))^2\,(a_z(r))^2}{r} + 10/3\,\frac{F_2(r)\,(\cos(\beta))^2\,(a_\theta(r))^2\,g}{r} \\
&- 4\,\frac{P_2(r)\,(\cos(\beta))^2\,(a_\theta(r))^2\,g\,(\sin(\beta))^2\,(a_z(r))^2}{r} + 4/3\,\frac{P_2(r)\,(\cos(\beta))^4\,(a_\theta(r))^4\,g}{r} \\
&+ 8/3\,\frac{P_1(r)\,g\,(\sin(\beta))^4\,(a_z(r))^4}{r} + 8/3\,\frac{P_2(r)\,g\,(\sin(\beta))^4\,(a_z(r))^4}{r} - 2\,g\mu\,a_r(r)\,\frac{d}{dr}a_r(r) \\
&- 2/3\left(\frac{d}{dr}F_1(r)\right)g\,(\cos(\beta))^2\,(a_\theta(r))^2 - 2/3\left(\frac{d}{dr}F_1(r)\right)g\,(\sin(\beta))^2\,(a_z(r))^2 \\
&- 2/3\left(\frac{d}{dr}F_2(r)\right)g\,(\cos(\beta))^2\,(a_\theta(r))^2 - 2/3\left(\frac{d}{dr}F_2(r)\right)g\,(\sin(\beta))^2\,(a_z(r))^2 \\
&+ 2/3\,gF_1(r)\,\frac{d}{dr}I_4(r) + 2/3\,g\left(\frac{d}{dr}F_1(r)\right)I_4(r) + 2/3\,gF_2(r)\,\frac{d}{dr}I_6(r) \\
&+ 2/3\,g\left(\frac{d}{dr}F_2(r)\right)I_6(r) + 2\,\frac{\mu\,a_r(r)\,\frac{d}{dr}a_r(r)}{gr^2} \\
&- 4/3\,F_1(r)\,g\,(\cos(\beta))^2\,a_\theta(r)\,\frac{d}{dr}a_\theta(r) - 4/3\,F_1(r)\,g\,(\sin(\beta))^2\,a_z(r)\,\frac{d}{dr}a_z(r) \\
&- 4/3\,F_2(r)\,g\,(\cos(\beta))^2\,a_\theta(r)\,\frac{d}{dr}a_\theta(r) - 4/3\,F_2(r)\,g\,(\sin(\beta))^2\,a_z(r)\,\frac{d}{dr}a_z(r)
\end{aligned}
$$

$$
\begin{aligned}
B_1 &= \mu\,(a_z(r))^2\, g + 8/3\, P_1(r)\, g\,(\sin(\beta))^4\,(a_z(r))^4 \\
&- 4/3\, P_1(r)\, g\,(\sin(\beta))^2\,(a_z(r))^2\,(\cos(\beta))^2\,(a_\theta(r))^2 \\
&+ 8/3\, P_2(r)\, g\,(\sin(\beta))^4\,(a_z(r))^4 - 4/3\, P_2(r)\,(\cos(\beta))^2\,(a_\theta(r))^2\, g\,(\sin(\beta))^2\,(a_z(r))^2 \\
&+ \frac{\mu\,(a_r(r))^2}{gr^2} - 2\,\frac{\mu\, a_r(r)\,\frac{d}{dr}a_r(r)}{gr} + 2/3\, F_1(r)\, g\,(\sin(\beta))^2\,(a_z(r))^2 \\
&+ 2/3\, F_2(r)\, g\,(\sin(\beta))^2\,(a_z(r))^2
\end{aligned}
$$

$$
C_1 = -2\,\frac{\mu\, a_r(r)\,\frac{d}{dr}a_r(r)}{g} - 2\,\frac{\mu\,(a_r(r))^2}{gr}
$$

$$
D_1 = -\frac{\mu\,(a_r(r))^2}{g}
$$

$$
E_1 = \mu g
$$

$$
\begin{aligned}
A_2 &= 8/3\,\frac{F_2(r)\,(\cos(\beta))^2\,a_\theta(r)\,\frac{d}{dr}a_\theta(r)}{r}+\mu\,(a_z(r))^2\,g^2\\
&+ 4/3\,\frac{\left(\frac{d}{dr}F_2(r)\right)(\cos(\beta))^2\,(a_\theta(r))^2}{r}-4/3\,\frac{\left(\frac{d}{dr}F_2(r)\right)(\sin(\beta))^2\,(a_z(r))^2}{r}\\
&+ 2/3\,\frac{F_2(r)\,(\cos(\beta))^2\,(a_\theta(r))^2}{r^2}+4/3\,\frac{F_2(r)\,(\sin(\beta))^2\,(a_z(r))^2}{r^2}\\
&+ 4/3\,\frac{\left(\frac{d}{dr}F_1(r)\right)(\cos(\beta))^2\,(a_\theta(r))^2}{r}-4/3\,\frac{\left(\frac{d}{dr}F_1(r)\right)(\sin(\beta))^2\,(a_z(r))^2}{r}\\
&+ 4/3\,\frac{\left(\frac{d}{dr}P_1(r)\right)(\cos(\beta))^4\,(a_\theta(r))^4}{r}-4/3\,\frac{\left(\frac{d}{dr}P_1(r)\right)(\sin(\beta))^4\,(a_z(r))^4}{r}\\
&+ 4/3\,\frac{\left(\frac{d}{dr}P_2(r)\right)(\cos(\beta))^4\,(a_\theta(r))^4}{r}-4/3\,\frac{\left(\frac{d}{dr}P_2(r)\right)(\sin(\beta))^4\,(a_z(r))^4}{r}\\
&+ 4/3\,\frac{P_2(r)\,(\sin(\beta))^4\,(a_z(r))^4}{r^2}+8/3\,\frac{P_2(r)\,(\cos(\beta))^4\,(a_\theta(r))^4}{r^2}\\
&+ 2/3\,\frac{F_1(r)\,(\cos(\beta))^2\,(a_\theta(r))^2}{r^2}+4/3\,\frac{F_1(r)\,(\sin(\beta))^2\,(a_z(r))^2}{r^2}\\
&+ 4/3\,\frac{P_1(r)\,(\sin(\beta))^4\,(a_z(r))^4}{r^2}+2\,F_1(r)\,(\sin(\beta))^2\,(a_z(r))^2\,g^2\\
&+ 2\,F_2(r)\,(\sin(\beta))^2\,(a_z(r))^2\,g^2+8/3\,\frac{F_1(r)\,(\cos(\beta))^2\,a_\theta(r)\,\frac{d}{dr}a_\theta(r)}{r}\\
&- 8/3\,\frac{F_1(r)\,(\sin(\beta))^2\,a_z(r)\,\frac{d}{dr}a_z(r)}{r}+16/3\,\frac{P1(r)\,(\cos(\beta))^4\,(a_\theta(r))^3\,\frac{d}{dr}a_\theta(r)}{r}\\
&- 16/3\,\frac{P_1(r)\,(\sin(\beta))^4\,(a_z(r))^3\,\frac{d}{dr}a_z(r)}{r}-8/3\,\frac{F_2(r)\,(\sin(\beta))^2\,a_z(r)\,\frac{d}{dr}a_z(r)}{r}\\
&- 4\,\frac{P_2(r)\,(\sin(\beta))^2\,(a_z(r))^2\,(\cos(\beta))^2\,(a_\theta(r))^2}{r^2}\\
&- 4\,\frac{P_1(r)\,(\sin(\beta))^2\,(a_z(r))^2\,(\cos(\beta))^2\,(a_\theta(r))^2}{r^2}\\
&- 16/3\,\frac{P_2(r)\,(\sin(\beta))^4\,(a_z(r))^3\,\frac{d}{dr}a_z(r)}{r}\\
&+ 16/3\,\frac{P_2(r)\,(\cos(\beta))^4\,(a_\theta(r))^3\,\frac{d}{dr}a_\theta(r)}{r}+\frac{\mu\,(a_\theta(r))^2}{r^2}\\
&+ 8/3\,\frac{P_1(r)\,(\cos(\beta))^4\,(a_\theta(r))^4}{r^2}
\end{aligned}
$$

$$
\begin{aligned}
B_2 &= -4/3\left(\frac{d}{dr}P_2(r)\right)(\sin(\beta))^4(a_z(r))^4 - 2\left(\frac{d}{dr}F_2(r)\right)(\sin(\beta))^2(a_z(r))^2 \\
&- 16/3\,P_1(r)(\sin(\beta))^4(a_z(r))^3\frac{d}{dr}a_z(r) - 4\,F_2(r)(\sin(\beta))^2 a_z(r)\frac{d}{dr}a_z(r) \\
&- 2\left(\frac{d}{dr}F_1(r)\right)(\sin(\beta))^2(a_z(r))^2 - 16/3\,P_2(r)(\sin(\beta))^4(a_z(r))^3\frac{d}{dr}a_z(r) \\
&- 4\,F_1(r)(\sin(\beta))^2 a_z(r)\frac{d}{dr}a_z(r) - 4/3\left(\frac{d}{dr}P_1(r)\right)(\sin(\beta))^4(a_z(r))^4 \\
&- 2/3\left(\frac{d}{dr}F_1(r)\right)(\cos(\beta))^2(a_\theta(r))^2 + 2/3\left(\frac{d}{dr}F_1(r)\right)I_4(r) + 2/3\,F_2(r)\frac{d}{dr}I_6(r) \\
&+ 2/3\,F_1(r)\frac{d}{dr}I_4(r) + 2/3\left(\frac{d}{dr}F_2(r)\right)I_6(r) - 2\frac{\mu\,(a_r(r))^2}{r} \\
&- 4/3\,F_1(r)(\cos(\beta))^2 a_\theta(r)\frac{d}{dr}a_\theta(r) - 4/3\,F_2(r)(\cos(\beta))^2 a_\theta(r)\frac{d}{dr}a_\theta(r) \\
&+ 10/3\frac{F_1(r)(\cos(\beta))^2(a_\theta(r))^2}{r} + 10/3\frac{F_2(r)(\cos(\beta))^2(a_\theta(r))^2}{r} \\
&- 4/3\frac{F_1(r)(\sin(\beta))^2(a_z(r))^2}{r} - 2/3\left(\frac{d}{dr}F_2(r)\right)(\cos(\beta))^2(a_\theta(r))^2 \\
&+ \frac{\mu\,(a_\theta(r))^2}{r} - 4\,\mu\,a_r(r)\frac{d}{dr}a_r(r) - 4\frac{P_1(r)(\sin(\beta))^2(a_z(r))^2(\cos(\beta))^2(a_\theta(r))^2}{r} \\
&- 8/3\,P_2(r)(\sin(\beta))^2(a_z(r))^2(\cos(\beta))^2 a_\theta(r)\frac{d}{dr}a_\theta(r) \\
&- 8/3\,P_1(r)(\sin(\beta))^2 a_z(r)\left(\frac{d}{dr}a_z(r)\right)(\cos(\beta))^2(a_\theta(r))^2 \\
&- 4/3\left(\frac{d}{dr}P_1(r)\right)(\sin(\beta))^2(a_z(r))^2(\cos(\beta))^2(a_\theta(r))^2 \\
&- 8/3\,P_1(r)(\sin(\beta))^2(a_z(r))^2(\cos(\beta))^2 a_\theta(r)\frac{d}{dr}a_\theta(r) \\
&- 4/3\left(\frac{d}{dr}P_2(r)\right)(\sin(\beta))^2(a_z(r))^2(\cos(\beta))^2(a_\theta(r))^2 \\
&- 8/3\,P_2(r)(\sin(\beta))^2 a_z(r)\left(\frac{d}{dr}a_z(r)\right)(\cos(\beta))^2(a_\theta(r))^2 \\
&- 4\frac{P_2(r)(\sin(\beta))^2(a_z(r))^2(\cos(\beta))^2(a_\theta(r))^2}{r} \\
&- 4/3\frac{F_2(r)(\sin(\beta))^2(a_z(r))^2}{r} - 4/3\frac{P_2(r)(\sin(\beta))^4(a_z(r))^4}{r} \\
&+ 4/3\frac{P_2(r)(\cos(\beta))^4(a_\theta(r))^4}{r} - 4/3\frac{P_1(r)(\sin(\beta))^4(a_z(r))^4}{r} \\
&+ 4/3\frac{P_1(r)(\cos(\beta))^4(a_\theta(r))^4}{r}
\end{aligned}
$$

$$\begin{aligned} C_2 &= -4/3\,P_2(r)(\sin(\beta))^2(a_z(r))^2(\cos(\beta))^2(a_\theta(r))^2 - 4/3\,F_1(r)(\sin(\beta))^2(a_z(r))^2 \\ &- 4/3\,F_2(r)(\sin(\beta))^2(a_z(r))^2 - 4/3\,P_1(r)(\sin(\beta))^2(a_z(r))^2(\cos(\beta))^2(a_\theta(r))^2 \\ &- \mu\,(a_r(r))^2 - 4/3\,P_2(r)(\sin(\beta))^4(a_z(r))^4 - 4/3\,P_1(r)(\sin(\beta))^4(a_z(r))^4 \end{aligned}$$

$$D_2 = \mu$$

$$\begin{aligned} a_1 &= 4/3\,\frac{P_1(r_{in})(\cos(\beta))^4(a_\theta(r_{in}))^4}{r_{in}} - 4/3\,\frac{F_1(r_{in})(\sin(\beta))^2(a_z(r_{in}))^2}{r_{in}} \\ &- 4/3\,\frac{P_1(r_{in})(\sin(\beta))^4(a_z(r_{in}))^4}{r_{in}} - 4/3\,\frac{F_2(r_{in})(\sin(\beta))^2(a_z(r_{in}))^2}{r_{in}} \\ &+ 4/3\,\frac{F_2(r_{in})(\cos(\beta))^2(a_\theta(r_{in}))^2}{r_{in}} + 4/3\,\frac{F_1(r_{in})(\cos(\beta))^2(a_\theta(r_{in}))^2}{r_{in}} \\ &- 4/3\,\frac{P_2(r_{in})(\sin(\beta))^4(a_z(r_{in}))^4}{r_{in}} + 4/3\,\frac{P_2(r_{in})(\cos(\beta))^4(a_\theta(r_{in}))^4}{r_{in}} \end{aligned}$$

$$\begin{aligned} a_2 &= -4/3\,P_2(r_{in})(\sin(\beta))^4(a_z(r_{in}))^4 - 2/3\,F_1(r_{in})I_4(r_{in}) - 2/3\,F_2(r_{in})I_6(r_{in}) \\ &- 2/3\,F_2(r_{in})(\cos(\beta))^2(a_\theta(r_{in}))^2 - 2\,F_1(r_{in})(\sin(\beta))^2(a_z(r_{in}))^2 - 2\,\mu\,q(r_{in}) \\ &- 4/3\,P_1(r_{in})(\sin(\beta))^2(a_z(r_{in}))^2(\cos(\beta))^2(a_\theta(r_{in}))^2 - 2\,F_2(r_{in})(\sin(\beta))^2(a_z(r_{in}))^2 \\ &- 2/3\,F_1(r_{in})(\cos(\beta))^2(a_\theta(r_{in}))^2 - 4/3\,P_2(r_{in})(\sin(\beta))^2(a_z(r_{in}))^2(\cos(\beta))^2(a_\theta(r_{in}))^2 \\ &- 4/3\,P_1(r_{in})(\sin(\beta))^4(a_z(r_{in}))^4 \end{aligned}$$

$$a_4 = \mu$$

$$\begin{aligned} b_1 &= -2\,g\mu\,q(r_{in}) + \frac{\mu\,(a_r(r_{in}))^2}{g{r_{in}}^2} - 2/3\,F_1(r_{in})\,g(\cos(\beta))^2(a_\theta(r_{in}))^2 \\ &- 2/3\,F_1(r_{in})\,g(\sin(\beta))^2(a_z(r_{in}))^2 - 2/3\,F_2(r_{in})\,g(\cos(\beta))^2(a_\theta(r_{in}))^2 \\ &- 2/3\,F_2(r_{in})\,g(\sin(\beta))^2(a_z(r_{in}))^2 + g\mu\,(a_r(r_{in}))^2 \\ &- 2/3\,gF_1(r_{in})I_4(r_{in}) - 2/3\,gF_2(r_{in})I_6(r_{in}) \end{aligned}$$

$$b_2 = -\frac{\mu\,(a_r(r_{in}))^2}{g r_{in}}$$

$$b_3 = -\frac{\mu\,(a_r(r_{in}))^2}{g}$$

$$\begin{aligned} c_5 &= 4/3\,\frac{F_2(r_{out})(\cos(\beta))^2(a_\theta(r_{out}))^2}{r_{out}} - 4/3\,\frac{F_2(r_{out})(\sin(\beta))^2(a_z(r_{out}))^2}{r_{out}} \\ &- 4/3\,\frac{P_1(r_{out})(\sin(\beta))^4(a_z(r_{out}))^4}{r_{out}} - 4/3\,\frac{P_2(r_{out})(\sin(\beta))^4(a_z(r_{out}))^4}{r_{out}} \\ &+ 4/3\,\frac{F_1(r_{out})(\cos(\beta))^2(a_\theta(r_{out}))^2}{r_{out}} + 4/3\,\frac{P_1(r_{out})(\cos(\beta))^4(a_\theta(r_{out}))^4}{r_{out}} \\ &+ 4/3\,\frac{P_2(r_{out})(\cos(\beta))^4(a_\theta(r_{out}))^4}{r_{out}} - 4/3\,\frac{F_1(r_{out})(\sin(\beta))^2(a_z(r_{out}))^2}{r_{out}} \end{aligned}$$

$$\begin{aligned} c_6 &= -\mu\,(a_r(r_{out}))^2 - 4/3\,P_2(r_{out})(\sin(\beta))^2(a_z(r_{out}))^2(\cos(\beta))^2(a_\theta(r_{out}))^2 \\ &- \mu\,q(r_{out}) - 2/3\,F_1(r_{out})(\cos(\beta))^2(a_\theta(r_{out}))^2 + P_{ext} - 4/3\,P_1(r_{out})(\sin(\beta))^4(a_z(r_{out}))^4 \\ &- 2/3\,F_2(r_{out})(\cos(\beta))^2(a_\theta(r_{out}))^2 - 4/3\,P_1(r_{out})(\sin(\beta))^2(a_z(r_{out}))^2(\cos(\beta))^2(a_\theta(r_{out}))^2 \\ &- 4/3\,P_2(r_{out})(\sin(\beta))^4(a_z(r_{out}))^4 - 2\,F_1(r_{out})(\sin(\beta))^2(a_z(r_{out}))^2 \\ &- 2\,F_2(r_{out})(\sin(\beta))^2(a_z(r_{out}))^2 \end{aligned}$$

$$c_8 = \mu$$

$$\begin{aligned} d_5 &= -\mu\,q(r_{out})\,g + \frac{\mu\,(a_r(r_{out}))^2}{g {r_{out}}^2} - 2/3\,F_1(r_{out})\,g(\cos(\beta))^2(a_\theta(r_{out}))^2 \\ &- 2/3\,F_1(r_{out})\,g(\sin(\beta))^2(a_z(r_{out}))^2 - 2/3\,F_2(r_{out})\,g(\cos(\beta))^2(a_\theta(r_{out}))^2 \\ &- 2/3\,F_2(r_{out})\,g(\sin(\beta))^2(a_z(r_{out}))^2 + P_{ext}\,g \end{aligned}$$

$$d_6 = -\frac{\mu\,(a_r(r_{out}))^2}{g r_{out}}$$

$$d_7 = -\frac{\mu\,(a_r(r_{out}))^2}{g}$$

$$\begin{aligned} s_{wr1}(r) &= 4/3\,\frac{P_2(r)(\cos(\beta))^4(a_\theta(r))^4}{r} + 4/3\,\frac{P_1(r)(\cos(\beta))^4(a_\theta(r))^4}{r} \\ &- 4/3\,\frac{P_2(r)(\sin(\beta))^4(a_z(r))^4}{r} - 4/3\,\frac{P_1(r)(\sin(\beta))^4(a_z(r))^4}{r} \\ &- 4/3\,\frac{F_1(r)(\sin(\beta))^2(a_z(r))^2}{r} + 4/3\,\frac{F_2(r)(\cos(\beta))^2(a_\theta(r))^2}{r} \\ &+ 4/3\,\frac{F_1(r)(\cos(\beta))^2(a_\theta(r))^2}{r} - 4/3\,\frac{F_2(r)(\sin(\beta))^2(a_z(r))^2}{r} \end{aligned}$$

$$\begin{aligned} s_{wr2}(r) &= -4/3\,P_1(r)(\sin(\beta))^4(a_z(r))^4 \\ &- 4/3\,P_2(r)(\sin(\beta))^2(a_z(r))^2(\cos(\beta))^2(a_\theta(r))^2 \\ &- 4/3\,P_2(r)(\sin(\beta))^4(a_z(r))^4 - 2\,F_1(r)(\sin(\beta))^2(a_z(r))^2 \\ &- \mu\,(a_r(r))^2 - 4/3\,P_1(r)(\sin(\beta))^2(a_z(r))^2(\cos(\beta))^2(a_\theta(r))^2 \\ &- \mu\,q(r) - 2\,F_2(r)(\sin(\beta))^2(a_z(r))^2 - 2/3\,F_2(r)(\cos(\beta))^2(a_\theta(r))^2 \\ &- 2/3\,F_1(r)(\cos(\beta))^2(a_\theta(r))^2 \end{aligned}$$

$$\begin{aligned} s_{uz1}(r) &= -\mu\,q(r)g + \frac{\mu\,(a_r(r))^2}{gr^2} - 2/3\,F_1(r)\,g(\cos(\beta))^2(a_\theta(r))^2 \\ &- 2/3\,F_1(r)\,g(\sin(\beta))^2(a_z(r))^2 - 2/3\,F_2(r)\,g(\cos(\beta))^2(a_\theta(r))^2 \\ &- 2/3\,F_2(r)\,g(\sin(\beta))^2(a_z(r))^2 \end{aligned}$$

$$s_{uz2}(r) = -\frac{\mu\,(a_r(r))^2}{gr}$$

$$s_{uz3}(r) = -\frac{\mu\,(a_r(r))^2}{g}$$

$$
\begin{aligned}
e_1 &= 4/3\,\frac{P_2\left(r_c\right)\left(\cos\left(\beta\right)\right)^4\left(a_\theta\left(r_c\right)\right)^4}{r_c} + 4/3\,\frac{F_1\left(r_c\right)\left(\cos\left(\beta\right)\right)^2\left(at\left(r_c\right)\right)^2}{r_c} \\
&+ 4/3\,\frac{P_1\left(r_c\right)\left(\cos\left(\beta\right)\right)^4\left(a_\theta\left(r_c\right)\right)^4}{r_c} - 4/3\,\frac{F_1\left(r_c\right)\left(\sin\left(\beta\right)\right)^2\left(a_z\left(r_c\right)\right)^2}{r_c} \\
&+ 4/3\,\frac{F_2\left(r_c\right)\left(\cos\left(\beta\right)\right)^2\left(a_\theta\left(r_c\right)\right)^2}{r_c} - 4/3\,\frac{P_2\left(r_c\right)\left(\sin\left(\beta\right)\right)^4\left(a_z\left(r_c\right)\right)^4}{r_c} \\
&- 4/3\,\frac{F_2\left(r_c\right)\left(\sin\left(\beta\right)\right)^2\left(a_z\left(r_c\right)\right)^2}{r_c} - 4/3\,\frac{P_1\left(r_c\right)\left(\sin\left(\beta\right)\right)^4\left(a_z\left(r_c\right)\right)^4}{r_c}
\end{aligned}
$$

$$
\begin{aligned}
e_2 &= -\mu\,Y_{b9} - 2/3\,F_2\left(r_c\right)\left(\cos\left(\beta\right)\right)^2\left(a_\theta\left(r_c\right)\right)^2 - 2/3\,F_1\left(r_c\right)\left(\cos\left(\beta\right)\right)^2\left(a_\theta\left(r_c\right)\right)^2 \\
&- 2\,F_2\left(r_c\right)\left(\sin\left(\beta\right)\right)^2\left(a_z\left(r_c\right)\right)^2 - 4/3\,P_2\left(r_c\right)\left(\sin\left(\beta\right)\right)^4\left(a_z\left(r_c\right)\right)^4 - 2\,F_1\left(r_c\right)\left(\sin\left(\beta\right)\right)^2\left(a_z\left(r_c\right)\right)^2 \\
&- \mu\,\left(a_r\left(r_c\right)\right)^2 - 4/3\,P_1\left(r_c\right)\left(\sin\left(\beta\right)\right)^4\left(a_z\left(r_c\right)\right)^4 \\
&- 4/3\,P_2\left(r_c\right)\left(\sin\left(\beta\right)\right)^2\left(a_z\left(r_c\right)\right)^2\left(\cos\left(\beta\right)\right)^2\left(a_\theta\left(r_c\right)\right)^2 \\
&- 4/3\,P_1\left(r_c\right)\left(\sin\left(\beta\right)\right)^2\left(a_z\left(r_c\right)\right)^2\left(\cos\left(\beta\right)\right)^2\left(a_\theta\left(r_c\right)\right)^2
\end{aligned}
$$

$$e_4 = \mu$$

$$
\begin{aligned}
e_5 &= 4/3\,\frac{P_2\left(r_c\right)\left(\cos\left(\beta\right)\right)^4\left(a_\theta\left(r_c\right)\right)^4}{r_c} + 4/3\,\frac{F_1\left(r_c\right)\left(\cos\left(\beta\right)\right)^2\left(at\left(r_c\right)\right)^2}{r_c} \\
&+ 4/3\,\frac{P_1\left(r_c\right)\left(\cos\left(\beta\right)\right)^4\left(a_\theta\left(r_c\right)\right)^4}{r_c} - 4/3\,\frac{F_1\left(r_c\right)\left(\sin\left(\beta\right)\right)^2\left(a_z\left(r_c\right)\right)^2}{r_c} \\
&+ 4/3\,\frac{F_2\left(r_c\right)\left(\cos\left(\beta\right)\right)^2\left(a_\theta\left(r_c\right)\right)^2}{r_c} - 4/3\,\frac{P_2\left(r_c\right)\left(\sin\left(\beta\right)\right)^4\left(a_z\left(r_c\right)\right)^4}{r_c} \\
&- 4/3\,\frac{F_2\left(r_c\right)\left(\sin\left(\beta\right)\right)^2\left(a_z\left(r_c\right)\right)^2}{r_c} - 4/3\,\frac{P_1\left(r_c\right)\left(\sin\left(\beta\right)\right)^4\left(a_z\left(r_c\right)\right)^4}{r_c}
\end{aligned}
$$

$$
\begin{aligned}
e_6 &= -\mu\,Y_{b10} - 2/3\,F_2\left(r_c\right)\left(\cos\left(\beta\right)\right)^2\left(a_\theta\left(r_c\right)\right)^2 - 2/3\,F_1\left(r_c\right)\left(\cos\left(\beta\right)\right)^2\left(a_\theta\left(r_c\right)\right)^2 \\
&- 2\,F_2\left(r_c\right)\left(\sin\left(\beta\right)\right)^2\left(a_z\left(r_c\right)\right)^2 - 4/3\,P_2\left(r_c\right)\left(\sin\left(\beta\right)\right)^4\left(a_z\left(r_c\right)\right)^4 - 2\,F_1\left(r_c\right)\left(\sin\left(\beta\right)\right)^2\left(a_z\left(r_c\right)\right)^2 \\
&- \mu\,\left(a_r\left(r_c\right)\right)^2 - 4/3\,P_1\left(r_c\right)\left(\sin\left(\beta\right)\right)^4\left(a_z\left(r_c\right)\right)^4 \\
&- 4/3\,P_2\left(r_c\right)\left(\sin\left(\beta\right)\right)^2\left(a_z\left(r_c\right)\right)^2\left(\cos\left(\beta\right)\right)^2\left(a_\theta\left(r_c\right)\right)^2 \\
&- 4/3\,P_1\left(r_c\right)\left(\sin\left(\beta\right)\right)^2\left(a_z\left(r_c\right)\right)^2\left(\cos\left(\beta\right)\right)^2\left(a_\theta\left(r_c\right)\right)^2
\end{aligned}
$$

$$e_8 = \mu$$

$$\begin{aligned} f_1 &= -\mu\, Y_{b9} g + \frac{\mu\, (a_r(r_c))^2}{g {r_c}^2} - 2/3\, F_1(r_c)\, g\, (\cos(\beta))^2\, (a_\theta(r_c))^2 - 2/3\, F_1(r_c)\, g\, (\sin(\beta))^2\, (a_z(r_c))^2 \\ &- 2/3\, F_2(r_c)\, g\, (\cos(\beta))^2\, (a_\theta(r_c))^2 - 2/3\, F_2(r_c)\, g\, (\sin(\beta))^2\, (a_z(r_c))^2 \end{aligned}$$

$$f_2 = -\frac{\mu\, (a_r(r_c))^2}{g r_c}$$

$$f_3 = -\frac{\mu\, (a_r(r_c))^2}{g}$$

$$\begin{aligned} f_5 &= -\mu\, Y_{b10} g + \frac{\mu\, (a_r(r_c))^2}{g {r_c}^2} - 2/3\, F_1(r_c)\, g\, (\cos(\beta))^2\, (a_\theta(r_c))^2 - 2/3\, F_1(r_c)\, g\, (\sin(\beta))^2\, (a_z(r_c))^2 \\ &- 2/3\, F_2(r_c)\, g\, (\cos(\beta))^2\, (a_\theta(r_c))^2 - 2/3\, F_2(r_c)\, g\, (\sin(\beta))^2\, (a_z(r_c))^2 \end{aligned}$$

$$f_6 = -\frac{\mu\, (a_r(r_c))^2}{g r_c}$$

$$f_7 = -\frac{\mu\, (a_r(r_c))^2}{g}$$

Appendix B

Coefficients for ODEs in the incremental crack problem of Chapter 5

Below equations are coefficients of ODEs for Jump in 'u' in Chapter 5.

$$
\begin{aligned}
A_1 &= \frac{\mu\,(a_z(r))^2\,g}{r} + 2/3\,\frac{F_1(r)\,g\,(\sin(\beta))^2\,(a_z(r))^2}{r} \\
&- 4\,\frac{P_1(r)\,(\cos(\beta))^2\,(a_\theta(r))^2\,g\,(\sin(\beta))^2\,(a_z(r))^2}{r} + 4/3\,\frac{P_1(r)\,(\cos(\beta))^4\,(a_\theta(r))^4\,g}{r} \\
&+ \frac{g\mu\,(a_\theta(r))^2}{r} - \frac{g\mu\,(a_r(r))^2}{r} - \frac{\mu\,(a_r(r))^2}{gr^3} + 10/3\,\frac{F_1(r)\,(\cos(\beta))^2\,(a_\theta(r))^2\,g}{r} \\
&+ 2/3\,\frac{F_2(r)\,g\,(\sin(\beta))^2\,(a_z(r))^2}{r} + 10/3\,\frac{F_2(r)\,(\cos(\beta))^2\,(a_\theta(r))^2\,g}{r} \\
&- 4\,\frac{P_2(r)\,(\cos(\beta))^2\,(a_\theta(r))^2\,g\,(\sin(\beta))^2\,(a_z(r))^2}{r} + 4/3\,\frac{P_2(r)\,(\cos(\beta))^4\,(a_\theta(r))^4\,g}{r} \\
&+ 8/3\,\frac{P_1(r)\,g\,(\sin(\beta))^4\,(a_z(r))^4}{r} + 8/3\,\frac{P_2(r)\,g\,(\sin(\beta))^4\,(a_z(r))^4}{r} - 2\,g\mu\,a_r(r)\,\frac{d}{dr}a_r(r) \\
&- 2/3\left(\frac{d}{dr}F_1(r)\right)g\,(\cos(\beta))^2\,(a_\theta(r))^2 - 2/3\left(\frac{d}{dr}F_1(r)\right)g\,(\sin(\beta))^2\,(a_z(r))^2 \\
&- 2/3\left(\frac{d}{dr}F_2(r)\right)g\,(\cos(\beta))^2\,(a_\theta(r))^2 - 2/3\left(\frac{d}{dr}F_2(r)\right)g\,(\sin(\beta))^2\,(a_z(r))^2 \\
&+ 2/3\,gF_1(r)\,\frac{d}{dr}I_4(r) + 2/3\,g\left(\frac{d}{dr}F_1(r)\right)I_4(r) + 2/3\,gF_2(r)\,\frac{d}{dr}I_6(r) \\
&+ 2/3\,g\left(\frac{d}{dr}F_2(r)\right)I_6(r) + 2\,\frac{\mu\,a_r(r)\,\frac{d}{dr}a_r(r)}{gr^2} \\
&- 4/3\,F_1(r)\,g\,(\cos(\beta))^2\,a_\theta(r)\,\frac{d}{dr}a_\theta(r) - 4/3\,F_1(r)\,g\,(\sin(\beta))^2\,a_z(r)\,\frac{d}{dr}a_z(r) \\
&- 4/3\,F_2(r)\,g\,(\cos(\beta))^2\,a_\theta(r)\,\frac{d}{dr}a_\theta(r) - 4/3\,F_2(r)\,g\,(\sin(\beta))^2\,a_z(r)\,\frac{d}{dr}a_z(r)
\end{aligned}
$$

$$
\begin{aligned}
B_1 &= \mu\,(a_z(r))^2\, g + 8/3\, P_1(r)\, g\,(\sin(\beta))^4\,(a_z(r))^4 \\
&- 4/3\, P_1(r)\, g\,(\sin(\beta))^2\,(a_z(r))^2\,(\cos(\beta))^2\,(a_\theta(r))^2 \\
&+ 8/3\, P_2(r)\, g\,(\sin(\beta))^4\,(a_z(r))^4 - 4/3\, P_2(r)\,(\cos(\beta))^2\,(a_\theta(r))^2\, g\,(\sin(\beta))^2\,(a_z(r))^2 \\
&+ \frac{\mu\,(a_r(r))^2}{gr^2} - 2\,\frac{\mu\, a_r(r)\,\frac{d}{dr}a_r(r)}{gr} + 2/3\, F_1(r)\, g\,(\sin(\beta))^2\,(a_z(r))^2 \\
&+ 2/3\, F_2(r)\, g\,(\sin(\beta))^2\,(a_z(r))^2
\end{aligned}
$$

$$
C_1 = -2\,\frac{\mu\, a_r(r)\,\frac{d}{dr}a_r(r)}{g} - 2\,\frac{\mu\,(a_r(r))^2}{gr}
$$

$$
D_1 = -\frac{\mu\,(a_r(r))^2}{g}
$$

$$
E_1 = \mu g
$$

$$
\begin{aligned}
A_2 &= -4/3\,\frac{P_1(r)\,(\sin(\beta))^4\,(a_z(r))^4}{r^2} - 4/3\,\frac{\left(\frac{d}{dr1}P_2(r)\right)(\cos(\beta))^4\,(a_\theta(r))^4}{r} \\
&+ 4/3\,\frac{\left(\frac{d}{dr}P_2(r)\right)(\sin(\beta))^4\,(a_z(r))^4}{r} - 8/3\,\frac{P_2(r)\,(\cos(\beta))^4\,(a_\theta(r))^4}{r^2} \\
&- 4/3\,\frac{P_2(r)\,(\sin(\beta))^4\,(a_z(r))^4}{r^2} - 2\,F_1(r)\,(\sin(\beta))^2\,(a_z(r))^2\,g^2 \\
&- 2\,F_2(r)\,(\sin(\beta))^2\,(a_z(r))^2\,g^2 - 4/3\,\frac{\left(\frac{d}{dr}F_1(r)\right)(\cos(\beta))^2\,(a_\theta(r))^2}{r} \\
&+ 4/3\,\frac{\left(\frac{d}{dr}F_1(r)\right)(\sin(\beta))^2\,(a_z(r))^2}{r} - 2/3\,\frac{F_1(r)\,(\cos(\beta))^2\,(a_\theta(r))^2}{r^2} \\
&- 4/3\,\frac{F_1(r)\,(\sin(\beta))^2\,(a_z(r))^2}{r^2} - 4/3\,\frac{\left(\frac{d}{dr}F_2(r)\right)(\cos(\beta))^2\,(a_\theta(r))^2}{r} \\
&+ 4/3\,\frac{\left(\frac{d}{dr}F_2(r)\right)(\sin(\beta))^2\,(a_z(r))^2}{r} - 2/3\,\frac{F_2(r)\,(\cos(\beta))^2\,(a_\theta(r))^2}{r^2} \\
&- 4/3\,\frac{F_2(r)\,(\sin(\beta))^2\,(a_z(r))^2}{r^2} - 16/3\,\frac{P_2(r)\,(\cos(\beta))^4\,(a_\theta(r))^3\,\frac{d}{dr}a_\theta(r)}{r} \\
&- \mu\,(a_z(r))^2\,g^2 - \frac{\mu\,(a_\theta(r))^2}{r^2} - 4/3\,\frac{\left(\frac{d}{dr}P_1(r)\right)(\cos(\beta))^4\,(a_\theta(r))^4}{r} \\
&+ 4/3\,\frac{\left(\frac{d}{dr}P_1(r)\right)(\sin(\beta))^4\,(a_z(r))^4}{r} - 8/3\,\frac{P_1(r)\,(\cos(\beta))^4\,(a_\theta(r))^4}{r^2} \\
&+ 8/3\,\frac{F_1(r)\,(\sin(\beta))^2\,a_z(r)\,\frac{d}{dr}a_z(r)}{r} + 16/3\,\frac{P_2(r)\,(\sin(\beta))^4\,(a_z(r))^3\,\frac{d}{dr}a_z(r)}{r} \\
&- 8/3\,\frac{F_2(r)\,(\cos(\beta))^2\,a_\theta(r)\,\frac{d}{dr}a_\theta(r)}{r} + 8/3\,\frac{F_2(r)\,(\sin(\beta))^2\,a_z(r)\,\frac{d}{dr}a_z(r)}{r} \\
&+ 4\,\frac{P_1(r)\,(\cos(\beta))^2\,(a_\theta(r))^2\,(\sin(\beta))^2\,(a_z(r))^2}{r^2} \\
&+ 4\,\frac{P_2(r)\,(\cos(\beta))^2\,(a_\theta(r))^2\,(\sin(\beta))^2\,(a_z(r))^2}{r^2} \\
&- 16/3\,\frac{P_1(r)\,(\cos(\beta))^4\,(a_\theta(r))^3\,\frac{d}{dr}a_\theta(r)}{r} \\
&+ 16/3\,\frac{P_1(r)\,(\sin(\beta))^4\,(a_z(r))^3\,\frac{d}{dr}a_z(r)}{r} \\
&- 8/3\,\frac{F_1(r)\,(\cos(\beta))^2\,a_\theta(r)\,\frac{d}{dr}a_\theta(r)}{r}
\end{aligned}
$$

$$
\begin{aligned}
B_2 &= 16/3\,P_2(r)(\sin(\beta))^4(a_z(r))^3\frac{d}{dr}a_z(r) + 4/3\,F_2(r)(\cos(\beta))^2 a_\theta(r)\frac{d}{dr}a_\theta(r)\\
&+ 4\,F_2(r)(\sin(\beta))^2 a_z(r)\frac{d}{dr}a_z(r) + 2\frac{\mu\,(a_r(r))^2}{r} + 4/3\frac{F_1(r)(\sin(\beta))^2(a_z(r))^2}{r}\\
&+ 4/3\,F_1(r)(\cos(\beta))^2 a_\theta(r)\frac{d}{dr}a_\theta(r)\\
&+ 8/3\,P_2(r)(\sin(\beta))^2(a_z(r))^2(\cos(\beta))^2 a_\theta(r)\frac{d}{dr}a_\theta(r)\\
&+ 4/3\left(\frac{d}{dr}P_1(r)\right)(\sin(\beta))^2(a_z(r))^2(\cos(\beta))^2(a_\theta(r))^2\\
&+ 4\frac{P_1(r)(\sin(\beta))^2(a_z(r))^2(\cos(\beta))^2(a_\theta(r))^2}{r}\\
&+ 4\frac{P_2(r)(\sin(\beta))^2(a_z(r))^2(\cos(\beta))^2(a_\theta(r))^2}{r}\\
&+ 8/3\,P_1(r)(\sin(\beta))^2 a_z(r)\left(\frac{d}{dr}a_z(r)\right)(\cos(\beta))^2(a_\theta(r))^2\\
&+ 8/3\,P_1(r)(\sin(\beta))^2(a_z(r))^2(\cos(\beta))^2 a_\theta(r)\frac{d}{dr}a_\theta(r)\\
&+ 4/3\left(\frac{d}{dr}P_2(r)\right)(\sin(\beta))^2(a_z(r))^2(\cos(\beta))^2(a_\theta(r))^2\\
&+ 8/3\,P_2(r)(\sin(\beta))^2 a_z(r)\left(\frac{d}{dr}a_z(r)\right)(\cos(\beta))^2(a_\theta(r))^2\\
&+ 2/3\left(\frac{d}{dr}F_1(r)\right)(\cos(\beta))^2(a_\theta(r))^2 + 2\left(\frac{d}{dr}F_2(r)\right)(\sin(\beta))^2(a_z(r))^2\\
&+ 2/3\left(\frac{d}{dr}F_2(r)\right)(\cos(\beta))^2(a_\theta(r))^2 + 4/3\left(\frac{d}{dr}P_2(r)\right)(\sin(\beta))^4(a_z(r))^4\\
&+ 4/3\frac{F_2(r)(\sin(\beta))^2(a_z(r))^2}{r} - 4/3\frac{P_2(r)(\cos(\beta))^4(a_\theta(r))^4}{r}\\
&+ 4/3\frac{P_2(r)(\sin(\beta))^4(a_z(r))^4}{r} - 10/3\frac{F_1(r)(\cos(\beta))^2(a_\theta(r))^2}{r}\\
&- 10/3\frac{F_2(r)(\cos(\beta))^2(a_\theta(r))^2}{r} + 16/3\,P_1(r)(\sin(\beta))^4(a_z(r))^3\frac{d}{dr}a_z(r)\\
&- 2/3\,F_1(r)\frac{d}{dr}I_4(r) - \frac{\mu\,(a_\theta(r))^2}{r} - 4/3\frac{P_1(r)(\cos(\beta))^4(a_\theta(r))^4}{r}\\
&+ 4/3\frac{P_1(r)(\sin(\beta))^4(a_z(r))^4}{r} + 4\,\mu\,a_r(r)\frac{d}{dr}a_r(r)\\
&+ 4/3\left(\frac{d}{dr}P_1(r)\right)(\sin(\beta))^4(a_z(r))^4 + 2\left(\frac{d}{dr}F_1(r)\right)(\sin(\beta))^2(a_z(r))^2\\
&+ 4\,F_1(r)(\sin(\beta))^2 a_z(r)\frac{d}{dr}a_z(r) - 2/3\left(\frac{d}{dr}F_2(r)\right)I_6(r)\\
&- 2/3\left(\frac{d}{dr}F_1(r)\right)I_4(r) - 2/3\,F_2(r)\frac{d}{dr}I_6(r)
\end{aligned}
$$

$$\begin{aligned} C_2 &= \mu\,(a_r(r))^2 + 4/3\,P_2(r)(\sin(\beta))^2(a_z(r))^2(\cos(\beta))^2(a_\theta(r))^2 \\ &+ 4/3\,P_1(r)(\sin(\beta))^2(a_z(r))^2(\cos(\beta))^2(a_\theta(r))^2 + 4/3\,P_1(r)(\sin(\beta))^4(a_z(r))^4 \\ &+ 4/3\,F_1(r)(\sin(\beta))^2(a_z(r))^2 + 4/3\,F_2(r)(\sin(\beta))^2(a_z(r))^2 \\ &+ 4/3\,P_2(r)(\sin(\beta))^4(a_z(r))^4 \end{aligned}$$

$$D_2 = -\mu$$

$$\begin{aligned} a_1 &= -4/3\,\frac{F_1(r_{in})(\cos(\beta))^2(a_\theta(r_{in}))^2}{r_{in}} + 4/3\,\frac{P_2(r_{in})(\sin(\beta))^4(a_z(r_{in}))^4}{r_{in}} \\ &- 4/3\,\frac{F_2(r_{in})(\cos(\beta))^2(a_\theta(r_{in}))^2}{r_{in}} + 4/3\,\frac{F_1(r_{in})(\sin(\beta))^2(a_z(rin))^2}{r_{in}} \\ &- 4/3\,\frac{P_1(rin)(\cos(\beta))^4(a_\theta(r_{in}))^4}{r_{in}} + 4/3\,\frac{P_1(r_{in})(\sin(\beta))^4(a_z(r_{in}))^4}{r_{in}} \\ &+ 4/3\,\frac{F_2(r_{in})(\sin(\beta))^2(a_z(r_{in}))^2}{r_{in}} - 4/3\,\frac{P_2(r_{in})(\cos(\beta))^4(a_\theta(r_{in}))^4}{r_{in}} \end{aligned}$$

$$\begin{aligned} a_2 &= 4/3\,P_1(r_{in})(\sin(\beta))^2(a_z(r_{in}))^2(\cos(\beta))^2(a_\theta(r_{in}))^2 + 4/3\,P_2(rin)(\sin(\beta))^4(a_z(r_{in}))^4 \\ &+ 4/3\,P_2(r_{in})(\sin(\beta))^2(a_z(r_{in}))^2(\cos(\beta))^2(a_\theta(r_{in}))^2 + 2\,F_1(r_{in})(\sin(\beta))^2(a_z(rin))^2 \\ &+ 2\,\mu\,q(r_{in}) + 2/3\,F_1(r_{in})(\cos(\beta))^2(a_\theta(r_{in}))^2 + 2\,F_2(r_{in})(\sin(\beta))^2(a_z(r_{in}))^2 \\ &+ 4/3\,P_1(r_{in})(\sin(\beta))^4(a_z(r_{in}))^4 + 2/3\,F_2(r_{in})(\cos(\beta))^2(a_\theta(r_{in}))^2 \\ &+ 2/3\,F_1(r_{in})\,I_4(r_{in}) + 2/3\,F_2(r_{in})\,I_6(r_{in}) \end{aligned}$$

$$a_4 = -\mu$$

$$\begin{aligned} b_1 &= -2\,g\mu\,q(r_{in}) + \frac{\mu\,(a_r(r_{in}))^2}{g{r_{in}}^2} - 2/3\,F_1(r_{in})\,g(\cos(\beta))^2(a_\theta(r_{in}))^2 \\ &- 2/3\,F_1(r_{in})\,g(\sin(\beta))^2(a_z(r_{in}))^2 - 2/3\,F_2(r_{in})\,g(\cos(\beta))^2(a_\theta(r_{in}))^2 \\ &- 2/3\,F_2(r_{in})\,g(\sin(\beta))^2(a_z(r_{in}))^2 + g\mu\,(a_r(r_{in}))^2 \\ &- 2/3\,gF_1(r_{in})\,I_4(r_{in}) - 2/3\,gF_2(r_{in})\,I_6(r_{in}) \end{aligned}$$

$$b_2 = -\frac{\mu\,(a_r(r_{in}))^2}{g r_{in}}$$

$$b_3 = -\frac{\mu\,(a_r(r_{in}))^2}{g}$$

$$\begin{aligned} c_5 &= -4/3\,\frac{P_2(r_{out})(\cos(\beta))^4(a_\theta(r_{out}))^4}{r_{out}} - 4/3\,\frac{F_1(r_{out})(\cos(\beta))^2(a_\theta(r_{out}))^2}{r_{out}} \\ &+ 4/3\,\frac{F_1(r_{out})(\sin(\beta))^2(a_z(r_{out}))^2}{r_{out}} + 4/3\,\frac{P_2(r_{out})(\sin(\beta))^4(a_z(r_{out}))^4}{r_{out}} \\ &- 4/3\,\frac{F_2(r_{out})(\cos(\beta))^2(a_\theta(r_{out}))^2}{r_{out}} + 4/3\,\frac{F_2(r_{out})(\sin(\beta))^2(a_z(r_{out}))^2}{r_{out}} \\ &- 4/3\,\frac{P_1(r_{out})(\cos(\beta))^4(a_\theta(r_{out}))^4}{r_{out}} + 4/3\,\frac{P_1(r_{out})(\sin(\beta))^4(a_z(r_{out}))^4}{r_{out}} \end{aligned}$$

$$\begin{aligned} c_6 &= 4/3\,P_1(r_{out})(\sin(\beta))^2(a_z(r_{out}))^2(\cos(\beta))^2(a_\theta(r_{out}))^2 + 4/3\,P_2(r_{out})(\sin(\beta))^4(a_z(r_{out}))^4 \\ &+ 4/3\,P_2(r_{out})(\sin(\beta))^2(a_z(r_{out}))^2(\cos(\beta))^2(a_\theta(r_{out}))^2 + 2\,F_1(r_{out})(\sin(\beta))^2(a_z(r_{out}))^2 \\ &+ \mu\,q(r_{out}) + 2/3\,F_1(r_{out})(\cos(\beta))^2(a_\theta(r_{out}))^2 + \mu\,(a_r(r_{out}))^2 \\ &+ 2\,F_2(r_{out})(\sin(\beta))^2(a_z(r_{out}))^2 + 4/3\,P_1(r_{out})(\sin(\beta))^4(a_z(r_{out}))^4 \\ &+ 2/3\,F_2(r_{out})(\cos(\beta))^2(a_\theta(r_{out}))^2 - P_{ext} \end{aligned}$$

$$c_8 = -\mu$$

$$\begin{aligned} d_5 &= -\mu\,q(r_{out})\,g + \frac{\mu\,(a_r(r_{out}))^2}{g {r_{out}}^2} - 2/3\,F_1(r_{out})\,g(\cos(\beta))^2(a_\theta(r_{out}))^2 \\ &- 2/3\,F_1(r_{out})\,g(\sin(\beta))^2(a_z(r_{out}))^2 - 2/3\,F_2(r_{out})\,g(\cos(\beta))^2(a_\theta(r_{out}))^2 \\ &- 2/3\,F_2(r_{out})\,g(\sin(\beta))^2(a_z(r_{out}))^2 + P_{ext}\,g \end{aligned}$$

$$d_6 = -\frac{\mu\,(a_r(r_{out}))^2}{g r_{out}}$$

$$d_7 = -\frac{\mu\,(a_r(r_{out}))^2}{g}$$

$$\begin{aligned} s_{ur1}(r) &= -4/3\,\frac{P_2(r)(\cos(\beta))^4(a_\theta(r))^4}{r} + 4/3\,\frac{P_1(r)(\sin(\beta))^4(a_z(r))^4}{r} \\ &- 4/3\,\frac{F_1(r)(\cos(\beta))^2(a_\theta(r))^2}{r} + 4/3\,\frac{F_1(r)(\sin(\beta))^2(a_z(r))^2}{r} \\ &+ 4/3\,\frac{P_2(r)(\sin(\beta))^4(a_z(r))^4}{r} - 4/3\,\frac{F_2(r)(\cos(\beta))^2(a_\theta(r))^2}{r} \\ &+ 4/3\,\frac{F_2(r)(\sin(\beta))^2(a_z(r))^2}{r} - 4/3\,\frac{P_1(r)(\cos(\beta))^4(a_\theta(r))^4}{r} \end{aligned}$$

$$\begin{aligned} s_{ur2}(r) &= 4/3\,P_1(r)(\sin(\beta))^2(a_z(r))^2(\cos(\beta))^2(a_\theta(r))^2 \\ &+ 4/3\,P_2(r)(\sin(\beta))^4(a_z(r))^4 \\ &+ 4/3\,P_2(r)(\sin(\beta))^2(a_z(r))^2(\cos(\beta))^2(a_\theta(r))^2 \\ &+ 2\,F_1(r)(\sin(\beta))^2(a_z(r))^2 + \mu\,q(r) + 2/3\,F_1(r)(\cos(\beta))^2(a_\theta(r))^2 \\ &+ \mu\,(a_r(r))^2 + 2\,F_2(r)(\sin(\beta))^2(a_z(r))^2 \\ &+ 4/3\,P_1(r)(\sin(\beta))^4(a_z(r))^4 + 2/3\,F_2(r)(\cos(\beta))^2(a_\theta(r))^2 \end{aligned}$$

$$\begin{aligned} s_{uz1}(r) &= -\mu\,q(r)\,g + \frac{\mu\,(a_r(r))^2}{gr^2} - 2/3\,F_1(r)\,g(\cos(\beta))^2(a_\theta(r))^2 \\ &- 2/3\,F_1(r)\,g(\sin(\beta))^2(a_z(r))^2 - 2/3\,F_2(r)\,g(\cos(\beta))^2(a_\theta(r))^2 \\ &- 2/3\,F_2(r)\,g(\sin(\beta))^2(a_z(r))^2 \end{aligned}$$

$$s_{uz2}(r) = -\frac{\mu\,(a_r(r))^2}{gr}$$

$$s_{uz3}(r) = -\frac{\mu\,(a_r(r))^2}{g}$$

$$
\begin{aligned}
e_1 &= -4/3\,\frac{P_2(r_c)(\cos(\beta))^4(a_\theta(r_c))^4}{r_c} + 4/3\,\frac{P_1(r_c)(\sin(\beta))^4(a_z(r_c))^4}{r_c} \\
&- 4/3\,\frac{F_1(r_c)(\cos(\beta))^2(a_\theta(r_c))^2}{r_c} + 4/3\,\frac{F_1(r_c)(\sin(\beta))^2(a_z(r_c))^2}{r_c} \\
&+ 4/3\,\frac{P_2(r_c)(\sin(\beta))^4(a_z(r_c))^4}{r_c} - 4/3\,\frac{F_2(r_c)(\cos(\beta))^2(a_\theta(r_c))^2}{r_c} \\
&+ 4/3\,\frac{F_2(r_c)(\sin(\beta))^2(a_z(r_c))^2}{r_c} - 4/3\,\frac{P_1(r_c)(\cos(\beta))^4(a_\theta(r_c))^4}{r_c}
\end{aligned}
$$

$$
\begin{aligned}
e_2 &= 4/3\,P_1(r_c)(\sin(\beta))^2(a_z(r_c))^2(\cos(\beta))^2(a_\theta(r_c))^2 + 4/3\,P_2(r_c)(\sin(\beta))^4(a_z(r_c))^4 \\
&+ 4/3\,P_2(r_c)(\sin(\beta))^2(a_z(r_c))^2(\cos(\beta))^2(a_\theta(r_c))^2 + 2\,F_1(r_c)(\sin(\beta))^2(a_z(r_c))^2 + \mu Y_{b9} \\
&+ 2/3\,F_1(r_c)(\cos(\beta))^2(a_\theta(r_c))^2 + \mu\,(a_r(r_c))^2 + 2\,F_2(r_c)(\sin(\beta))^2(a_z(r_c))^2 \\
&+ 4/3\,P_1(r_c)(\sin(\beta))^4(a_z(r_c))^4 + 2/3\,F_2(r_c)(\cos(\beta))^2(a_\theta(r_c))^2
\end{aligned}
$$

$$e_4 = \mu$$

$$
\begin{aligned}
e_5 &= -4/3\,\frac{P_2(r_c)(\cos(\beta))^4(a_\theta(r_c))^4}{r_c} + 4/3\,\frac{P_1(r_c)(\sin(\beta))^4(a_z(r_c))^4}{r_c} \\
&- 4/3\,\frac{F_1(r_c)(\cos(\beta))^2(a_\theta(r_c))^2}{r_c} + 4/3\,\frac{F_1(r_c)(\sin(\beta))^2(a_z(r_c))^2}{r_c} \\
&+ 4/3\,\frac{P_2(r_c)(\sin(\beta))^4(a_z(r_c))^4}{r_c} - 4/3\,\frac{F_2(r_c)(\cos(\beta))^2(a_\theta(r_c))^2}{r_c} \\
&+ 4/3\,\frac{F_2(r_c)(\sin(\beta))^2(a_z(r_c))^2}{r_c} - 4/3\,\frac{P_1(r_c)(\cos(\beta))^4(a_\theta(r_c))^4}{r_c}
\end{aligned}
$$

$$
\begin{aligned}
e_6 &= 4/3\,P_1(r_c)(\sin(\beta))^2(a_z(r_c))^2(\cos(\beta))^2(a_\theta(r_c))^2 + 4/3\,P_2(r_c)(\sin(\beta))^4(a_z(r_c))^4 \\
&+ 4/3\,P_2(r_c)(\sin(\beta))^2(a_z(r_c))^2(\cos(\beta))^2(a_\theta(r_c))^2 + 2\,F_1(r_c)(\sin(\beta))^2(a_z(r_c))^2 + \mu Y_{b10} \\
&+ 2/3\,F_1(r_c)(\cos(\beta))^2(a_\theta(r_c))^2 + \mu\,(a_r(r_c))^2 + 2\,F_2(r_c)(\sin(\beta))^2(a_z(r_c))^2 \\
&+ 4/3\,P_1(r_c)(\sin(\beta))^4(a_z(r_c))^4 + 2/3\,F_2(r_c)(\cos(\beta))^2(a_\theta(r_c))^2
\end{aligned}
$$

$$e_8 = \mu$$

$$\begin{aligned} f_1 &= -\mu\, Y_{b9} g + \frac{\mu\, (a_r(r_c))^2}{g {r_c}^2} - 2/3\, F_1(r_c)\, g\, (\cos(\beta))^2\, (a_\theta(r_c))^2 \\ &- 2/3\, F_1(r_c)\, g\, (\sin(\beta))^2\, (a_z(r_c))^2 - 2/3\, F_2(r_c)\, g\, (\cos(\beta))^2\, (a_\theta(r_c))^2 \\ &- 2/3\, F_2(r_c)\, g\, (\sin(\beta))^2\, (a_z(r_c))^2 \end{aligned}$$

$$f_2 = -\frac{\mu\, (a_r(r_c))^2}{g r_c}$$

$$f_3 = -\frac{\mu\, (a_r(r_c))^2}{g}$$

$$\begin{aligned} f_5 &= -\mu\, Y_{b10} g + \frac{\mu\, (a_r(r_c))^2}{g {r_c}^2} - 2/3\, F_1(r_c)\, g\, (\cos(\beta))^2\, (a_\theta(r_c))^2 \\ &- 2/3\, F_1(r_c)\, g\, (\sin(\beta))^2\, (a_z(r_c))^2 - 2/3\, F_2(r_c)\, g\, (\cos(\beta))^2\, (a_\theta(r_c))^2 \\ &- 2/3\, F_2(r_c)\, g\, (\sin(\beta))^2\, (a_z(r_c))^2 \end{aligned}$$

$$f_6 = -\frac{\mu\, (a_r(r_c))^2}{g r_c}$$

$$f_7 = -\frac{\mu\, (a_r(r_c))^2}{g}$$

Appendix C

Coefficients for ODEs in the incremental inner pressure of Chapter 5

Below equations are coefficients of ODEs for incremental inner pressure in Chapter 5.

$$
\begin{aligned}
f_5(r) &= 2\,a_r\left(r\right)\frac{d}{dr}a_r\left(r\right) - 2/3\,\frac{\left(\frac{d}{dr}F_1\left(r\right)\right)I_4\left(r\right)}{\mu} - 2/3\,\frac{F_1\left(r\right)\frac{d}{dr}I_4\left(r\right)}{\mu} \\
&- 2/3\,\frac{\left(\frac{d}{dr}F_2\left(r\right)\right)I_6\left(r\right)}{\mu} - 2/3\,\frac{F_2\left(r\right)\frac{d}{dr}I_6\left(r\right)}{\mu} + \frac{\left(a_r\left(r\right)\right)^2}{r} \\
&- \frac{\left(a_\theta\left(r\right)\right)^2}{r} - 2\,\frac{F_1\left(r\right)\left(\cos\left(\beta\right)\right)^2\left(a_\theta\left(r\right)\right)^2}{\mu\,r} \\
&- 2\,\frac{F_2\left(r\right)\left(\cos\left(\beta\right)\right)^2\left(a_\theta\left(r\right)\right)^2}{\mu\,r}
\end{aligned}
$$

$$
\begin{aligned}
f_2(r) &= -4/3\,\frac{P_1(r)\,(\cos(\beta))^4\,(a_\theta(r))^4}{\mu\,r^2} - 4/3\,\frac{P_2(r)\,(\cos(\beta))^4\,(a_\theta(r))^4}{\mu\,r^2} \\
&+ 8/3\,\frac{P_1(r)\,(\cos(\beta))^2\,(a_\theta(r))^2\,(\sin(\beta))^2\,(a_z(r))^2}{\mu\,r^2} \\
&+ 8/3\,\frac{P_2(r)\,(\cos(\beta))^2\,(a_\theta(r))^2\,(\sin(\beta))^2\,(a_z(r))^2}{\mu\,r^2} \\
&- 4\,\frac{F_2(r)\,(\cos(\beta))^2\,a_\theta(r)\,\frac{d}{dr}a_\theta(r)}{\mu\,r} - 4/3\,\frac{F_2(r)\,(\sin(\beta))^2\,a_z(r)\,\frac{d}{dr}a_z(r)}{\mu\,r} \\
&- 4/3\,\frac{\left(\frac{d}{dr}P_1(r)\right)(\cos(\beta))^2\,(a_\theta(r))^2\,(\sin(\beta))^2\,(a_z(r))^2}{\mu\,r} \\
&- 16/3\,\frac{P_1(r)\,(\cos(\beta))^4\,(a_\theta(r))^3\,\frac{d}{dr}a_\theta(r)}{\mu\,r} \\
&- 8/3\,\frac{P_1(r)\,(\cos(\beta))^2\,a_\theta(r)\left(\frac{d}{dr}a_\theta(r)\right)(\sin(\beta))^2\,(a_z(r))^2}{\mu\,r} \\
&- 8/3\,\frac{P_1(r)\,(\cos(\beta))^2\,(a_\theta(r))^2\,(\sin(\beta))^2\,a_z(r)\,\frac{d}{dr}a_z(r)}{\mu\,r} \\
&- 4/3\,\frac{\left(\frac{d}{dr}P_2(r)\right)(\cos(\beta))^2\,(a_\theta(r))^2\,(\sin(\beta))^2\,(a_z(r))^2}{\mu\,r} \\
&- 16/3\,\frac{P_2(r)\,(\cos(\beta))^4\,(a_\theta(r))^3\,\frac{d}{dr}a_\theta(r)}{\mu\,r} \\
&- 4/3\,\frac{\left(\frac{d}{dr}P_1(r)\right)(\cos(\beta))^4\,(a_\theta(r))^4}{\mu\,r} - 4/3\,\frac{\left(\frac{d}{dr}P_2(r)\right)(\cos(\beta))^4\,(a_\theta(r))^4}{\mu\,r} \\
&- 2\,\frac{\left(\frac{d}{dr}F_1(r)\right)(\cos(\beta))^2\,(a_\theta(r))^2}{\mu\,r} - 2/3\,\frac{\left(\frac{d}{dr}F_1(r)\right)(\sin(\beta))^2\,(a_z(r))^2}{\mu\,r} \\
&- 2\,\frac{\left(\frac{d}{dr}F_2(r)\right)(\cos(\beta))^2\,(a_\theta(r))^2}{\mu\,r} - 2/3\,\frac{\left(\frac{d}{dr}F_2(r)\right)(\sin(\beta))^2\,(a_z(r))^2}{\mu\,r} \\
&+ 8/3\,\frac{F_1(r)\,(\cos(\beta))^2\,(a_\theta(r))^2}{\mu\,r^2} + 8/3\,\frac{F_2(r)\,(\cos(\beta))^2\,(a_\theta(r))^2}{\mu\,r^2} + 2/3\,\frac{\left(\frac{d}{dr}F_1(r)\right)I_4(r)}{\mu\,r} \\
&+ 2/3\,\frac{F_1(r)\,\frac{d}{dr}I_4(r)}{\mu\,r} + 2/3\,\frac{\left(\frac{d}{dr}F_2(r)\right)I_6(r)}{\mu\,r} + 2/3\,\frac{F_2(r)\,\frac{d}{dr}I_6(r)}{\mu\,r} \\
&- 8/3\,\frac{P_2(r)\,(\cos(\beta))^2\,a_\theta(r)\left(\frac{d}{dr}a_\theta(r)\right)(\sin(\beta))^2\,(a_z(r))^2}{\mu\,r} \\
&- 8/3\,\frac{P_2(r)\,(\cos(\beta))^2\,(a_\theta(r))^2\,(\sin(\beta))^2\,a_z(r)\,\frac{d}{dr}a_z(r)}{\mu\,r} - 4\,\frac{F_1(r)\,(\cos(\beta))^2\,a_\theta(r)\,\frac{d}{dr}a_\theta(r)}{\mu\,r} \\
&- 4/3\,\frac{F_1(r)\,(\sin(\beta))^2\,a_z(r)\,\frac{d}{dr}a_z(r)}{\mu\,r} - 4\,\frac{a_r(r)\,\frac{d}{dr}a_r(r)}{r}
\end{aligned}
$$

$$
\begin{aligned}
p_1(r_{in}) &= -2\,\frac{\mu\,Y_{a5}}{r_{in}} - 2/3\,\frac{F_1\left(r_{in}\right)\left(\sin\left(\beta\right)\right)^2\left(a_z\left(r_{in}\right)\right)^2}{r_{in}} \\
&- 2/3\,\frac{F_2\left(r_{in}\right)\left(\sin\left(\beta\right)\right)^2\left(a_z\left(r_{in}\right)\right)^2}{r_{in}} - 2\,\frac{F_2\left(r_{in}\right)\left(\cos\left(\beta\right)\right)^2\left(a_\theta\left(r_{in}\right)\right)^2}{r_{in}} \\
&- 4/3\,\frac{P_1\left(r_{in}\right)\left(\cos\left(\beta\right)\right)^4\left(a_\theta\left(r_{in}\right)\right)^4}{r_{in}} - 2\,\frac{F_1\left(r_{in}\right)\left(\cos\left(\beta\right)\right)^2\left(a_\theta\left(r_{in}\right)\right)^2}{r_{in}} \\
&- 4/3\,\frac{P_2\left(r_{in}\right)\left(\cos\left(\beta\right)\right)^4\left(a_\theta\left(r_{in}\right)\right)^4}{r_{in}} \\
&- 4/3\,\frac{P_2\left(r_{in}\right)\left(\cos\left(\beta\right)\right)^2\left(a_\theta\left(r_{in}\right)\right)^2\left(\sin\left(\beta\right)\right)^2\left(a_z\left(r_{in}\right)\right)^2}{r_{in}} \\
&- 2/3\,\frac{F_1\left(r_{in}\right)I_4\left(r_{in}\right)}{r_{in}} - 2/3\,\frac{F_2\left(r_{in}\right)I_6\left(r_{in}\right)}{r_{in}} \\
&- 4/3\,\frac{P_1\left(r_{in}\right)\left(\cos\left(\beta\right)\right)^2\left(a_\theta\left(r_{in}\right)\right)^2\left(\sin\left(\beta\right)\right)^2\left(a_z\left(r_{in}\right)\right)^2}{r_{in}}
\end{aligned}
$$

$$
\begin{aligned}
p_2(r_{in}) &= -\frac{\mu\,Y_{a6}}{r_{out}} - \frac{\mu\,\left(a_r\left(r_{out}\right)\right)^2}{r_{out}} - 4/3\,\frac{P_1\left(r_{out}\right)\left(\cos\left(\beta\right)\right)^4\left(a_\theta\left(r_{out}\right)\right)^4}{r_{out}} \\
&- 4/3\,\frac{P_1\left(r_{out}\right)\left(\cos\left(\beta\right)\right)^2\left(a_\theta\left(r_{out}\right)\right)^2\left(\sin\left(\beta\right)\right)^2\left(a_z\left(r_{out}\right)\right)^2}{r_{out}} \\
&- 4/3\,\frac{P_2\left(r_{out}\right)\left(\cos\left(\beta\right)\right)^4\left(a_\theta\left(r_{out}\right)\right)^4}{r_{out}} \\
&- 4/3\,\frac{P_2\left(r_{out}\right)\left(\cos\left(\beta\right)\right)^2\left(a_\theta\left(r_{out}\right)\right)^2\left(\sin\left(\beta\right)\right)^2\left(a_z\left(r_{out}\right)\right)^2}{r_{out}} \\
&- 2\,\frac{F_1\left(r_{out}\right)\left(\cos\left(\beta\right)\right)^2\left(a_\theta\left(r_{out}\right)\right)^2}{r_{out}} - 2/3\,\frac{F_1\left(r_{out}\right)\left(\sin\left(\beta\right)\right)^2\left(a_z\left(r_{out}\right)\right)^2}{r_{out}} \\
&- 2\,\frac{F_2\left(r_{out}\right)\left(\cos\left(\beta\right)\right)^2\left(a_\theta\left(r_{out}\right)\right)^2}{r_{out}} - 2/3\,\frac{F_2\left(r_{out}\right)\left(\sin\left(\beta\right)\right)^2\left(a_z\left(r_{out}\right)\right)^2}{r_{out}} + \frac{P_{ext}}{r_{out}}
\end{aligned}
$$

$$
\begin{aligned}
p_3(r_c) &= -\frac{\mu\,Y_{b5}}{r_c} - \frac{\mu\,\left(a_r\left(r_c\right)\right)^2}{r_c} - 4/3\,\frac{P_1\left(r_c\right)\left(\cos\left(\beta\right)\right)^4\left(a_\theta\left(r_c\right)\right)^4}{r_c} \\
&- 4/3\,\frac{P_1\left(r_c\right)\left(\cos\left(\beta\right)\right)^2\left(a_\theta\left(r_c\right)\right)^2\left(\sin\left(\beta\right)\right)^2\left(a_z\left(r_c\right)\right)^2}{r_c} - 4/3\,\frac{P_2\left(r_c\right)\left(\cos\left(\beta\right)\right)^4\left(a_\theta\left(r_c\right)\right)^4}{r_c} \\
&- 4/3\,\frac{P_2\left(r_c\right)\left(\cos\left(\beta\right)\right)^2\left(a_\theta\left(r_c\right)\right)^2\left(\sin\left(\beta\right)\right)^2\left(a_z\left(r_c\right)\right)^2}{r_c} - 2\,\frac{F_1\left(r_c\right)\left(\cos\left(\beta\right)\right)^2\left(a_\theta\left(r_c\right)\right)^2}{r_c} \\
&- 2/3\,\frac{F_1\left(r_c\right)\left(\sin\left(\beta\right)\right)^2\left(a_z\left(r_c\right)\right)^2}{r_c} - 2\,\frac{F_2\left(r_c\right)\left(\cos\left(\beta\right)\right)^2\left(a_\theta\left(r_c\right)\right)^2}{r_c} \\
&- 2/3\,\frac{F_2\left(r_c\right)\left(\sin\left(\beta\right)\right)^2\left(a_z\left(r_c\right)\right)^2}{r_c}
\end{aligned}
$$

$$
\begin{aligned}
p_4(r_c) &= -\frac{\mu\, Y_{b6}}{r_c} - \frac{\mu\ (a_r\,(r_c))^2}{r_c} - 4/3\,\frac{P_1\,(r_c)\,(\cos(\beta))^4\,(a_\theta\,(r_c))^4}{r_c} \\
&- 4/3\,\frac{P_1\,(r_c)\,(\cos(\beta))^2\,(a_\theta\,(r_c))^2\,(\sin(\beta))^2\,(a_z\,(r_c))^2}{r_c} \\
&- 4/3\,\frac{P_2\,(r_c)\,(\cos(\beta))^4\,(a_\theta\,(r_c))^4}{r_c} \\
&- 4/3\,\frac{P_2\,(r_c)\,(\cos(\beta))^2\,(a_\theta\,(r_c))^2\,(\sin(\beta))^2\,(a_z\,(r_c))^2}{r_c} - 2\,\frac{F_1\,(r_c)\,(\cos(\beta))^2\,(a_\theta\,(r_c))^2}{r_c} \\
&- 2/3\,\frac{F_1\,(r_c)\,(\sin(\beta))^2\,(a_z\,(r_c))^2}{r_c} - 2\,\frac{F_2\,(r_c)\,(\cos(\beta))^2\,(a_\theta\,(r_c))^2}{r_c} \\
&- 2/3\,\frac{F_2\,(r_c)\,(\sin(\beta))^2\,(a_z\,(r_c))^2}{r_c}
\end{aligned}
$$

$$
\begin{aligned}
S_1(r) &= -\frac{\mu\, q\,(r)}{r} - \frac{\mu\ (ar\,(r))^2}{r} - 4/3\,\frac{P1\,(r)\,(\cos(\beta))^4\,(at\,(r))^4}{r} \\
&- 4/3\,\frac{P1\,(r)\,(\cos(\beta))^2\,(at\,(r))^2\,(\sin(\beta))^2\,(az\,(r))^2}{r} \\
&- 4/3\,\frac{P2\,(r)\,(\cos(\beta))^4\,(at\,(r))^4}{r} \\
&- 4/3\,\frac{P2\,(r)\,(\cos(\beta))^2\,(at\,(r))^2\,(\sin(\beta))^2\,(az\,(r))^2}{r} \\
&- 2\,\frac{F1\,(r)\,(\cos(\beta))^2\,(at\,(r))^2}{r} - 2/3\,\frac{F1\,(r)\,(\sin(\beta))^2\,(az\,(r))^2}{r} \\
&- 2\,\frac{F2\,(r)\,(\cos(\beta))^2\,(at\,(r))^2}{r} - 2/3\,\frac{F2\,(r)\,(\sin(\beta))^2\,(az\,(r))^2}{r}
\end{aligned}
$$

$$
\begin{aligned}
A(r) &= 2\,a_r\,(r)\,\frac{d}{dr}a_r\,(r) - 2/3\,\frac{\left(\frac{d}{dr}F_1\,(r)\right)I_4\,(r)}{\mu} - 2/3\,\frac{F_1\,(r)\,\frac{d}{dr}I_4\,(r)}{\mu} \\
&- 2/3\,\frac{\left(\frac{d}{dr}F_2\,(r)\right)I_6\,(r)}{\mu} - 2/3\,\frac{F_2\,(r)\,\frac{d}{dr}I_6\,(r1)}{\mu} + \frac{(a_r\,(r))^2}{r} \\
&- \frac{(a_\theta\,(r))^2}{r} - 2\,\frac{F_1\,(r)\,(\cos(\beta))^2\,(a_\theta\,(r))^2}{\mu\, r} - 2\,\frac{F_2\,(r)\,(\cos(\beta))^2\,(a_\theta\,(r))^2}{\mu\, r}
\end{aligned}
$$

$$
\begin{aligned}
B(r) &= -8/3\,\frac{P_1(r)\,(\cos(\beta))^2\,a_\theta(r)\left(\frac{d}{dr}a_\theta(r)\right)(\sin(\beta))^2\,(a_z(r))^2}{r} \\
&+ 8/3\,\frac{P_2(r)\,(\cos(\beta))^2\,(a_\theta(r))^2\,(\sin(\beta))^2\,(a_z(r))^2}{r^2} - 16/3\,\frac{P_1(r)\,(\cos(\beta))^4\,(a_\theta(r))^3\,\frac{d}{dr}a_\theta(r)}{r} \\
&- 4/3\,\frac{\left(\frac{d}{dr}P_1(r)\right)(\cos(\beta))^2\,(a_\theta(r))^2\,(\sin(\beta))^2\,(a_z(r))^2}{r} \\
&- 16/3\,\frac{P_2(r)\,(\cos(\beta))^4\,(a_\theta(r))^3\,\frac{d}{dr}a_\theta(r)}{r} \\
&- 8/3\,\frac{P_2(r)\,(\cos(\beta))^2\,a_\theta(r)\left(\frac{d}{dr}a_\theta(r)\right)(\sin(\beta))^2\,(a_z(r))^2}{r} \\
&- 8/3\,\frac{P_2(r)\,(\cos(\beta))^2\,(a_\theta(r))^2\,(\sin(\beta))^2\,a_z(r)\,\frac{d}{dr}a_z(r)}{r} \\
&+ 8/3\,\frac{P_1(r)\,(\cos(\beta))^2\,(a_\theta(r))^2\,(\sin(\beta))^2\,(a_z(r))^2}{r^2} \\
&- 8/3\,\frac{P_1(r)\,(\cos(\beta))^2\,(a_\theta(r))^2\,(\sin(\beta))^2\,a_z(r)\,\frac{d}{dr}a_z(r)}{r} \\
&- 4/3\,\frac{\left(\frac{d}{dr}P_2(r)\right)(\cos(\beta))^2\,(a_\theta(r))^2\,(\sin(\beta))^2\,(a_z(r))^2}{r} \\
&- 4\,\frac{F_2(r)\,(\cos(\beta))^2\,a_\theta(r)\,\frac{d}{dr}a_\theta(r)}{r} - 4/3\,\frac{F_2(r)\,(\sin(\beta))^2\,a_z(r)\,\frac{d}{dr}a_z(r)}{r} \\
&- 4\,\frac{F_1(r)\,(\cos(\beta))^2\,a_\theta(r)\,\frac{d}{dr}a_\theta(r)}{r} - 4/3\,\frac{F_1(r)\,(\sin(\beta))^2\,a_z(r)\,\frac{d}{dr}a_z(r)}{r} \\
&- 4/3\,\frac{\left(\frac{d}{dr}P_1(r)\right)(\cos(\beta))^4\,(a_\theta(r))^4}{r} + 8/3\,\frac{F_1(r)\,(\cos(\beta))^2\,(a_\theta(r))^2}{r^2} - 4\,\frac{\mu\,a_r(r)\,\frac{d}{dr}a_r(r)}{r} \\
&- 4/3\,\frac{\left(\frac{d}{dr}P_2(r)\right)(\cos(\beta))^4\,(a_\theta(r))^4}{r} - 4/3\,\frac{P_2(r)\,(\cos(\beta))^4\,(a_\theta(r))^4}{r^2} \\
&- 2\,\frac{\left(\frac{d}{dr}F_1(r)\right)(\cos(\beta))^2\,(a_\theta(r))^2}{r} + 8/3\,\frac{F_2(r)\,(\cos(\beta))^2\,(a_\theta(r))^2}{r^2} \\
&- 4/3\,\frac{P_1(r)\,(\cos(\beta))^4\,(a_\theta(r))^4}{r^2} - 2/3\,\frac{\left(\frac{d}{dr}F_1(r)\right)(\sin(\beta))^2\,(a_z(r))^2}{r} \\
&- 2\,\frac{\left(\frac{d}{dr}F_2(r)\right)(\cos(\beta))^2\,(a_\theta(r))^2}{r} - 2/3\,\frac{\left(\frac{d}{dr}F_2(r)\right)(\sin(\beta))^2\,(a_z(r))^2}{r} + 2/3\,\frac{\left(\frac{d}{dr}F_1(r)\right)I_4(r)}{r} \\
&+ 2/3\,\frac{\left(\frac{d}{dr}F_2(r)\right)I_6(r)}{r} + 2/3\,\frac{F_2(r)\,\frac{d}{dr}I_6(r)}{r} + 2/3\,\frac{F_1(r)\,\frac{d}{dr}I_4(r)}{r}
\end{aligned}
$$

$$
\begin{aligned}
a(r) &= -2\,\frac{\mu\ Y_{a1}}{r_{in}} - 4/3\,\frac{P_1\left(r_{in}\right)\left(\cos\left(\beta\right)\right)^4\left(a_\theta\left(r_{in}\right)\right)^4}{r_{in}} \\
&- 4/3\,\frac{P_1\left(r_{in}\right)\left(\cos\left(\beta\right)\right)^2\left(a_\theta\left(r_{in}\right)\right)^2\left(\sin\left(\beta\right)\right)^2\left(a_z\left(r_{in}\right)\right)^2}{r_{in}} \\
&- 4/3\,\frac{P_2\left(r_{in}\right)\left(\cos\left(\beta\right)\right)^4\left(a_\theta\left(r_{in}\right)\right)^4}{r_{in}} \\
&- 4/3\,\frac{P_2\left(r_{in}\right)\left(\cos\left(\beta\right)\right)^2\left(a_\theta\left(r_{in}\right)\right)^2\left(\sin\left(\beta\right)\right)^2\left(a_z\left(r_{in}\right)\right)^2}{r_{in}} \\
&- 2\,\frac{F_1\left(r_{in}\right)\left(\cos\left(\beta\right)\right)^2\left(a_\theta\left(r_{in}\right)\right)^2}{r_{in}} - 2/3\,\frac{F_1\left(r_{in}\right)\left(\sin\left(\beta\right)\right)^2\left(a_z\left(r_{in}\right)\right)^2}{r_{in}} \\
&- 2\,\frac{F_2\left(r_{in}\right)\left(\cos\left(\beta\right)\right)^2\left(a_\theta\left(r_{in}\right)\right)^2}{r_{in}} - 2/3\,\frac{F_2\left(r_{in}\right)\left(\sin\left(\beta\right)\right)^2\left(a_z\left(r_{in}\right)\right)^2}{r_{in}} \\
&- 2/3\,\frac{F_1\left(r_{in}\right)I_4\left(r_{in}\right)}{r_{in}} - 2/3\,\frac{F_2\left(r_{in}\right)I_6\left(r_{in}\right)}{r_{in}}
\end{aligned}
$$

$$
\begin{aligned}
b(r) &= -\frac{\mu\ Y_{a1}}{r_{out}} - \frac{\mu\ \left(a_r\left(r_{out}\right)\right)^2}{r_{out}} - 4/3\,\frac{P_1\left(r_{out}\right)\left(\cos\left(\beta\right)\right)^4\left(a_\theta\left(r_{out}\right)\right)^4}{r_{out}} \\
&- 4/3\,\frac{P_1\left(r_{out}\right)\left(\cos\left(\beta\right)\right)^2\left(a_\theta\left(r_{out}\right)\right)^2\left(\sin\left(\beta\right)\right)^2\left(a_z\left(r_{out}\right)\right)^2}{r_{out}} \\
&- 4/3\,\frac{P_2\left(r_{out}\right)\left(\cos\left(\beta\right)\right)^4\left(a_\theta\left(r_{out}\right)\right)^4}{r_{out}} \\
&- 4/3\,\frac{P_2\left(r_{out}\right)\left(\cos\left(\beta\right)\right)^2\left(a_\theta\left(r_{out}\right)\right)^2\left(\sin\left(\beta\right)\right)^2\left(a_z\left(r_{out}\right)\right)^2}{r_{out}} \\
&- 2\,\frac{F_1\left(r_{out}\right)\left(\cos\left(\beta\right)\right)^2\left(a_\theta\left(r_{out}\right)\right)^2}{r_{out}} - 2/3\,\frac{F_1\left(r_{out}\right)\left(\sin\left(\beta\right)\right)^2\left(a_z\left(r_{out}\right)\right)^2}{r_{out}} \\
&- 2\,\frac{F_2\left(r_{out}\right)\left(\cos\left(\beta\right)\right)^2\left(a_\theta\left(r_{out}\right)\right)^2}{r_{out}} - 2/3\,\frac{F_2\left(r_{out}\right)\left(\sin\left(\beta\right)\right)^2\left(a_z\left(r_{out}\right)\right)^2}{r_{out}} + \frac{P_{ext}}{r_{out}}
\end{aligned}
$$

References

Walter R. Benson, Joseph E. Hamilton, and Clarence E. Claugus. Dissection of aorta: Report of a case treated by fenestration procedure. *Annals of surgery*, 146:111–116, 1957.

M.E. DeBakey, W.S. Henly, D.A. Cooley, G.C. Morris, E.S. Crawford, and A.C. Beall. Surgical management of dissecting aneurysms of the aorta. *Journal of the American Heart Association*, 24:290–303, 1961.

I. Demir, J. P. Hirth, and H. M. Zbib. The somigliana ring dislocation. *Journal of Elasticity*, 28(3):223–246, 1992.

T. C. Gasser and G. A. Holzapfel. Geometrically non-linear and consistently linearized embedded strong discontinuity models for 3d problems with an application to the dissection analysis of soft biological tissues. *Computer Methods In Applied Mechanics and Engineering*, 192(47-48):5059–5098, 2003. doi: 10.1016/j.cma.2003.06.001.

T. C. Gasser and G. A. Holzapfel. Modeling the propagation of arterial dissection. *European Journal of Mechanics A-solids*, 25(4):617–633, 2006. doi: 10.1016/j.euromechsol.2006.05.004.

G. A. Holzapfel. Arterial tissue in health and disease: Experimental data, collagen-based modeling and simulation, including aortic dissection. *Biomechanical Modelling at the Molecular, Cellular and Tissue Levels*, 508:259–344, 2009.

G. A. Holzapfel, T. C. Gasser, and R. W. Ogden. A new constitutive framework for arterial wall mechanics and a comparative study of material models. *Journal of Elasticity*, 61 (1-3):1–48, 2000.

D. Kamalakannan, Howard S. Rosman, and Kim A. Eagle. Acute aortic dissection. *Critical Care Clinics*, 23:779–800, 2007.

I. A. Khan and C. K. Nair. Clinical, diagnostic, and management perspectives of aortic dissection. *Chest*, 122(1):311–328, 2002.

Alexander M. Korsunsky. Fundamental eigenstrain solutions for axisymmetric crack problems. *Journal of the Mechanics and Physics of Solids*, 43:1221–1241, 1995.

T. L. Leise, J. R. Walton, and Y. Gorb. A boundary integral method for a dynamic, transient mode i crack problem with viscoelastic cohesive zone. *International Journal of Fracture*, 162:69–76, 2010.

M. J. Lighthill. *Introduction to Fourier Analysis and Generalised Functions.* Cambridge University Press, 1958.

Fred Nilsson. A tentative method for determination of cohesive zone properties in soft materials. *International Journal of Fracture*, 136:133–142, 2005.

M. Ortiz and A. Pandolfi. Finite-deformation irreversible cohesive elements for three-dimensional crack-propagation analysis. *International Journal For Numerical Methods In Engineering*, 44(9):1267–1282, 1999.

F. B. Parker, John F. Neville, E. Lawrence Hanson, Sultan Mohiuddin, and Watts R. Webb. Management of acute aortic dissection. *The Annals of Thoracic Surgery*, 19: 436–442, 1975.

R.W.Ogden. *Non-linear elastic deformations.* Dover Publications Inc., 1997.

L.K.v. Segesser, Igor Killer FACS, Marcel Ziswiler, Andre Linka, Manfred Ritter, Rolf Jenni, Peter C. Baumann MSEE, and Marko I. Turina. Dissection of the descending thoracic aorta extending into the ascending aortaa therapeutic challenge. *Thoracic and Cardiovascular Surgery*, 108:755–761, 1994.

W.S. Slaughter. *The linearized theory of elasticity.* Birkhuser Boston, 2002.

T. Suzuki, Rajendra H. Mehta, Hseyin Ince, Ryozo Nagai, Yasunari Sakomura, Frank Weber, Tetsuya Sumiyoshi, Eduardo Bossone, Santi Trimarchi, Jeanna V. Cooper, Dean E. Smith, Eric M. Isselbacher, Kim A. Eagle, and Christoph A. Nienaber. Clinical profiles and outcomes of acute type b aortic dissection in the current era: Lessons from the international registry of aortic dissection (irad). *Journal of the American Heart Association*, 108:312–317, 2003.

A. S.M. Tam, M. Catherine Sapp, and Margot R. Roach. The effect of tear depth on the propagation of aortic dissections in isolated porcine thoracic aorta. *Journal of Biomechanics*, 31:673–676, 1998.

J. Wei, Chung-Yi Chang, Yi-Cheng Chuang, Sung-How Sue, Kuo-Chen Lee, and David Tung. A new vascular ring connector in surgery for aortic dissection. *The Journal of Thoracic and Cardiovascular Surgery*, 138:674–677, 2009.

M.D.B Wilks, D. Nowell, and D.A. Hills. The evaluation of stress intensity factors for plane cracks in residual stress fields. *Journal of Strain Analysis*, 28:145–152, 1993.

B. Yang, S. Mall, and K. Ravi-Chandar. A cohesive zone model for fatigue crack growth in quasibrittle materials. *International Journal of Solids and Structures*, 38:3927–3944, 2001.